Universidade de Lisboa
Faculdade de Ciências
Departamento de Química e Bioquímica

Characterization of Erv2p and Pdi1p, two thiol oxidoreductases involved in protein disulfide bond formation in the endoplasmic reticulum of *Saccharomyces cerevisiae*

Andrea Lages Lino Vala

Doutoramento em Bioquímica
(Especialidade: Regulação Bioquímica)

2008

Universidade de Lisboa
Faculdade de Ciências
Departamento de Química e Bioquímica

Characterization of Erv2p and Pdi1p, two thiol oxidoreductases involved in protein disulfide bond formation in the endoplasmic reticulum of *Saccharomyces cerevisiae*

Andrea Lages Lino Vala

Doutoramento em Bioquímica
(Especialidade: Regulação Bioquímica)

Tese orientada pelo Professor Chris Kaiser e
pela Professora Dra. Ana Ponces Freire

2008

A presente tese foi realizada no Departamento de Biologia do Massachussets Institute of Technology (Instituto de Tecnologia de Massachussets) sob a orientação do Professor Chris Kaiser e com a co-orientação da Professora Dra. Ana Ponces Freire (Faculdade de Ciências da Universidade de Lisboa).

Characterization of Erv2p and Pdi1p, two thiol oxidoreductases involved in protein disulfide bond formation in the endoplasmic reticulum of *Saccharomyces cerevisiae*

by Andrea Lages Lino Vala

Submitted to the Department of Chemistry and Biochemistry
Faculty of Sciences
University of Lisbon

©2008 Andrea Lages Lino Vala
All rights reserved

Declaração

Para os devidos efeitos, e de acordo com o n˚2 do artigo 8 do Decreto-Lei n˚ 388/70, a autora desta dissertação declara que interveio na concepção e execução do trabalho experimental apresentado nesta dissertação, excepto quando indicado.

Na presente dissertação incluem-se os resultados das seguintes publicações:

Sevier, C.S., Cuozzo, J.W., **Vala, A**., Åslund, F. and Kaiser, C.A. (2001) A flavoprotein oxidase defines a new endoplasmic reticulum pathway for biosynthetic disulphide bond formation. *Nat Cell Biol*, **3**, 874-882.

Gross, E., Sevier, C.S., **Vala, A.**, Kaiser, C.A. and Fass, D. (2002) A new FAD-binding fold and intersubunit disulfide shuttle in the thiol oxidase Erv2p. *Nat Struct Biol*, **9**, 61-67.

Vala, A., Sevier, C.S. and Kaiser, C.A. (2005) Structural determinants of substrate access to the disulfide oxidase Erv2p. *J Mol Biol*, **354**, 952-966.

Sevier, C.S, **Vala, A.** and Kaiser, C.A. (2007) Role of glutathione in the isomerization of protein disulfide bonds in *S. cerevisiae*. *In preparation*.

Characterization of Erv2p and Pdi1p, two thiol oxidoreductases involved in protein disulfide bond formation in the endoplasmic reticulum of *Saccharomyces cerevisiae*

by Andrea Lages Lino Vala

Abstract

Disulfide bonds are essential for the folding and stability of a variety of secretory proteins. One well-characterized pathway for disulfide bond formation involves a membrane-bound oxidoreductase, Ero1p, and a lumenal protein, Pdi1p. In a sequence of thiol-disulfide exchange reactions, Ero1p transfers its oxidizing equivalents, obtained from molecular oxygen, to Pdi1p, which in turn transfers its to substrate proteins. Consistent with its proposed role, a conditional allele of *ERO1* (*ero1-1*) is DTT sensitive and has defects in disulfide bond formation. Furthermore, in this strain Pdi1p is in its reduced state, while it is oxidized in wild-type cells.

Using genetic and biochemical assays, we isolated and characterized Erv2p, a small dimeric FAD-dependent sulfhydryl oxidase that that can generate disulfide bonds in the endoplasmic reticulum lumen of *Saccharomyces cerevisiae*. Overexpression of Erv2p suppresses the growth defect of *ero1-1* mutants and the DTT sensitivity at the restrictive temperature and restores disulfide bond formation in substrate proteins.

Mutagenic and structural data show that Erv2p uses an internal relay between two conserved pairs of cysteines to transfer disulfides to substrate proteins: the FAD-proximal active site pair of cysteines and the C-terminal pair of cysteines located in a flexible tail. Oxidizing equivalents obtained from oxygen are transferred to Pdi1p *via* these pairs of essential cysteines. Site-directed mutagenesis of the Erv2p tail suggests that tail cysteine residues and their spatial localization, and not the other residues, are required for Erv2p activity.

Furthermore, the shuttle mechanism seems to provide specificity in the disulfide transfer by preventing direct access to the active site cysteines. We found that mutations in the dimer interface that convert Erv2p into a monomeric protein bypass the need to transfer between two pairs of cysteines. Analysis of the activity of various mutants suggests that converting Erv2p to a monomeric form yields an active but less specific protein. Thus my work suggests that the Erv2p tail confers substrate specificity by preventing access to the active site cysteine pair. This mechanism seems to be a common mechanism of disulfide bond transfer since it is shared by Ero1p and members of the QSOX/ERV family.

To better understand the role of Pdi1p in disulfide oxidation and isomerization pathways, we isolated and characterized temperature-sensitive mutants of Pdi1p. One set of *pdi1* ts mutants is impaired in CPY maturation, indicating that this mutant has defective oxidase activity. These mutants are trapped in mixed-disulfide complexes; therefore they will be invaluable tools for identifying Pdi1p substrates and subsequently studying the mechanism of interaction between Pdi1p and substrate. The second set of mutants accumulates a precursor of CPY, suggesting a novel role for Pdi1p in the translocation of secretory proteins into the ER.

Keywords (5): disulfide bond; oxidative folding; Erv2p; Pdi1p; substrate specificity; sulfhydryl oxidase; *Saccharomyces cerevisiae*

Caracterização da Erv2p e da Pdi1p, duas oxidoreductases envolvidas na formação de pontes persulfureto no lúmen do retículo endoplasmático de *Saccharomyces cerevisiae*

Andrea Lages Lino Vala

Resumo

A ponte persulfureto é uma ligação covalente simples formada a partir da oxidação de grupos tiol (ou sulfídrilo, -SH). As pontes persufureto sao essenciais para a formação e estabilidade de uma variedade de proteínas da via secretória. Previamente, vários estudos definiram quais os intervenientes principais deste processo. As proteínas envolvidas neste processo possuem um centro catalítico onde ocorre a oxidação e redução reversível de dois resíduos de cisteína. O processo de criação de pontes persulfureto é devido à acção conjunta de uma oxidoredutase localizada na membrana do retículo endoplasmático, Ero1p, e de uma proteína localizada no lúmen do retículo endoplasmático, Pdi1p. Numa sequência de reações de intercâmbio tiol-persulfureto, a proteína Ero1p transfere uma ponte persulfureto, que obteve do oxigênio molecular, para a proteína Pdi1p, que por sua vez transfere esta ponte persulfureto para proteínas substrato. De acordo com a função proposta, um mutante condicional do gene *ERO1* (*ero1-1*) é sensível a agentes redutores, tais como o ditiotreitol, e tem defeitos na formação de pontes persulfureto em proteínas da via secretória. Além do mais, no mutante condicional do *ero1-1*, a proteína Pdi1p encontra-se no seu estado reduzido, enquanto que em células *wild-type* encontra-se no estado oxidado.

Com a ajuda de ensaios genéticos e bioquímicos, fomos capazes de isolar e caracterizar a proteína Erv2p, uma proteína de tamanho pequeno, dimérica, e que usa FAD como grupo prostético. A proteína Erv2p possui actividade de tiol oxidase e é capaz de gerar pontes persulfureto no lumen do retículo endoplásmico da levedura *Saccharomyces cerevisiae*. A sobre-expressão desta proteína suprime tanto o defeito de crescimento do mutante condicional *ero1-1*, como a sensibilidade a agentes reductores e restabelece a formação de pontes persulfureto em proteínas substrato. Dados estruturais e estudos mutagénicos da proteína Erv2p permitiram demonstrar que esta usa um sistema de transmissão em cadeia de pontes de persulfureto entre dois

pares de cisteínas conservados. O par de cisteínas activas localizadas próximo do grupo prostético FAD transfere a ponte persulfureto para o par de cisteínas localizadas numa região flexível da parte C-terminal da proteína da outra sub-unidade, e deste último par para as proteínas substrato.

Estudos em que a proteína Erv2p foi mutada em resíduos específicos da região C-terminal sugerem que as características necessárias para a sua actividade de tiol oxidase sao: 1) a presença das cisteínas da região flexível da parte C-terminal, e 2) a localização espacial deste par de cisteínas. Mais importante, este mecanismo de transmissão em cadeia de pontes persulfureto entre dois pares de cisteínas conservados parece conferir especificidade à transferência de pontes persulfureto, pois permite prevenir o acesso directo às cisteinas activas localizadas perto do grupo prostético FAD.

Descobrimos que mutações na interface dos monómeros da Erv2p convertem-a numa proteína monomérica e eliminam a necessidade de transferir a ponte persulfureto entre dois pares de cisteínas. A análise da actividade dos vários mutantes sugere que a conversão da proteína Erv2p duma forma dimérica numa forma monomérica dá origem a uma proteína activa mas menos específica. Deste modo, o meu trabalho sugere que esta região flexível da parte C-terminal da proteína Erv2p confere especificidade na transferência de pontes persulfureto a substratos, pois previne o acesso ao par de cisteínas activo. Este mecanismo parece ser um mecanismo geral de transferência de pontes persulfureto pois é tambem usado pela oxidoreductase Ero1p e por membros da família QSOX/ERV.

Para melhor entender o papel fundamental da Pdi1p no processo de oxidação e de isomerização de tióis, isolamos mutantes desta proteína que são sensíveis à temperatura. Foram obtidos mutantes da *pdi1* sensíveis à temperatura que foram caracterizados bioquimica- e geneticamente. Um dos grupos de mutantes de *pdi1* sensíveis à temperatura é deficiente na oxidação de proteínas da via secretória, tais como a carboxipeptidase Y, sugerindo uma deficiência na actividade de oxidoredutase. Uma vez que estes mutantes estao em complexos estáveis com o seu substrato, serão uma ferramenta valiosa que permitirá a identificacao de subtratos e o estudo em detalhe do mecanismo de interação da proteína Pdi1p com os seus substratos. O segundo grupo de mutantes da *pdi1* sensíveis à temperatura parece ser deficiente na translocação de proteínas do citosol para o lúmen do retículo endoplasmático. Estes estudos atribuem uma nova funcao à proteína Pdi1p.

Palavras-chave (5): ponte persulfureto; *folding* oxidativo; Erv2p; Pdi1p; especificidade de transferência ao substrato; actividade de tiol oxidase; *Saccharomyces cerevisiae*

Acknowledgments

I would like to thank my supervisor, **Prof. Chris Kaiser**, for accepting me as a Ph.D. student in his laboratory. While in the lab, I had the opportunity to learn science with one of the most critical person I have met, and to interact with great minds. I am grateful for his guidance, advice and support throughout the course of these years.

I would like to thank **Prof. Ana Ponces Freire**, my Portuguese advisor, who has been there for me all the times, for her encouragement and especially for her enthusiasm.

I would like to thank **Prof. Antonio Coutinho** for selecting me out of a group of people to join the Gulbenkian Ph.D. Program in Biology and Medicine and for believing in me and in my scientific capacities. By doing this, he gave me the wonderful opportunity to interact with a variety of excellent professors, who taught us about the fabulous aspects of biology in the first year of my Ph.D, and to spread my wings and fly to a different continent. I would also like to thank the students of the **7th PGDBM** and **Manuela Cordeiro** for their support and friendships.

I would like to thanks current and past members of the Kaiser lab for making this experience, in various ways, an unforgettable one: Sascha Losko, Stephen Helliwell, Rachna Ram, Esther Chen, Aron Eklund, Hak Chang, Kelly Curtis, Michelle Crotwell, Marta Rubio, Carolyn Sevier, April Risinger, Minggeng Gao, Hongging Qu, Barbara Karampalas, Eduardo Cebollero, Darcy Morse, Rajini Haraksingh, Natalie Cain, Nina Gaissert, Eric Spear, Polly McGahan and Erica Beade. I would like to specially thank Barbara Karampalas for making my experiences run smoother, by making sure all the reagents I needed were there on time, for putting up with my complaints about life in general and for all the words of advice.

I would like to express my gratitude to the **Fundação para a Ciência e Tecnologia** that awarded me a Ph.D. Fellowship (SFRH/BD/2735/2000).

I am grateful to the laboratories of Steve Bell, Robert Sauer and Bob Horvitz for sharing equipment, and especially **Jason Bower**, **David Wah**, **Peter Chivers**, **Shilpa Joshi** and **Daniel Bolon** for helping me with protein stuff, for their advices and useful contributions to my work.

I would like to thanks **Rachna** and **George** for being my friends, being there for me every time I needed, for putting up with my complaints and specially for all the good times (candle pin bowling, the flea circus, etc).

I would like to thanks **Joyce** and **Vicki** for being the friends they are, helping me through bad moments and specially for the mahjong nights, that make me forget the lab for a couple of hours...

I would like to thank the Portuguese group that hangs around the Boston/Cambridge area for all the good times. I specially want to thank **Rita Oliveira** for all the cooking moments, all the craziness and her friendship and **Susana Silva** for making sure I get out of this Ph.D. with my head still in the same spot it was when I started.

I would like to thank **Andreia Fernandes** and **Rodrigo Almeida** for being my friends and for putting up with my long lack of emails.

I would like to thank **Marina** and **Francisco** for their support, encouragement and for being there when I need it them in the final part of this adventure. I would like to thanks **Andi**, **Ted** and **Teresa** for all the fun times that made me forget the lab stress, and specially for their support and friendship.

Needless to say, I want to say a big thanks to my family, for all the help and support and for believing in me and setting me free to pursue my dreams, even though it meant being so so far away from them. I want to say a big thanks to **Anita**, my aunt and closest friend in the world, with whom I share all my thoughts, for all the love you have given me through out the years, for all the advices and reproaches that made me a better person, for always making me see the other side of things and for being there every time I need it.

Finally but not the least I would like to say that this thesis would have not been possible without the help of **Aron**. Your patience, love and caring made me overcome lots of obstacles. Thanks for always being there to pick me up from the lab at late hours in the evening (or should I say early morning?!) and also for putting up with "I am almost done, just another 15 minutes" that are always another hour or two.

Table of contents

Title page i
Declaração vii
Abstract ix
Keywords x
Resumo xi
Palavras-chave xiii
Acknowledgments xv
Table of contents xvii
List of figures xxiii
List of tables xxvi
Chapter One. Players in disulfide bond formation pathways: Current knowledge. 1
    Initial studies of disulfide bond formation 3
    Chemistry of thiol-disulfide exchange reactions 3
    Oxidative folding in the endoplasmic reticulum of eukaryotes 5
        The main pathway of disulfide bond formation requires Ero1 and Pdi1p 5
        An alternative pathway of disulfide bond formation is present in fungi 8
        Comparison between Ero1p and Erv2p mechanisms and structures 9
    Sulfhydryl oxidases of the QSOX/ERV family: their role in oxidative folding 11
        ERV1 is required for mitochondrial disulfide bond formation 12
        Augmenter of liver regeneration 16
        Vaccinia virus E10R: sulfhydryl oxidase involved in cytoplasmic disulfide bond formation pathway 18
        QSOX 19
        Members of the QSOX/ERV family share the same mechanism 20
    PDI - Its role in disulfide bond formation 22
        Thioredoxin fold 24
        Homologs of PDI in the yeast ER 25
            Mpd1p 26
            Mpd2p 28
            Eug1p 29
            Eps1p 30
        Mammalian homologs of PDI 31

The Role of other factors in oxidative folding 35
    Role of glutathione in oxidative folding 35
    Role of flavin 36
Disulfide bond formation in the periplasm of prokaryotes 36
    Oxidation pathway - DsbA & DsbB 36
    Isomerization pathway - DsbC/DsbG & DsbD 37
Comparison of the disulfide bond formation pathways in prokaryotes and eukaryotes 38
References 40
Chapter Two. Structural and biochemical characterization of Erv2p, a small FAD-dependent sulfhydryl oxidase 50
    Preface 52
    Part I. A flavoprotein oxidase defines a new endoplasmic reticulum pathway for biosynthetic disulfide bond formation 54
        Abstract 56
        Introduction 57
        Results 58
            ERV2 defines a novel pathway for disulfide bond formation 58
            Erv2p is a luminal ER protein 60
            Erv2p is a flavin-binding thiol oxidase 61
            In vivo function of Erv2p 63
            Trapping of Pdi1p-Erv2p mixed disulfides *in vivo* 64
            Oxidation of Pdi1p by Erv2p *in vitro* 65
        Discussion 66
        Material and methods 69
            Strains and growth conditions 70
            Isolation of P_{GAL1}-*ERV2* 71
            Tagging of *ERV2* 71
            Detection of CPY, Erv2p and Pdi1p by immunoblotting 71
            Localization of Erv2p 72
            Expression and purification of Erv2p 73
            Mutagenesis of *ERV2* 74
            ERV2 assays 75
            Trapping mixed disulfides between Erv2-HA and Pdi1p 75
            Expression and purification of His-tagged Pdi1p 76

Oxidation of Pdi1p by *ERV2 in vitro* 76
References 77
Tables 82
Figures 84
Part II. New FAD-binding fold and intersubunit disulfide shuttle in the thiol oxidase Erv2p. 95
Abstract 97
Introduction 98
Results and discussion 99
Crystallization of the Erv2p thiol-oxidase module 99
New fold for FAD binding proteins 100
Key structural and functional residues in the fold 101
Erv2p structure suggests a disulfide relay mechanism 102
Secondary Cys-X_n-Cys motifs in Erv2p homologs 104
Mechanisms for interaction with substrate proteins 104
Material and methods 105
Protein expression and purification 105
Circular dichroism 106
Crystallization and structure determination 106
Construction and analysis of Cys mutants 107
References 109
Tables 113
Figures 115
Chapter Three. Structural determinants of substrate access to the disulfide oxidase Erv2p. 123
Preface 125
Summary 127
Introduction 128
Results 130
Intragenic complementation of *erv2* mutations 130
Cys176 and Cys178 are the only tail residues essential for Erv2p activity 130
Erv2p activity depends on the spacing between Cys176 and Cys178 131

Erv2p activity depends on the position of Cys176 and Cys178 within the tail 132
Identification of intragenic suppressors of Erv2p tail cysteine mutants 133
Monomeric Erv2p has decreased substrate selectivity 134
Monomeric Erv2p mutants can oxidize Pdi1p in the absence of tail cysteine residues 136
Discussion 136
Specificity conferred by the disulfide relay 137
Generality of the disulfide relay mechanism 139
Materials and methods 140
Media and yeast strains 141
Plasmid construction 141
Radiolabeling and immunoprecipitation 142
Erv2p antibody production 142
Isolation of *ERV2-C176A-C178A* intragenic suppressors 142
Protein expression and purification 143
Protein molecular mass determination 143
Thermal denaturation assay 144
Activity assay 144
Pdi1p oxidation *in vitro* 145
References 146
Tables 149
Figures 153
Chapter Four. Further mutagenic studies performed in Erv2p. 165
Preface 167
Results 169
An additional pair of cysteines seems to be required for Erv2p activity *in vivo* 169
The tail of Erv2p is consisted mainly of charged residues 169
Altering Gly177 to a negatively charged residue affects Erv2p activity 170
Cys121 of the active site cysteine pair is attacked by Cys176 170
Intragenic suppressors of the tail cysteines mutants are monomers 170

Intragenic suppressor mutations do not rescue an Erv2p-C150A or Erv2p-C167A or Erv2p-C150A-C167A double mutant or an Erv2p-L171Stop mutant 171
Intragenic suppressor mutations are conserved in QSOX/ERV family 172
Sulfhydryl oxidase activity of Erv2p 172
Discussion 173
Erv2p and members of the in the QSOX/ERV family seem to share the same disulfide relay mechanism 174
Transfer between two pairs of cysteines confers specificity in the disulfide transfer 175
Specificity conferred by the disulfide transfer reaction 176
Materials and methods 177
Media and yeast strains 177
Plasmid construction 177
Radiolabeling and immunoprecipitation 178
Erv2p antibody production 179
Protein expression and purification 179
Gel filtration 179
FAD reduction assay 180
References 181
Tables 183
Figures 191
Chapter Five. Isolation and biochemical characterization of *pdi1* temperature-sensitive mutants. 199
Abstract 201
Results 203
Isolation of temperature-sensitive *pdi1* alleles 204
Characterization of *pdi1* ts mutants 204
The temperature-sensitive alleles of *PDI* are impaired in oxidative folding 205
In *pdi1* ts mutants secretion of invertase is not impaired 206
The *pdi1* ts mutants are unable to oxidize CPY 206
Function of Ero1p and Pdi1p in oxidative folding 207

        Genetic interactions of *pdi1* mutations with mutations in the disulfide bond pathway genes 207
        Location of the mutations in the predicted secondary structure of Pdi1p 208
        Trapping *pdi1* ts-substrate mixed disulfides *in vivo* 208
        Future directions 209
    Materials and methods 209
        Strains, plasmids and media 209
        Plasmid construction 211
        Isolation and integration of *pdi1* temperature-sensitive alleles 211
        Assays for growth in the presence of DTT, diamide or BSO 211
        CPY immunoprecipitation 212
        Induction of the unfolded protein response 213
        Protein extracts, and immunoblotting 213
    References 215
    Tables 219
    Figures 229
Chapter Six. Players in disulfide bond formation pathways: Open questions. 237
    Ero1-dependent and -independent disulfide bond formation pathways 239
    Search for substrates of Erv2p 239
    The function of Erv2p: still a mystery 239
    Erv2p homologs are involved in disulfide bond formation in non-ER locations 240
    How is FAD transported into the ER lumen? 240
    ER redox homeostasis and oxidative folding 240
    Specificity in disulfide transfer - variations on a theme 241
    Is there an isomerization pathway in yeast? PDI, GSH or an uncharacterized reductase - who's to blame? 242
    Role of PDI homologs? Different specificity? 243
    References 244

List of figures

Chapter 1. Players in disulfide bond formation pathways: Current knowledge.

Figure 1. Thiol-disulfide exchange reactions.
Figure 2. Pathway of disulfide bond formation in the ER of *S. cerevisiae*. Disulfide
Figure 3. Similarities between the structures and catalytic mechanisms of Erv2p and Ero1p.
Figure 4. Schematic representation of the QSOX/ERV family members.
Figure 5. Pathways of disulfide bond formation in the IMS of mitochondria of *S. cerevisiae*.
Figure 6. Pathways of disulfide bond formation (oxidation) in the cytoplasm of *vaccinia virus*.
Figure 7. Erv2p (A) and rat ALR (B) share the same catalytic core.
Figure 8. Schematic representation (domain structure) of the protein disulfide isomerase family (PDI-related proteins) from *S. cerevisiae* **(A)** and *Homo sapiens* **(B)**.
Figure 9. Structure of the thioredoxin fold.
Figure 10. Pathways of disulfide bond formation (oxidation) and isomerization in the periplasm of *E. coli*.

Chapter 2. Structural and biochemical characterization of Erv2p, a small FAD-dependent sulfhydryl oxidase.

Chapter 2. Part A. A flavoprotein oxidase defines a new endoplasmic reticulum pathway for biosynthetic disulfide bond formation.

Figure 1. *ERV2* overexpression restores growth, resistance to DTT, and the formation of disulfide bonds to an *ero1-1* mutant.
Figure 2. Erv2p is a membrane protein located in the ER.
Figure 3. Erv2p contains a conserved domain shared between yeast and human proteins.
Figure 4. Erv2p is a flavin-binding thiol oxidase that consumes oxygen to form disulfide bonds.
Figure 5. Erv2p uses oxygen in a pathway for thiol oxidation *in vivo*.
Figure 6. Erv2p transfers oxidizing equivalents to Pdi1p *via* a direct thiol-disulfide exchange.
Figure 7. Pathways for thiol oxidation in the ER.

Chapter 2. Part B. New FAD-binding fold and intersubunit disulfide shuttle in the thiol oxidase Erv2p.

- **Figure 1.** Sequence and secondary structure of Erv2p.
- **Figure 2.** CD of Erv2-ΔN and Erv2-c.
- **Figure 3.** Structure of Erv2p.
- **Figure 4.** FAD binding site.
- **Figure 5.** Electron density map in the vicinity of the Erv2p active site.
- **Figure 6.** Erv2p flexible C-terminal tail.
- **Figure 7.** Cys residues required for disulfide bond formation between Erv2p protomers and for Erv2p function *in vivo*.

Chapter 3. Structural determinants of substrate access to the disulfide oxidase Erv2p.

- **Figure 1.** Evidence of electron transfer between pairs of cysteine residues.
- **Figure 2.** Conservation of the C terminus of Erv2p among fungal species.
- **Figure 3.** In the tail, only Cys176 and Cys178 are required for activity.
- **Figure 4.** The position of Cys176 and Cys178 relative to the Cys121-Cys124 cysteine pair is important for disulfide transfer.
- **Figure 5.** Localization of Cys176 and Cys178 relative to Cys121-Cys124 is important for disulfide transfer.
- **Figure 6.** Intragenic suppressors of the cysteine tail mutant.
- **Figure 7.** Thermal denaturation curves for Erv2p wild-type and mutant variants.
- **Figure 8.** Erv2p intragenic suppressors have different substrate specificities.
- **Figure 9.** Crystal-structure of Erv2p showing accessibility of the active site cysteine residues.

Chapter 4. Further mutagenic studies performed in Erv2p.

- **Figure 1.** Erv2p Cys150 and Cys167 are required for activity.
- **Figure 2.** Conservation of the C-terminus of Erv2p among fungal species.
- **Figure 3.** Cys176 interacts with Cys121 in Erv2p-(DYD)Δ.
- **Figure 4.** Erv2p-F111S-C176A-C178A is a monomer.
- **Figure 5.** Catalytic mechanism of dimeric Erv2p (A) and monomeric Erv2p (B).

Chapter 5. Isolation and biochemical characterization of *pdi1* temperature-sensitive mutants.

- **Figure 1.** Isolation of a *pdi1* ts alleles.
- **Figure 2.** Addition of oxidant rescues *pdi1 ts* alleles.
- **Figure 3.** Blocking the excess of GSH rescues the *pdi1* ts alleles.
- **Figure 4.** CPY transport is impaired in *pdi1* ts alleles.

Figure 5. The *pdi1-16* ts mutant accumulates the intracellular form of invertase.

Figure 6. The *pdi1* ts alleles are required for oxidation of CPY.

Figure 7. Isolation of mutaions of *pdi1* ts alleles.

Figure 8. The *pdi1* ts alleles accumulate *pdi1* ts-substrate complexes.

List of tables

Chapter 1. Players in disulfide bond formation pathways: Current knowledge.

Table 1. Characteristics of *S. cerevisiae* PDI-like proteins and comparison to TrxA and DsbA from *E. coli*.

Table 2 - Characteristics of mammalian PDI-like proteins and comparison to TrxA and DsbA from *E. coli*.

Chapter 2. Structural and biochemical characterization of Erv2p, a small FAD-dependent sulfhydryl oxidase.

Chapter 2. Part A. A flavoprotein oxidase defines a new endoplasmic reticulum pathway for biosynthetic disulfide bond formation.

Table 1. Analysis of Erv2p mutants in the conserved Cys-X-X-Cys motif.

Table 2. Yeast strains used in this study.

Chapter 2. Part B. New FAD-binding fold and intersubunit disulfide shuttle in the thiol oxidase Erv2p.

Table 1. Crystallographic and refinement statistics.

Chapter 3. Structural determinants of substrate access to the disulfide oxidase Erv2p.

Table 1. Molecular mass of His$_6$-Erv2p and His$_6$-Erv2p mutants.

Table 2. Rate of O_2 consumption of His$_6$-Erv2p and His$_6$-Erv2p mutants.

Table 3. Plasmids used in this work.

Table 4. Primers used in this study.

Chapter 4. Further mutagenic studies performed in Erv2p.

Table 1. Erv2p C-terminal tail charge residues mutants.

Table 2. Gly177 mutants of Erv2p.

Table 3. Erv2p-(DYD) mutants.

Table 4. Erv2p suppressor mutants.

Table 5. Rate of O_2 consumption for of His$_6$-Erv2p and His$_6$-Erv2p mutants.

Table 6. Structure and properties of thiol compounds used in this study.

Table 7. Plasmids used in this work.

Table 8. Primers used in this study.

Chapter 5. Isolation and biochemical characterization of *pdi1* temperature-sensitive mutants.

Table 1. Temperature-sensitive alleles of Pdi1p.

Table 2. Characterization of *pdi1* temperature-sensitive alleles.

Table 3. Further characterization of *pdi1* temperature-sensitive alleles.

Table 4. Suppression of growth defect of the temperature-sensitive alleles of Pdi1p by blocking GSH synthesis.

Table 5. Synthetic lethality of temperature-sensitive alleles of Pdi1p with *ero1-1*, *ire1Δ*, and *hut1Δ*.

Table 6. Synthetic lethality of temperature-sensitive alleles of Pdi1p with genomic deletion of Pdi1p homologs.

Table 7. Mutations in *pdi1* temperature-sensitive alleles.

Table 8. Yeast strains used in this study.

Table 9. Plasmids used in this work

Chapter One

Players in disulfide bond formation pathways: Current knowledge

Initial studies of disulfide bond formation

Pioneer studies by Anfinsen and colleagues on *in vitro* protein folding demonstrated that the presence of oxygen or another strong oxidant, such as oxidized glutathione, is sufficient to promote disulfide bond formation between free cysteine thiols. However, disulfide bond formation *in vitro* is often a very slow and inefficient process, requiring hours to days (Anfinsen *et al.*, 1961). In cells, this process is more rapid, suggesting the existence of catalyst.

The formation of disulfide bonds is a critical step in the folding and maturation of secretory proteins and cell-surface proteins. The formation of disulfide bonds influences the thermodynamics of protein folding: disulfide bonds stabilize the native conformation of a protein by destabilizing the unfolded form. *In vivo* oxidative folding is a catalyzed process that is possibly coupled to protein translation/translocation. Further studies by Anfinsen and colleagues lead to the discovery of protein disulfide isomerase (PDI), a protein that can accelerate the oxidative folding of ribonuclease A (RNaseA), a protein containing four disulfide bonds (Goldberger *et al.*, 1963). Since then, a variety of other proteins involved in disulfide bond formation have been discovered and studied and entire pathways of disulfide bond formation have been described (reviewed in (Sevier *et al.*, 2006a; Thorpe *et al.*, 2002; Tu *et al.*, 2004).

Recent studies have made it clear that the role of disulfide bonds is not limited to structural stability. Reversible formation of disulfides takes part in the catalytic mechanism of various enzymes, in the regulation of enzyme activity and in signaling cascades (see review (Biswas *et al.*, 2006). Some proteins, such as ribonucleotide reductase, cycle between a reduced and an oxidized state during their catalytic cycle. Others, such as OxyR, use the redox state of the cysteines as a redox switch to modulate protein function (Biswas et al., 2006; Ghezzi, 2005).

In this chapter I will review the current knowledge on the pathways of formation of disulfide bonds.

Chemistry of thiol-disulfide exchange reactions

Disulfide bond formation is a two-electron oxidation of two thiols, in which two reducing equivalents are released ($2\ e^- + 2H^+$). Biologically, the formation of disulfide bonds is linked to the reduction of molecular oxygen. The reverse reaction, the reduction of a disulfide bond occurs at the expense of reducing equivalents, which are obtained from NADH or NADPH (Gilbert, 1963).

Thiol-disulfide exchange reactions provide a mechanism for transfering reducing or oxidizing equivalents between two thiol-disulfide pairs. A thiolate anion (–S^-), formed by deprotonation of a free thiol, reacts with a disulfide bond of an oxidized species, resulting in the formation of a transient mixed disulfide complex between both species. In a second thiol-disulfide exchange reaction, the free thiolate anion reacts with the mixed-disulfide bond, thus “resolving” it. The net result of the thiol-disulfide exchange reaction is the oxidation of the previously reduced species, with the concomitant reduction of the initially oxidized species (Figure 1A). *In vivo*, oxidation, reduction and isomerization reactions are catalyzed by cellular thiol-disulfide oxidoreductases (Figure 1B).

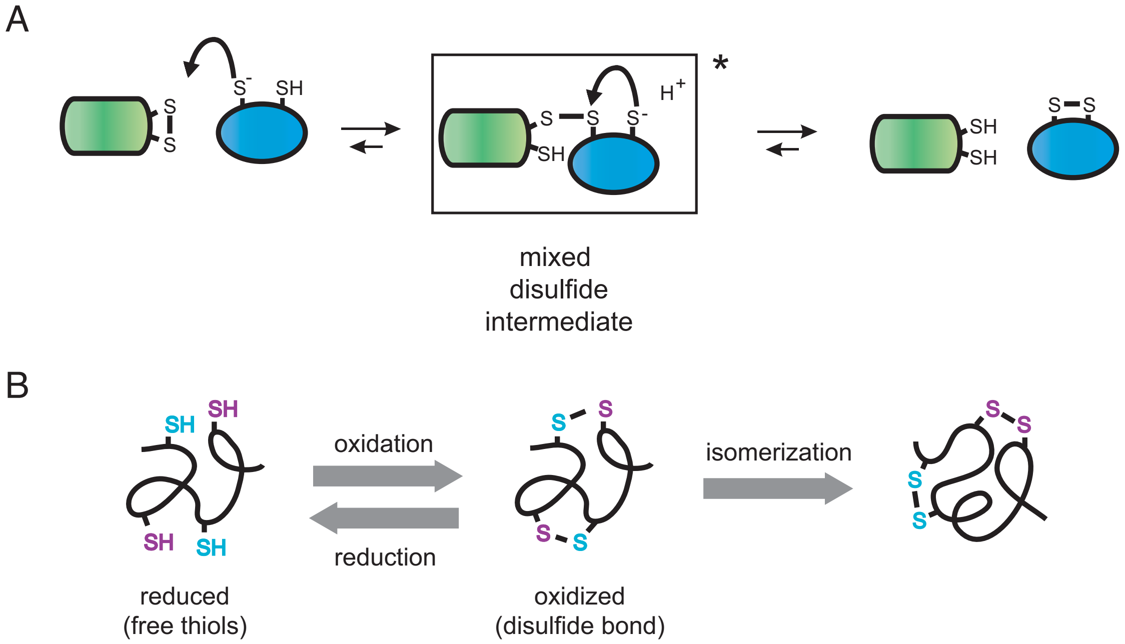
A
S
S
S-
SH
S
S
SH
H+
S-
*
SH
SH
S
S
mixed disulfide intermediate
B
SH
SH
SH
SH
reduced (free thiols)
oxidation
reduction
S
S
S
S
oxidized (disulfide bond)
isomerization
S
S
S
S

Figure 1. Thiol-disulfide exchange reactions. (A) A thiolate anion formed by deprotonation of a cysteine residue reacts with a disulfide bonded species through a nucleophilic substitution reaction. This mixed-disulfide is a transient species that is resolved by the attack of a thiolate anion, resulting in a reduced and an oxidized species. (B) Three types of thiol-disulfide exchange reactions are possible: oxidation, reduction and isomerization.

Oxidative folding in the endoplasmic reticulum of eukaryotes

Proteins that are destined for the secretory pathway normally contain disulfide bonds while cytosolic proteins are devoid of them. Disulfide bonds are formed in the endoplasmic reticulum of eukaryotes or in the periplasm of bacteria (reviewed in (Frand *et al.*, 2000a)).

The main pathway of disulfide bond formation requires Ero1p and Pdi1p

The main pathway of disulfide bond formation in the ER of *Saccharomyces cerevisiae* has been studied intensively. Disulfide bonds are formed in substrate proteins by the concerted action of Ero1p and Pdi1p (Figure 2) (Frand *et al.*, 1998; Pollard *et al.*, 1998).

The *ERO1* (ER oxidoreductin 1) gene was identified by two independent screens: 1) a screen for temperature sensitive mutants with defects in export of secretory proteins from the ER, and 2) a screen for DTT sensitive mutants (Frand et al., 1998; Pollard et al., 1998). The *ERO1* gene is essential for yeast viability (Frand et al., 1998; Pollard et al., 1998). Ero1p is a 65 kDa flavoprotein that is localized to the ER membrane and possesses eight potential N-linked glycosylation sites (Frand et al., 1998; Pollard et al., 1998).

The conditional mutant of *ERO1* (*ero1-1*) not only exhibits a higher sensitivity to external reductants, such as dithiothreitol (DTT) but it has a constitutive unfolded protein response (UPR) (Frand et al., 1998; Pollard et al., 1998). At the restrictive temperature, this mutant exhibits a complete block in the maturation of proteins containing disulfide bonds (such as carboxypeptidase Y (CPY) and the GPI-linked plasma membrane protein, Gas1p), yet it has no defect in secretion of invertase, a periplasmic protein that does not contains disulfides (Frand et al., 1998). Various other evidence suggests that Ero1p plays a role in disulfide bond formation: 1) at the restrictive temperature, the *ero1-1* mutant is no longer able to oxidize CPY, 2) Ero1p is found in mixed-disulfide complexes with Pdi1p and Mpd2p, two proteins that had been previously shown to be involved in disulfide bond formation (see below), 3) at the restrictive temperature, the *ero1-1* mutant Pdi1p is mainly in the reduced state, and 4) overexpression of ERO1 gene leads to DTT resistance (Frand et al., 1998; Frand *et al.*, 1999; Pollard et al., 1998).

Mutagenesis studies have revealed that two pairs of cysteines, Cys100-Cys105 and Cys352-Cys355, are required for Ero1p activity, as assayed by viability and CPY maturation (Frand *et al.*, 2000b). Recent elucidation of the Ero1p structure confirmed that through a series of thiol-disulfide exchange reactions, Ero1p receives its oxidizing equivalents from oxygen and passes them on to Pdi1p and/or Mpd2p (Frand et al., 2000b; Gross *et al.*, 2004).

dithiol substrate →[Cys100-Cys105] → [Cys352-Cys355] → FAD → O_2

Ero1p is a monomeric flavoenzyme that contains a core domain formed by a four-helix bundle (helixes $\alpha2$, $\alpha7$, $\alpha8$ and $\alpha3$) and two extended flexible loops. At least two different conformations of the proteins were observed in the crystal structure: 1) one conformation in which the cysteine pair (Cys100-Cys105) in the flexible loop is near the cysteine pair (Cys352-Cys355) proximal to the FAD cofactor, and 2) one conformation in which the flexible loop is displaced from the core (Gross et al., 2004). The crystal structure thus showed a snapshot of the mechanism of internal disulfide transfer in Ero1p: oxidizing equivalents flow from the FAD cofactor to the active site cysteine pair (Cys352-Cys355), from active site cysteines to the loop cysteines (Cys100-Cys105), and from the latter to substrates proteins, such as Pdi1p.

Mutagenesis studies have demonstrated that Ero1p uses an internal disulfide transfer mechanism to impart selectivity to protein oxidation of substrates (Sevier *et al.*, 2006b). Mutants that allow substrates increased access to the Cys352-Cys355 pair presented a higher thiol oxidase activity toward small thiols (Sevier et al., 2006b). Interestingly, the most divergent regions between the Ero1p homologs are found within the loop region, which contains the second redox-active cysteine pair that interacts with PDI. The differences within this region might facilitate the interaction between Ero1p and specific PDI homologs (Sevier et al., 2006b)

Similar disulfide bond formation pathways exists in higher eukaryotes, although the number and/or diversity of pathways seems to be higher. *Schizosaccharomyces pombe* contains two homologs of Ero1p, SpEro1a and SpEro1b, and three PDI-like proteins. Like Ero1p, they are membrane proteins that are required for disulfide bond formation (Kettner *et al.*, 2004). Although both SpEro1a and SpEro1b are able to complement the growth defect of an *S. cerevisiae ero1-1* mutant, SpEro1b can suppress only at low levels, because it becomes toxic at higher levels of expression (Kettner et al., 2004). Furthermore, a *S. cerevisiae ero1-*

1 mutant expressing SpEro1a is sensitive to DTT, while *ero1-1* expressing SpEro1b is DTT resistant (Kettner et al., 2004). At present it is unknown whether these proteins are required for disulfide bond formation in specific targets or if they have overlapping activities, but the previous results suggest that the SpEro1a and SpEro1b have different activities (Kettner et al., 2004).

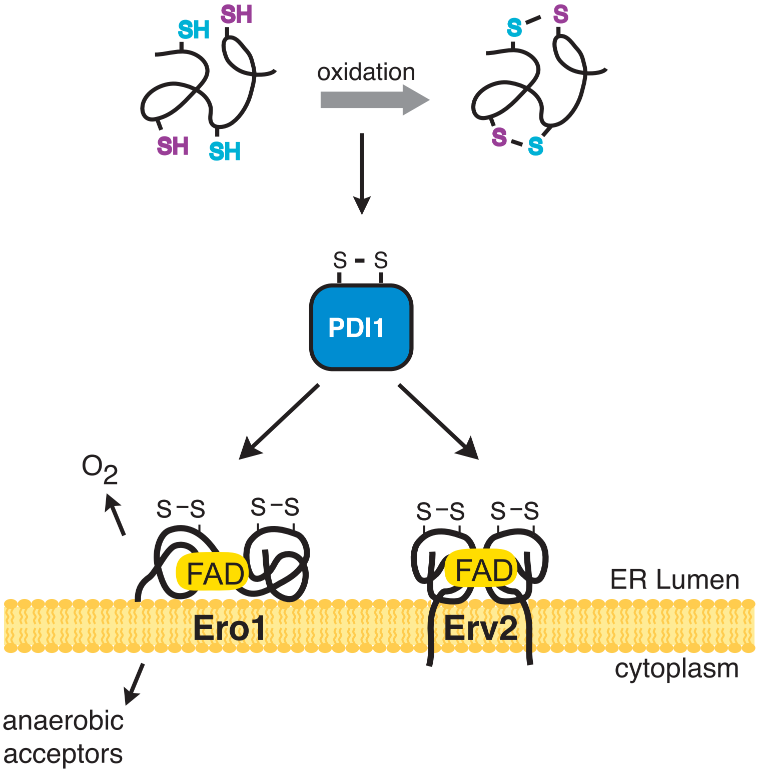

Figure 2. Pathway of disulfide bond formation in the ER of *S. cerevisiae*. Disulfide bond formation occurs in the ER of eukaryotes. The membrane associated protein, Ero1p and the soluble protein, Pdi1p are the main players. Together they transfer oxidizing equivalents, through a series of thiol-disulfide exchange reactions, to the substrate proteins that traverse the secretory pathway. In an alternative pathway, which seems to exist only in fungal eukaryotes, Erv2p can function together with Pdi1p to generate disulfide bonds in substrate proteins.

Two human homologs of Ero1p have also been identified, HsEro1-Lα and HsEro1-Lβ which have 48.5% and 50.6% similarity to ScERO1, respectively, and 50.6% similarity between each other (Cabibbo *et al.*, 2000). Both HsEro1-Lα and HsEro1-Lβ are integral membrane glycoproteins that are localized to the ER (Cabibbo et al., 2000; Pagani *et al.*, 2000). HsEro1-Lα and HsEro1-Lβ differ in their tissue distribution, and while regulation of expression of HsEro1-Lα is mainly controlled by cellular oxygen (Gess *et al.*, 2003), the expression of HsEro1-Lβ is induced by the unfolded protein response (UPR) (Pagani et al., 2000). The different tissue expression and conditions of expression suggest that HsEro1-Lα and HsEro1-Lβ have undergone functional specialization in response to different demands of oxygen tension and high throughput protein folding (Dias-Gunasekara *et al.*, 2005b).

Both HsEro1-Lα and HsEro1-Lβ suppress the growth defect and restore CPY maturation in *S.* cerevisiae *ero1-1* (Cabibbo et al., 2000; Pagani et al., 2000). Both HsEro1-Lα and HsEro1-Lβ form mixed disulfides with PDI (Benham *et al.*, 2000; Mezghrani *et al.*, 2001) but do not interact with ERp72, ERp57 and P5 (Mezghrani et al., 2001). HsEro1-Lα can form complexes with PDI, ERp44 and PDILT (ref in (Dias-Gunasekara *et al.*, 2005a; Dias-Gunasekara et al., 2005b)

An alternative pathway of disulfide bond formation is present in fungi

Fungi contain a second pathway for disulfide bond formation that uses Erv2p as a thiol oxidase. The *ERV2* (Essential for respiration and viability 2) gene was first identified by its similarity to *ERV1* (Lisowsky, 1996; Stein *et al.*, 1998). Erv2p was later identified as a gene that when overexpressed could suppress the growth defect of *ero1-1* mutants (Sevier *et al.*, 2001). Biochemical and genetic data suggest that Erv2p might act in an Ero1p-independent pathway of disulfide bond formation (Sevier et al., 2001). In the absence of Ero1p, Erv2p is able to transfer its oxidizing equivalents to Pdi1p. Aside from Pdi1p, other potential substrates of Erv2p have not been found.

Analysis of mRNA transcription has shown that *ERV2* mRNA is expressed under various conditions, being highly expressed in glucose medium, galactose medium, medium supplemented with mating factor a, growth at 17 ˚C and in stationary phase (Stein et al., 1998).

Mutagenesis studies have shown that two cysteine pairs (Cys121-Cys124 and Cys171-Cys178) are required for Erv2p activity (Gross *et al.*, 2002). The other cysteine pair (Cys 150-Cys167) is not required for activity (see Chapter 4). Recent elucidation of the Erv2p structure gave light into its mechanism. Erv2p is a homodimer, each subunit containing a four helix bundle (helixes α1-α4) and an additional turn of helix (α5) packed perpendicular to the bundle (Gross et al., 2002). The dimer interface is made of contacts between α1 and α2 helixes packing against the symmetric-related helixes (Gross et al., 2002). The dimer interface is made of hydrophobic residues and the hydrophobic nature of 10 residues in the interface is conserved among homologs (Gross et al., 2002). The active site cysteine pair, in a Cys-X-X-Cys motif, is found at the N-terminus of a helix, in this case α3 (like Cys-X-X-Cys motif of thioredoxin). The second cysteine pair required for activity is located on a flexible C-terminal tail. Two different conformations for the tail were observed: one in which the tail cysteine pair (Cys176-Cys178) were in close proximity active site cysteine pair (the FAD-proximal Cys121-Cys124), and another conformation where the tail was displaced these two cysteine pairs were not in close proximity. These studies show that Erv2p uses an internal transfer relay between two conserved cysteine pairs to transfer disulfides to substrate proteins (see scheme)

dithiol substrate →[Cys176-Cys178]$_{\text{subA}}$ → [Cys121-Cys124]$_{\text{subB}}$ → FAD]$_{\text{subB}}$ → O_2

Random and site-directed mutagenesis showed that in mutants where the transfer oxidizing equivalents from the active site cysteine pair (Cys121-Cys124) occurs directly to the substrate protein, loose specificity in the disulfide transfer becoming more promiscuous (for more details see chapter 3).

Comparison between Ero1p and Erv2p mechanisms and structures

Ero1p and Erv2p seem to share the same catalytic mechanism. Both proteins require two cysteine pairs for the transfer oxidizing equivalents from oxygen to the substrate proteins through thiol-disulfide exchange reactions (Gross et al., 2004; Gross et al., 2002).

Although the two proteins do not share any sequence similarity, they share the same core domain composed of a 4 helix bundle that holds the FAD cofactor (Gross et al., 2004). In both proteins, the active cysteine pair in a conserved Cys-X-X-Cys motif is located at the N-terminus of a helix. A second cysteine pair, essential for activity, and is located in an unstructured flexible region (C-terminal tail of Erv2p or loop of Ero1p) that can be found in at least two different conformations. In one conformation, this flexible region is flipped out, and its cysteine pair oxidizes substrate proteins, such as Pdi1p, while becoming reduced. In another conformation, the flexible region moves closer to the active site cysteine pair and the former cysteine pair reoxidizes the reduced cysteine pair in the flexible region. The active site cysteine pair is in close proximity to the FAD cofactor and is then reoxidized by the flavin, which is then reoxidized by molecular oxygen (Gross et al., 2004; Gross et al., 2002).

In Erv2p, a short channel lined with hydrophobic residues that leads to the N5 nitrogen atom of FAD seems to be the potential channel through which oxygen interacts with the flavin cofactor (Gross et al., 2002). No such channel has been found in the Ero1p structure, and this difference might suggest differences in final electron acceptor (Gross et al., 2004).

(Next page)

Figure 3. Similarities between the structures and catalytic mechanisms of Erv2p and Ero1p. The structures of Erv2p (left panel; PDB files 1JR8 and 1JRA) and Ero1p (right panel; PDB files 1RP4 and 1RQ1) are shown in a side view (A) and a top view (B and C) using Pymol (DeLano, 2002). The four helices composing the four helix bundle are colored yellow, red, green and blue. Both cysteine residues of the active site and the FAD cofactor are represented in a ball-and-stick representation and are colored in magenta and orange, respectively. (C) In Erv2p, the second pair of cysteines is provided by the C-terminus of the other subunit while in Ero1p the second pair of cysteines is located in a mobile loop. Both the Erv2p tail and the Ero1p mobile loop have at least two different conformations and are colored in light blue. The cysteine residues located in these regions are colored in light pink.

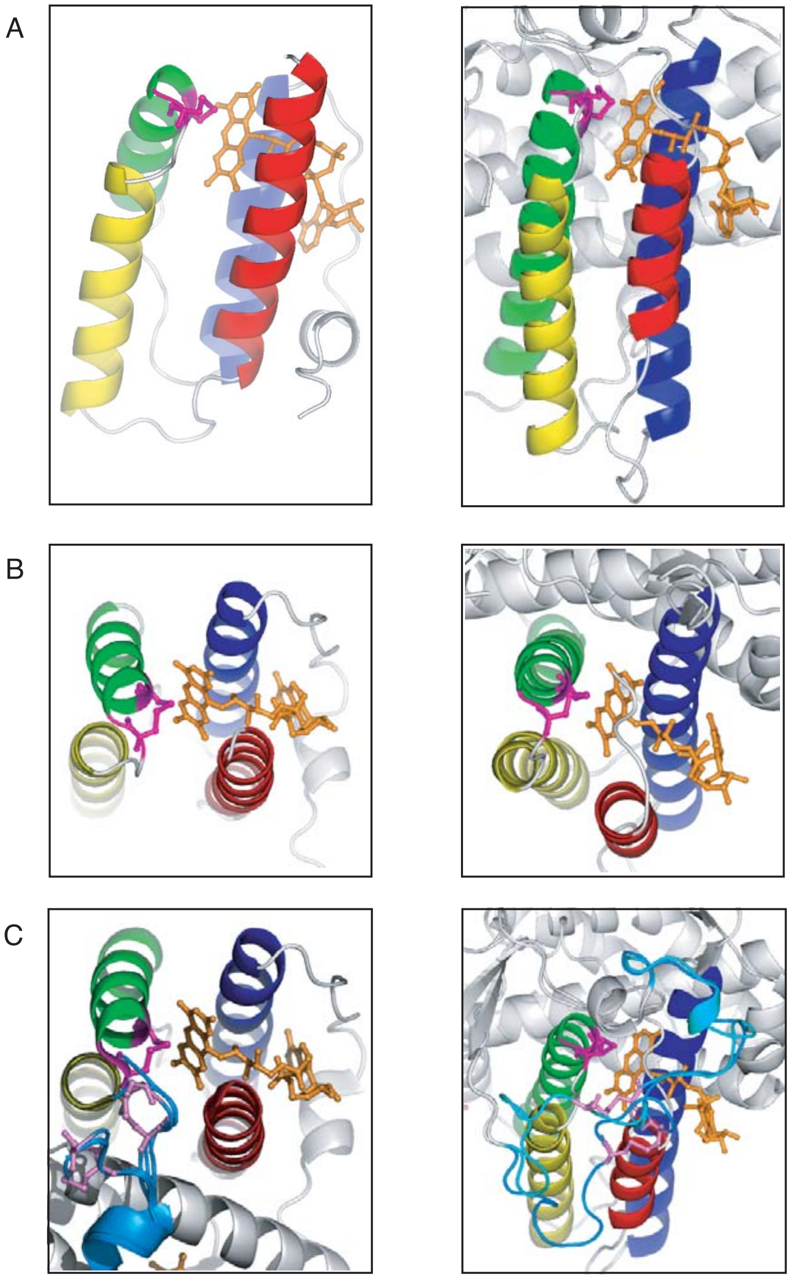

Sulfhydryl oxidases of the QSOX/ERV family: their role in oxidative folding

Erv2p belongs to an emerging family of flavoproteins. One of the main features of the members of this family is their ability to catalyze the oxidation of thiol substrates to disulfides, with the associated reduction of oxygen and production of hydrogen peroxide (Coppock *et al.*, 2000; Francavilla *et al.*, 1994; Lisowsky, 1992; Lisowsky *et al.*, 2001; Senkevich *et al.*, 2000b).

Sequence analysis reveals that the QSOX/ERV family members share a core domain of about 100 amino acids that includes a conserved Cys-X-X-Cys motif and that this family can be subdivided into two different types of proteins (Figure 4): small ERV-like proteins (such as Erv1p, Erv2p, ALR and E10R) that are approximately 100 to 200 amino acids in size and the QSOX-like proteins that are about 400 to 600 amino acids (such as Quiescin Q6 and the Sox proteins). The latter are a fusion between an N-terminal thioredoxin-like domain and an ERV-like domain and seem to be present only in genomes of higher eukaryotes. All eukaryotic genomes sequenced so far contain at least one member of the QSOX/ERV family.

The members of this family are located in several subcellular compartments and are involved in a variety of different cellular processes (Coppock et al., 2000; Francavilla et al., 1994; Lisowsky, 1992; Lisowsky et al., 2001; Senkevich et al., 2000b). For example, while the mitochondrial protein Erv1p is involved in cytoplasmic iron-sulfur cluster assembly and mitochondrial protein import, the vaccinia virus protein E10R is involved in disulfide bond formation in viral proteins in the cytoplasm of infected cells (Lange *et al.*, 2001; Mesecke *et al.*, 2005; Senkevich *et al.*, 2004; Senkevich *et al.*, 2000a; Senkevich et al., 2000b). The QSOX proteins are secreted proteins that may be involved in the formation of disulfide bonds in the extracellular space (Thorpe et al., 2002).

***ERV1* is required for mitochondrial disulfide bond formation**

ERV1 (Essential for respiration and viability 1) was first identified as a gene that suppresses the growth defect of the *pet-ts492* (*erv1-1*) mutant (Lisowsky, 1992). It is essential for viability, for the synthesis of mitochondrial proteins such as Cox2p, and for oxidative phosphorylation (Lisowsky, 1992). Furthermore, *ERV1* may be involved in the biogenesis of mitochondria (Stein et al., 1998). Inactivation of *ERV1* leads to the loss of the mitochondrial genome and an aberrant distribution of mitochondria at the two poles of the cell. In addition, lack of the typical formation of crystae for some mitochondria is observed in an *erv1-1* mutant at the permissive temperature (Becher *et al.*, 1999; Lisowsky, 1994).

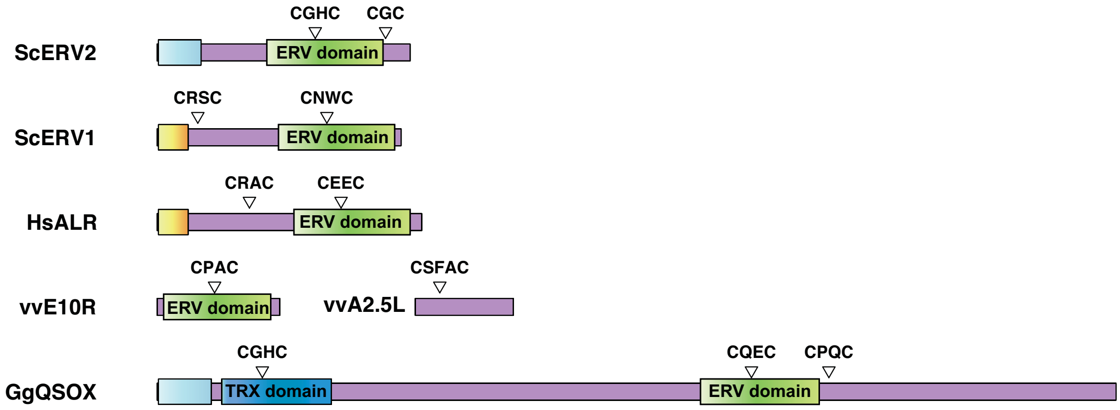

Figure 4. Schematic representation of the QSOX/ERV family members. Signal sequences were predicted by SignalP (Bendtsen *et al.*, 2004; Nielsen *et al.*, 1997; Nielsen *et al.*, 1998) and are shown in light blue. Mitochondrial signal sequences were predicted by Mitoprot II (Claros, 1995; Claros *et al.*, 1996) and are shown in light orange. The ERV domain was predicted by sequence similarity between the proteins using ClustalX (Thompson *et al.*, 1997) and the boundaries suggested in Pfam (Bateman *et al.*, 2004) and is shown in green. The TRX domain was predicted by sequence similarity to the thioredoxin fold using the boundaries suggested in Pfam (Bateman et al., 2004) and is shown in blue. The two pairs of essential cysteines are represented by a triangle and their sequence is shown. The following amino acid sequences were used: *Sacharomyces cerevisiae* Erv2p (ScErv2p, NCBI accession number NP_015362) and Erv1p (ScErv1p, NCBI accession number NP_011543), *Homo sapien*s ALR, (HsALR, NCBI accession number NP_005253), vaccinia virus E10R (vvE10R, NCBI accession number NP_063714) and *Gallus gallus* QSOX (GgQSOX, accession number NP_989456)

Erv1p is a mitochondrial protein located in the mitochondrial intermembrane space (IMS). Recent data suggest that Erv1p and Mia40p are involved in a disulfide cascade pathway in the intermembrane space (IMS) of mitochondria, which controls the import of IMS-localized proteins that contain a Cys-X_3-Cys or Cys-X_9-Cys motif, such as Tim13p and Cox17p (Mesecke et al., 2005). Newly synthesized mitochondrial proteins are translocated into the IMS in an unfolded reduced form through the translocase of the mitochondrial outer membrane (TOM complex). After translocation into the IMS, these proteins are oxidized through interaction with oxidized Mia40p. Reduced Mia40p is subsequently reoxidized via interaction with oxidized Erv1p, thus promoting the next round of formation of disulfide bonds in IMS proteins. Erv1p transfers its electrons to oxygen via its two cysteine pairs and flavin-bound cofactor, after which it becomes reoxidized and ready for another cycle (Figure 5) (Mesecke et al., 2005). Cytochrome c is the final electron acceptor for Erv1p (Bihlmaier *et al.*, 2007). Cytochrome c transfers its electrons to cytochrome c oxidase, which in turn transfers its electrons to oxygen. This interaction directly connects the disulfide bond formation to the respiratory chain, thus preventing the generation of hydrogen peroxide (Bihlmaier et al., 2007).

In both *erv1-1* and *mia40-3* mutants, the levels of IMS proteins that contain a Cys-X_3-Cys or Cys-X_9-Cys motif, such as the small Tim proteins (Tim9, Tim10p, Tim12p and Tim13p) and Cox17p, were reduced, whereas the levels of IMS proteins that lack conserved cysteine signatures and proteins of the outer membrane, inner membrane or the matrix were not affected (Mesecke et al., 2005; Rissler *et al.*, 2005; Terziyska *et al.*, 2005). Furthermore, the formation of a complex between Erv1p and Mia40p that is sensitive to reducing conditions suggests that this interaction occurs via their cysteines and that Mia40p accumulates in the reduced state when Erv1p is depleted (Mesecke et al., 2005; Rissler et al., 2005). The fact that in both wild-type and *erv1-1* cells, Tim10p is found in its oxidized form suggests that Erv1p does not directly oxidize the small Tim proteins, but rather transfers its oxidizing equivalents through Mia40p (Allen *et al.*, 2005). Moreover, cells depleted of Erv1p are DTT sensitive (Mesecke et al., 2005). The presence of homologs of Mia40p and Erv1p in higher eukaryotes suggests that this disulfide bond formation pathway and import into the IMS might be conserved process.

Erv1p is thought to be involved in the process of assembly of cytoplasmic iron-sulphur (Fe/S) proteins (Lange et al., 2001). Maturation of Leu1p and Ril1p, two Fe/S cytosolic proteins, is impaired in an *erv1-1* mutant at the restrictive temperature, while the maturation of mitochondrial Fe/S proteins, such as Bio2p, aconitase, and succinate dehydrogenase, is not. Furthermore, the *erv1-1* mutant accumulates free iron, a characteristic of mutants that are impaired in biogenesis of cellular Fe/S proteins. In addition, overexpression of wild-type Erv1p is able to restore the maturation of Leu1p in an *erv1-1* strain (Lange et al., 2001). It is possible that the role of Erv1p in Fe/S cluster assembly is an indirect effect, since Erv1p interferes with the formation of the Tim complex (translocation into the inner membrane) and thus might interfere with transport of proteins essential for the assembly of Fe/S clusters in the matrix. The other possibility is that Erv1p is necessary for the transport of a component that is synthesized in the matrix but needs to be transported to the cytosol (Sipos *et al.*, 2002).

Erv1p is a mitochondrial FAD-dependent sulfhydryl oxidase that contains three pairs of essential cysteines. As in Erv2p, the first cysteine pair (Cys131 and Cys133 in Erv1p) is located in the core domain present in all members of the QSOX/ERV family juxtaposed to the FAD cofactor. It forms a conserved Cys-X_2-Cys motif that can interact with the flavin cofactor. The second cysteine pair (Cys30 and Cys33) is located in the N-terminus and is thought to receive oxidizing equivalents from the first pair and subsequently transfer them to the substrate protein (Hofhaus *et al.*, 2003). Finally, the third cysteine pair (Cys159 and Cys176) seems to form a structural bond. All three cysteine pairs are necessary for activity *in vivo* and *in vitro* (Hofhaus et al., 2003). The existence of a disulfide-linked intermediate between the Cys30-Cys33 pair and the active site confirms that these two pairs of cysteines interact during the catalytic mechanism of Erv1p. The electron flow is as follows:

$$\text{dithiol substrate} \rightarrow [\text{Cys30-Cys33}]_{\text{subA}} \rightarrow [\text{Cys130-Cys133}]_{\text{subB}} \rightarrow [\text{FAD}]_{\text{subB}} \rightarrow O_2$$

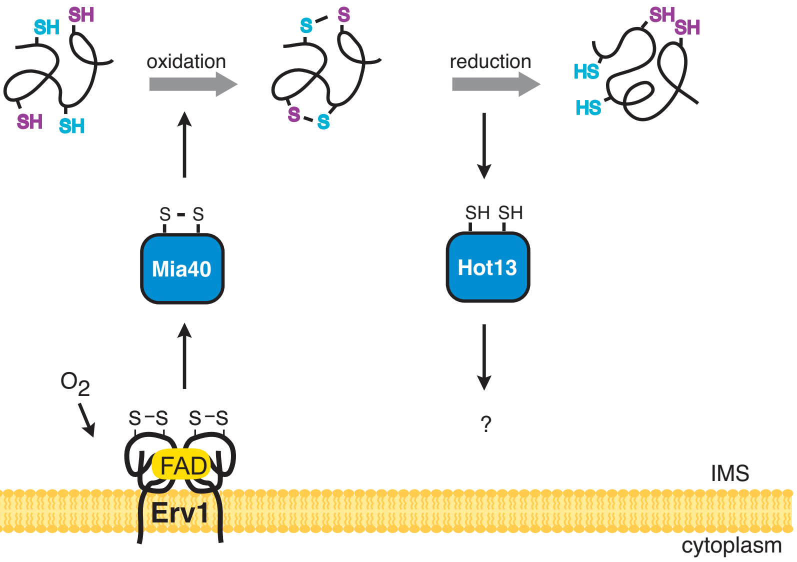

Figure 5. Pathways of disulfide bond formation in the IMS of mitochondria of *S. cerevisiae*. Mia40p oxidizes substrate proteins, such as Tim13p and Cox17p, after their translocation through the TOM complex. Oxidized Mia40p is recycled by interaction with Erv1p, which in turn obtains its oxidizing equivalents from oxygen or from cytochrome c through its flavin-bound cofactor.

Recombinant wild-type Erv1p can oxidize reduced lysozyme, DTT and cysteine, with apparent turnover numbers of 8.6, 52.8 and 5 min^{-1}, respectively (Hofhaus et al., 2003; Hofhaus *et al.*, 2002; Lee *et al.*, 2000; Lisowsky et al., 2001). Substitution of the active site cysteines with serine abolishes the sulfhydryl oxidase activity towards DTT, whereas substitution of the Cys30 or Cys33 with serine only diminishes the activity towards DTT (Hofhaus et al., 2003).

Augmenter of liver regeneration

Mammalian ALR (augmenter of liver regeneration) is a homolog of ScErv1p and was first identified as a cytoplasmic human growth factor that was able to stimulate regeneration of liver after partial hepatectomy (Francavilla et al., 1994). Recent studies suggest that it might be involved in the formation of cytoplasmic iron-sulphur proteins (Lange et al., 2001) and in spermatogenesis (Klissenbauer *et al.*, 2002).

Two forms of ALR formed due to alternative splicing are found in hepatocytes (Thasler *et al.*, 2005). The 15 kDa shorter form consists of 125 amino acids, lacks the N-terminal region, and is localized to the nucleus. The 23 kDa longer form is 205 amino acids and is mainly located to the cytosol and mitochondrial intermembrane space (Thasler et al., 2005).

Three mechanisms have been proposed by which ALR promotes liver regeneration. First, during liver regeneration, ALR is secreted from hepatocytes, and through the interaction with a membrane receptor for ALR, activates a MAPK pathway, which in turn increases gene expression (Li *et al.*, 2001). In a second mechanism, intracellular ALR interacts with the Jun activation domain-binding protein 1 (JAB1), which leads to C-jun phosphorylation and the subsequent activation of the activation protein-1 (AP-1) in a MAPK independent manner. In a third mechanism, ALR reduces the lytic activity of liver-resident NK cells and produces a burst in mitochondrial metabolism (Francavilla *et al.*, 1997). These effects are mediated by the down regulation of IFN-γ (as indicated by the reduction of IFN-γ mRNA in rats after ALRp administration and by the reduction of IFN-γ protein levels in liver resident NK cells). Whether these signaling pathways cooperate with each other or act separately remains to be elucidated (Lu *et al.*, 2002).

Like Erv2p and Erv1p, ALR contains 3 pairs of cysteines, two of them essential. The first cysteine pair (Cys62 and Cys65 in ALR) forms a conserved Cys-X_2-Cys motif that is required for *H. sapiens* ALR (HsALR) activity *in vitro* (Lisowsky et al., 2001). The crystal structure of rat ALR (rALR) has been solved, revealing that it possesses the same overall structure as Erv2p: a four helical bundle core domain containing the FAD cofactor (Wu *et al.*, 2003). In the case of rALR, a second cysteine pair is formed by the Cys15 or one subunit and the Cys124 of the other subunit (Farrell *et al.*, 2005). A comparison between Erv2p and ALR crystal structures and the biochemical data has defined a disulfide bond transfer mechanism in the ALR protein.

$$\text{dithiol substrate} \rightarrow [\text{Cys15/Cys124}]_{\text{subAB}} \rightarrow [\text{Cys62-Cys65}]_{\text{subB}} \rightarrow [\text{FAD}]_{\text{subB}} \rightarrow O_2$$

This intersubunit disulfide bond (Cys15A-Cys124B and Cys15B-Cys124A) is not conserved in other members of the ERV/QSOX family, and it is not required for dimerization of ALR (Farrell et al., 2005). Structural modeling of human ALR indicates that this intersubunit disulfide bond is in close proximity to the active site cysteines (Farrell et al., 2005).

Both Erv1p and mature ALR contain an extra Cys-X-X-Cys motif in the N-terminus that might play a role in the relay mechanism (Wu et al., 2003). As in the Erv2p mutants lacking the Cys176-Cys178 cysteine pair, an N-terminal truncated ALRp (Δ1-80-ALRp fused to the signal sequence of Cytb2 for proper localization to the intermembrane space) lacking the extra Cys-X-X-Cys motif is able to rescue *erv1-1*, but cells containing this construct are less active than the wild type ALRp or Erv1p in incorporation of ^{55}Fe into cytosolic Leu1p (Lange et al., 2001). However, as observed for Erv2p-Cys176A/Cys178A, recombinant Δ1-73-Erv1p and Δ1-81-ALRp still exhibit sulfhydryl oxidase activity *in vitro* as indicated by oxidation of reduced lysozyme or DTT (Hofhaus et al., 2003; Lee et al., 2000; Lisowsky et al., 2001).

A chimera made of the N-terminal region of Erv1p (amino acid residues 1-93) fused to the C-terminal region of human ALR (amino acid residues 81-205) is able to complement the *erv1Δ* or *erv1-1* growth defect, suggesting that the ALR core domain is able to substitute for Erv1p. In addition, this fusion protein is localized to the IMS and is able to restore the assembly of cytoplasmic Fe/S clusters when expressed in the *erv1-1* mutant. This result suggests that ALR might also be involved in assembly of Fe/S clusters in mitochondria (Lange et al., 2001).

Vaccinia virus E10R: sulfhydryl oxidase involved in cytoplasmic disulfide bond formation pathway

One of the members of the QSOX/ERV family, a viral protein E10R, has been implicated in disulfide bond formation in the cytoplasm of vaccinia virus infected cells (Senkevich et al., 2000a). The E10R protein is the smallest of the family, containing approximately 100 amino acids and only a single pair of cysteines in a Cys-X-X-Cys motif (Senkevich et al., 2000a). Recent studies have shown that E10R is essential for vaccinia virus assembly and that its cysteine residues are required for the *in vivo* oxidation of viral proteins, such as L1R, F9L and A28L (Senkevich et al., 2004; Senkevich et al., 2000a; Senkevich et al., 2000b).

Various studies have defined the pathway of disulfide bond formation in the cytoplasm of vaccinia virus-infected cells (Figure 6). E10R oxidizes an adaptor protein A2.5L (Senkevich *et al.*, 2002b), which contains a pair of cysteines that probably fulfills the function of the tail cysteines in Erv2p. Next, A2.5L interacts with a glutaredoxin-like protein, G4L, that in turn oxidizes coat proteins in the cytoplasm (Senkevich et al., 2004; Senkevich *et al.*, 2002a; White *et al.*, 2002). Based on its homology with ERV-like members of the QSOX/ERV family, it is thought that E10R is a FAD-dependent sulfhydryl oxidase and that it becomes reoxidized by transferring electrons to O_2, forming H_2O_2, but no *in vitro* studies have been performed to directly confirm this.

Various pieces of evidence confirm this pathway: 1) E10R repression prevents the formation of disulfide bonds in the cytoplasmic domain of virion attached L1R protein or the closely related F9L (Senkevich et al., 2000a), 2) the cysteines in the conserved Cys-X-X-Cys motif of E10R are essential for its function, and when these residues are mutated to Ser, the F1L and F9L proteins are reduced, 3) each cysteine in A2.5L is also essential for the formation of disulfide bonds in substrate proteins that are essential for formation of the mature virion (Senkevich et al., 2000a; Senkevich et al., 2000b; White et al., 2002), 4) G4L is also required for virus assembly and is required for the formation of disulfide bonds in L1R and F9L proteins and 5) Repression of E10R prevents thiol oxidation of G4L, whereas the reverse is not true.

The three components of this pathway (Figure 6) are present/conserved in all sequenced poxviruses and are essential for vaccinia virus assembly, suggesting that this is a conserved mechanism in poxvirures (Senkevich et al., 2000a; Senkevich et al., 2002b; White et al., 2002).

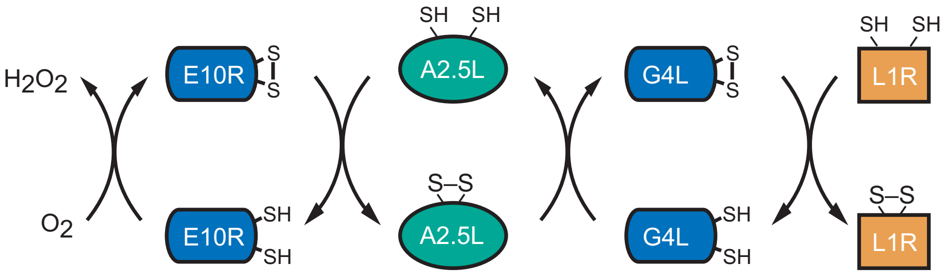

Figure 6. Pathways of disulfide bond formation (oxidation) in the cytoplasm of *vaccinia virus*. Arrows indicate flow of electrons. The vaccinia virus L1R (or F9L or A28L) is oxidized by glutaredoxin homolog G4L, which in turn is reduced. Reduced G4L is reoxidized by interaction with A2.5L. A2.5L is reoxidized by E10R, which in turn is reoxidized by molecular oxygen, producing hydrogen peroxide.

QSOX

The Quiescin/Sox-like proteins, such as chicken sulfhydryl oxidase and Quiescin Q6, are secreted proteins that might be involved in the formation of disulfide bonds in the extracellular space (Thorpe et al., 2002). They consist of a fusion of thioredoxin and ERV/ALR motifs (Hoober *et al.*, 1999a). Members of the QSOX family include the avian egg white oxidase, the rat seminal vesicle flavoprotein, and Quiescin Q6, a cell growth inhibitory factor. Quiescin Q6, the best understood member of this family is highly induced when human fibroblasts enter reversible quiescence (Hoober et al., 1999a).

QSOX are found in metazoans, such as *Caenorhabditis elegans* and *Drosophila melanogaster*, plants and certain protists, while Erv2-like proteins are found only in fungal genome (Thorpe et al., 2002). Interestingly, Erv2p and QSOX proteins have not been found in the same organism (Thorpe et al., 2002). Furthermore, although QSOX proteins have been found in protists such as *trypanosoma brucei*, some protist genomes such as *Giardia lamblia* and *Entamoeba histolytica* seem to have neither QSOX nor ERV-like proteins in their genomes (Hoober et al., 1999a). Although little is known about the role of the QSOX family members, it has been suggested that members of this family introduce disulfide bonds in the extracellular medium (Thorpe et al., 2002).

The Chicken QSOX (cQSOX) is by far the best studied sulfhydryl oxidase of the QSOX/ERV family. It is a homodimeric protein containing one molecule of FAD per subunit (Hoober *et al.*, 1996). The protein cQSOX is able to oxidize a variety of small thiols, such as DTT, GSH, and cysteine *in vitro* (Hoober et al., 1996). The cQSOX flavoenzyme is also able to introduce disulfide bonds *in vitro* to a wide variety of proteins and peptides, such as insulin A and B chains, lysozyme, ovalbumin, riboflavin-binding protein and reduced RNase, although the K_m obtained for these substrates are significantly lower than those for small monothiols (Thorpe et al., 2002). This result suggests that there is little dependence on substrate molecular weight or isolelectric point (Thorpe et al., 2002). It has also been reported that cQSOX can oxidize reduced PDI and reduced *E. coli* Trx (Hoober *et al.*, 1999b; Hoober *et al.*, 2002).

A mechanism for substrate specificity similar to the one observed for Erv2p is found in chicken QSOX, which is a fusion of a thioredoxin-like domain and an ERV-like domain (Raje *et al.*, 2003). Partial proteolysis studies showed that while the thioredoxin-like fragment or the ERV-like fragment alone has little or no activity toward thiol substrates, the two fragments combined exhibit substantial activity. The ERV-like fragment is a dimer and probably shares the overall structure of Erv2p, including a flexible C-terminal tail containing the second cysteine pair (Raje et al., 2003). As in Erv2p, this second pair of cysteine residues in the ERV-like fragment confers specificity in the disulfide transfer to the redox active cysteine pair in the thioredoxin-like fragment. In contrast, the rat QSOX protein is a monomeric enzyme (Ostrowski *et al.*, 1980), showing that subunit communication in the dimeric avian enzyme may not be a prerequisite for activity (Thorpe et al., 2002).

Members of the QSOX/ERV family share the same mechanism

Structural and biochemical data suggest that all members of the QSOX/ERV family share the same catalytic mechanism. Structural studies on Erv2p and rat ALR have shown that the conserved core domain is composed of a four helix bundle that contains the active site cysteine pair at the N-terminus of a helix (helix $\alpha3$ in the case of Erv2p) (Figure 7) (Gross et al., 2002; Wu et al., 2003). Site-directed mutagenesis studies showed that all members of this family require two pairs of cysteines for their catalytic activity *in vivo* or *in vitro*, suggesting that they might share the same catalytic mechanism (Hofhaus et al., 2003; Lisowsky et al., 2001; Senkevich et al., 2000b; Senkevich et al., 2002a; Sevier et al., 2001). One pair of cysteines is located in the conserved core near the flavin cofactor, while the second pair of cysteines is located in a flexible region, in either the N- or C-terminal regions of the proteins, and has variable spacing between cysteine residues. The latter pair of cysteines seems to be an electron carrier between the active site cysteines and the substrate. After transfer of oxidizing equivalents to the tail cysteine pair, the active site cysteines become reduced. To be recycled, the active site pair of cysteines interacts with the flavin-bound cofactor becoming oxidized. Subsequently, molecular oxygen or another electron acceptor reoxidizes the reduced flavin.

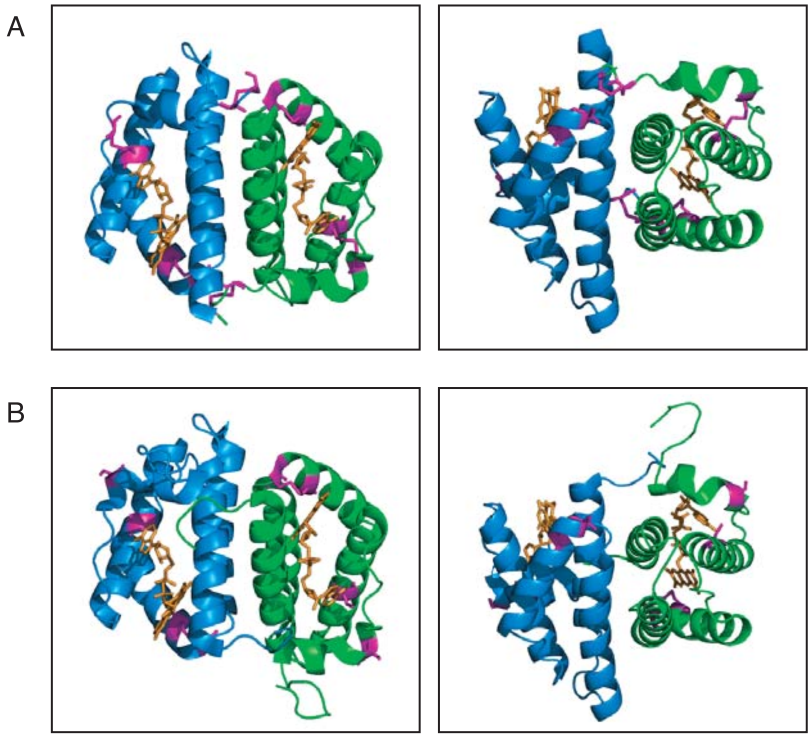

Figure 7. Erv2p (A) and rat ALR (B) share the same catalytic core. The structures of Erv2p (PDB file 1JR8) and rat ALR (PDB file 1OQC) are shown in a side view (left panel) and a top view (right panel) using Pymol (DeLano, 2002). One subunit is colored in blue while the other is colored in green. Both cysteine residues and the FAD cofactor are represented in a ball-and-stick representation and are colored magenta and orange, respectively.

PDI - Its role in disulfide bond formation

PDI proteins can catalyze thiol oxidation, reduction and isomerization reactions; isomerization may occur directly through intramolecular rearrangement of through cycles or reduction and oxidation (Schwaller *et al.*, 2003).

To date, several homologues of PDI have been found, but the role of these proteins is only now being uncovered. Each PDI-like protein consists of active (a domains), containing a characteristic CXXC active site motif, and inactive (b domains) thioredoxin-like modules. The structure might have evolved by means of partial gene duplication or shuffling of common thioredoxin-like modules (Kemmink *et al.*, 1997).

PDI-family proteins differ from thioredoxin (Trx) in two main aspects: their redox potentials are usually higher, and the presence of domains devoid of the active site cysteine confers additional properties on them, such as the capacity to bind peptides or proteins and consequently display chaperone and isomerase activities. It has been suggested that the multi-domain structure of PDI enhances and diversifies substrate specificity (Ellgaard *et al.*, 2005).

(Next page)

Figure 8. Schematic representation (domain structure) of the protein disulfide isomerase family (PDI-related proteins) from *S. cerevisiae* **(A)** and *Homo sapiens* **(B)**. Signal sequences were predicted by SignalP (Bendtsen et al., 2004; Nielsen et al., 1997; Nielsen et al., 1998) and are shown in light blue. Active thioredoxin-like domains (a domains) are represented by blue rectangles. The cysteine residues of the active domains are represented by a triangle and their sequence is shown. The catalytically inactive thioredoxin-like domains (b and b' domains) are shown in green, pink and purple, respectively. Transmembrane regions were predicted by the program TMHMM 2.0 (Krogh *et al.*, 2001; Sonnhammer *et al.*, 1998) and are shown in orange. The a and b domains boundaries were predicted by sequence similarity between the proteins using ClustalX (Thompson et al., 1997) and the boundaries suggested in Pfam (Bateman et al., 2004). Adapted from (Ellgaard et al., 2005).

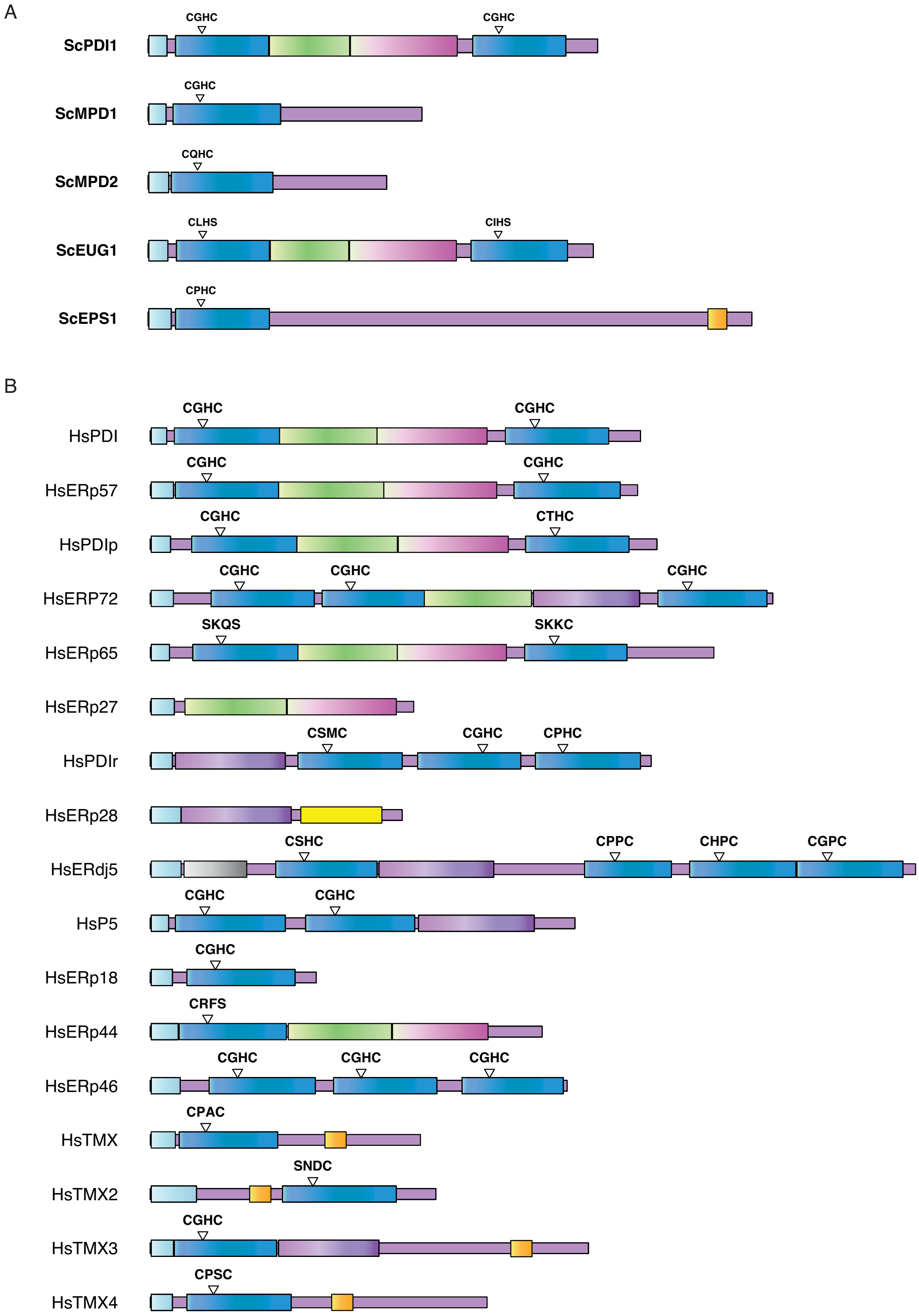
A
ScPDI1
CGHC
CGHC
ScMPD1
CGHC
ScMPD2
CQHC
ScEUG1
CLHS
CIHS
ScEPS1
CPHC
B
HsPDI
CGHC
CGHC
HsERp57
CGHC
CGHC
HsPDIp
CGHC
CTHC
HsERP72
CGHC
CGHC
CGHC
HsERp65
SKQS
SKKC
HsERp27
HsPDIr
CSMC
CGHC
CPHC
HsERp28
HsERdj5
CSHC
CPPC
CHPC
CGPC
HsP5
CGHC
CGHC
HsERp18
CGHC
HsERp44
CRFS
HsERp46
CGHC
CGHC
CGHC
HsTMX
CPAC
HsTMX2
SNDC
HsTMX3
CGHC
HsTMX4
CPSC

Thioredoxin fold

The thioredoxin fold is an ancient structural fold consisting of four stranded β-sheets and three flanking α-helixes that was named after the protein in which it was first observed, the *E. coli* thioredoxin (Martin, 1995). A variety of proteins have been shown to belong to the thioredoxin superfamily, such as thioredoxin, glutaredoxin, glutathione peroxidase (GPx), peroxiredoxin (Prx), glutathione S-transferase (GST), PDI and its bacterial homolog DsbA.

The thioredoxin fold is composed of an N-terminal βαβ motif and a C-terminal ββα motif connected by a loop of residues that incorporate a third helix (Figure 9A) (Martin, 1995). The β strands from the N- and C-terminal motifs form a β-sheet of parallel (β1 and β2) and antiparallel (β3 and β4) β-strand pairs that is characteristic of the thioredoxin fold (Martin, 1995). On one side of the β-sheet and parallel to it are the helices from the N- and C-terminal motifs (α1 and α3, respectively). On the other side of the β-sheet and opposite to the α1 and a3 helices, the helix that connects both N- and C-terminal motifs is located in a perpendicular orientation (Martin, 1995).

The core thioredoxin fold comprises about 80 residues, but each protein in the family contains extra residues beyond the core (Martin, 1995). Structural and sequence analysis between proteins of the thioredoxin superfamily has shown that the thioredoxin fold can tolerate insertions at various positions without disruption of the overall structure (Figure 9B). *E. coli* thioredoxin, DsbA and glutathione peroxidase contain an extra domain of around 20 to 30 residues inserted at the N-terminus of the β and α domains. Both DsbA and glutathione peroxidase have an additional insertion of a 40-70 amino acid helical domain or loop after the N-terminal motif (βαβ) of the thioredoxin fold, while glutathione S-transferase has a whole domain inserted into the C-terminus of the thioredoxin fold.

These extra domains inserted into the thioredoxin fold have been shown to provide these proteins with extra functionality. For example, the insertion in DsbA forms a deep hydrophobic groove near the active site that seems to be important for substrate binding, while the extra domain in GST contributes residues that help to stabilize GSH and the electrophilic substrate (Martin, 1995).

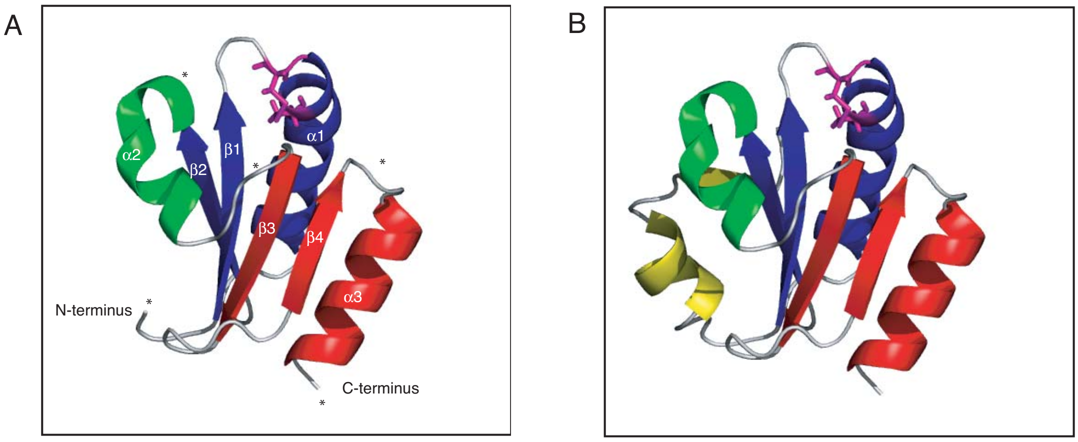

Figure 9. Structure of the thioredoxin fold. (A) Thioredoxin fold of *E. coli* thioredoxin A (PDB file 2TRX) was generated using Pymol (DeLano, 2002). The N-terminal βαβ domain is colored in blue, the C-terminal ββα domain is colored in red and the connecting α helix is colored in green. The cysteine residues are shown in a stick-and-ball representation and are colored in magenta. Asterisks represent areas of the thioredoxin fold that can tolerate insertions. (B) Structure of *E. coli* thioredoxin A (PDB file 2TRX) as in (A). In yellow are represented extra domains of thioredoxin A not found in the core thioredoxin fold. Adapted from (Martin, 1995).

Homologs of PDI in the yeast ER

Yeast PDI (Pdi1p) was isolated by various groups using different approaches (Farquhar *et al.*, 1991; Gunther *et al.*, 1991; LaMantia *et al.*, 1991). It contains 5 potential sites for Asn-linked glycosylation on Asn residues positioned at amino acid 82, 117, 155, 174 and 425; an ER retention signal HDEL and two WCGHC motifs. Pdi1p is an essential protein for growth and viability that is required for the maturation of carboxypeptidase Y (Farquhar et al., 1991; Gunther et al., 1991; LaMantia et al., 1991). In a glucose repression of *PDI1* experiment, proCPY (p2form - 67-69 kDa) is accumulated (Farquhar et al., 1991; Gunther et al., 1991; LaMantia et al., 1991).

PDI1 under the gal promoter is able to rescue *pdi1Δ* (Gunther *et al.*, 1993). Under the same conditions, a deletion of the C-terminal 38 amino acids of Pdi1p is also able to rescue this strain. This deletion is not able to rescue a *pdi1Δ* strain under the ADC1 promoter (Farquhar et al., 1991; Gunther et al., 1991; LaMantia et al., 1991). The C-terminal domain contains the KDEL ER retention signal, so the likely explanation is that PDI1 must be retained in the ER to perform its function.

In vitro, PDI can catalyze the oxidation, reduction or isomerization of disulfide bonds depending upon the redox conditions of the assay and the nature of the substrate protein (ref in (Frand et al., 2000a)). It is unknown which of these activities, if any, is the essential function of Pdi1p. Overexpression of Pdi1p-Cys-X-X-Ser mutant can restore viability of *pdi1Δ* cells suggesting an essential role for Pdi1p in the isomerization of non-native disulfide bonds. Futhermore, this mutant lacks detectable oxidase and reductase activities *in vitro*. However, Pdi1p was shown to be involved, together with Ero1p, in the oxidation pathway.

S. cerevisiae contains four nonessential genes with homology to Pdi1p, namely, *MPD1* , *MPD2*, *EUG1* and *EPS1*, each of which contain at least one active TRX-like domain (Figure 8) (Tachibana *et al.*, 1992; Tachikawa *et al.*, 1997; Tachikawa *et al.*, 1995; Wang *et al.*, 1999).

Mpd1p

Mpd1p (**m**ulticopy suppressor of ***PDI1*** deletion) was isolated in a screen for multicopy suppressors of a strain lacking *PDI1* (Tachikawa et al., 1995). In contrast to *PDI1*, *MPD1* is a non-essential gene. Genetic analyses of strains lacking both *PDI1* and its homologs indicates that Mpd1p is the only of the homologs that can fully compensate for the absence of Pdi1p (Norgaard *et al.*, 2001).

Mpd1p is a glycoprotein of 318 amino acid residues that has homology to Pdi1p. It contains an N-terminal signal sequence, a C-terminal ER retention signal (HDEL) and a TRX-like domain that contains a Cys-X-X-Cys motif (Tachikawa et al., 1995). Mpd1p does not seem to have homology to the b and b' domains of *PDI1* and its C-terminal region is not homologous to any other protein in the protein database. Homologs of Mpd1p have been found in fungal genomes but to date, no human homologs of Mpd1p have been found.

The *MPD1* promoter region contains a TATA box and a sequence related to the unfolded protein response (UPR). The *MPD1* gene is slightly upregulated in response to treatment with DTT or tunicamycin (inducers of the UPR) (Norgaard *et al.*, 2003). In contrast, *MPD1* is strongly upregulated in response to *PDI1* deficiency (Norgaard et al., 2003). The *MPD1* promoter contains both UPR response elements (ERES) and CERP (**c**is-acting **e**lement **r**esponding to **P**DI deficiency) (Norgaard et al., 2003; Tachikawa et al., 1995).

Mpd1p is able to suppress a *PDI1* deleted strain when expressed from a high copy plasmid or under the control of the *PDI1* promoter (Holst *et al.*, 1997; Tachikawa et al., 1995). Furthermore, a strain depleted for *PDI1* is unable to process CPY, which accumulates in the p1 form (ER form). But, overexpression of Mpd1p in Pdi1p-depleted cells restores CPY maturation (80% of the CPY becomes mature after 60 minutes chase) (Tachikawa et al., 1995).

In vitro studies with recombinant Mpd1p have shown that it has weak reductase activity (measured by the reduction of insulin) but no chaperone activity (measured by the aggregation of denatured rhodanase and mastoparan binding - no binding) (Kimura *et al.*, 2004). Recombinant Mpd1p has been shown to have an oxidase activity when using denatured lysozyme as substrate, but its activity is 13.8% of that of wild-type (Kimura *et al.*, 2005).

Mpd1p binds Mpd2p and Eps1p with K_D values of 5.97x10^{-5} M and 3.88 x 10^{-6} M, respectively (Kimura et al., 2004; Kimura et al., 2005). Mpd1p does not affect the chaperone activity of Mpd2p, and Mpd2p does not affect the reductive activity of Mpd1p (Kimura et al., 2005). Also, the interaction between Mpd1p and Mpd2p does not appear to promote isomerase activity (Kimura et al., 2004).

Mpd1p is the only yeast PDI homolog that has been shown to be able to interact with Cne1p, a calnexin homolog, with a K_D value of 2.27 x 10^{-7} M (Kimura et al., 2005).

Cne1p has no reductive activity, while Mpd1p has no chaperone activity. The reductase activity of Mpd1p is increased in the presence of Cne1p (from 100% to 115%), and the chaperone activity of Cne1p is quenched by interaction with Mpd1p (100% to 47%) (Kimura et al., 2005). The inhibition of Cne1p chaperone activity by Mpd1p could be overcome by increasing the concentration of Cne1p, suggesting that the binding interface between Cne1p and Mpd1p is near the peptide binding site of Cne1p and that its chaperone activity requires that peptide binding site (Kimura et al., 2005).

Although the function of Mpd1p in the ER is unknown, it has been suggested to play a role in quality control in the ER. First, Mpd1p is more similar to human Erp57 than to human PDI, and although Mpd1p has different domain architecture than human Erp57, it is thought to be its yeast counterpart (Tachikawa et al., 1997). Furthermore, Mpd1p interacts with Cne1p, a homolog of calnexin and calreticulin, two lectins known to interact with Erp57 (Kimura et al., 2005).

Mpd2p

Mpd2p (**m**ulticopy suppressor of ***PDI1*** deletion 2) was isolated together with Mpd1p in a screen for multicopy suppressors of PDI1 (Tachikawa et al., 1995). In contrast with *PDI1*, *MPD2* is a non-essential gene. No phenotype has been found for the strain deleted for MPD2.

Mpd2p is a glycoprotein with 277 amino acid residues that contains an N-terminal signal-sequence, a C-terminal ER retention signal (HDEL) and TRX-like domain that contains a Cys-X-X-Cys motif (Tachikawa et al., 1997). The active site sequence is similar to, but distinct from, the active site sequence of Pdi1p and Mpd1p (TSWCQHCK). The C-terminal region of Mpd2 shows no homology with any other protein in the protein database. No human homologs of Mpd2p have been found, although it has been suggested to have a C-terminal helical domain similar to the PDI-D family (ERp28) (personal observation).

MPD2 can partially suppress the phenotype caused by the loss of *PDI1* function. Overexpression of Mpd2p can suppress a yeast strain lacking *PDI1* but this strain has a growth defect when compared to the wild-type strain (3.3 hours versus 1.7 hours doubling time) and is sensitive to exogenous reducing agents (DTT) (Tachikawa et al., 1997). Furthermore, It can rescue the CPY maturation defect of a *pdi1Δ* strain, although after 15 minutes chase only 60% of the CPY becomes mature (Tachikawa et al., 1997). The active site cysteines are required for function, since active site cysteine to serine mutants of Mpd2p (Mpd2-SXXS) are not able to suppress the growth defect of a *pdi1Δ* strain (Tachikawa et al., 1997).

MPD2 expression is slightly induced in response to ER stress, such as treatment with DTT or tunicamycin (inducers of the UPR) (Norgaard et al., 2003). *MPD2*, as *MPD1*, also contains a CERP (**c**is-acting **e**lement **r**esponding to **P**DI deficiency) and is induced by deficiency of *PDI1* (Norgaard et al., 2003).

Mpd2p has reductase activity (reduction of insulin) that is extremely low compared to Pdi1p (Kimura et al., 2005). Mpd2p has the highest chaperone activity of the yeast PDI homologs, which is 68% of that of yPdi1p and 27-fold that of hPDI (measured by the aggregation of denatured rhodanase and mastoparan binding with a K_D of 2.68×10^{-5}) (Kimura et al., 2004; Kimura et al., 2005). Mpd2p has oxidative refolding activities towards denatured lysozyme as substrate, but its activity is 16 % of that of wild-type (Kimura et al., 2005).

Mpd2p and Mpd1p interact with each other with a K_D value of 5.97×10^{-5}, but Mpd1p does not affect the chaperone activity of Mpd2p, while Mpd2p does not affect the reductive activity of Mpd1p (Kimura et al., 2005).

Few studies have addressed the function of Mpd2p *in vivo*. The fact that Mpd2p can only partially complement *pdi1Δ* might reflect the fact that Mpd2p has only one of the activities of Pdi1p, or it might indicate that the two proteins act upon a different set of substrates.

Eug1p

Eug1p (ER protein unnecessary for growth 1) was isolated in a screen of a yeast genomic library for genes that hybridized to an oligonucleotide encoding the PDI active site sequence (Tachibana et al., 1992).

Eug1p is an ER glycoprotein with 517 amino acid residues. It contains an N-terminal signal-sequence, a C-terminal ER retention signal (HDEL) and two TRX-like domains that contain a non-classical Cys-X-X-Ser motif (Tachibana et al., 1992). It is highly similar to PDI from yeast and mammals, with the same domain organization as Pdi1p (Norgaard et al., 2001).

Cells lacking the *EUG1* gene do not exhibit growth defects, although a slight defect in the sorting of soluble vacuolar proteins CPY and proteinase A has been reported (Tachibana et al., 1992). Eug1p overexpression in a *pdi1Δ* strain allowed growth in the absence of Pdi1p but did not suppress the phenotype of accumulation of proCPY in the early secretory pathway, suggesting that Eug1p cannot fully compensate for the lack of Pdi1p (Tachibana et al., 1992).

The observation that a mutant Pdi1p with active sites mutated to Cys-X-X-Ser has almost no oxidase activity, while its isomerase activity is not affected, has lead to the idea that Eug1p might act as a dedicated isomerase in the yeast ER; however, its specific substrates are not known (Norgaard et al., 2001).

In an *in vitro* assay, Eug1p exhibited a chaperone activity (measured by the aggregation of denatured rhodanase and mastoparan binding with a K_D value of 4.21×10^{-4}) (Kimura et al., 2004), while its oxidative refolding activities (using denatured lysozyme as substrate) was only 2.16 % of that of Pdi1p (Kimura et al., 2004).

Eug1p and Eps1 interact *in vitro* with a K_D value of 6.06×10^{-6} M, but the role of this interaction is unknown (Kimura et al., 2005). Furthermore, the reductive activity of a mixture of Eps1p and Eug1p is greater that the sum of the individual reductive activities of both proteins (122% vs. 0 % or 100% for the mixture, Eug1p or Eps1p) suggesting that Eug1p and Eps1p might work together *in vivo* (Kimura et al., 2005).

Eps1p

Eps1p (**E**R-retained **P**ma1 **s**uppressing) was identified in a screen for mutants that suppress the dominant-negative growth effect of Pma1-D378N (a dominant negative allele of Pma1) (Wang et al., 1999). Eps1p is an ER type I transmembrane protein containing a C-terminal KKKNQD motif, which confers retention of transmembrane proteins in the ER (Wang et al., 1999). It contains a thioredoxin domain that is facing the ER and a second Cys-X-X-Cys motif (Cys-Asp-Lys-Cys) in a region (150-290) with no obvious sequence similarity to the disulfide isomerase/thioredoxin family (Wang *et al.*, 2003).

Overexpression of Eps1p (2*μ*, under its own promoter) suppresses the growth defect of the *pdi1Δ* strain (Wang et al., 1999). Eps1p seems be a homolog of TMX (see below) (Kimura et al., 2005). In vitro studies using denatured lysozyme as substrate suggest that Eps1p has no oxidative refolding activity (Kimura et al., 2005). Using the BIAcore system they found that Eps1p binds to Pdi1p, Eug1p, Mpd1p, Kar2p and Cne1p, with K_D value of 7.33×10^{-6} M, 6.06×10^{-6} M, 3.88×10^{-6} M, 1.03×10^{-6} M, and 1.38×10^{-5} M respectively. The Eps1p-Cne1p interaction is of low affinity (Kimura et al., 2005).

Characterization of deletion mutants of *EPS1* showed that cells lacking *EPS1* do not show any detectable growth defects, and that there are no differences between the kinetics of CPY folding between the wild-type and the *eps1Δ* strain (Wang et al., 1999)

Although the localization of wild-type Pma1p is not affected in *eps1Δ*, in these cells one can observe ER accumulation of the plasma membrane Gas1p (Wang et al., 1999). Cells expressing pma1-D378N allele cannot grow even though there is a chromosomal copy of PMA1. In wild-type cells, wild-type Pma1p is relatively stable while the pma1-D378N mutant is rapidly degraded. In *eps1Δ* cells, degradation of pma1-D378N is slowed, while overexpression of Eps1p leads to an increase in pma1-D378N degradation (Wang et al., 1999).

It has been shown that Eps1p is not required for CPY* degradation, while in *eps1Δ* mutant cells H-2K^b seems to be stabilized and its degradation is slowed (Wang et al., 2003). Wild-type cells and *eps1Δ* cells do not shown significant differences in the secretion of wild-type lysozyme. In contrast, secretion of a lysozyme mutant (lysozyme-C99A) was higher in *eps1Δ* cells (He *et al.*, 2005). Furthermore, compared to wild-type cells there is an enhancement of the secretion of unstable proteins, such as amyloid prone chicken cystatin, in *eps1Δ* cells (He et al., 2005). These studies suggest that Eps1p plays a role in ERAD as a redox-sensitive chaperone (independent of its enzymatic function as a oxidoreductase) (He et al., 2005).

Mammalian homologs of PDI

The mammalian ER contains several PDI-like proteins containing various combinations of active and inactive thioredoxin domains (see Table 1). Their roles are just now being uncovered, and various studies suggest that they might participate in discrete disulfide bond formation pathways (reviewed in (Ellgaard et al., 2005)).

For example, ERp57 interacts with the lectin-like chaperone calnexin and calreticulin to promote disulfide bond formation in glycoproteins, such as MHC-Class I. ERdj5 contains both a J domain and a thioredoxin-like motif (Hosoda *et al.*, 2003). Biochemical studies have shown that the J domain of ERdj5 specifically interacts with BIP in vitro and that this interaction is ATP-dependent (Cunnea *et al.*, 2003; Hosoda et al., 2003). This could be a novel example of synergy between a chaperone and a folding enzyme (Hosoda et al., 2003).

TMX, also a member of the mammalian PDI family, contains a transmembrane domain. It has been suggested that TMX might function to help relieve ER stresses (Cunnea et al., 2003; Hosoda et al., 2003; Matsuo *et al.*, 2001). Overexpression of TMX increases the resistance to apoptosis induced by treatment with brefeldin A (BFA), an inhibitor of ER to Golgi transport, but not apoptosis induced by agents that disrupt the intracellular calcium homeostasis, such as thapsigargin or the calcium ionophore A23187 (Matsuo et al., 2001). Furthermore, the active site cysteines seem to be required for its function *in vivo*, since the increased resistance to apoptosis induced by treatment with brefeldin A (BFA) was not observed in TMX-C56S-C59S (Matsuo et al., 2001).

Table 1 - Characteristics of *S. cerevisiae* PDI-like proteins and comparison to TrxA and DsbA from *E. coli*.

Protein	Alias	NCBI accession	Length (aa)	Domain structure	a-like domains	Interactions with other proteins	ER retention
***S. cerevisiae* homologs**							
Pdi1p	Trg1	NP_009887	522	a-b-b'-a'-c	-C-G-H-C-	Ero1p, Kar2p, Eps1p, Prc1p	HDEL
Mpd1		NP_014931	318	a	-C-G-H-C-	Cne1p, Mpd2p, Eps1p	HDEL
Mpd2		NP_014553	277	a	-C-Q-H-C-	Ero1p	HDEL
Eug1		NP_010806	517	b0-b-b'-b'0	-C-L-H-S- -C-I-H-S-	Eps1p	HDEL
Eps1		NP_012261	701	a	-C-P-H-C-	Pma1p, Kar2p, Eug1p, Pdi1p, Mpd1p	KKXXX TM segment
Others							
TrxA (E. coli)		AAY89720	109	a	-C-G-P-C-	TrxR, substrates	NA
DsbA (E. coli)		CAA56736	208	a	-C-P-H-C-	DsbB, substrates	NA

Domains a, a' and a^0 are redox active with thioredoxin fold. In contrast, b and b' domains are redox inactive with possible a thioredoxin fold (the b domain of hPDI has a thioredoxin-like fold although it does not contain the CXXC motif). The D domain is a unique helical domain present in the PDI-D family. The domain c represents a highly acidic region. NA non-applicable.

Table 2 - Characteristics of mammalian PDI-like proteins and comparison to TrxA and DsbA from *E. coli*.

Protein	Alias	NCBI accession	Length	Domain structure	a-like domains	Interactions with other proteins	ER retention
***H. sapiens* homologs**							
PDI	P4HB, P55	AAH71892	508	a-b-b'-a'-c	-C-G-H-C- -C-G-H-C-	Ero1-L	KDEL
ERp57	GRP58, P58, ERp60, ERp61	NP_005304	505	a-b-b'-a'	-C-G-H-C- -C-G-H-C-	calnexin/calreticulin	QDEL
ERp72	(CaBP2, ERP70	NP_004902	645	c-a^0-a-b-b'-a'	-C-G-H-C- -C-G-H-C- -C-G-H-C-	ND	KEEL
PDIp	PDIP	NP_006840	525	a-b-b'-a'	-C-G-H-C- -C-T-H-C-	ND	KEEL
PDIr	PDIR	BAA08451	519	b-a^0-a-a'	-C-S-M-C- -C-G-H-C- -C-P-H-C-	ND	KEEL
ERdj5	jPDI	AAN73271	793	a^0-X-a-a'-a''	-C-S-H-C- -C-P-P-C- -C-H-P-C- -C-G-P-C-	BIP	KDEL
ERp27		NP_689534	273	b	None	ND	
ERp28	ERp29	P30040	261	b-D	None	ND	
P5	CaBP1, ERp5	NP_005733	440	a^0-a-b-c	-C-G-H-C-	ND	KDEL
ERp46	EndoPDI	NP_110437	432	a-a'-a''	-C-G-H-C- -C-G-H-C- -C-G-H-C-	ND	
ERp44		NP_055866	406	a	-C-R-F-S-	Ero1-L	RDEL
ERp18	ERp19, TLP19	NP_056997	172	a	-C-G-H-C- I	ND	EDEL
ERp65	PDILT	AAH44936	584	a-b-b-a-	-S-K-Q-S- -S-K-K-C-	Ero1-L	KEEL

Table 2 (Continued) - Characteristics of mammalian PDI-like proteins and comparison to TrxA and DsbA from *E. coli*.

Protein	Alias	NCBI accession	Length	Domain structure	a-like domains	Interactions with other proteins	ER retention
***H. sapiens* homologs**							
TMX		NP_110283	280	a	-C-P-A-C	ND	TM segment TDKS
TMX2		NP_057043	296	a	-S-N-D-C	ND	KKDK
TMX3		NP_061895	454	a	-C-G-H-C	ND	TM segment -KKKD
TMX4		AAQ89363	349	a	-C-P-S-C-	ND	TM segment -DKGLL
Others						ND	
TrxA (E. coli)		AAY89720	109	a	-C-G-P-C-	TrxR, substrates	NA
DsbA (E. coli)		CAA56736	208	a	-C-P-H-C-	DsbB, substrates	NA

Domains a, a' and a^0 are redox active with thioredoxin-fold. In contrast, b and b' domains are redox inactive with possible a thioredoxin- fold (the b domain of hPDI has a thioredoxin-like fold although it does not contain the CXXC motif). The D domain is a unique helical domain present in the PDI-D family. The domain c represents a highly acidic region.

The Role of other factors in oxidative folding

Role of glutathione in oxidative folding

Whereas the redox potential of the cytosol is strongly reducing, the redox potential of the ER is more oxidizing due to its higher GSSG content (Hwang *et al.*, 1992). Glutathione is a major source of thiols in the ER and the ratio of the concentration of reduced to oxidized (GSH/GSSG) in the ER is 1:1 to 3:1 (Hwang et al., 1992). These studies suggested that glutathione acts as a protein oxidant in the ER. Furthermore, oxidative refolding *in vitro* requires a redox buffer with a similar ratio of GSH/GSSG (Gilbert, 1963).

The current model is that GSH is not required for disulfide bond formation, but acts as a net reductant in the ER to counteract the Ero1p-driven oxidation pathway (Cuozzo *et al.*, 1999). First, glutathione is not essential for the formation of disulfide bond formation, since mutants in *gsh1Δ* are able to mature CPY (Frand et al., 1998). Second, deletion of the *GSH1* gene (which lacks γ-glutamylcysteine synthetase, the enzyme for the first and rate-limiting step in glutathione synthesis) not only restores disulfide bond formation to cells containing a mutant *ERO1* allele but also causes oxidative protein folding to be more readily compromised by the addition of a small molecule oxidant (Frand et al., 1998).

Similar experiments performed in permeabilized mammalian cells have shown that reduced glutathione is necessary to counteract the Ero1p-Pdi1p oxidation pathway (Molteni *et al.*, 2004). Furthermore, like *GSH1* deletions mutants, glutathione-depleted mammalian cells (treated with an inhibitor of γ-glutamylcysteine synthetase) do not exhibit defects in oxidative folding or secretion (Chakravarthi *et al.*, 2004; Frand et al., 1998). GSH has been shown to be required to keep ERp57 in its reduced state. Furthermore, mammalian cells depleted for glutathione cannot reduce ERp57 after oxidative stress. However, a large fraction of the glutathione in the ER forms mixed-disulfide bonds with proteins, thus making it unclear whether reduced glutathione acts by maintaining thioredoxin-like reductases in their active reduced form or by directly reducing folding substrates (Bass *et al.*, 2004).

Role of flavin

FAD1 and *FMN1*, genes involved in the synthesis of flavin, were found to be high copy suppressors of the *ero1-1* mutant (Tu *et al.*, 2002). Furthermore, the observation that CPY maturation is defective in the *rib5Δ* strain (deficient in production of FAD), while there is no observable defect in *coq5Δ* or *hem1Δ* strains (deficient in production of ubiquinone and heme, respectively), suggests that flavin levels influence oxidative folding *in vivo* (Tu et al, 2000). Various other pieces of evidence suggest a role of flavin in the process of disulfide bond formation: 1) *ero1-1* is synthetic lethal with *fad1-1* mutant, 2) the *fad1-1* mutant is DTT sensitive under anaerobic conditions, 3) overexpression of *FAD1* in *ero1-1* mutants can suppress the growth defect in anaerobic conditions, and 4) addition of free FAD to recombinant Ero1p accelerates the formation of disulfides in RNAseA (Tu et al., 2002).

All together, these data suggest that flavin might play an important role in disulfide bond formation under anerobic conditions. The FAD levels in yeast vary with the growth condition and the growth phase (Tu et al., 2004).

Flavin also seems to play a role in mammalian disulfide bond formation pathways. In HepG2 cells, secretion of apolipoprotein B-100 (apoB) into the culture medium is lower in riboflavin-deficient cells compared to cells grown in normal medium (Manthey *et al.*, 2005). In addition, riboflavin deficiency causes decreased secretion and intracellular accumulation of IL-2 in Jurkat cells (Varsanyi *et al.*, 2004).

Disulfide bond formation in the periplasm of prokaryotes

Oxidation pathway - DsbA & DsbB

The oxidation pathway of gram negative bacteria such as *E. coli* is composed of two proteins, the disulfide oxidase DsbA and the membrane protein DsbB (reviewed in (Kadokura *et al.*, 2003). After transfer of its disulfide bond to a substrate protein, DsbA becomes reduced. To start a new catalytic cycle, DsbA must become reoxidized. DsbB reoxidizes reduced DsbA, thus becoming reduced itself. Reduced DsbB is reoxidized by oxidizing equivalents provided from the respiratory chain through its quinone cofactor (Figure 10).

Inactivation of either DsbA or DsbB leads to accumulation of reduced proteins in the periplasm of *E. coli*. This, and the fact that both mutants exhibit the same phenotypes (such as sensitive to dithiothreitol, benzylpenicilim and some metal ions such as Hg^{2+} and Cd^{2+}), suggested that these two proteins were acting on the same pathway. Moreover, $dsbA^{-}$ strains have reduced levels of proteins that contain disulfide bonds, such as alkaline phosphatase and β-lactamase.

Isomerization pathway - DsbC/DsbG & DsbD

The fact that DsbA was found not to be a specific oxidant, and therefore could lead to the formation of non-native disulfides in proteins with more than 2 cysteines, suggested the presence of an isomerization pathway in *E. coli* (reviewed in (Kadokura et al., 2003)). To correct the non-native disulfides formed by DsbA, *E. coli* possesses an isomerization system composed of protein disulfide isomerase DsbC or DsbG and a membrane protein DsbG.

DsbC/DsbG catalyses the reoxidzation of misoxidized substrates, thus becoming oxidized in the process. In turn, DsbC is reduced by DsbG protein, which gets oxidized in the process. DsbG must be kept reduced in the periplasm to perform its function; thus it receives electrons from cytoplasmic thioredoxin. Thioredoxin is kept reduced by thioredoxin reductase, which uses NADPH.

DsbC and DsbD are kept reduced in the oxidative environment of the periplasm. Structural and mutagenesis studies showed that while DsbC/DsbD are dimeric proteins, DsbA is a monomeric protein. These studies found that turning DsbC into a monomeric protein allow it to be oxidized by DsbB. This elegant mechanism allows two opposite pathways (oxidation and isomerization) to occur simultaneously without short-circuiting the system.

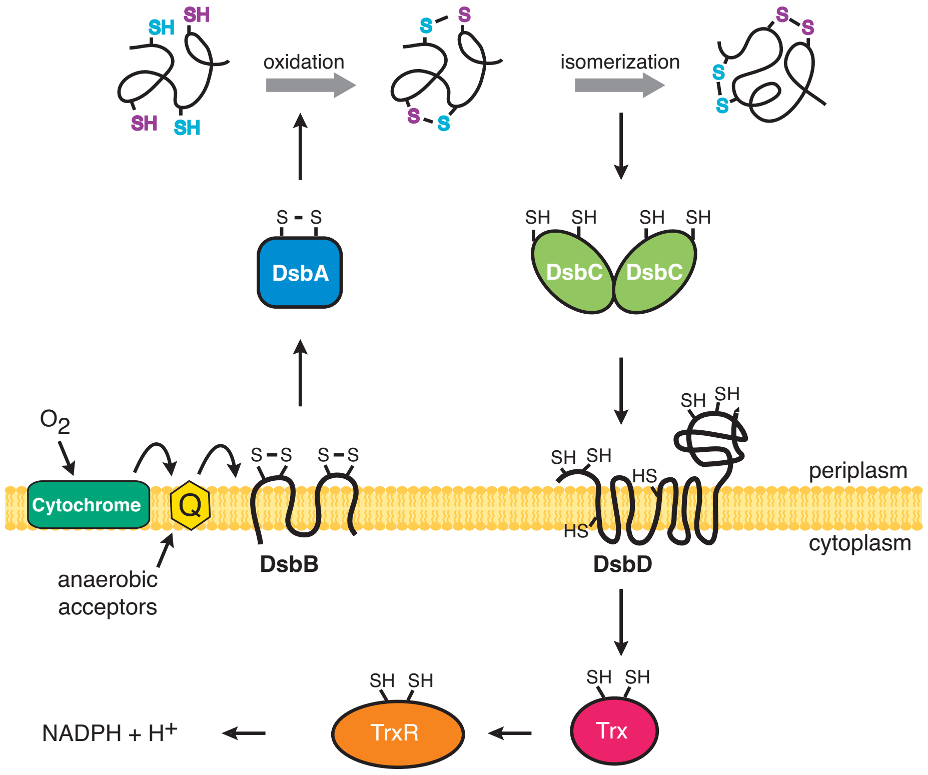
SH
SH
SH
SH
oxidation
S
S
S
S
isomerization
S
S
S
S
S - S
DsbA
SH
SH
SH
SH
DsbC
DsbC
O2
Cytochrome
Q
S-S
S-S
DsbB
anaerobic acceptors
SH
SH
HS
HS
SH
SH
DsbD
periplasm
cytoplasm
SH
SH
TrxR
SH
SH
Trx
NADPH + H+

Figure 10. Pathways of disulfide bond formation (oxidation) and isomerization in the periplasm of *E. coli*.

Comparison of the disulfide bond formation pathways in prokaryotes and eukaryotes

Despite the differences between eukaryotes and prokaryotes, their disulfide bond formation pathways share a number of features. The secretion of various oxidized proteins is affected by disruption of either DsbA or PDI (Bardwell *et al.*, 1991; Frand et al., 1998). The fact that PDI is also able to complement a dsbA$^-$ mutant when targeted to the bacterial periplasm suggests an overlap of the biochemical activities of PDI and DsbA (Humphreys *et al.*, 1995). Their main job is to oxidize substrate proteins in the ER and in the periplasm, respectively.

The loss of either *ERO1* or DsbB results in the accumulation of reduced Pdi1p or DsbA, their respective substrates (Bardwell *et al.*, 1993; Frand et al., 1998). Both mutants seem to accumulate proteins in the reduced state (CPY, Gas1p in the case of Ero1 and alkaline phosphatase in the case of DsbB). Both *ero1-1* and dsbB$^-$ mutants are DTT sensitive, and defects in disulfide bond formation in both mutants are rescued by addition of oxidants (diamide in the case of Ero1p and GSSG or cysteine in the case of DsbB).

Both Ero1p and DsbB are membrane associated oxidoreductases that transfer disulfides to soluble thioredoxin-like proteins (Pdi1p/Mpd2p and DsbA respectively) suggesting that they are functional homologs. Moreover, comparison of the structural features of both DsbB and Ero1p showed that both contain an active site cysteine pair in a four helix bundle containing the redox cofactor (FAD or quinone, respectively), and another cysteine pair located in an unstructured flexible loop that is posed to interact with the substrate (Sevier *et al.*, 2005).

The main difference between the prokaryotic and the eukaryotic disulfide bond formation pathways is the lack of a dedicated isomerization pathway in eukaryotes. Oxidation and isomerization systems in prokayotes are separate (DsbA-DsbB and DsbC-DsbD systems), while eukaryotes have become dependent on forming disulfides by consolidating the oxidase and isomerization functions into one single protein.

Why do the two pathways not exist in yeast or higher eukaryotes? The periplasm is more leaky to the external environment, so if bacteria used a small thiol it would be difficult to maintain its concentration in the periplasm. Thus, the two separate pathways for disulfide bond formation and isomerization might be a necessity in bacteria.

Although eukaryotes lack a dedicated pathway of isomerization there are still some interesting analogies that can be made between the two systems. Both dsbC$^-$ and *gsh1Δ* mutants are rescued by reducing agents (ref in (Frand et al., 2000a)). Reducing equivalents delivered to DsbC from DsbD are derived from cytoplasmic thioredoxin, which is linked to NADPH (ref in (Frand et al., 2000a)). Similarly, reducing equivalents delivered to the ER are derived from the cytoplasm, which is linked to NADPH metabolism through glutathione reductase. Although the sequence similarity of Pdi1p and DsbC is almost undetectable, their crystal structures suggest a similar fold.

References

Allen, S., Balabanidou, V., Sideris, D.P., Lisowsky, T. and Tokatlidis, K. (2005) Erv1 mediates the Mia40-dependent protein import pathway and provides a functional link to the respiratory chain by shuttling electrons to cytochrome c. *J Mol Biol*, 353, 937-944.

Anfinsen, C.B. and Haber, E. (1961) Studies on the reduction and re-formation of protein disulfide bonds. *J Biol Chem*, 236, 1361-1363.

Bardwell, J.C., Lee, J.O., Jander, G., Martin, N., Belin, D. and Beckwith, J. (1993) A pathway for disulfide bond formation in vivo. *Proc Natl Acad Sci U S A*, 90, 1038-1042.

Bardwell, J.C., McGovern, K. and Beckwith, J. (1991) Identification of a protein required for disulfide bond formation in vivo. *Cell*, 67, 581-589.

Bass, R., Ruddock, L.W., Klappa, P. and Freedman, R.B. (2004) A major fraction of endoplasmic reticulum-located glutathione is present as mixed disulfides with protein. *J Biol Chem*, 279, 5257-5262.

Bateman, A., Coin, L., Durbin, R., Finn, R.D., Hollich, V., Griffiths-Jones, S., Khanna, A., Marshall, M., Moxon, S., Sonnhammer, E.L., Studholme, D.J., Yeats, C. and Eddy, S.R. (2004) The Pfam protein families database. *Nucleic Acids Res*, 32, D138-141.

Becher, D., Kricke, J., Stein, G. and Lisowsky, T. (1999) A mutant for the yeast scERV1 gene displays a new defect in mitochondrial morphology and distribution. *Yeast*, 15, 1171-1181.

Bendtsen, J.D., Nielsen, H., von Heijne, G. and Brunak, S. (2004) Improved prediction of signal peptides: SignalP 3.0. *J Mol Biol*, 340, 783-795.

Benham, A.M., Cabibbo, A., Fassio, A., Bulleid, N., Sitia, R. and Braakman, I. (2000) The CXXCXXC motif determines the folding, structure and stability of human Ero1-Lalpha. *Embo J*, 19, 4493-4502.

Bihlmaier, K., Mesecke, N., Terziyska, N., Bien, M., Hell, K. and Herrmann, J.M. (2007) The disulfide relay system of mitochondria is connected to the respiratory chain. *J Cell Biol*, 179, 389-395.

Biswas, S., Chida, A.S. and Rahman, I. (2006) Redox modifications of protein-thiols: emerging roles in cell signaling. *Biochem Pharmacol*, 71, 551-564.

Cabibbo, A., Pagani, M., Fabbri, M., Rocchi, M., Farmery, M.R., Bulleid, N.J. and Sitia, R. (2000) ERO1-L, a human protein that favors disulfide bond formation in the endoplasmic reticulum. *J Biol Chem*, 275, 4827-4833.

Chakravarthi, S. and Bulleid, N.J. (2004) Glutathione is required to regulate the formation of native disulfide bonds within proteins entering the secretory pathway. *J Biol Chem*, 279, 39872-39879.

Claros, M.G. (1995) MitoProt, a Macintosh application for studying mitochondrial proteins. *Comput Appl Biosci*, 11, 441-447.

Claros, M.G. and Vincens, P. (1996) Computational method to predict mitochondrially imported proteins and their targeting sequences. *Eur J Biochem*, 241, 779-786.

Coppock, D., Kopman, C., Gudas, J. and Cina-Poppe, D.A. (2000) Regulation of the quiescence-induced genes: quiescin Q6, decorin, and ribosomal protein S29. *Biochem Biophys Res Commun*, 269, 604-610.

Cunnea, P.M., Miranda-Vizuete, A., Bertoli, G., Simmen, T., Damdimopoulos, A.E., Hermann, S., Leinonen, S., Huikko, M.P., Gustafsson, J.A., Sitia, R. and Spyrou, G. (2003) ERdj5, an endoplasmic reticulum (ER)-resident protein containing DnaJ and thioredoxin domains, is expressed in secretory cells or following ER stress. *J Biol Chem*, 278, 1059-1066.

Cuozzo, J.W. and Kaiser, C.A. (1999) Competition between glutathione and protein thiols for disulphide-bond formation. *Nat Cell Biol*, 1, 130-135.

DeLano, W.L. (2002) The Pymol Molecular Graphics System.

Dias-Gunasekara, S. and Benham, A.M. (2005a) Defining the protein-protein interactions of the mammalian endoplasmic reticulum oxidoreductases (EROs). *Biochem Soc Trans*, 33, 1382-1384.

Dias-Gunasekara, S., Gubbens, J., van Lith, M., Dunne, C., Williams, J.A., Kataky, R., Scoones, D., Lapthorn, A., Bulleid, N.J. and Benham, A.M. (2005b) Tissue-specific expression and dimerization of the endoplasmic reticulum oxidoreductase Ero1beta. *J Biol Chem*, 280, 33066-33075.

Ellgaard, L. and Ruddock, L.W. (2005) The human protein disulphide isomerase family: substrate interactions and functional properties. *EMBO Rep*, 6, 28-32.

Farquhar, R., Honey, N., Murant, S.J., Bossier, P., Schultz, L., Montgomery, D., Ellis, R.W., Freedman, R.B. and Tuite, M.F. (1991) Protein disulfide isomerase is essential for viability in Saccharomyces cerevisiae. *Gene*, 108, 81-89.

Farrell, S.R. and Thorpe, C. (2005) Augmenter of liver regeneration: a flavin-dependent sulfhydryl oxidase with cytochrome c reductase activity. *Biochemistry*, 44, 1532-1541.

Francavilla, A., Hagiya, M., Porter, K.A., Polimeno, L., Ihara, I. and Starzl, T.E. (1994) Augmenter of liver regeneration: its place in the universe of hepatic growth factors. *Hepatology*, 20, 747-757.

Francavilla, A., Vujanovic, N.L., Polimeno, L., Azzarone, A., Iacobellis, A., Deleo, A., Hagiya, M., Whiteside, T.L. and Starzl, T.E. (1997) The in vivo effect of hepatotrophic factors augmenter of liver regeneration, hepatocyte growth factor, and insulin-like growth factor-II on liver natural killer cell functions. *Hepatology*, 25, 411-415.

Frand, A.R., Cuozzo, J.W. and Kaiser, C.A. (2000a) Pathways for protein disulphide bond formation. *Trends Cell Biol*, 10, 203-210.

Frand, A.R. and Kaiser, C.A. (1998) The ERO1 gene of yeast is required for oxidation of protein dithiols in the endoplasmic reticulum. *Mol Cell*, 1, 161-170.

Frand, A.R. and Kaiser, C.A. (1999) Ero1p oxidizes protein disulfide isomerase in a pathway for disulfide bond formation in the endoplasmic reticulum. *Mol Cell*, 4, 469-477.

Frand, A.R. and Kaiser, C.A. (2000b) Two pairs of conserved cysteines are required for the oxidative activity of Ero1p in protein disulfide bond formation in the endoplasmic reticulum. *Mol Biol Cell*, 11, 2833-2843.

Gess, B., Hofbauer, K.H., Wenger, R.H., Lohaus, C., Meyer, H.E. and Kurtz, A. (2003) The cellular oxygen tension regulates expression of the endoplasmic oxidoreductase ERO1-Lalpha. *Eur J Biochem*, 270, 2228-2235.

Ghezzi, P. (2005) Oxidoreduction of protein thiols in redox regulation. *Biochem Soc Trans*, 33, 1378-1381.

Gilbert, H.F. (1963) Molecular and cellular aspects of thiol-disulfide exchange. *Advances In enzymology and Related Areas of Molecular Biology*, 63, 69-172.

Goldberger, R.F., Epstein, C.J. and Anfinsen, C.B. (1963) Acceleration of reactivation of reduced bovine pancreatic ribonuclease by a microsomal system from rat liver. *J Biol Chem*, 238, 628-635.

Gross, E., Kastner, D.B., Kaiser, C.A. and Fass, D. (2004) Structure of Ero1p, source of disulfide bonds for oxidative protein folding in the cell. *Cell*, 117, 601-610.

Gross, E., Sevier, C.S., Vala, A., Kaiser, C.A. and Fass, D. (2002) A new FAD-binding fold and intersubunit disulfide shuttle in the thiol oxidase Erv2p. *Nat Struct Biol*, 9, 61-67.

Gunther, R., Brauer, C., Janetzky, B., Forster, H.H., Ehbrecht, I.M., Lehle, L. and Kuntzel, H. (1991) The Saccharomyces cerevisiae TRG1 gene is essential for growth and encodes a lumenal endoplasmic reticulum glycoprotein involved in the maturation of vacuolar carboxypeptidase. *J Biol Chem*, 266, 24557-24563.

Gunther, R., Srinivasan, M., Haugejorden, S., Green, M., Ehbrecht, I.M. and Kuntzel, H. (1993) Functional replacement of the Saccharomyces cerevisiae Trg1/Pdi1 protein by members of the mammalian protein disulfide isomerase family. *J Biol Chem*, 268, 7728-7732.

He, J., Sakamoto, T., Song, Y., Saito, A., Harada, A., Azakami, H. and Kato, A. (2005) Effect of EPS1 gene deletion in Saccharomyces cerevisiae on the secretion of foreign proteins which have disulfide bridges. *FEBS Lett*, 579, 2277-2283.

Hofhaus, G., Lee, J.E., Tews, I., Rosenberg, B. and Lisowsky, T. (2003) The N-terminal cysteine pair of yeast sulfhydryl oxidase Erv1p is essential for in vivo activity and interacts with the primary redox centre. *Eur J Biochem*, 270, 1528-1535.

Hofhaus, G. and Lisowsky, T. (2002) Sulfhydryl oxidases as factors for mitochondrial biogenesis. *Methods Enzymol*, 348, 314-324.

Holst, B., Tachibana, C. and Winther, J.R. (1997) Active site mutations in yeast protein disulfide isomerase cause dithiothreitol sensitivity and a reduced rate of protein folding in the endoplasmic reticulum. *J Cell Biol*, 138, 1229-1238.

Hoober, K.L., Glynn, N.M., Burnside, J., Coppock, D.L. and Thorpe, C. (1999a) Homology between egg white sulfhydryl oxidase and quiescin Q6 defines a new class of flavin-linked sulfhydryl oxidases. *J Biol Chem*, 274, 31759-31762.

Hoober, K.L., Joneja, B., White, H.B., 3rd and Thorpe, C. (1996) A sulfhydryl oxidase from chicken egg white. *J Biol Chem*, 271, 30510-30516.

Hoober, K.L., Sheasley, S.L., Gilbert, H.F. and Thorpe, C. (1999b) Sulfhydryl oxidase from egg white. A facile catalyst for disulfide bond formation in proteins and peptides. *J Biol Chem*, 274, 22147-22150.

Hoober, K.L. and Thorpe, C. (2002) Flavin-dependent sulfhydryl oxidases in protein disulfide bond formation. *Methods Enzymol*, 348, 30-34.

Hosoda, A., Kimata, Y., Tsuru, A. and Kohno, K. (2003) JPDI, a novel endoplasmic reticulum-resident protein containing both a BiP-interacting J-domain and thioredoxin-like motifs. *J Biol Chem*, 278, 2669-2676.

Humphreys, D.P., Weir, N., Mountain, A. and Lund, P.A. (1995) Human protein disulfide isomerase functionally complements a dsbA mutation and enhances the yield of pectate lyase C in Escherichia coli. *J Biol Chem*, 270, 28210-28215.

Hwang, C., Sinskey, A.J. and Lodish, H.F. (1992) Oxidized redox state of glutathione in the endoplasmic reticulum. *Science*, 257, 1496-1502.

Kadokura, H., Katzen, F. and Beckwith, J. (2003) Protein disulfide bond formation in prokaryotes. *Annu Rev Biochem*, 72, 111-135.

Kemmink, J., Darby, N.J., Dijkstra, K., Nilges, M. and Creighton, T.E. (1997) The folding catalyst protein disulfide isomerase is constructed of active and inactive thioredoxin modules. *Curr Biol*, 7, 239-245.

Kettner, K., Blomberg, A. and Rodel, G. (2004) Schizosaccharomyces pombe ER oxidoreductin-like proteins SpEro1a p and SpEro1b p. *Yeast*, 21, 1035-1044.

Kimura, T., Hosoda, Y., Kitamura, Y., Nakamura, H., Horibe, T. and Kikuchi, M. (2004) Functional differences between human and yeast protein disulfide isomerase family proteins. *Biochem Biophys Res Commun*, 320, 359-365.

Kimura, T., Hosoda, Y., Sato, Y., Kitamura, Y., Ikeda, T., Horibe, T. and Kikuchi, M. (2005) Interactions among yeast protein-disulfide isomerase proteins and endoplasmic reticulum chaperone proteins influence their activities. *J Biol Chem*, 280, 31438-31441.

Klissenbauer, M., Winters, S., Heinlein, U.A. and Lisowsky, T. (2002) Accumulation of the mitochondrial form of the sulphydryl oxidase Erv1p/Alrp during the early stages of spermatogenesis. *J Exp Biol*, 205, 1979-1986.

Krogh, A., Larsson, B., von Heijne, G. and Sonnhammer, E.L. (2001) Predicting transmembrane protein topology with a hidden Markov model: application to complete genomes. *J Mol Biol*, 305, 567-580.

LaMantia, M., Miura, T., Tachikawa, H., Kaplan, H.A., Lennarz, W.J. and Mizunaga, T. (1991) Glycosylation site binding protein and protein disulfide isomerase are identical and essential for cell viability in yeast. *Proc Natl Acad Sci U S A*, 88, 4453-4457.

Lange, H., Lisowsky, T., Gerber, J., Muhlenhoff, U., Kispal, G. and Lill, R. (2001) An essential function of the mitochondrial sulfhydryl oxidase Erv1p/ALR in the maturation of cytosolic Fe/S proteins. *EMBO Rep*, 2, 715-720.

Lee, J., Hofhaus, G. and Lisowsky, T. (2000) Erv1p from Saccharomyces cerevisiae is a FAD-linked sulfhydryl oxidase. *FEBS Lett*, 477, 62-66.

Li, Y., Xing, G., Wang, Q., Li, M., Wei, H., Fan, G., Chen, J., Yang, X., Wu, C., Chen, H. and He, F. (2001) Hepatopoietin acts as an autocrine growth factor in hepatoma cells. *DNA Cell Biol*, 20, 791-795.

Lisowsky, T. (1992) Dual function of a new nuclear gene for oxidative phosphorylation and vegetative growth in yeast. *Mol Gen Genet*, 232, 58-64.

Lisowsky, T. (1994) ERV1 is involved in the cell-division cycle and the maintenance of mitochondrial genomes in Saccharomyces cerevisiae. *Curr Genet*, 26, 15-20.

Lisowsky, T. (1996) Removal of an intron with unique 3' branch site creates an amino-terminal protein sequence directing the scERV1 gene product to mitochondria. *Yeast*, 12, 1501-1510.

Lisowsky, T., Lee, J.E., Polimeno, L., Francavilla, A. and Hofhaus, G. (2001) Mammalian augmenter of liver regeneration protein is a sulfhydryl oxidase. *Dig Liver Dis*, 33, 173-180.

Lu, J., Xu, W.X., Zhan, Y.Q., Cui, X.L., Cai, W.M., He, F.C. and Yang, X.M. (2002) Identification and characterization of a novel isoform of hepatopoietin. *World J Gastroenterol*, 8, 353-356.

Manthey, K.C., Chew, Y.C. and Zempleni, J. (2005) Riboflavin deficiency impairs oxidative folding and secretion of apolipoprotein B-100 in HepG2 cells, triggering stress response systems. *J Nutr*, 135, 978-982.

Martin, J.L. (1995) Thioredoxin--a fold for all reasons. *Structure*, 3, 245-250.

Matsuo, Y., Akiyama, N., Nakamura, H., Yodoi, J., Noda, M. and Kizaka-Kondoh, S. (2001) Identification of a novel thioredoxin-related transmembrane protein. *J Biol Chem*, 276, 10032-10038.

Mesecke, N., Terziyska, N., Kozany, C., Baumann, F., Neupert, W., Hell, K. and Herrmann, J.M. (2005) A disulfide relay system in the intermembrane space of mitochondria that mediates protein import. *Cell*, 121, 1059-1069.

Mezghrani, A., Fassio, A., Benham, A., Simmen, T., Braakman, I. and Sitia, R. (2001) Manipulation of oxidative protein folding and PDI redox state in mammalian cells. *Embo J*, 20, 6288-6296.

Molteni, S.N., Fassio, A., Ciriolo, M.R., Filomeni, G., Pasqualetto, E., Fagioli, C. and Sitia, R. (2004) Glutathione limits Ero1-dependent oxidation in the endoplasmic reticulum. *J Biol Chem*, 279, 32667-32673.

Nielsen, H., Engelbrecht, J., Brunak, S. and von Heijne, G. (1997) Identification of prokaryotic and eukaryotic signal peptides and prediction of their cleavage sites. *Protein Eng*, 10, 1-6.

Nielsen, H. and Krogh, A. (1998) Prediction of signal peptides and signal anchors by a hidden Markov model. *Proc Int Conf Intell Syst Mol Biol*, 6, 122-130.

Norgaard, P., Tachibana, C., Bruun, A.W. and Winther, J.R. (2003) Gene regulation in response to protein disulphide isomerase deficiency. *Yeast*, 20, 645-652.

Norgaard, P., Westphal, V., Tachibana, C., Alsoe, L., Holst, B. and Winther, J.R. (2001) Functional differences in yeast protein disulfide isomerases. *J Cell Biol*, 152, 553-562.

Ostrowski, M.C. and Kistler, W.S. (1980) Properties of a flavoprotein sulfhydryl oxidase from rat seminal vesicle secretion. *Biochemistry*, 19, 2639-2645.

Pagani, M., Fabbri, M., Benedetti, C., Fassio, A., Pilati, S., Bulleid, N.J., Cabibbo, A. and Sitia, R. (2000) Endoplasmic reticulum oxidoreductin 1-lbeta (ERO1-Lbeta), a human gene induced in the course of the unfolded protein response. *J Biol Chem*, 275, 23685-23692.

Pollard, M.G., Travers, K.J. and Weissman, J.S. (1998) Ero1p: a novel and ubiquitous protein with an essential role in oxidative protein folding in the endoplasmic reticulum. *Mol Cell*, 1, 171-182.

Raje, S. and Thorpe, C. (2003) Inter-domain redox communication in flavoenzymes of the quiescin/sulfhydryl oxidase family: role of a thioredoxin domain in disulfide bond formation. *Biochemistry*, 42, 4560-4568.

Rissler, M., Wiedemann, N., Pfannschmidt, S., Gabriel, K., Guiard, B., Pfanner, N. and Chacinska, A. (2005) The essential mitochondrial protein Erv1 cooperates with Mia40 in biogenesis of intermembrane space proteins. *J Mol Biol*, 353, 485-492.

Schwaller, M., Wilkinson, B. and Gilbert, H.F. (2003) Reduction-reoxidation cycles contribute to catalysis of disulfide isomerization by protein-disulfide isomerase. *J Biol Chem*, 278, 7154-7159.

Senkevich, T.G., Ward, B.M. and Moss, B. (2004) Vaccinia virus entry into cells is dependent on a virion surface protein encoded by the A28L gene. *J Virol*, 78, 2357-2366.

Senkevich, T.G., Weisberg, A.S. and Moss, B. (2000a) Vaccinia virus E10R protein is associated with the membranes of intracellular mature virions and has a role in morphogenesis. *Virology*, 278, 244-252.

Senkevich, T.G., White, C.L., Koonin, E.V. and Moss, B. (2000b) A viral member of the ERV1/ALR protein family participates in a cytoplasmic pathway of disulfide bond formation. *Proc Natl Acad Sci U S A*, 97, 12068-12073.

Senkevich, T.G., White, C.L., Koonin, E.V. and Moss, B. (2002a) Complete pathway for protein disulfide bond formation encoded by poxviruses. *Proc Natl Acad Sci U S A*, 99, 6667-6672.

Senkevich, T.G., White, C.L., Weisberg, A., Granek, J.A., Wolffe, E.J., Koonin, E.V. and Moss, B. (2002b) Expression of the vaccinia virus A2.5L redox protein is required for virion morphogenesis. *Virology*, 300, 296-303.

Sevier, C.S., Cuozzo, J.W., Vala, A., Aslund, F. and Kaiser, C.A. (2001) A flavoprotein oxidase defines a new endoplasmic reticulum pathway for biosynthetic disulphide bond formation. *Nat Cell Biol*, 3, 874-882.

Sevier, C.S., Kadokura, H., Tam, V.C., Beckwith, J., Fass, D. and Kaiser, C.A. (2005) The prokaryotic enzyme DsbB may share key structural features with eukaryotic disulfide bond forming oxidoreductases. *Protein Sci*, 14, 1630-1642.

Sevier, C.S. and Kaiser, C.A. (2006a) Conservation and diversity of the cellular disulfide bond formation pathways. *Antioxid Redox Signal*, 8, 797-811.

Sevier, C.S. and Kaiser, C.A. (2006b) Disulfide transfer between two conserved cysteine pairs imparts selectivity to protein oxidation by Ero1. *Mol Biol Cell*, 17, 2256-2266.

Sipos, K., Lange, H., Fekete, Z., Ullmann, P., Lill, R. and Kispal, G. (2002) Maturation of cytosolic iron-sulfur proteins requires glutathione. *J Biol Chem*, 277, 26944-26949.

Sonnhammer, E.L., von Heijne, G. and Krogh, A. (1998) A hidden Markov model for predicting transmembrane helices in protein sequences. *Proc Int Conf Intell Syst Mol Biol*, 6, 175-182.

Stein, G. and Lisowsky, T. (1998) Functional comparison of the yeast scERV1 and scERV2 genes. *Yeast*, 14, 171-180.

Tachibana, C. and Stevens, T.H. (1992) The yeast EUG1 gene encodes an endoplasmic reticulum protein that is functionally related to protein disulfide isomerase. *Mol Cell Biol*, 12, 4601-4611.

Tachikawa, H., Funahashi, W., Takeuchi, Y., Nakanishi, H., Nishihara, R., Katoh, S., Gao, X.D., Mizunaga, T. and Fujimoto, D. (1997) Overproduction of Mpd2p suppresses the lethality of protein disulfide isomerase depletion in a CXXC sequence dependent manner. *Biochem Biophys Res Commun*, 239, 710-714.

Tachikawa, H., Takeuchi, Y., Funahashi, W., Miura, T., Gao, X.D., Fujimoto, D., Mizunaga, T. and Onodera, K. (1995) Isolation and characterization of a yeast gene, MPD1, the overexpression of which suppresses inviability caused by protein disulfide isomerase depletion. *FEBS Lett*, 369, 212-216.

Terziyska, N., Lutz, T., Kozany, C., Mokranjac, D., Mesecke, N., Neupert, W., Herrmann, J.M. and Hell, K. (2005) Mia40, a novel factor for protein import into the intermembrane space of mitochondria is able to bind metal ions. *FEBS Lett*, 579, 179-184.

Thasler, W.E., Schlott, T., Thelen, P., Hellerbrand, C., Bataille, F., Lichtenauer, M., Schlitt, H.J., Jauch, K.W. and Weiss, T.S. (2005) Expression of augmenter of liver regeneration (ALR) in human liver cirrhosis and carcinoma. *Histopathology*, 47, 57-66.

Thompson, J.D., Gibson, T.J., Plewniak, F., Jeanmougin, F. and Higgins, D.G. (1997) The CLUSTAL_X windows interface: flexible strategies for multiple sequence alignment aided by quality analysis tools. *Nucleic Acids Res*, 25, 4876-4882.

Thorpe, C., Hoober, K.L., Raje, S., Glynn, N.M., Burnside, J., Turi, G.K. and Coppock, D.L. (2002) Sulfhydryl oxidases: emerging catalysts of protein disulfide bond formation in eukaryotes. *Arch Biochem Biophys*, 405, 1-12.

Tu, B.P. and Weissman, J.S. (2002) The FAD- and O(2)-dependent reaction cycle of Ero1-mediated oxidative protein folding in the endoplasmic reticulum. *Mol Cell*, 10, 983-994.

Tu, B.P. and Weissman, J.S. (2004) Oxidative protein folding in eukaryotes: mechanisms and consequences. *J Cell Biol*, 164, 341-346.

Varsanyi, M., Szarka, A., Papp, E., Makai, D., Nardai, G., Fulceri, R., Csermely, P., Mandl, J., Benedetti, A. and Banhegyi, G. (2004) FAD transport and FAD-dependent protein thiol oxidation in rat liver microsomes. *J Biol Chem*, 279, 3370-3374.

Wang, Q. and Chang, A. (1999) Eps1, a novel PDI-related protein involved in ER quality control in yeast. *Embo J*, 18, 5972-5982.

Wang, Q. and Chang, A. (2003) Substrate recognition in ER-associated degradation mediated by Eps1, a member of the protein disulfide isomerase family. *Embo J*, 22, 3792-3802.

White, C.L., Senkevich, T.G. and Moss, B. (2002) Vaccinia virus G4L glutaredoxin is an essential intermediate of a cytoplasmic disulfide bond pathway required for virion assembly. *J Virol*, 76, 467-472.

Wu, C.K., Dailey, T.A., Dailey, H.A., Wang, B.C. and Rose, J.P. (2003) The crystal structure of augmenter of liver regeneration: A mammalian FAD-dependent sulfhydryl oxidase. *Protein Sci*, 12, 1109-1118.

Chapter Two

Structural and biochemical characterization of Erv2p, a small FAD-dependent sulfhydryl oxidase

Preface

Chapter 2 contains two papers that have been published as:

Sevier, C.S., Cuozzo, J.W., **Vala, A**., Åslund, F. and Kaiser, C.A. (2001) A flavoprotein oxidase defines a new endoplasmic reticulum pathway for biosynthetic disulphide bond formation. *Nat Cell Biol*, **3**, 874-882.

Gross, E., Sevier, C.S., **Vala, A.**, Kaiser, C.A. and Fass, D. (2002) A new FAD-binding fold and intersubunit disulfide shuttle in the thiol oxidase Erv2p. *Nat Struct Biol*, **9**, 61-67.

Chapter 2 represents primarily the work of Fredrick Åslund, John W. Cuozzo, and Einav Gross. Fredrick Åslund performed the screen from where *ERV2* was identified and John W. Cuozzo did the characterization of Erv2p. Einav Gross resolved the crystal structure of Erv2p.

In the first paper I performed the experiments represented in Figures 2B, C and D. In the second paper, I contributed to Figure 7B and C by constructing the plasmids and strains, and by generating preliminary results.

A flavoprotein oxidase defines a new endoplasmic reticulum pathway for biosynthetic disulfide bond formation

Abstract

Ero1p and Pdi1p are essential elements of the pathway for the formation of disulfide bonds within the endoplasmic reticulum (ER). By screening for alternative oxidation pathways in *Saccharomyces cerevisiae*, we identified *ERV2* as a gene that when overexpressed can restore viability and disulfide bond formation to an *ero1-1* mutant strain. *ERV2* encodes a luminal ER protein of relative molecular mass 22,000. Purified recombinant Erv2p is a flavoenzyme that can catalyze O_2-dependent formation of disulfide bonds. Erv2p transfers oxidizing equivalents to Pdi1p by a dithiol-disulfide exchange reaction, indicating that the Erv2p-dependent pathway for disulfide bond formation closely parallels that of the previously identified Ero1p-dependent pathway.

Introduction

Secreted proteins and the extracellular domains of membrane proteins often contain disulfide bonds that are required for proper protein folding, function and stability. The process of disulfide bond formation has been studied intensively by the use of assays for the oxidative refolding of reduced and denatured proteins such as ribonuclease A (Lyles and Gilbert, 1991). Such *in vitro* assays have revealed the importance of both a source of oxidizing equivalents (usually provided by a mixture of oxidized and reduced glutathione) and a catalyst for disulfide formation and rearrangement such as protein disulfide isomerase (PDI). In eukaryotic cells, protein disulfide bonds are formed as the nascent polypeptide chains of secretory proteins enter the lumen of the endoplasmic reticulum (ER). The cellular pathways that provide oxidizing equivalents to the ER of living cells conducive for disulfide bond formation have recently begun to come to light.

The product of the *ERO1* gene is important in generating oxidizing equivalents in the ER. *ERO1* encodes an ER-membrane glycoprotein that in yeast is essential for viability and for the generation of disulfide bonds in secretory proteins (Cuozzo and Kaiser, 1999; Frand and Kaiser, 1998; Pollard *et al*., 1998). ER oxidation by *ERO1* seems to be a broadly conserved mechanism, because homologues of yeast *ERO1* are present in every eukaryote for which extensive genomic sequence data are available and a mammalian version of the gene can functionally complement yeast *ero1* mutations (Cabibbo *et al*., 2000). PDI is a highly abundant resident of the ER lumen that *in vitro* can catalyze either protein disulfide rearrangements or dithiol oxidation to disulfides according to the conditions of the assay (Gilbert, 1994). The activity of PDI depends on two pairs of cysteines found in the motif Cys-X-X-Cys, which is a conserved feature of the oxidoreductases of the thioredoxin superfamily (Chivers *et al*., 1997; Martin, 1995). Pdi1p is essential for cell viability, and Pdi1p has been implicated in the catalysis of both disulfide bond formation and isomerization *in vivo* (Frand and Kaiser, 1999; Holst *et al*., 1997; Laboissiere *et al*., 1995; LaMantia and Lennarz, 1993; Scherens *et al*., 1991).

We have recently delineated a core pathway for disulfide bond formation in the yeast ER in which oxidizing equivalents flow from Ero1p to Pdi1p and then to substrate proteins (Frand *et al*., 2000). Evidence for this pathway comes from mutational studies demonstrating that Ero1p is required for oxidation of the cysteine pairs of Pdi1p, and that Pdi1p is required for the oxidation of cysteine thiols in substrate proteins. Direct transfer of oxidizing equivalents by dithiol-disulfide exchange reactions was demonstrated by the capture of Ero1p-Pdi1p and Pdi1p-substrate mixed disulfides, which are the intermediates for these transfer reactions (Frand and Kaiser, 1999). Finally, this pathway for protein disulfide formation has been confirmed by *in vitro* reconstitution of substrate protein oxidation with the use of purified Ero1p and Pdi1p (Tu *et al.*, 2000). The mechanism for oxidation of Ero1p itself is not yet understood, nor has the ultimate physiological source of oxidizing equivalents for the ER disulfide bond formation been identified.

Ero1p is required for the oxidation of intraluminal glutathione as well as for the oxidation of protein thiols. However, the production of oxidized glutathione in the ER is not an obligatory intermediate step in protein thiol oxidation; instead, the presence of reduced glutathione seems to buffer the ER lumen against hyper-oxidizing conditions (Cuozzo and Kaiser, 1999; Frand and Kaiser, 1998). A key observation indicating that glutathione effectively competes with protein thiols for oxidizing equivalents derived from Ero1p is that the temperature sensitivity of an *ero1-1* mutant can be suppressed by *gsh1Δ,* a mutation that blocks the synthesis of intracellular glutathione (Cuozzo and Kaiser, 1999). We have also found that a complete chromosomal deletion of *ERO1* can be suppressed in this manner; an *ero1Δ gsh1Δ* double mutant will grow and form normal disulfide bonds (J.W.C. and C.A.K., unpublished work). This observation indicates the existence of a bypass pathway for disulfide bond formation that can function independently of Ero1p. We found that an *ero1Δ gsh1Δ* double mutant can grow under aerobic but not anaerobic conditions, indicating that bypass of Ero1p requires O_2 as an ultimate electron acceptor. Here we used an overexpression screen to identify a component of the presumptive bypass pathway, Erv2p, which is a luminal ER oxidase that can consume O_2 for the production of protein disulfide bonds.

Results

ERV2 defines a novel pathway for disulfide bond formation

To identify components of disulfide bond formation pathways that can function independently of *ERO1*, we screened for genes that when overexpressed could suppress the temperature sensitivity of an *ero1-1* mutant. An *ero1-1* strain was transformed with a library of *Saccharomyces cerevisiae* cDNAs expressed from the powerful *GAL1* promoter, and 50 clones were identified that could grow at the restrictive temperature of 37 °C from a collection of 106 transformants. Plasmid recovered from these strains revealed that 45 contained cDNA of the *ERO1* gene itself, whereas 5 plasmids contained the yeast open reading frame (ORF) YPR037C, which had previously been designated *ERV2* because of its homology with the yeast gene *ERV1* (Figure 1A) (Stein and Lisowsky, 1998).

We tested whether overexpression of *ERV2* could suppress the lethality of a complete deletion of *ERO1*. A heterozygous *ERO1/ero1Δ* diploid strain carrying the P_{GAL1}-*ERV2* plasmid was sporulated and tetrads were dissected onto galactose medium. The *ero1Δ* P_{GAL1}-*ERV2* spore clones could grow slowly, whereas *ero1Δ* spores that did not receive the plasmid could not progress beyond two or three cells. The growth of the *ero1Δ* P_{GAL1}-*ERV2* strain depended on *ERV2* overexpression because this strain could not grow on glucose medium (data not shown).

We found previously that the capacity of *ero1-1* mutants for disulfide bond formation is compromised even at temperatures permissive for growth. As a consequence, *ero1-1* strains are hypersensitive to the presence of a reductant such as dithiothreitol (DTT) or 2-mercaptoethanol in the growth medium (Frand and Kaiser, 1998). Activation of a parallel pathway for disulfide bond formation would therefore be expected to increase the resistance of the *ero1-1* strain to DTT. Accordingly, we assayed a *ero1-1* P_{GAL1}-*ERV2* strain for DTT resistance and found that *ERV2* overexpression conferred resistance to DTT, as shown by a decrease in the diameter of the zone of growth inhibition caused by DTT in a plate assay (Figure 1B).

Finally, in the most specific test for a role of Erv2p in disulfide bond formation *in vivo*, we assayed the ability of overexpressed *ERV2* to restore the capacity of *ero1* mutants to form disulfide bonds in secretory proteins. Carboxypeptidase Y (CPY) is a convenient substrate for this purpose because native CPY contains five disulfide bonds and a failure to form these bonds causes the incompletely folded pro-CPY to accumulate in the ER (Jamsa *et al.*, 1994; Simons *et al.*, 1995). Therefore, in an *ero1-1* mutant at the restrictive temperature (37 °C) pro-CPY accumulates in the ER in its core-glycosylated, unprocessed p1 form (Figure 1C, lane 1). This is in contrast to wild-type cells, in which CPY is exported from the ER, progresses through the secretory pathway and becomes converted to the mature (m) form after cleavage by vacuolar proteases (Figure 1C, lane 5). Both *ero1-1* and *ero1-1* P_{GAL1}-*ERV2* strains were grown in galactose medium at a permissive temperature of 24 °C and then shifted to 37 °C for 4 h. Under these conditions, the *ero1-1* P_{GAL1}-*ERV2* strain accumulated much less of the p1 form of CPY than the *ero1-1* strain as detected by immunoblotting (Figure 1C, compare lane 2 with lane 1). The accumulation of some p1 CPY in the *ero1-1* P_{GAL1}-*ERV2* strain when incubated at 37 °C for 4 h indicated a partial defect in disulfide bond formation. This strain seemed eventually to adapt and to restore apparently normal efficiencies of disulfide bond formation, because after incubation of the *ero1-1* P_{GAL1}-*ERV2* strain at 37 °C for 20 h, conditions under which this strain continues to grow, the p1 form of CPY was only barely detectable (Figure 1C, lane 3). The total amount of CPY in this strain was similar to that in the wild-type, demonstrating that normal CPY synthesis continues at 37 °C and that the p1 form does not accumulate because it can be converted to mature CPY. Finally, an *ero1Δ* P_{GAL1}-*ERV2* strain did not accumulate the p1 form of CPY, demonstrating that overproduced Erv2p had the capacity to drive native disulfide bond formation even in the complete absence of Ero1p (Figure 1C, lane 4). Neither the *ero1Δ* P_{GAL1}-*ERV2* strain nor the *ero1-1* P_{GAL1}-*ERV2* strain (at 37 °C) would grow on glucose medium, confirming that the suppression of the CPY trafficking defect in these strains depended on overexpression of *ERV2* and was not the result of cryptic extragenic suppressor mutations (data not shown). Taken together, the increased resistance to DTT and the restoration of CPY maturation that is conferred by overexpression of *ERV2* in either *ero1-1* or *ero1Δ* genetic backgrounds show that overproduced Erv2p forms the basis of a disulfide-bond-formation pathway that can function independently of Ero1p.

Erv2p is a luminal ER protein

The *ERV2* gene encodes a protein of predicted relative molecular weight 22,000 (Mr 20K), containing a putative amino-terminal hydrophobic ER localization sequence. To examine the intracellular localization of Erv2p, a carboxy-terminal fusion to a hemagglutinin (HA) epitope tag was constructed. The HA-tagged fusion protein could be detected by immunoblotting and was able to suppress the *ero1-1* temperature-sensitive defect, indicating that the tagged protein was functional (data not shown). Extracts were prepared from cells expressing the tagged construct, and Erv2p was followed by fractionation under conditions intended to reveal properties such as membrane localization and peripheral localization in the ER. Erv2p could be solubilized by detergent (1% Triton X-100) but not by Na_2CO_3 at pH 11.5, indicating that Erv2p is an integral membrane protein and that the hydrophobic N-terminal sequence acts as both a signal sequence and a membrane anchor (Figure 2A).

Immunofluorescence microscopy showed that HA-tagged Erv2p was distributed at the perimeter of the nucleus, coincident with the ER-resident protein Pdi1p (Figure 2B). The localization of Erv2p to the ER permits it to function directly at the site of protein disulfide bond formation. Because Erv2p has no distinguishable ER retention signal (such as an HDEL-motif), Erv2p is presumably retained in the ER by its transmembrane segment. To determine the membrane topology of Erv2p, membranes from a medium-spin pellet fraction (see Materials and methods) were subjected to digestion by proteinase K in the presence and absence of Triton X-100. Erv2p-HA was resistant to protease digestion in the absence of detergent but was degraded in the presence of detergent, like the luminal ER protein Pdi1p, showing that the carboxy-terminal domain of Erv2p-HA is luminal (Figure 2C). To exclude the possibility that the C-terminal domain of Erv2p was intrinsically protease resistant, purified recombinant C-terminal domain of Erv2p (described below) was treated with protease under the same conditions as those used for the membrane samples and was shown to be sensitive to protease in the absence of detergent (Figure 2D). We therefore conclude that Erv2p is normally a type II transmembrane protein with an N-terminal membrane anchor with the bulk of the protein residing within the lumen of the ER.

Erv2p is a flavin-binding thiol oxidase

The *ERV2* gene sequence shares significant homology with the yeast *ERV1* gene, encoding an essential mitochondrial matrix protein (Hofhaus *et al.*, 1999; Lisowsky, 1992), the cytoplasmic human protein ALR (Augmenter of Liver Regeneration), which has been shown to stimulate regeneration of the liver after partial hepatectomy (Francavilla *et al.*, 1994; Hagiya *et al.*, 1994), the C-terminal domain of the secreted human protein quiescin Q6, a Mr-93K protein that is induced when fibroblasts reach senescence (Coppock *et al.*, 1998), and cytoplasmic proteins encoded by vaccinia and African swine fever viruses (Lewis *et al.*, 2000; Senkevich *et al.*, 2000). All four proteins share a Cys-X-X-Cys motif, indicative of the active site of thioredoxin-like thiol oxidoreductases, but no other similarity to proteins of the thioredoxin family of proteins is evident in this domain (Figure 3). Importantly, the avian homologue of quiescin Q6 (designated SOX) and Erv1p have been shown to be flavoproteins that catalyze the reaction (Hoober *et al.*, 1999; Lee *et al.*, 2000)

$$2\text{R-SH} + O_2 \rightarrow \text{R-S-S-R} + H_2O_2$$

To examine the possible enzymatic activity of Erv2p, the *ERV2* coding sequence with a C-terminal His_6 tag was expressed in *Escherichia coli* from the T7 promoter. Although some full-length Erv2p could be expressed in this way, we found that a much greater yield of soluble protein was obtained by expression of a truncated protein (designated Erv2-ΔN) that lacked 29 residues of the hydrophobic N terminus. Purification of Erv2-ΔN from a cytosolic extract by Ni-nitrilotriacetate (NTA) affinity chromatography produced a protein of M_r 20K that was of >90% purity as assessed by staining with Coomassie Blue after SDS-PAGE.

Purified recombinant Erv2-ΔN protein was bright yellow, and spectroscopic analysis of the protein revealed absorbance peaks at 382 and 454 nm, indicative of a bound FAD moiety (Figure 4A). We found that the yield of flavin-bound Erv2-ΔN (as determined by the ratio of Abs_{280} to Abs_{454} for the purified protein) could be improved about twofold if FAD was added to the *E. coli* growth medium during the period of protein induction. The flavin moiety could be released from the protein either by boiling or by precipitation of the protein in trichloroacetic acid (TCA), indicating that the flavin was not covalently bound to the protein. The fluorescence (excitation at 450 nm and emission at 535 nm) of released flavin increased 4.7-fold on transfer from neutral to acidic pH; this is a characteristic of FAD, not FMN (Faeder and Siegel, 1973). The FAD moiety was found to bind tightly to the protein, because the protein retained 98% of its FAD absorbance at 454 nm after dialysis for 20 h. When purified Erv2-ΔN was denatured in 8 M guanidinium chloride, the absorbance at 454 nm was identical to that of the folded protein; we therefore calculated the concentration of protein with bound flavin in our preparations from the absorption coefficient for pure flavin. The ratio of the protein concentration of purified recombinant Erv2-ΔN and the flavin concentration (using an absorption coefficient of 12.5 mM^{-1} cm^{-1} at 454 nm) was 0.74, indicating that the normal stoichiometry of FAD binding is one FAD molecule per monomer of protein. The overexpressed recombinant protein is most probably not completely loaded with FAD.

We tested the ability of purified Erv2-ΔN to catalyze the transfer of reducing equivalents from free thiols to FAD. Reduction of the bound FAD could be monitored by a corresponding decrease in Abs_{454}. The addition of 5 mM DTT to a solution containing 4 μM Erv2-ΔN caused complete reduction of bound FAD (Figure 4B). Because 5 mM DTT alone would not reduce FAD in solution, Erv2-ΔN must act as an efficient catalyst for the transfer of electrons from the thiol groups of DTT to the protein-associated FAD. The observed time lag between the moment of DTT addition and the ensuing reduction of FAD probably corresponds to the time that it takes for the oxidase activity to consume a significant quantity of the O_2 in the spectrophotometer cuvette. A similar delay in the DTT reduction of the FAD moiety of SOX has been observed (Hoober *et al.*, 1999). The reduced FAD produced after the addition of DTT to Erv2-ΔN could be re-oxidized by the introduction of oxygen to the solution as detected by an increase in Abs_{454} after the addition of oxygen (data not shown). Erv2-ΔN exhibited specificity for the type of thiol-containing compound that could be coupled to FAD reduction because reduced glutathione at concentrations up to 100 mM did not produce detectable reduction of the FAD in Erv2-ΔN even after prolonged incubation (data not shown).

To determine whether O_2 could serve as an electron acceptor for Erv2-ΔN, consumption of soluble O_2 was measured with an oxygen electrode. When Erv2-ΔN was mixed with DTT in a buffer saturated with O_2, a steady decrease in the soluble O_2 could be recorded. In addition, the concomitant production of H_2O_2 could be detected by the peroxidase-catalyzed oxidation of o-dianisidine (data not shown). This consumption of O_2 and production of H_2O_2 depended on both DTT and Erv2-ΔN. The corresponding oxidation of DTT was confirmed by following a decrease in the reactivity of DTT with Ellman's reagent (5,5'-dithiobis-(2-nitrobenzoic acid)) (data not shown). The rate of DTT oxidation was equal within experimental error to the rate of oxygen consumption, indicating a stoichiometry of 1 mol of molecular oxygen consumed per mole of disulfide produced. The rate of O_2 consumption was saturable with increasing concentrations of DTT and the K_m of Erv2-ΔN for DTT was calculated to be 6.9 mM with a turnover number of 239 mol O_2 min^{-1} per mole Erv2-ΔN (Figure 4C). In concordance with the results from the FAD reduction assay described above, we found that the addition of glutathione to the enzyme did not cause a detectable increase in oxygen consumption or H_2O_2 production, showing that Erv2p alone will not react with glutathione. Overall, these results led to the conclusion that Erv2p can use molecular oxygen as a source of oxidizing equivalents for thiol oxidation *in vitro*.

In vivo function of Erv2p

Using the ability of *ERV2* overexpression to suppress the temperature sensitivity of *ero1-1* as a measure of Erv2p activity *in vivo*, we tested whether suppression requires O_2. Wild-type, *ero1-1*, *ero1-1* P_{GAL1}-*ERV2* and *ero1-1* P_{GAL1}-*ERO1* strains were incubated at 37 °C in an anaerobic chamber. *ERV2* was unable to rescue the *ero1-1* strain anaerobically, whereas overexpression of *ERO1* allowed the strain to grow nearly as well as the wild-type under the same conditions (Figure 5A). Thus, oxygen is necessary for Erv2p to function *in vivo* as well as *in vitro*.

Deletion of the *ERV2* gene in the *ero1-1* background significantly increases DTT sensitivity. When grown with 1 mM DTT, the double mutant grows much more slowly than *ero1-1* alone (Figure 5B). The hypersensitivity of an *ero1-1 erv2*Δ double mutant to

DTT was confirmed by determining the size of the growth inhibition zone caused by DTT on solid medium (data not shown). The Erv2p pathway is not essential for disulfide bond formation under standard growth conditions; deletion of *ERV2* in a wild-type background does not result in a disulfide bond formation defect. It is therefore likely that Erv2p is directly involved in maintaining the oxidizing conditions of the ER, although the inherent capacity for generation of oxidizing equivalents in the ER of endogenous Erv2p seems to be considerably less than that of Ero1p.

Since the cysteine residues in the Cys-X-X-Cys motif (Cys121 and Cys124) of Erv2p are conserved between the Erv2p homologues, we were interested in whether either of these residues was essential for the activity of the protein *in vivo*. The single mutants Cys121→Ala and Cys124→Ala and the Cys121→Ala,Cys124→Ala double mutant of Erv2p were generated by site-directed mutagenesis and found not to be able to suppress the temperature-sensitivity of the *ero1-1* strain (Table 1). All three mutant proteins were expressed at the same level as wild-type protein, as determined by immunoblotting (data not shown). To examine the FAD binding of the mutants, all of the mutants were expressed in *E. coli*, then purified and assayed for FAD binding by examining their absorbance spectra. All three mutants had absorbance maxima near 454 nm, and the ratio of Abs_{454} to the total protein Abs_{280} was significantly higher than the ratio for the BSA control protein. These results indicated that the cysteine mutants were able to fold normally and to bind FAD (Table 1). The activity of each of the mutants with DTT was tested with the oxygen consumption assay and none of the Erv2p Cys-X-X-Cys mutants was found to be active in this assay. These results demonstrate that the cysteine residues in the conserved Cys-X-X-Cys motif of Erv2p are required for its activity as an oxidase *in vitro* and *in vivo*.

Trapping of Pdi1p-Erv2p mixed disulfides *in vivo*

We next wished to examine the relationship between the oxidase activity of Erv2p observed *in vitro* and the oxidation of substrate proteins *in vivo*. Other pathways for protein disulfide bond formation, including Ero1p-Pdi1p in the ER and DsbB-DsbA in the bacterial periplasm, employ a protein from the thioredoxin family of thiol oxidoreductases for the purpose of disulfide transfer, suggesting that Erv2p might similarly operate in conjunction with Pdi1p or one of the yeast PDI homologues. We therefore examined whether Erv2p participates in a thiol-disulfide exchange pathway with Pdi1p.

During the transfer of a disulfide bond, a mixed-disulfide intermediate is generated when a disulfide bond in the oxidized partner is attacked by a cysteine-derived thiolate anion in the reduced partner. To assay for this mixed-disulfide intermediate, cells overproducing both Erv2p-HA and Pdi1p were labeled with [^{35}S]methionine and subsequently treated with TCA to block thiol exchange and precipitate cellular proteins. Free thiols were then blocked with the thiol-alkylating agent N-ethylmaleimide (NEM) and proteins were immunoprecipitated with anti-HA under non-reducing but denaturing conditions. Primary anti-HA immunoprecipitates were divided and reimmunoprecipitated with anti-Pdi1p or anti-HA. The most prominent species detected on the non-reducing gel have Mr values of 25K and 50K. The Mr 25K species corresponds to an Erv2p-HA monomer, whereas the Mr 50K species corresponds to an Erv2p-HA homodimer. Purified recombinant Erv2-ΔN also forms a prominent disulfide-bonded homodimer, which is evident when preparations of Erv2-ΔN are resolved on non-reducing gels (data not shown). Also evident when Erv2p-HA was immunoprecipitated from yeast extracts under non-reducing conditions were high-molecular-weight complexes that contained Pdi1p as shown by reprecipitation with anti-Pdi1p antibody (Figure 6A, lanes 1 and 2). On reduction with DTT, the high-molecular-weight complex resolved into two bands corresponding to Erv2p-HA and Pdi1p (Figure 6A, lanes 3 and 4). These results show that Erv2p can engage Pdi1p in a thiol-disulfide exchange reaction *in vivo*.

Oxidation of Pdi1p by Erv2p *in vitro*

The expected product of a disulfide transfer between Pdi1p and Erv2p is oxidized Pdi1p. Given that we had preparations of enzymatically active recombinant Erv2-ΔN, we tested the ability of pure Erv2-ΔN to oxidize purified Pdi1p *in vitro*. Functional recombinant Pdi1p was prepared in a reduced state and then incubated with Erv2-ΔN for 15 min at 30 °C. At the end of the reaction, TCA was added to preserve the oxidation state by rapidly blocking thiol exchange, and then the oxidation state of Pdi1p was assessed by reaction with the thiol-conjugating reagent 4-acetamido-4'-maleimidylstilbene-2,2'-disulphonic acid (AMS) at neutral pH. The reduced and oxidized forms of AMS-modified Pdi1p were resolved by SDS-PAGE. When reduced Pdi1p and Erv2-ΔN were mixed, Pdi1p exhibited redox changes consistent with quantitative disulfide bond transfer from Erv2p to Pdi1p (Figure 6B, lanes 4-6). Reduced Pdi1p incubated with an excess of the oxidizing agent diamide was used as the mobility standard for fully oxidized Pdi1p (Figure 6B, lane 3). The cysteine residues in the conserved Cys-X-X-Cys motif of Erv2p are required for disulfide bond transfer to Pdi1p, because mixing the Erv2-Cys121→Ala,Cys124→Ala mutant with Pdi1p did not result in the oxidation of Pdi1p (Figure 6B, lane 7). Additionally, FAD alone could not transfer oxidizing equivalents to Pdi1p in the absence of Erv2p (Figure 6B, lane 8).

Discussion

We previously identified Ero1p as a major conduit for introducing oxidizing equivalents into the lumen of the ER. Here we show that an *ero1Δ* mutant can be bypassed by overexpression of Erv2p, indicating that Erv2p can supplant Ero1p for the generation of biosynthetic protein disulfide bonds in the ER. Erv2p is an ER protein with an N-terminal hydrophobic membrane anchor and a luminal domain that binds FAD and can catalyze the formation of disulfide bonds with O_2 as an electron acceptor. Parallel physiological experiments show that the capacity of Erv2p to drive disulfide bond formation *in vivo* in an *ero1-1* mutant requires O_2 and depends on two conserved cysteine residues within Erv2p that are necessary for thiol oxidase activity *in vitro*. Erv2p seems to drive the oxidation of substrate proteins *in vivo* as part of a disulfide-bond-formation cascade involving Pdi1p.

The Erv2p sequence includes an N-terminal hydrophobic segment (amino acids 10-30) that seems to be a transmembrane anchor because Erv2p fractionates with the membrane and resists extraction by treatment with high pH or chaotropic agents. An algorithm to assess topology based on a comparison of the net charge difference between amino acid sequences flanking the transmembrane domain (Claros and von Heijne, 1994) leads to the prediction that most of Erv2p (amino acids 31-196) should reside within the lumen of the ER. We confirmed this prediction experimentally by demonstrating that Erv2p present in an isolated microsomal membrane fraction is inaccessible to protease. In parallel experiments we showed that the soluble luminal domain of Erv2p, when expressed in *E. coli*, binds tightly to FAD and uses this flavin cofactor to catalyze thiol oxidation. Similar experiments, published while this manuscript was under review, also demonstrate that Erv2p is an FAD-linked thiol oxidase present in a yeast microsomal fraction (Gerber *et al.*, 2001). These results, in addition to the recent discovery that Ero1p also binds FAD (Tu *et al.*, 2000), indicate that yeast cells contain a pool of FAD within the lumen of the ER that, in turn, implies the existence of a transporter for FAD (or $FADH_2$) in the ER membrane. Transporters for the nucleotide-sugar precursors of luminal glycosylation reactions that reside in the ER or Golgi membranes have been studied extensively (Hirschberg *et al.*, 1998), but a transporter specific for FAD derived from these organelles has not been described. It might be possible to identify this transporter biochemically by an assay for FAD transport activity in microsomal membrane preparations. Alternatively, it might be possible to use Erv2p function as the basis for a genetic screen for FAD transport mutants.

Figure 7 summarizes the relationships between the different pathways for disulfide formation and consumption that we have defined in the ER of living *S. cerevisiae* cells. The primary pathway for introducing oxidizing equivalents into the ER involves two essential proteins, Ero1p and Pdi1p (Frand *et al.*, 2000; Frand and Kaiser, 1999). Disulfide bonds that form within Ero1p are transferred, by a dithiol-disulfide exchange reaction, to the active site of Pdi1p and are then transferred to substrate proteins (Frand *et al.*, 2000). Thus, Ero1p seems to link the redox chemistry of the cell to the formation of disulfide bonds within the ER, whereas Pdi1p seems to act as a mobile carrier of oxidizing equivalents adapted for the introduction of disulfide bonds into substrate proteins. We now know of two different ways of bypassing the requirement for Ero1p in disulfide bond formation. The first is to decrease the overall load on the ER oxidation pathways. Glutathione within the ER competes with protein thiols for the oxidizing equivalents generated by Ero1p; the load on the protein oxidation pathways presented by glutathione can be greatly decreased by blocking the cellular synthesis of glutathione (Cuozzo and Kaiser, 1999). The second method of bypassing the need for Ero1p is to overexpress Erv2p. Erv2p seems to participate in a disulfide bond cascade in parallel with Ero1p. As expected, bypass *via* the Erv2p pathway is only effective during aerobic growth, when O_2 is available as an electron acceptor for Erv2p. The Erv2p pathway is not essential for disulfide bond formation under standard growth conditions, but in a sensitized genetic background with impaired Ero1p function we can detect a contribution of Erv2p to the capacity of the ER for disulfide bond formation. *ERV2* expression is induced in cells that have entered stationary phase (Stein and Lisowsky, 1998), suggesting that under these conditions Erv2p might have a larger part in providing oxidizing equivalents to the ER.

Ero1p and Erv2p differ in their use of electron acceptors. Ero1p contributes to ER oxidation in either the presence or the absence of O_2, implying that the physiological electron acceptor(s) for Ero1p is not O_2 and does not depend on O_2 for its generation. In the recent reconstruction of the Ero1p pathway *in vitro*, the oxidation of protein substrates by purified Ero1p and Pdi1p required a stoichiometric excess FAD (Tu *et al.*, 2000). Thus, for this reaction *in vitro*, the source of oxidizing equivalents seems to be added free FAD, implying that Ero1p becomes reoxidized by the acquisition of FAD from solution. Accordingly, it is possible that *in vivo* Ero1p exchanges $FADH_2$ for free FAD in the ER lumen and that free FAD and $FADH_2$ shuttle between the cytosol and ER lumen. However, it seems unlikely that this is the normal physiological mechanism for oxidation of Ero1p. The concentration of FAD in yeast cells is much less than that required for the oxidation of Ero1p *in vitro* (Gliszczynska and Koziolowa, 1998). In addition, most flavoproteins bind their cofactors tightly, which precludes the use of a catalytic cycle based on flavin exchange with solution. In contrast to what has been found for Ero1p, we show here that Erv2p binds tightly to its FAD cofactor and uses O_2 as a direct and obligatory electron acceptor. The Erv2p pathway therefore represents the first eukaryotic pathway for biosynthetic disulfide bond formation in the ER for which the ultimate electron acceptor has been defined.

The physiological implications of two parallel pathways for disulfide bond formation in the yeast ER are not yet understood. Our results demonstrate that Erv2p can transfer oxidizing equivalents directly to Pdi1p *in vivo* and *in vitro*. However, the role of the four additional PDI homologues present in the yeast ER as potential substrates for Ero1p or Erv2p has not been fully explored. An intriguing possibility is that Ero1p and Erv2p might transfer oxidizing equivalents to different PDI homologues, which in turn might perform specialized functions in the oxidation of different substrate proteins. Preliminary experiments suggest that Ero1p and Erv2p might prefer different substrates in that a dithiol-disulfide exchange reaction between Ero1p and Mpd2p has been detected (Frand and Kaiser, 1999), whereas a corresponding mixed-disulfide intermediate has not been detected between Erv2p and Mpd2p (data not shown). Although the ability to capture mixed disulfides provide strong evidence for a dithiol-disulfide transfer reaction, the mixed-disulfide species is an evanescent intermediate and there is no reason to assume that the amount of mixed disulfide should be correlated with the overall rate of disulfide transfer between proteins. Accordingly, a full description of the fluxes of disulfides from Ero1p and Erv2p to the different PDI homologues will probably require reconstitution of each of the possible exchange reactions *in vitro* and measurement of the corresponding kinetic constants.

Erv2p is a member of a family of thiol oxidases that are distributed widely among eukaryotic organisms and their viruses (Coppock *et al.*, 1998; Hofhaus *et al.*, 1999; Hoober *et al.*, 1999; Senkevich *et al.*, 2000). Although the different members of this family reside in a variety of cellular locations, a common mechanism for disulfide transfer to substrate proteins has begun to emerge. Our results show that Erv2p can operate in conjunction with Pdi1p to mediate the transfer of disulfide bonds to thiol substrate proteins within the yeast ER. Recent studies on cytoplasmic disulfide bonds that form during the maturation of vaccinia virus particles show that the vaccinia E10R protein, which is homologous to Erv2p, is responsible for the oxidation of the viral G4L gene product, which is homologous to glutaredoxin (Senkevich *et al.*, 2000). The natural substrates for oxidation by Erv1p within the mitochondrion have not been identified. However, it seems possible that the *TRX3* gene product, a thioredoxin targeted to the mitochondrial matrix, might be the oxidoreductase partner for Erv1p (Pedrajas *et al.*, 1999). Similarly, the cytoplasmic ALR proteins have been shown to have protein thiol oxidase activity (Lisowsky *et al.*, 2001). It is possible that ALR uses cytoplasmic thioredoxin or glutaredoxin as a cofactor, but the ultimate substrate for ALR is not known. Finally, although a requirement for the thioredoxin-like domain of SOX in protein disulfide formation has not been established, it seems possible that an internal disulfide transfer between the ERV-like and thioredoxin-like domains is part of the mechanism by which a disulfide bond is ultimately transferred to a substrate protein in the extracellular space.

The members of the QSOX/ERV family that are targeted to the secretory pathway can be classified into two general types, ERV-like and QSOX-like. The ERV-like sequences have a hydrophobic N terminus and are about 200 amino acids in length. Sequences of this type can be identified in fungal genomes, including *S. cerevisiae*, *Candida albicans*, *Botrytis cinerea* and *Saccharomyces pombe*. These proteins presumably function as thiol oxidases within the ER of their respective organisms. ERV-like sequences are not evident in the genomic or expressed sequence tag databases for multicellular eukaryotes, including *Arabidopsis thaliana*, *Caenorhabditis elegans*, *Drosophila melanogaster* and *Homo sapiens*. However, these metazoan genomes all encode proteins with the same overall sequence organization of QSOX (including a signal sequence, an N-terminal thioredoxin domain and a C-terminal ERV-like domain with an overall length of 400-600 amino acids). If we extrapolate from the physiological characterization of Erv2p presented here and the characterization of SOX as a secreted protein of avian egg whites, it seems that the fungi have evolved to use the ERV-like domain for biosynthetic protein disulfide formation within the ER, whereas multicellular organisms use the same domain in the context of a secreted protein for disulfide bond formation in the extracellular space.

Material and methods

Strains and growth conditions

YPD is rich medium with 2% glucose and YPGal is rich medium with 2% galactose. Some experiments were performed with YEP medium containing 2% raffinose and 1% galactose to induce the *GAL1* promoter. To grow strains under anaerobic conditions, 0.002% ergosterol and 0.5% Tween 80 were added to the medium. Anaerobic conditions were maintained in a sealed BBL GasPak chamber with a H_2 and CO_2 generator envelope (Becton Dickinson). Minimal medium (SMM) contains either 2% glucose or a specified carbon source and is supplemented with 16 amino acids not including cysteine.

Genotypes of the strains used in this study are listed in Table 2. The isolation and characterization of the *ero1-1* temperature-sensitive strain (CKY559) were as described previously (Frand and Kaiser, 1998).

The *erv2Δ* strain (CKY688) was constructed by transforming a wild-type strain (CKY8) with a linear DNA fragment containing 45 base pair segments derived from the 5' and 3' non-coding regions of *ERV2* flanking the *kanMX4* gene. This fragment was designed so that homologous recombination of the fragment would give a complete deletion of the *ERV2* coding sequence. The DNA fragment was synthesized by PCR with Vent polymerase (New England Biolabs) and the *kanMX4*-containing plasmid pFA6a-*kanMX4* (Wach *et al.*, 1994). The primers used for PCR were 5'-TTT GTA AAG AGG AAA GTC TGG ACA GAT TGT GCA AGG AAC GAA GGG CGT ACG CTG CAG GTC GAC-3' and 5'-AAA AAT TTA CTA TTA CTA TAA TTG ATT AAT GTA ATC TTT CTT TGT ATC GAT GAA TTC GAG CTC G-3'. Mutants containing the integrated *kanMX4* gene were selected on rich medium containing geneticin (20 μg ml^{-1}) and were verified by PCR amplification of the insert sequences.

The *erv2Δ ero1-1* strain (CKY689) was constructed by crossing the *erv2Δ* strain (CKY688) to a *MAT**a*** *ero1-1* strain (CKY687); the resulting *erv2Δ ero1-1* spore clones were identified by their temperature sensitivity and geneticin resistance. A sister spore clone (CKY690) of the double mutant that contained only the *ero1-1* allele was used for comparisons of growth rate and DTT sensitivity with the double-mutant strain.

The *ero1Δ* strain containing the P_{GAL1}-*ERV2* plasmid was constructed by transforming the heterozygous *ERO1/ero1Δ* diploid strain (CKY467) with P_{GAL1}-*ERV2* (pFA11; see below). The transformants were sporulated and tetrads dissected on YPGal plates. Spores containing the *ero1Δ* allele and the P_{GAL1}-*ERV2* plasmid were able to grow slowly on galactose but not at all on glucose medium.

Isolation of P$_{GAL1}$-*ERV2*

The *ero1-1* mutant strain (CKY598) was transformed with a yeast cDNA library under the regulation of the *GAL1* promoter (Liu *et al.*, 1992). Approximately 106 colonies were replica-plated onto YEP plates supplemented with 2% raffinose and 1% galactose and incubated at 37 °C for 2 d. A total of 50 colonies that grew under these conditions were analyzed. Plasmid DNA was screened by PCR with primers specific for *GAL1* promoter (5'-TGC ATA ACC ACT TTA ACT-3') and ERO1 (5'-CGT GTT CAA ATA TTC CTT TGA-3'): 45 of the plasmid preparations gave rise to a PCR product of the size expected from an *ERO1* insert. Five plasmids that did not encode *ERO1* contained the yeast ORF YPR037C, *ERV2*; a representative plasmid was named pFA11. pFA11 was re-transformed into the *ero1-1* strain (CKY598). This strain could grow at 37 °C on both minimal and rich medium containing galactose, but could not grow on glucose-containing medium at 37 °C.

Tagging of *ERV2*

The insert in pFA11 was amplified with the primers Gal1 (see above) and Erv2Coxp: 5'-ATT ACC GCG GTT AGC GGC CG CCG TGC TGT TTA GCC TCC-3' and was digested with BamHI and SacII and ligated to pFA11 digested with the same enzymes. The resulting plasmid was named pFA12. An in-frame HA tag was then ligated into the NotI site at the 3' end of *ERV2*; the resulting *P$_{GAL1}$-ERV2-HA* construct was named pFA13. *P$_{GAL1}$-ERV2-HA* from pFA13 was inserted into a centromeric plasmid marked with *LEU2* to form pJC16.

Detection of CPY, Erv2p and Pdi1p by immunoblotting

For the detection of CPY, cells were cultured in SMM lacking uracil with the addition of 2% galactose and a total of 5 OD$_{600}$ units of cells were pelleted and then suspended in 50 μl sample buffer (80 mM Tris-HCl [pH 6.8], 2% SDS, 10% glycerol, 25 mM DTT, 0.01% bromophenol blue) and boiled for 2 min. Cells were lysed by agitation with glass beads, an additional 50 μl sample buffer was added and the samples were centrifuged briefly. The equivalent of 0.75 OD$_{600}$ units of cells for each sample were subjected to SDS-PAGE (8% gel). Immunoblotting was performed as described (Elrod-Erickson and Kaiser, 1996), with anti-CPY (1:1,000 dilution) and horseradish-peroxidase

(HRP)-conjugated donkey anti-rabbit IgG (1:10,000 dilution; Amersham). Erv2p-HA immunoblots used monoclonal anti-HA antibody 16B12 (1:500 dilution; Covance) and sheep anti-mouse IgG-HRP (1:3,000 dilution, Amersham). Pdi1p immunoblots used polyclonal anti-Pdi1p antibody (1:1,000 dilution, a gift from T. Stevens, Eugene, Oregon) and donkey anti-rabbit IgG-HRP (1:10,000 dilution; Amersham). Blots were developed by chemiluminescence (ECL system; Amersham) and detected on a Kodak Image Station 440.

Localization of Erv2p

A wild-type yeast strain (CKY263) was transformed with pFA13 encoding the HA-tagged version of Erv2p. This strain was grown to exponential phase in SMM lacking uracil and containing 2% raffinose and 1% galactose; cells were suspended in 10 mM Tris-HCl [pH 7.5], 1 mM EDTA, 0.1 mM PMSF, and lysed with glass beads. Unlysed cells were removed by centrifugation at 500 g for 1 min. The resulting extract was treated with 10 mM Tris-HCl [pH 7.5], 1 mM EDTA, 0.1 mM PMSF containing 1% Triton X-100, 2.5 M urea or 0.1 M Na_2CO_3 [pH 11]. After incubation on ice for 1 h, the samples were fractionated by centrifugation at 100,000 g for 1 h. Supernatants were collected and mixed with sample buffer, and membrane pellets were solubilized in sample buffer at the same final volume as supernatants. The samples were separated by SDS-PAGE (12% gel) and Erv2p-HA was detected by immunoblotting.

For the localization of Erv2p by immunofluorescence, CKY263 containing pJC16 was grown to exponential phase in SMM lacking leucine and containing 2% galactose and 2% raffinose, and the cells were fixed with 1/10 culture volume of 37% formaldehyde. Fixed cells were treated with lyticase followed by monoclonal anti-HA 12CA5 (1:5,000 dilution; Covance) and polyclonal anti-Pdi (1:2,500 dilution; a gift from T. Stevens). A secondary Alexa 488 goat anti-mouse (1:200 dilution; Molecular Probes) and a secondary Texas Red donkey anti-rabbit antibody (1:200 dilution; Amersham) were used for the detection of Erv2p-HA and Pdi1p, respectively. Staining with 4',6-diamidino-2-phenylindole (DAPI) was used to identify the localization of the yeast nucleus. Images were acquired with a Nikon E800 microscope equipped with a charge-coupled device camera (model C4742-95; Hamamatsu) and Improvision Open lab software.

For protease accessibility experiments, CKY263 containing pJC16 was grown to exponential phase in SMM lacking leucine and containing 2% galactose and 2%

raffinose. Cells were converted to spheroplasts by digestion with lyticase, lysed by Dounce homogenization in buffer 88 (20 mM HEPES [pH 6.8], 150 mM potassium acetate, 250 mM sorbitol, 1 mM magnesium acetate) and centrifuged at 370 g. The supernatant fraction was centrifuged at 12,000 g, and the membrane fraction suspended in buffer 88 was used as the starting material for digestion with protease. Samples were treated on ice with 50 μg ml^{-1} proteinase K (Sigma) in the presence or absence of 1% Triton X-100; digestion was stopped by the addition of 40 mM PMSF. Erv2p-HA and Pdip were detected by immunoblotting. In parallel, samples of purified Erv2-ΔN were subjected to digestion with proteinase K under identical conditions. Digestion was stopped after 30 min by addition of 60 mM PMSF and Erv2-ΔN was detected by SDS-PAGE and Coomassie Blue stain.

Expression and purification of Erv2p

The *ERV2* gene was subcloned into the bacterial expression vector pET-21b(+) (Novagen) containing the T7 promoter and the His6 tag, using PCR to amplify the gene from the original library clone pFA11. To increase expression, the first 29 amino acids encoding the hydrophobic N-terminal signal sequence were not included in the bacterial expression vector. The 5' primer contains an NheI site followed by a sequence homologous to *ERV2* bases 88-120 (5'-AAA AAA GCT AGC GAA CTA TCC ATC GCT ACG CCG GGC-3'). The 3' primer contains a HindIII site followed by the reverse complement of *ERV2* bases 565-588 (5'-AAA AAA AAG CTT ACC GTG CTG TTT AGC CTC CTT CTC-3'). The *ERV2* gene was amplified with Vent polymerase and the resulting PCR product was digested with NheI and HindIII and ligated into these sites in the pET-21b(+) vector. The resulting construct (pJC11) expressed Erv2-ΔN, which corresponded to Erv2p without the signal sequence followed by an in-frame His6 tag.

The bacterial host BL21 was transformed with pJC11. A saturated 10 ml culture of this strain was diluted into 1 liter of 2 times YT plus ampicillin, grown to exponential phase, and the expression of Erv2-ΔN was induced with 1 mM isopropyl beta-D-thiogalactoside (IPTG) for 2 h at 30 °C. To maximize loading of Erv2-ΔN with flavin, FAD (Sigma) was added to a final concentration of 10 μM at the time of induction. The cells were harvested in 25 ml lysis buffer (50 mM sodium phosphate [pH 8.0], 300 mM NaCl, 10 mM imidazole, 1 mM PMSF) and were lysed by incubation for 20 min on ice with 1 mg ml^{-1} lysozyme, followed by sonication. Insoluble material was removed by centrifugation (25,000 g for 20 min) and the cleared lysate was bound to 1 ml 50% Ni-

NTA (Qiagen) resin by batch incubation for 1 h at 4 °C. The resin was washed with 20 ml 50 mM sodium phosphate [pH 8.0], 300 mM NaCl, 20 mM imidazole followed by 10 ml 50 mM sodium phosphate [pH 8.0], 300 mM NaCl, 50 mM imidazole. Bound protein was eluted with 50 mM sodium phosphate [pH 8.0], 300 mM NaCl, 250 mM imidazole and then dialyzed for 20 h against 50 mM sodium phosphate [pH 7.5], 150 mM NaCl. The dialyzed fractions were analyzed by staining with Coomassie Blue and were found to contain a major band running at a Mr of 21K, consistent with the predicted molecular mass of the Erv2-ΔN construct.

The absorbance spectrum of Erv2-ΔN was recorded on a Hewlett-Packard 8452A diode array spectrophotometer and showed peaks characteristic of a bound flavin. The flavin group of recombinant Erv2-ΔN was further characterized by fluorescence spectroscopy. The bound flavin was released by boiling a sample of the protein for 5 min in a foil-covered tube. The boiled sample was centrifuged to remove the precipitated protein, and aliquots of the supernatant were diluted 1:50 into 50 mM Tris-HCl [pH 7.5] or 10 mM HCl. The fluorescence of both samples was determined on a Hitachi F4500 fluorescence spectrophotometer with an excitation wavelength of 450 nm and an emission range of 490-600 nm. The fluorescence of the acidified supernatant at 535 nm was 4.7-fold that of the neutral solution, which is characteristic of FAD and not FMN (Faeder and Siegel, 1973).

Mutagenesis of *ERV2*

Mutants of *ERV2* that converted Cys121 or Cys124 to Ala were made with the QuikChange site-directed mutagenesis kit (Stratagene), which allowed the mutations to be made directly in pFA13. Complementary primers were used for each mutant constructed: Cys121→Ala (1), 5'-GCA GAA CTC TAT CCA GCC GGG GAA TGT TCA TAT C-3'; Cys121→Ala (2), 5'-GAT ATG AAC ATT CCC CGG CTG GAT AGA GTT CTG C-3'; Cys124→Ala (1), 5'-CTA TCC ATG CGG GGA AGC TTC ATA TCA CTT TGT AAA G-3'; Cys124→Ala (2), 5'-CTT TAC AAA GTG ATA TGA AGC TTC CCC GCA TGG ATA G-3'; both Cys residues (1), 5'-GCA GAA CTC TAT CCA GCC GGG GAA GCT TCA TAT CAC TTT GTA AAG-3'; both Cys residues (2), 5'-CTT TAC AAA GTG ATA TGA AGC TTC CCC GGC TGG ATA GAG TTC TGC-3'. The mutated plasmids were verified by sequencing, and the protein expression levels in each of the mutants were assessed by immunoblotting protein extracts from the overexpressing strains with anti-HA antibody. The mutants were subcloned into the pET-21b(+) vector by using the NheI and XhoI sites for subsequent expression in *E. coli* as His_6-tagged proteins without the N-terminal signal sequence as described above for the wild-type protein.

ERV2 **assays**

The activities of recombinant purified Erv2-ΔN and the active-site cysteine mutants were assayed by determining the rate of O_2 consumption with the use of a Clark oxygen electrode (YSI 4004). Activity was assayed at 25 °C in an oxygen-saturated (240 μM O_2) 50 mM sodium phosphate [pH 7.5] buffer. The buffer was stirred continuously throughout the assay. DTT was added first; the assay was then started by the addition of 0.17 μM Erv2-ΔN. Oxygen consumption rate was recorded as the decrease in oxygen concentration over the first 4 min after the addition of the enzyme. In control experiments, no non-enzymatic oxygen consumption was observed over the duration of the assay.

Trapping mixed disulfides between Erv2-HA and Pdi1p

A wild-type yeast strain (CKY263) containing plasmids encoding *ERV2-HA* and *PDI1* was grown to exponential phase. Cells were radiolabeled with [^{35}S]methionine and [^{35}S]cysteine (EXPRESS, NEN) for 60 min at 30 °C in SMM lacking uracil, leucine and methionine but containing 3% galactose. Extracts corresponding to 40 OD_{600} units were collected by centrifugation and suspended in 10% (w/v) TCA. Cell membranes were disrupted by agitation with glass beads and proteins were collected by centrifugation at 4 °C. Protein pellets were resuspended in urea sample buffer (50 mM Tris-HCl [pH 7.5], 2% SDS, 6 M urea, 1 mM PMSF, bromophenol blue) containing 40 mM NEM (Sigma). The pH of the samples was adjusted by the gradual addition of 1 M Tris-HCl [pH 8] until samples turned blue. After incubation on ice for 15 min and at 24 °C for 10 min, samples were diluted 1:10 in immunoprecipitation buffer (50 mM Tris-HCl [pH 7.4], 150 mM NaCl, 1% Triton X-100, 1 mM PMSF) and immunoprecipitated with monoclonal anti-HA antibody (12CA5) as described previously (Frand and Kaiser, 1998). Immunoprecipitated samples were boiled for 2 min in non-reducing sample buffer, diluted in immunoprecipitation buffer; one-quarter was reimmunoprecipitated with anti-HA antibody and three-quarters of each sample was reimmunoprecipitated with anti-Pdi1p antibody. Before electrophoresis, 0.1 M DTT was added to one-half of each sample and all samples were boiled for 2 min. Samples were analyzed by SDS-PAGE (8% gel) and proteins were revealed with a 445si PhosphorImager (Molecular Dynamics).

Expression and purification of His-tagged Pdi1p

Plasmid encoding wild-type, His_6-tagged yeast Pdi1p without the signal sequence was kindly provided by J. Winther (Copenhagen, Denmark). The *E. coli* strain BL21(DE3) containing the yPDI plasmid was grown to exponential phase in Luria-Bertani medium containing ampicillin, and expression of Pdi1p was induced with 1 mM IPTG for 4 h at 30 °C. Cells from 1 liter of culture were collected in 10 ml sonication buffer (50 mM sodium phosphate [pH 8.0], 300 M NaCl, 1 mM PMSF) and lysed by incubation for 30 min on ice with 1 mg ml^{-1} lysozyme, followed by sonication. Insoluble material was removed by centrifugation at 20,000 g for 20 min and by filtration through a 0.45 μm pore-size filter. The cleared lysate was incubated in a batch with 4 ml 50% Ni-NTA (Qiagen) resin for 1 h at 4 °C. The resin was loaded into a column, washed with 40 ml sonication buffer containing 1 mM 2-mercaptoethanol, and then with 20 ml 50 mM sodium phosphate [pH 8.0], 300 M NaCl, 20 mM imidazole, 1 mM 2-mercaptoethanol. Bound protein was eluted with 50 mM sodium phosphate [pH 8.0], 300 M NaCl, 100 mM imidazole. Fractions containing Pdi1p were pooled and dialyzed for 20 h against 50 mM sodium phosphate [pH 7.5], 150 mM NaCl.

Oxidation of Pdi1p by *ERV2 in vitro*

Purified Pdi1p was reduced by incubation with 10 mM DTT for 30 min at 30 °C. Reduced Pdi1p was diluted 1:100 to a final concentration of 3 μM in buffer containing 50 mM sodium phosphate [pH 7.5], 61.5 mM NaCl, 0.8 mM EDTA. Pdi1p samples were incubated for 15 min at 30 °C alone or in the presence of 1 mM diamide (Molecular Probes), 1, 3 or 9 μM Erv2-ΔN, 9 μM Erv2-ΔN-Cys121→Ala, Cys124→Ala or 9 μM FAD. Disulfide exchange reactions were quenched by the addition of an equal amount of 20% (w/v) TCA. Proteins were collected by centrifugation for 10 min at 4 °C and samples were washed with 200 μl acetone before resuspension in 15 μl urea sample buffer with or without 15 mM AMS (Molecular Probes). Proteins were solubilized by vortex-mixing for 15 min at 4 °C and were subsequently incubated for 15 min at 30 °C; 15 μl of 2 times non-reducing sample buffer was added to samples, which were boiled for 2 min and resolved by non-reducing SDS-PAGE (8% gel). Pdi1p was detected by immunoblotting.

References

Cabibbo, A., Pagani, M., Fabbri, M., Rocchi, M., Farmery, M.R., Bulleid, N.J. and Sitia, R. (2000) ERO1-L, a human protein that favors disulfide bond formation in the endoplasmic reticulum. *J Biol Chem*, **275**, 4827-4833.

Chivers, P.T., Prehoda, K.E. and Raines, R.T. (1997) The CXXC motif: a rheostat in the active site. *Biochemistry*, **36**, 4061-4066.

Claros, M.G. and von Heijne, G. (1994) TopPred II: an improved software for membrane protein structure predictions. *Comput Appl Biosci*, **10**, 685-686.

Coppock, D.L., Cina-Poppe, D. and Gilleran, S. (1998) The quiescin Q6 gene (QSCN6) is a fusion of two ancient gene families: thioredoxin and ERV1. *Genomics*, **54**, 460-468.

Cuozzo, J.W. and Kaiser, C.A. (1999) Competition between glutathione and protein thiols for disulphide-bond formation. *Nat Cell Biol*, **1**, 130-135.

Elrod-Erickson, M.J. and Kaiser, C.A. (1996) Genes that control the fidelity of endoplasmic reticulum to Golgi transport identified as suppressors of vesicle budding mutations. *Mol Biol Cell*, **7**, 1043-1058.

Faeder, E.J. and Siegel, L.M. (1973) A rapid micromethod for determination of FMN and FAD in mixtures. *Anal Biochem*, **53**, 332-336.

Francavilla, A., Hagiya, M., Porter, K.A., Polimeno, L., Ihara, I. and Starzl, T.E. (1994) Augmenter of liver regeneration: its place in the universe of hepatic growth factors. *Hepatology*, **20**, 747-757.

Frand, A.R., Cuozzo, J.W. and Kaiser, C.A. (2000) Pathways for protein disulphide bond formation. *Trends Cell Biol*, **10**, 203-210.

Frand, A.R. and Kaiser, C.A. (1998) The ERO1 gene of yeast is required for oxidation of protein dithiols in the endoplasmic reticulum. *Mol Cell*, **1**, 161-170.

Frand, A.R. and Kaiser, C.A. (1999) Ero1p oxidizes protein disulfide isomerase in a pathway for disulfide bond formation in the endoplasmic reticulum. *Mol Cell*, **4**, 469-477.

Gerber, J., Muhlenhoff, U., Hofhaus, G., Lill, R. and Lisowsky, T. (2001) Yeast ERV2p is the first microsomal FAD-linked sulfhydryl oxidase of the Erv1p/Alrp protein family. *J Biol Chem*, **276**, 23486-23491.

Gilbert, H.F. (1994) The formation of native disulfide bonds. In *Mechanisms of Protein folding*. (ed. Pain, R.H.), Oxford Univ. Press, New York, pp. 104-135.

Gliszczynska, A. and Koziolowa, A. (1998) Chromatographic determination of flavin derivatives in baker's yeast. *J Chromatogr A*, **822**, 59-66.

Hagiya, M., Francavilla, A., Polimeno, L., Ihara, I., Sakai, H., Seki, T., Shimonishi, M., Porter, K.A. and Starzl, T.E. (1994) Cloning and sequence analysis of the rat augmenter of liver regeneration (ALR) gene: expression of biologically active recombinant ALR and demonstration of tissue distribution. *Proc Natl Acad Sci U S A*, **91**, 8142-8146.

Hirschberg, C.B., Robbins, P.W. and Abeijon, C. (1998) Transporters of nucleotide sugars, ATP, and nucleotide sulfate in the endoplasmic reticulum and Golgi apparatus. *Annu Rev Biochem*, **67**, 49-69.

Hofhaus, G., Stein, G., Polimeno, L., Francavilla, A. and Lisowsky, T. (1999) Highly divergent amino termini of the homologous human ALR and yeast scERV1 gene products define species specific differences in cellular localization. *Eur J Cell Biol*, **78**, 349-356.

Holst, B., Tachibana, C. and Winther, J.R. (1997) Active site mutations in yeast protein disulfide isomerase cause dithiothreitol sensitivity and a reduced rate of protein folding in the endoplasmic reticulum. *J Cell Biol*, **138**, 1229-1238.

Hoober, K.L., Glynn, N.M., Burnside, J., Coppock, D.L. and Thorpe, C. (1999) Homology between egg white sulfhydryl oxidase and quiescin Q6 defines a new class of flavin-linked sulfhydryl oxidases. *J Biol Chem*, **274**, 31759-31762.

Jamsa, E., Simonen, M. and Makarow, M. (1994) Selective retention of secretory proteins in the yeast endoplasmic reticulum by treatment of cells with a reducing agent. *Yeast*, **10**, 355-370.

Laboissiere, M.C., Sturley, S.L. and Raines, R.T. (1995) The essential function of protein-disulfide isomerase is to unscramble non-native disulfide bonds. *J Biol Chem*, **270**, 28006-28009.

LaMantia, M.L. and Lennarz, W.J. (1993) The essential function of yeast protein disulfide isomerase does not reside in its isomerase activity. *Cell*, **74**, 899-908.

Lee, J., Hofhaus, G. and Lisowsky, T. (2000) Erv1p from Saccharomyces cerevisiae is a FAD-linked sulfhydryl oxidase. *FEBS Lett*, **477**, 62-66.

Lewis, T., Zsak, L., Burrage, T.G., Lu, Z., Kutish, G.F., Neilan, J.G. and Rock, D.L. (2000) An African swine fever virus ERV1-ALR homologue, 9GL, affects virion maturation and viral growth in macrophages and viral virulence in swine. *J Virol*, **74**, 1275-1285.

Lisowsky, T. (1992) Dual function of a new nuclear gene for oxidative phosphorylation and vegetative growth in yeast. *Mol Gen Genet*, **232**, 58-64.

Lisowsky, T., Lee, J.E., Polimeno, L., Francavilla, A. and Hofhaus, G. (2001) Mammalian augmenter of liver regeneration protein is a sulfhydryl oxidase. *Dig Liver Dis*, **33**, 173-180.

Liu, H., Krizek, J. and Bretscher, A. (1992) Construction of a GAL1-regulated yeast cDNA expression library and its application to the identification of genes whose overexpression causes lethality in yeast. *Genetics*, **132**, 665-673.

Lyles, M.M. and Gilbert, H.F. (1991) Catalysis of the oxidative folding of ribonuclease A by protein disulfide isomerase: dependence of the rate on the composition of the redox buffer. *Biochemistry*, **30**, 613-619.

Martin, J.L. (1995) Thioredoxin-a fold for all reasons. *Structure*, **3**, 245-250.

Pedrajas, J.R., Kosmidou, E., Miranda-Vizuete, A., Gustafsson, J.A., Wright, A.P. and Spyrou, G. (1999) Identification and functional characterization of a novel mitochondrial thioredoxin system in Saccharomyces cerevisiae. *J Biol Chem*, **274**, 6366-6373.

Pollard, M.G., Travers, K.J. and Weissman, J.S. (1998) Ero1p: a novel and ubiquitous protein with an essential role in oxidative protein folding in the endoplasmic reticulum. *Mol Cell*, **1**, 171-182.

Scherens, B., Dubois, E. and Messenguy, F. (1991) Determination of the sequence of the yeast YCL313 gene localized on chromosome III. Homology with the protein disulfide isomerase (PDI gene product) of other organisms. *Yeast*, **7**, 185-193.

Senkevich, T.G., White, C.L., Koonin, E.V. and Moss, B. (2000) A viral member of the ERV1/ALR protein family participates in a cytoplasmic pathway of disulfide bond formation. *Proc Natl Acad Sci U S A*, **97**, 12068-12073.

Simons, J.F., Ferro-Novick, S., Rose, M.D. and Helenius, A. (1995) BiP/Kar2p serves as a molecular chaperone during carboxypeptidase Y folding in yeast. *J Cell Biol*, **130**, 41-49.

Stein, G. and Lisowsky, T. (1998) Functional comparison of the yeast scERV1 and scERV2 genes. *Yeast*, **14**, 171-180.

Tu, B.P., Ho-Schleyer, S.C., Travers, K.J. and Weissman, J.S. (2000) Biochemical basis of oxidative protein folding in the endoplasmic reticulum. *Science*, **290**, 1571-1574.

Wach, A., Brachat, A., Pohlmann, R. and Philippsen, P. (1994) New heterologous modules for classical or PCR-based gene disruptions in Saccharomyces cerevisiae. *Yeast*, **10**, 1793-1808.

Table 1. Analysis of Erv2p mutants in the conserved Cys-X-X-Cys motif.

Protein	**$\mathrm{Abs}_{454}/\mathrm{Abs}_{280}$**	**Activity with 20 mM DTT (nmol O_2 min^{-1})**	**Suppression of *ero1-1* at 37 °C?**
Erv2p-WT	0.157	117	Yes
Erv2p-C121A	0.121	0	No
Erv2p-C124A	0.168	0	No
Erv2p-C121A-C124A	0.122	0	No
Albumin	0.003	0	-

C121A, Cys121→Ala; C124A, Cys124→Ala; C121A-C124A, Cys121→Ala, Cys124→Ala double mutant

Table 2. Yeast strains used in this study.

Strain	**Genotype**	**Source**
CKY8	*MATα ura3-52 leu2-3,112*	Kaiser lab collection
CKY263	*MAT***a** *ura3-52 leu2-3,112 GAL2*	Kaiser lab collection
CKY467	*MAT***a**/*α ero1Δ::LEU2/ERO1 ura3-52/ura3-52 leu2-3,112/leu2-3,112*	Kaiser lab collection
CKY598	*MAT***a** *ero1-1 ura3-52 leu2-3,112 GAL2*	Kaiser lab collection
CKY687	*MAT***a** *ero1-1 ura3-52 leu2-3,112*	Kaiser lab collection
CKY688	*MATα erv2Δ::kanMX4 ura3-52 leu2-3,112*	This study
CKY689	*MATα ero1-1 erv2Δ::kanMX4 ura3-52 leu2-3,112*	This study
CKY690	*MAT***a** *ero1-1 ura3-52 leu2-3,112*	This study

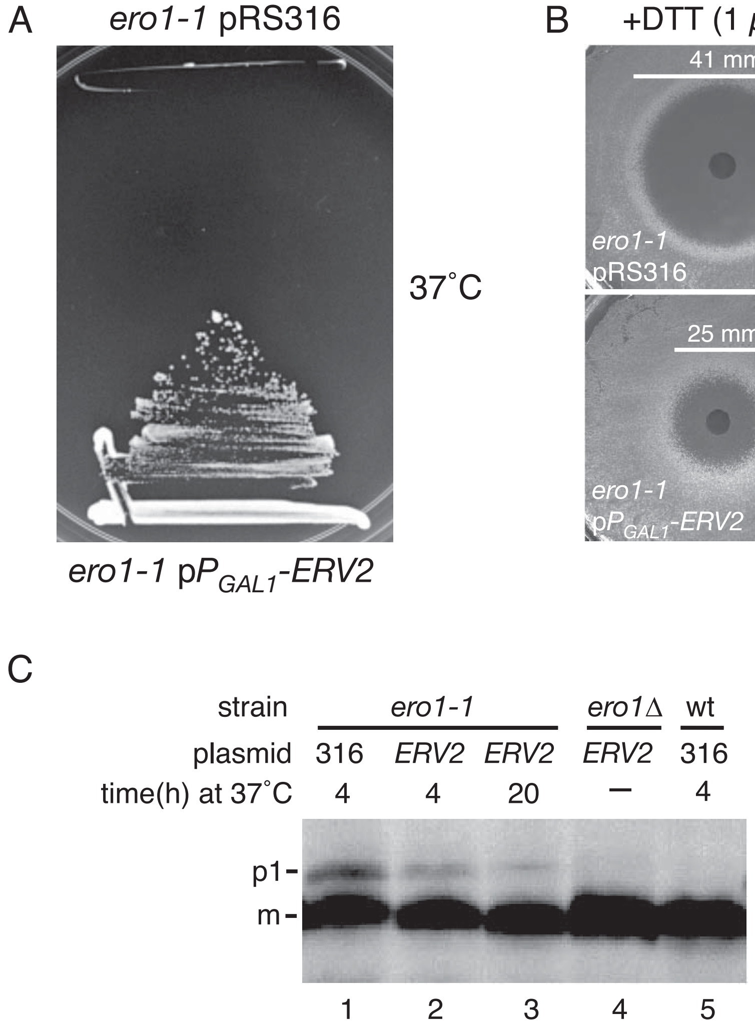
A
ero1-1 pRS316
37˚C
ero1-1 pPGAL1-ERV2
B
+DTT (1 µmol)
41 mm
ero1-1
pRS316
25 mm
ero1-1
pPGAL1-ERV2
C
strain
ero1-1
ero1Δ
wt
plasmid 316 ERV2 ERV2 ERV2 316
time(h) at 37˚C 4 4 20 — 4
p1
m
1 2 3 4 5

Figure 1. *ERV2* overexpression restores growth, resistance to DTT, and the formation of disulfide bonds to an *ero1-1* mutant. **(A)** An *ero1-1* strain (CKY598) was transformed with the control plasmid, pRS316, or with P_{GAL1}-*ERV2*. These strains were plated on minimal medium with 2% galactose and were incubated at 37 °C for 4 d. **(B)** The two strains used in (A) were plated as a lawn of 4×10^6 cells on minimal medium with 2% galactose. A 6-mm filter disk was placed in the centre of each lawn and 10 µl 0.1 M DTT was applied to the disks. The lawns were incubated for 2 d at the semi-permissive temperature of 30 °C. **(C)** Immunoblot showing the relative amounts of the ER (p1) and vacuolar (m) forms of CPY in the wild-type (WT) strain (CKY263) containing the control plasmid pRS316, and in *ero1-1* (CKY598) with either pRS316 or the P_{GAL1}-*ERV2* plasmid. The strains were grown to exponential phase at 24 °C in YPGal and then shifted to the restrictive temperature (37 °C) for the indicated durations. The *ero1Δ* P_{GAL1}-*ERV2* strain was grown in YPGal medium at 30 °C. CPY was detected by immunoblotting.

(Next page)

Figure 2. Erv2p is a membrane protein located in the ER. **(A)** Extract from cells overexpressing *ERV2-HA* (pFA13) was fractionated by centrifugation under the following conditions: 50 mM Tris-HCl [pH 7.5], 1% Triton X-100, 2.5 M urea, or 0.1 M Na_2CO_3 [pH 11.5]. The supernatant (S) and pellet (P) fractions were separated by SDS-PAGE followed by detection of Erv2p by immunoblotting for the HA epitope. **(B)** Cells overexpressing Erv2p-HA were grown to exponential phase and then fixed for microscopy. Erv2p-HA and Pdi1p are revealed by immunofluorescence (bottom left and bottom right panels, respectively), the cell bodies are observed under differential interference contrast (top left panel), and the nucleus is revealed by staining with DAPI (top right panel). **(C)** Membranes prepared from cells overexpressing Erv2p-HA were either mock-digested or treated with 50 μg ml^{-1} proteinase K in the absence or presence of 1% Triton X-100, as indicated. Digests were terminated at the indicated times with 40 mM PMSF. The samples were separated by SDS-PAGE and Erv2p and Pdi1p were detected by immunoblotting. Proteolysis fragments of Pdi1p are indicated with asterisks. **(D)** The intrinsic sensitivity of Erv2p to protease was shown by treatment of purified Erv2-ΔN with 50 μg ml^{-1} proteinase K in the absence or presence of 1% Triton X-100. Erv2-ΔN was revealed by Coomassie Blue stain. A proteolysis fragment of Erv2-ΔN is indicated by an asterisk.

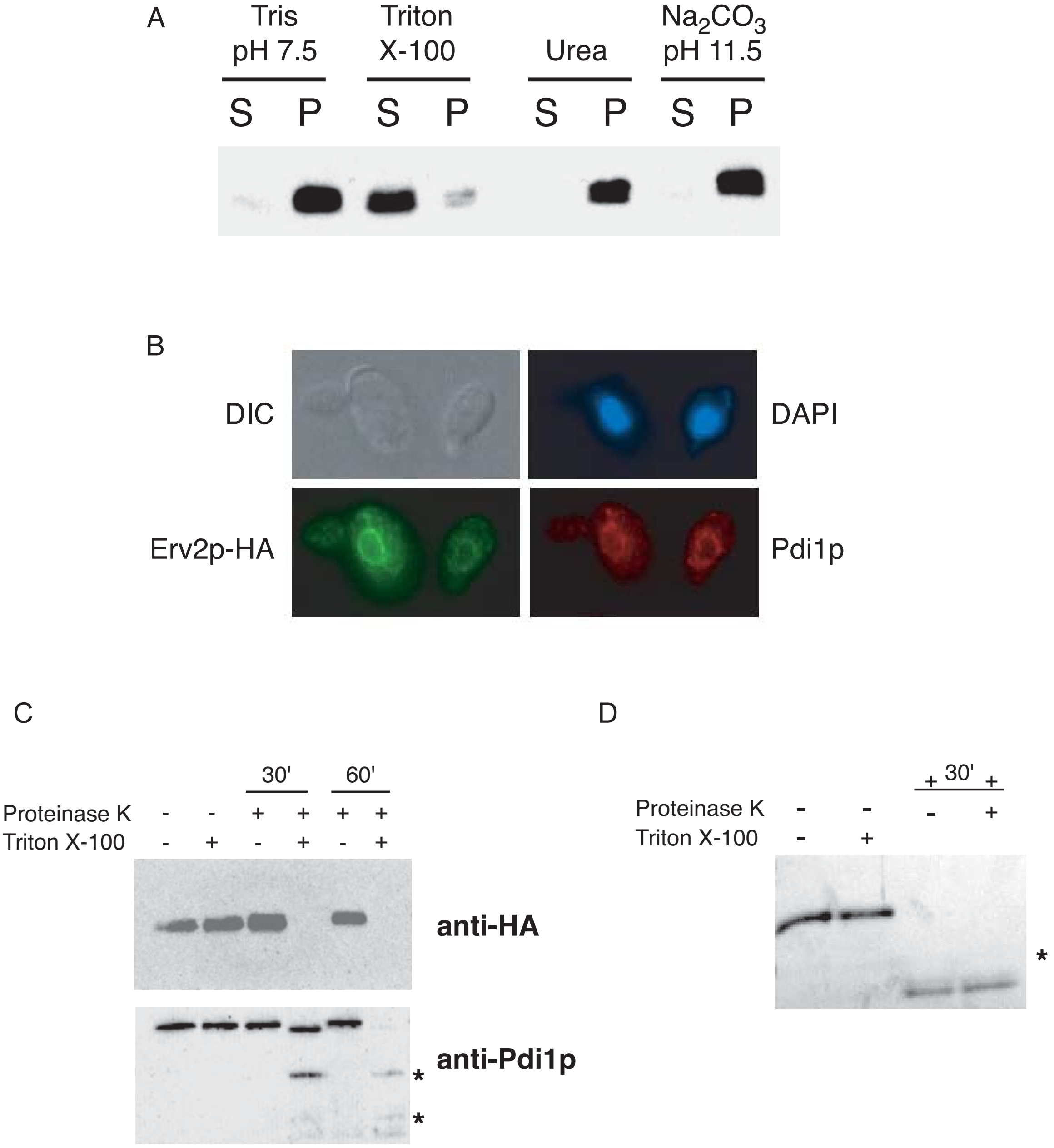
A
Tris pH 7.5
Triton X-100
Urea
Na₂CO₃ pH 11.5
S P S P S P S P
B
DIC
DAPI
Erv2p-HA
Pdi1p
C
30'
60'
Proteinase K - - + + + +
Triton X-100 - + - + - +
anti-HA
anti-Pdi1p
*
*
D
+ 30' +
Proteinase K - - - +
Triton X-100 - +
*

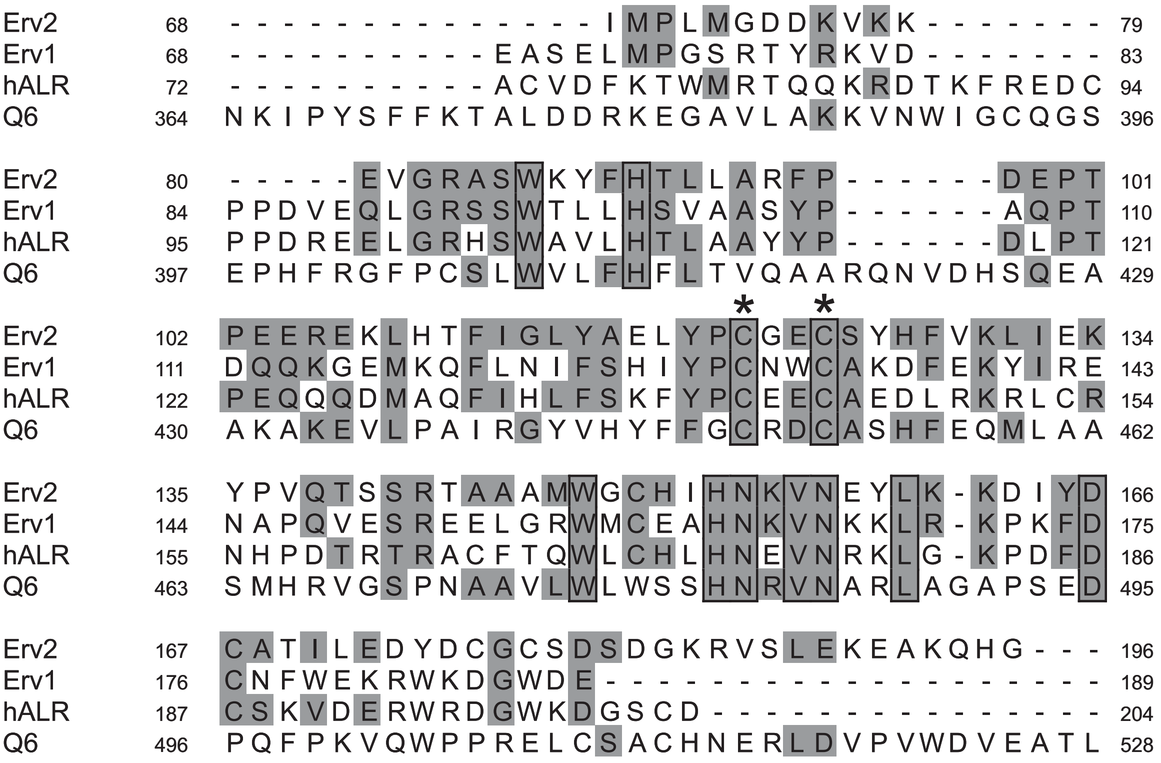

```
Erv2   68  - - - - - - - - - - - - - - I M P L M G D D K V K K - - - - - - -  79
Erv1   68  - - - - - - - - - - E A S E L M P G S R T Y R K V D - - - - - - -  83
hALR   72  - - - - - - - - - - A C V D F K T W M R T Q Q K R D T K F R E D C  94
Q6    364  N K I P Y S F F K T A L D D R K E G A V L A K K V N W I G C Q G S  396

Erv2   80  - - - - - E V G R A S W K Y F H T L L A R F P - - - - - - D E P T  101
Erv1   84  P P D V E Q L G R S S W T L L H S V A A S Y P - - - - - - A Q P T  110
hALR   95  P P D R E E L G R H S W A V L H T L A A Y Y P - - - - - - D L P T  121
Q6    397  E P H F R G F P C S L W V L F H F L T V Q A A R Q N V D H S Q E A  429

                                               *     *
Erv2  102  P E E R E K L H T F I G L Y A E L Y P C G E C S Y H F V K L I E K  134
Erv1  111  D Q Q K G E M K Q F L N I F S H I Y P C N W C A K D F E K Y I R E  143
hALR  122  P E Q Q Q D M A Q F I H L F S K F Y P C E E C A E D L R K R L C R  154
Q6    430  A K A K E V L P A I R G Y V H Y F F G C R D C A S H F E Q M L A A  462

Erv2  135  Y P V Q T S S R T A A A M W G C H I H N K V N E Y L K - K D I Y D  166
Erv1  144  N A P Q V E S R E E L G R W M C E A H N K V N K K L R - K P K F D  175
hALR  155  N H P D T R T R A C F T Q W L C H L H N E V N R K L G - K P D F D  186
Q6    463  S M H R V G S P N A A V L W L W S S H N R V N A R L A G A P S E D  495

Erv2  167  C A T I L E D Y D C G C S D S D G K R V S L E K E A K Q H G - - -  196
Erv1  176  C N F W E K R W K D G W D E - - - - - - - - - - - - - - - - - - -  189
hALR  187  C S K V D E R W R D G W K D G S C D - - - - - - - - - - - - - - -  204
Q6    496  P Q F P K V Q W P P R E L C S A C H N E R L D V P V W D V E A T L  528
```

Figure 3. Erv2p contains a conserved domain shared between yeast and human proteins. The amino acid sequences of Erv2p, the yeast homologue Erv1p and the human proteins ALR (hALR; NCBI accession no. CAB87993) and quiescin Q6 (Q6; NCBI accession no. NP_002817) were aligned with CLUSTALX. Conserved residues are boxed and homologous amino acids shared between Erv2p and at least one other sequence are shaded. The conserved cysteine residues in the Cys-X-X-Cys motif, Cys121 and Cys124 in the Erv2p sequence, are indicated with asterisks.

(next page)

Figure 4. Erv2p is a flavin-binding thiol oxidase that consumes oxygen to form disulfide bonds. **(A)** The absorbance spectrum of 23 μM purified recombinant Erv2-ΔN in 50 mM sodium phosphate [pH 7.5] was recorded from 300 to 600 nm. The absorbance spectrum of 20 μM FAD in is shown for comparison. **(B)** Recombinant Erv2-ΔN was diluted to a concentration of 4 μM in 50 mM sodium phosphate [pH 7.5]; DTT was added to 5 mM and the change in flavin absorbance at 454 nm was recorded. **(C)** The variation in rate of oxygen consumption (nmol O_2 min^{-1}) by Erv2-ΔN with DTT concentration was measured by using an oxygen electrode. The concentration of Erv2-ΔN in these assays was 0.17 μM. The kinetic constants reported in the text were obtained from an Eadie-Hofstee plot of the data (inset).

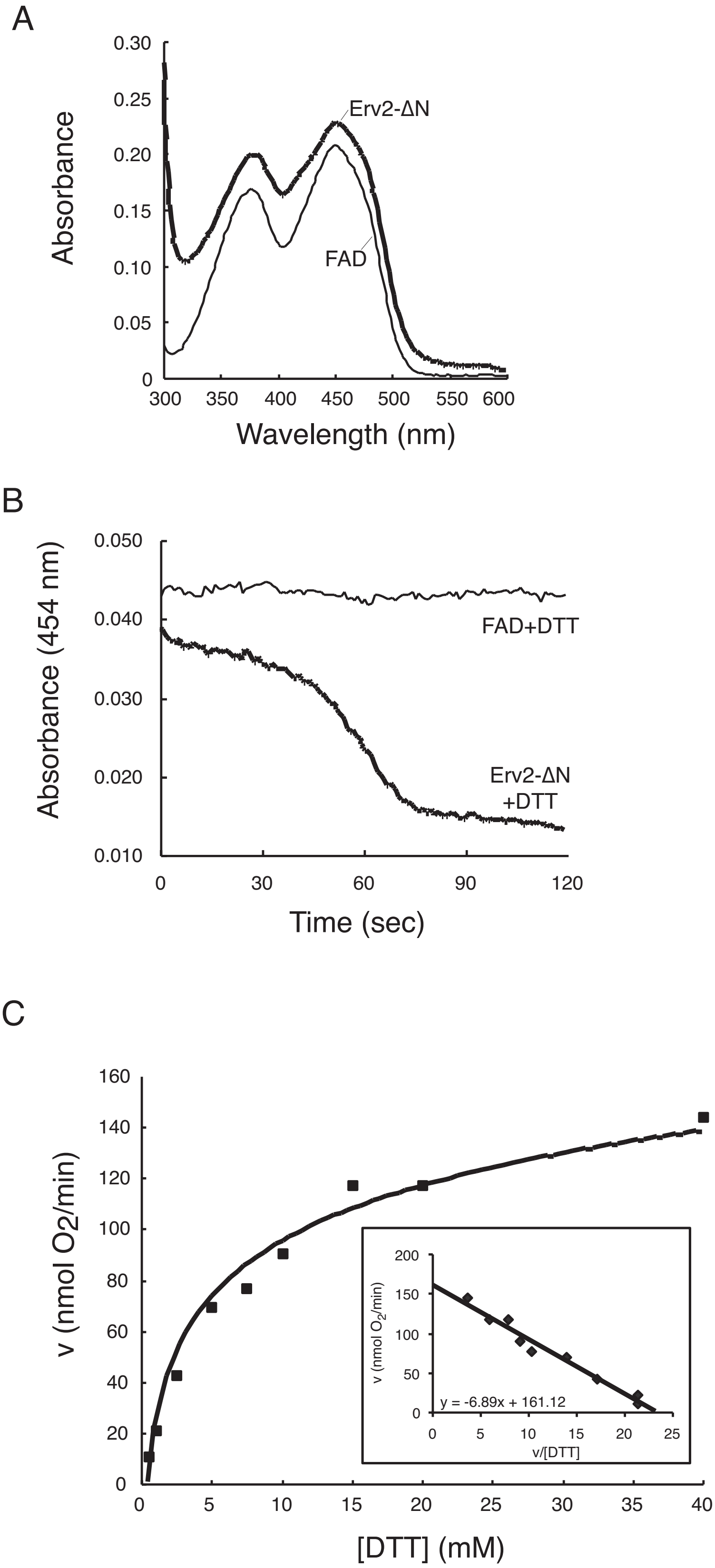
A
Absorbance
0.30
0.25
0.20
0.15
0.10
0.05
0
300
350
400
450
500
550
600
Wavelength (nm)
Erv2-ΔN
FAD
B
Absorbance (454 nm)
0.050
0.040
0.030
0.020
0.010
0
30
60
90
120
Time (sec)
FAD+DTT
Erv2-ΔN
+DTT
C
v (nmol O2/min)
160
140
120
100
80
60
40
20
0
0
5
10
15
20
25
30
35
40
[DTT] (mM)
v (nmol O2/min)
200
150
100
50
0
0
5
10
15
20
25
v/[DTT]
y = -6.89x + 161.12

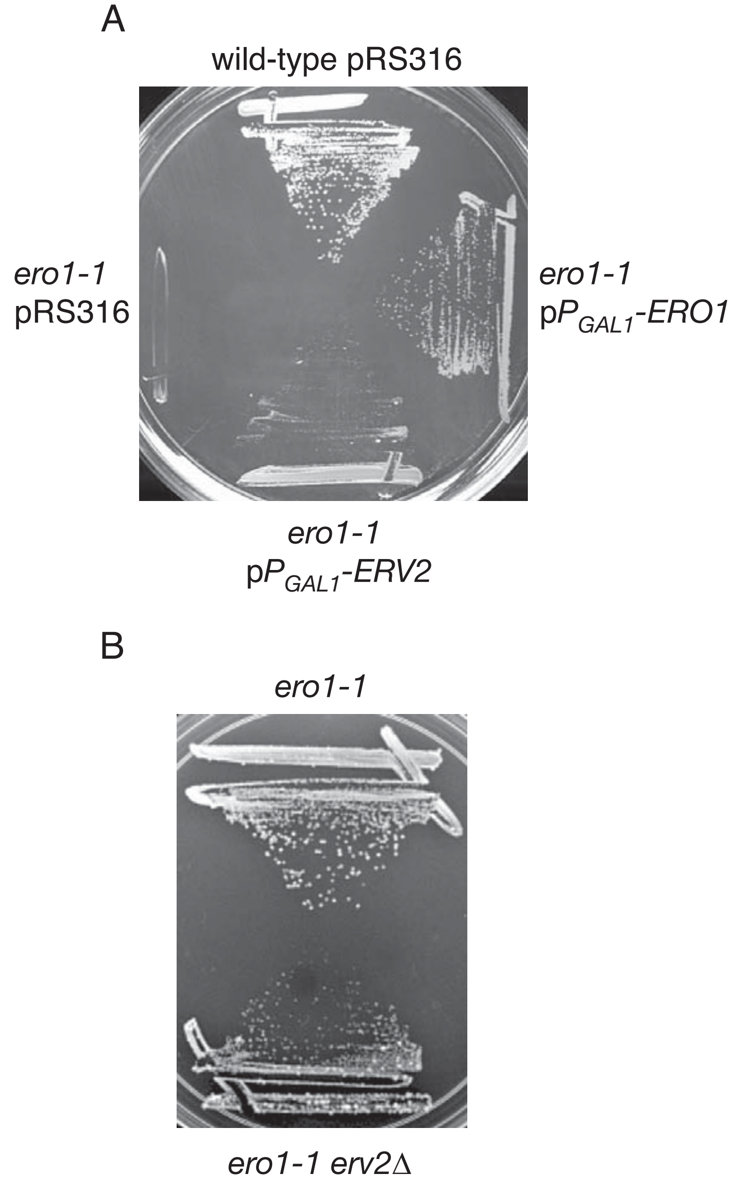
A
wild-type pRS316
ero1-1
pRS316
ero1-1
pP_{GAL1}-ERO1
ero1-1
pP_{GAL1}-ERV2
B
ero1-1
ero1-1 erv2Δ

Figure 5. Erv2p uses oxygen in a pathway for thiol oxidation *in vivo*. **(A)** The *ero1-1* strain (CKY598) containing a control plasmid, pRS316, P_{GAL1}-*ERV2* or P_{GAL1}-*ERO1*, along with the wild-type strain (CKY263) containing pRS316 were plated on YPGal medium containing ergosterol and Tween 80, and incubated under anaerobic conditions at 37 °C for 6 d. **(B)** The *ero1-1 erv2Δ* (CKY689) and *ero1-1* (CKY690) strains were plated on YPD medium containing 1 mM DTT and incubated for 2 d at 30 °C.

(Next page)

Figure 6. Erv2p transfers oxidizing equivalents to Pdi1p *via* a direct thiol-disulfide exchange. **(A)** Radiolabeled cells overproducing Erv2p-HA and Pdi1p were lysed in 10% TCA and free thiols were alkylated with NEM before immunoprecipitation with anti-HA under non-reducing conditions. The samples were reimmunoprecipitated with either anti-Pdi1p or anti-HA, as indicated. Before electrophoresis, half of each sample was reduced with DTT (lanes 3 and 4) and the remaining samples were analyzed under non-reducing conditions (lanes 1 and 2). Three times the amount of material was used in the anti-Pdi1p immunoprecipitations than in the anti-HA samples. **(B)** Reduced Pdi1p (3 μM) was incubated in buffer with 50 mM sodium phosphate [pH 7.5], 61.5 mM NaCl, 0.8 mM EDTA, 0.1 mM DTT either alone (lanes 1 and 2) or with the following additions: 1 mM diamide (lane 3); 1, 3 or 9 μM Erv2-ΔN (lanes 4, 5 and 6, respectively); 9 μM Erv2-ΔN-Cys121→Ala, Cys124→Ala (lane 7) or 9 μM FAD (lane 8). All samples were incubated at 30 °C for 15 min before trapping of thiols with 10% TCA followed by alkylation with AMS. Samples were resolved by SDS-PAGE and Pdi1p was detected by immunoblotting. The reduced (red.) and oxidized (ox.) forms of Pdi1p are indicated.

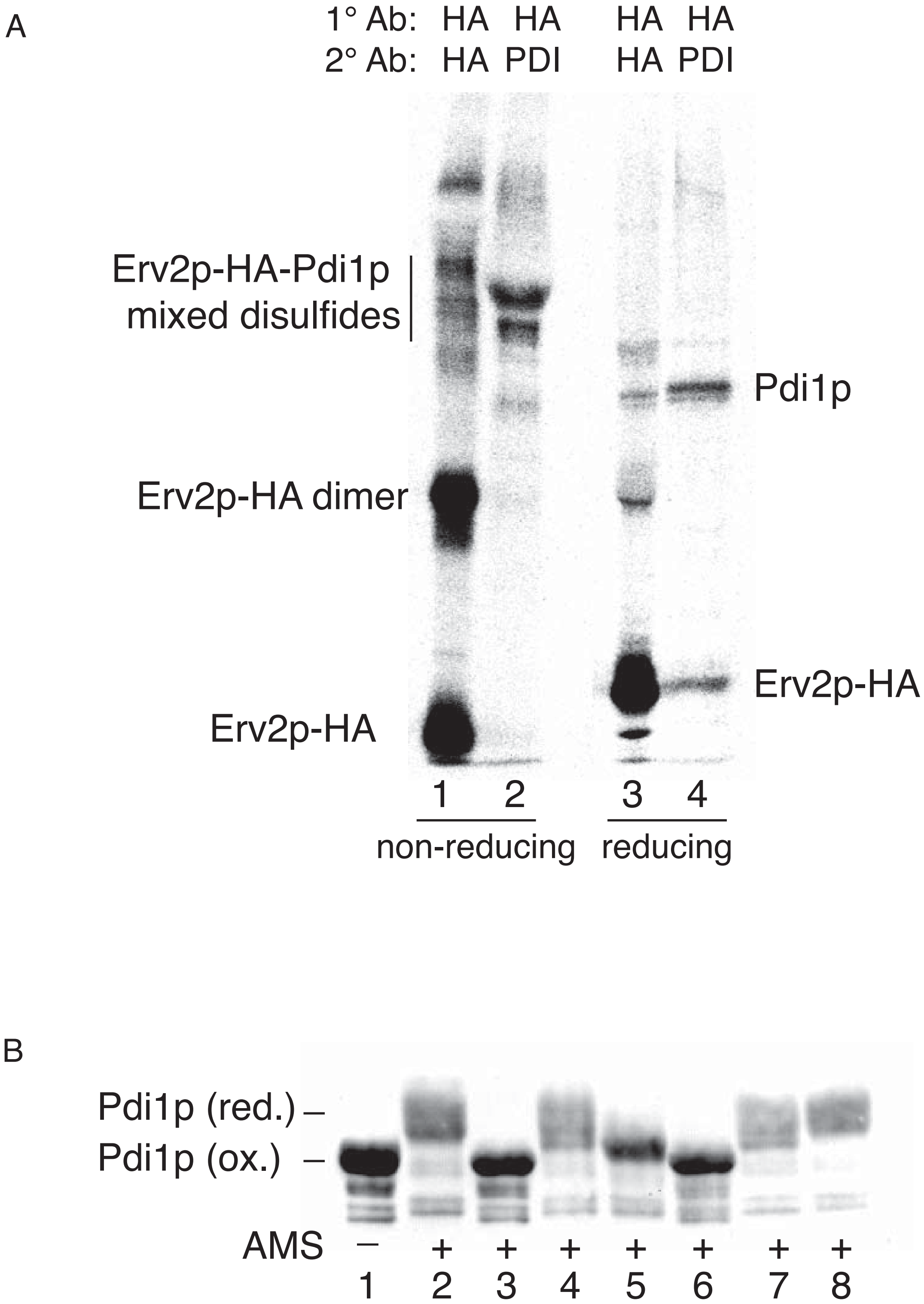
A
1° Ab: HA HA HA HA
2° Ab: HA PDI HA PDI
Erv2p-HA-Pdi1p mixed disulfides
Erv2p-HA dimer
Erv2p-HA
Pdi1p
Erv2p-HA
1 2 3 4
non-reducing
reducing
B
Pdi1p (red.)
Pdi1p (ox.)
AMS – + + + + + + +
1 2 3 4 5 6 7 8

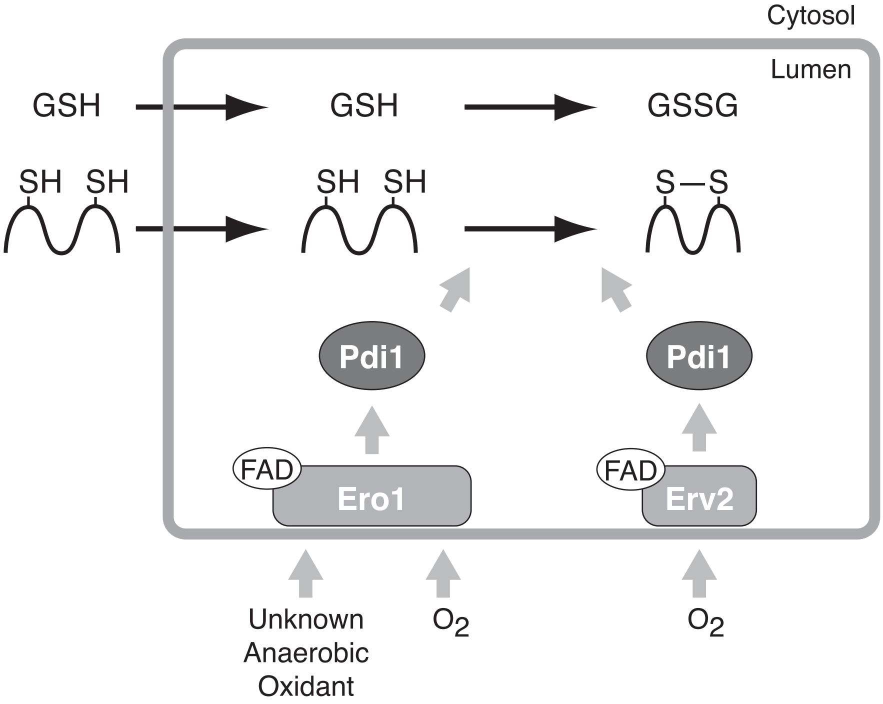
Cytosol
Lumen
GSH
GSH
GSSG
SH SH
SH SH
S—S
Pdi1
Pdi1
FAD
Ero1
FAD
Erv2
Unknown Anaerobic Oxidant
O2
O2

Figure 7. Pathways for thiol oxidation in the ER. Black arrows represent the entry of free thiols into the ER either as cysteine residues on newly translocated polypeptides or as reduced glutathione (GSH), which enters the ER by an unknown mechanism. Two different pathways exist for the flow of oxidizing equivalents into the ER, as represented by grey arrows. In the first pathway, disulfide bonds are transferred from Ero1p to Pdi1p and then to substrate proteins. Ero1p itself can be oxidized in either the presence or the absence of O_2 and might use FAD as a cofactor. In the second pathway, Erv2p uses luminal FAD as a cofactor and is oxidized directly by O_2. Erv2p also transfers disulfide bonds to Pdi1p before substrate oxidation. GSSG, oxidized glutathione.

New FAD-binding fold and intersubunit disulfide shuttle in the thiol oxidase Erv2p

Abstract

Erv2p is an FAD-dependent sulfhydryl oxidase that can promote disulfide bond formation during protein biosynthesis in the yeast endoplasmic reticulum. The structure of Erv2p, determined by X-ray crystallography to 1.5 Å resolution, reveals a helix-rich dimer with no global resemblance to other known FAD-binding proteins or thiol oxidoreductases. Two pairs of cysteine residues are required for Erv2p activity. The first (Cys-Gly-Glu-Cys) is adjacent to the isoalloxazine ring of the FAD. The second (Cys-Gly-Cys) is part of a flexible C-terminal segment that can swing into the vicinity of the first cysteine pair in the opposite subunit of the dimer and may shuttle electrons between substrate protein dithiols and the FAD-proximal disulfide.

Introduction

Disulfide bonds stabilize many secreted proteins, cell-surface proteins and proteins residing in intracellular membrane-bound compartments. The primary disulfide-bond donor in eukaryotes is the endoplasmic reticulum oxidoreductin 1 protein (Ero1p) (Frand and Kaiser, 1998; Pollard *et al.*, 1998). Ero1p is an essential membrane-associated (Frand and Kaiser, 1998) flavoenzyme (Tu *et al.*, 2000) that directly oxidizes a member of the thioredoxin fold family, protein disulfide isomerase (PDI) (Frand and Kaiser, 1999), a soluble factor that in turn oxidizes a wide variety of target proteins (Noiva, 1999).

A screen for proteins that restore viability to an Ero1p mutant when overexpressed in yeast uncovered Erv2p (Sevier *et al.*, 2001). Although Erv2p is normally expressed only under certain growth conditions (Stein and Lisowsky, 1998) and deletion of the *ERV2* gene is not lethal (Stein and Lisowsky, 1998), Erv2p expressed under a heterologous promoter efficiently rescues the temperature-sensitive *ero1-1* mutant at the non-permissive temperature (Sevier *et al.*, 2001). Prior to these experiments, Erv2p had been recognized (Gerber *et al.*, 2001; Stein and Lisowsky, 1998) as a homolog of the essential for respiration and viability 1 protein (Erv1p), a mitochondrial FAD-binding sulfhydryl oxidase (Lee *et al.*, 2000). In recent years, additional homologs have been discovered, including a hepatotrophic growth factor called ALR (augmenter of liver regeneration) (Hagiya *et al.*, 1994) and virally encoded enzymes that promote disulfide-bond formation in poxvirus coat proteins (Senkevich *et al.*, 2000), which assemble in the reducing environment of the cell cytosol. A domain homologous to Erv2p is fused to a thioredoxin-like domain in a family of proteins (Hoober *et al.*, 1999a) that includes an egg white sulfhydryl oxidase (Hoober *et al.*, 1999b) and Quiescin Q6, a protein that is highly expressed (Coppock *et al.*, 1998) and secreted (Coppock *et al.*, 2000) when fibroblasts enter quiescence. Although enzymes bearing the ERV-like domain differ in their protein substrates, a key feature of these enzymes appears to be the ability to catalyze the reaction $2R\text{-}SH + O_2 \leftrightarrows R\text{-}S\text{-}S\text{-}R + H_2O_2$. Thus, the basic sulfhydryl oxidase module of the Erv2p family can exist in a variety of compartmental and quaternary structural contexts to serve diverse physiological functions.

The Erv2p family has unusual features for sulfhydryl oxidoreductase flavoproteins. According to sequence alignments, the FAD-binding domain appears to comprise only ~100 residues, making it considerably smaller than typical flavin binding oxidoreductases (Senkevich *et al*., 2000). Furthermore, the secondary structure prediction for Erv2p suggested a highly α-helical protein (Senkevich *et al*., 2000). In contrast, classical FAD-binding folds (Fraaije and Mattevi, 2000) and the thioredoxin fold contained within other known endoplasmic reticulum (ER) (Kemmink *et al*., 1996; Kemmink *et al*., 1999) and bacterial periplasmic (Martin *et al*., 1993; McCarthy *et al*., 2000) thiol oxidoreductases are mixed α/β structures. Finally, FAD-binding thiol oxidoreductases that have been studied in depth, such as thioredoxin reductase, glutathione reductase and dihydrolipoamide dehydrogenase, use NADH (or NAD^+) as a substrate, whereas the Erv2p family uses O_2 as an electron acceptor. For the above reasons, Erv2p-like proteins differ from the flavoprotein families as currently described (Massey, 1995; van Berkel *et al*., 1999).

Results and discussion

Crystallization of the Erv2p thiol-oxidase module

To begin to elucidate the mechanism of the newly described class of disulfide bond donor enzymes to which Erv2p belongs and to further our understanding of the origin of the disulfide-rich environment of the ER, we determined the structure of Erv2p by X-ray crystallography. Erv2p retains its N-terminal signal sequence *in vivo* and remains fixed in the ER membrane (Sevier *et al*., 2001). For crystallization, we expressed a soluble fragment of Erv2p, called Erv2-ΔN, which lacks the signal sequence and begins at Glu30 (Figure 1). The first crystals obtained were found to be proteolytically cleaved to a shorter fragment beginning in the vicinity of Thr67, as determined by N-terminal peptide sequencing of the major degradation product in the crystallization stock solution. Data were collected to 2.0 Å resolution from these crystals, which were of space group $P2_1$ with unit cell dimensions a = 53.6 Å, b = 66.8 Å, c = 60.4 Å and β = 91.4°, and four molecules per asymmetric unit.

To increase the reproducibility of crystallization, a limited proteolysis step was added to the Erv2-ΔN purification procedure. Cleavage with thermolysin removed an N-terminal fragment, leaving a protease-resistant domain. The predominant N-terminal residue of this stable product was Leu71, and the molecular weight obtained by mass spectrometry was 13,395 ± 10 Da. This mass is consistent with Ser187 being the C-terminal residue of the protease-resistant domain (Figure 1), which gives a calculated mass of 13,390 Da. This fragment spans the region of high sequence homology with other proteins of the family and will be referred to as Erv2-core (Erv2-c).

The protease-resistant fragment Erv2-c was compared by circular dichroism (CD) spectroscopy to Erv2-ΔN. Both intact and truncated enzymes gave CD spectra typical of highly helical proteins (Figure 2). Subtraction of the spectrum for Erv2-c from that of Erv2-ΔN yielded a difference spectrum typical of an irregular structure. The lack of fixed secondary structure and the extreme protease sensitivity of the N-terminal 40 residues of Erv2-ΔN suggest that this region is flexible. Thus, Erv2-c comprises the structural core of the Erv2p protein. The FAD bound to Erv2-c is sensitive to reduction by concentrations of dithiothreitol (DTT) that do not reduce free flavin, demonstrating that Erv2-c is catalytically active (data not shown).

Erv2-c crystals nucleated poorly but grew rapidly under a variety of conditions when seeded from existing crystals. Data were collected to 1.5 Å from a crystal of space group $P2_1$, unit cell dimensions a = 47.6 Å, b = 45.2 Å, c = 53.8 Å and β = 100.2°, with two molecules per asymmetric unit. Crystals were grown with SeMet in place of the single methionine residue in the domain, and phases were obtained by multiwavelength anomalous dispersion (MAD). The structure built into the MAD electron density maps of Erv2-c was used in molecular replacement to provide phases for diffraction data from the crystal of degraded Erv2-ΔN. The structures were then refined independently for each crystal form.

New fold for FAD binding proteins

In total, six copies of the Erv2p protomer were observed between the two crystal forms, distributed as two dimers in the crystals grown from the Erv2-ΔN preparation (one is shown in Figure 3) and one dimer in the crystals of Erv2-c. Most of Erv2-c is structurally similar in all six protomers; the region between Asp75 and Tyr174 has an average root mean square (r.m.s.) deviation of 0.30 Å for backbone atoms. This region contains a four-helix bundle (helices $\alpha1$–$\alpha4$) and an additional single turn of helix ($\alpha5$) packed perpendicular to the bundle (Figure 3C). The $\alpha4$ helix (Arg142-Tyr159) crosses $\alpha3$ at an angle of ~50°, which is typical of helix-crossing angles in globular proteins but not in four-helix bundles (Kamtekar and Hecht, 1995). The $\alpha3$ helix (Gly122-Lys134) is at an ~30° angle to $\alpha2$, and $\alpha4$ makes an ~20° angle with $\alpha1$. The C terminus of $\alpha4$ splays out from the N terminus of $\alpha1$, and FAD binds between these helices (Figure 3C). The $\alpha1$ and $\alpha2$ helices (Asp75-Ala94 and Pro102-Leu118, respectively) are nearly antiparallel to one another and form the dimer interface by packing against the symmetry-related helices at an angle of ~55°. The dimer interface is hydrophobic with a contact area of ~700 Å^2, and the hydrophobic nature of 10 residues in the interface is conserved among homologs.

A search using DALI (Holm and Sander, 1996) for folds similar to that of Erv2p returned relatively weak matches with other four-helix bundle proteins. The three highest-scoring proteins were the transmembrane subunit c of ATP synthase (PDB accession code 1C17, Z-score 4.5, r.m.s. deviation 2.9 Å over 76 residues), cytochrome c' (1CPQ, Z-score 4.1, r.m.s. deviation 4.1 Å over 81 residues) and myohemerythrin (2MHR, Z-score 3.9, r.m.s. deviation 3.4 Å over 71 residues). The first match is likely to arise from the fortuitous convergence of topology and helix-helix crossing angles in two proteins that are otherwise unrelated (ATP synthase subunit c helices are much longer and are membrane-imbedded). Cytochrome c' and myohemerythrin are more similar to Erv2-c in that they are soluble and bind cofactors. Furthermore, cytochrome c' is involved in electron transport and myohemerythrin transports oxygen, whereas Erv2p transfers electrons from sulfhydryl groups to oxygen. However, Erv2p helix α3 aligns very poorly to cytochrome c' and myohemerythrin, and Erv2p appears to be an atypical member of the four-helix bundle fold family. To our knowledge, Erv2p is the first FAD-binding protein found to belong to the 'all α' fold class.

Key structural and functional residues in the fold

Among proteins that are related by homology to Erv2p (Senkevich *et al.*, 2000), conserved residues are predominantly in the FAD-binding site. For example, the lack of an amino acid side chain at Gly82 accommodates the flavin. The invariant Trp86 packs against the *si* face of the isoalloxazine ring and is in position to make a hydrogen bond to the hydrocarbon tail of the FAD flavin unit. The conserved Tyr119 packs against the *re* face of the FAD. His153 packs between Trp86 and the adenine ring of the FAD, and is also poised to interact with a FAD phosphate group. Residue 165 is either a Tyr or a Phe residue in all family members, and the side chain of this residue backs the adenine on the opposite face from His153. This series of aromatic residues, with intercalation of the isoalloxazine ring and adenine portions of the FAD, mimics base stacking in polynucleotides (Figure 4).

The only other non-Cys amino acid, aside from Trp86, that is invariant in all family members is Asn157. This residue is in position to make hydrogen bonds from its side chain NH_2 group to N7 of the FAD adenine moiety and to the side chain of Asn154. In addition, Asn147 makes water-mediated contacts *via* its side chain carbonyl group to the AMP phosphate group of the FAD and to a hydroxyl group in the flavin unit of the FAD. The FAD assumes a roughly semicircular structure so that the ribose and phosphates remain exposed to solvent while the two ends of the cofactor are buried (Figure 4).

Of the six Cys residues in Erv2p, only the two in the active-site Cys-X-X-Cys motif are conserved in every known family member. The Erv2p Cys-Gly-Glu-Cys sequence, like the Cys-X-X-Cys motif in thioredoxin, is found at the N terminus of a helix - in this case, $\alpha 3$ - and these Cys residues are disulfide-bonded to each other (Figure 5). Similar to *Escherichia coli* thioredoxin reductase (Kuriyan *et al.*, 1991), but different from glutathione reductase (Schulz *et al.*, 1978), the Erv2p active site Cys residues are on the *re* face of the FAD isoalloxazine ring (Figure 5). Erv1p, Erv2p and ALR, but not quiescin or the viral enzymes, share a second Cys pair found at positions 150 and 167 in Erv2p. These Cys residues form a disulfide bond near the adenine portion of the FAD and fix the short C-terminal helix $\alpha 5$ against the side of helix $\alpha 4$ (Figure 3B and C).

Erv2p structure suggests a disulfide relay mechanism

The final two Cys residues of Erv2p, Cys176 and Cys178, are disulfide bonded to each other in the C-terminal tail of the enzyme. Disulfide bonds between Cys residues separated by a single amino acid are extremely rare, with only a few examples in the protein structure database. For example, a disulfide bond is found within a Cys-Ser-Cys sequence in a Mengo encephalomyelitis virus coat protein (Krishnaswamy and Rossman, 1990) and within a Cys-Asp-Cys sequence in a thermostable serine protease (Smith *et al.*, 1999). As determined biochemically, but not yet crystallographically, a Cys-X-Cys sequence involved in coordination of zinc in the inactive form of the heat shock protein Hsp33 forms a disulfide bond (Barbirz *et al.*, 2000) upon conversion to the active chaperone conformation (Jakob *et al.*, 1999; Graumann *et al.*, 2001). Equilibrium constants for formation of small disulfide bonded loops are lower for Cys-X_m-Cys motifs when m equals one than for any other value of m from zero to five (Zhang and Snyder, 1989). Site-directed mutation of the thioredoxin active site from Cys-Gly-Pro-Cys to Cys-Ala-Cys produced an ineffective reducing agent that tended to form dimers when oxidized, thereby avoiding closure of the 11-membered ring, which would be formed upon disulfide bonding between the Cys residues of Cys-Ala-Cys (Gleason *et al.*, 1990). When strained disulfide bonds form, they become good oxidizing agents; a disulfide bond in the Erv2p Cys-Gly-Cys sequence is expected to transfer readily to substrate protein dithiols.

Although residues after Ser179 in the Erv2-c structure could not be traced in the electron density maps, the region from Asp175 to Ser179, including the disulfide bond between Cys176 and Cys178, was clearly observed in either of two conformations (Figure 6). In three of the six copies of the protomer (both chains in one dimer and one chain of another dimer), this C-terminal tail swings away from the dimer interface, and the Cys-Gly-Cys region packs back against the α5 helix of the same protomer. In the remaining three molecules, the tail extends away from the α5 helix and lies across the active site of the opposite subunit in the dimer. The Cβ atom of Cys178 approaches within ~4 Å of the Cβ of Cys121 (as opposed to 14 Å in the alternate conformation), and a mere change in the side chain torsion angles of these residues would permit formation of a disulfide bond between them (Figure 6, inset).

An intersubunit disulfide bond was detected between Erv2p protomers *in vivo*. When an epitope-tagged version of Erv2p was immunoprecipitated from yeast cells under denaturing, non-reducing conditions, bands corresponding to Erv2p monomer and dimer were apparent after electrophoresis on a non-reducing SDS-PAGE gel (Figure 7A). Addition of DTT prior to electrophoresis converted all of Erv2p to the monomeric species, confirming that the upper band represents disulfide bonded Erv2p protomers (Figure 7A).

To determine which Cys residues are required for the formation of the intersubunit disulfide bond, we constructed mutant forms of the enzyme containing Cys-to-Ala substitutions. A disulfide-linked dimer of Erv2p was not detected when Cys121 or both Cys176 and Cys178 were mutated (Figure 7B, lanes 2 and 7), confirming that these Cys residues are necessary for the formation of an intersubunit disulfide bond. The individual replacement of either Cys176 or Cys178 with Ala did not significantly alter the amount of disulfide-linked dimer formed, suggesting that the C-terminal tail has sufficient conformational flexibility to allow either Cys176 or Cys178 to form a disulfide with Cys121 (Figure 7B, lanes 5 and 6).

A simple test of the activity of Erv2p mutants *in vivo* is their ability, when overexpressed, to suppress the temperature sensitivity of an *ero1-1* mutant (Sevier *et al.*, 2001). Each of the individual Cys mutants was placed under control of the powerful *GAL1* promoter and tested for the ability to suppress the lethality of *ero1-1* at the restrictive temperature. The P_{GAL1}-*ERV2* plasmid bearing a wild-type copy of Erv2p restored growth to the *ero1-1* mutant at 37 °C (Sevier *et al.*, 2001). However, none of the Cys mutants expressed to approximately the same levels from the same plasmid, including single mutants in the Cys-Gly-Cys sequence, had the capacity to suppress *ero1-1*, showing that they lack activity *in vivo* (Figure 7C). The wild-type enzyme may function by accepting electrons from target proteins to open the Cys-Gly-Cys disulfide, which is reoxidized by shuttling electrons to the FAD-proximal Cys-Gly-Glu-Cys disulfide.

Secondary Cys-X_n-Cys motifs in Erv2p homologs

Although Erv2p is the only member of the family with a Cys-X-Cys motif, a similar disulfide shuttle may occur between Cys pairs in other homologs. Sequence alignments reveal that the quiescin family has a second conserved Cys-X-X-Cys sequence (Coppock *et al.*, 1998) in a position comparable to the Cys-Gly-Cys of Erv2p. Furthermore, Erv1p, like Erv2p, has been observed to form disulfide bonded dimers (Lee *et al.*, 2000). Erv1p and ALR have second Cys-X-X-Cys motifs N-terminal, rather than C-terminal, to the primary Cys-X-X-Cys active site. The N-terminal region of Erv1p (Lee *et al.*, 2000), but not that of Erv2p (Gerber *et al.*, 2001), is necessary for the formation of dimers. In Erv1p, 50 residues separate the N-terminal auxiliary Cys-Arg-Ser-Cys sequence from the beginning of helix $\alpha 1$. These 50 residues are rich in Gly and Ser and are predicted to have little secondary structure, indicating that they could easily span the 30 Å between the active site of the opposite protomer and the N terminus of helix $\alpha 1$. Although Ero1p is not homologous to Erv2p and its structure is unknown, the Ero1p protein may operate by a similar disulfide-shuttle mechanism. Ero1p has two pairs of conserved Cys residues, one of which interacts directly with PDI and the other of which reoxidizes the PDI-interacting pair (Frand and Kaiser, 2000).

Mechanisms for interaction with substrate proteins

Much effort has focused on understanding the role of the residues in the immediate vicinity of the active site Cys residues on the redox properties of thiol-disulfide oxidoreductases (Chivers *et al.*, 1997). However, attention is now turning to issues such as steric exclusion of substrates by the tertiary and quaternary structural contexts of Cys-X_n-Cys motifs. For example, the bacterial periplasmic protein DsbC, which normally acts in reduced form to isomerize disulfides and avoids oxidation by the DsbB protein, instead becomes oxidized by DsbB and in turn acts as a disulfide oxidase when mutated to destroy its dimerization interface (Bader *et al.*, 2001). No changes in the vicinity of the active site were necessary. Furthermore, two thioredoxin folds may not be able to interact with one another, for steric reasons, to accomplish intermolecular dithiol-disulfide exchange (Katzen and Beckwith, 2000). Although the Erv2p active site disulfide is not in a thioredoxin fold, it is at the N terminus of a helix, and its local geometry is similar to that of the DsbA and thioredoxin active sites (r.m.s. deviation ~0.25 Å for Cys-X-X-Cys backbone atoms). Erv2p may naturally oxidize ER enzymes with thioredoxin folds (Sevier *et al.*, 2001), and substrates that are sterically unable to access the Cys-Gly-Glu-Cys region of Erv2p may instead interact with the Cys-Gly-Cys in the C-terminal tail. The flexibility of the region containing Cys176 and Cys178 in Erv2p, as indicated by the protease sensitivity of the polypeptide chain at neighboring residues and the multiple conformations observed crystallographically, may further facilitate transfer of oxidizing equivalents to substrate dithiols. Erv2p can also oxidize lysozyme, a test substrate lacking a thioredoxin fold (Gerber *et al.*, 2001); whether the C-terminal Cys pair is required for this activity remains to be determined. In general, the structure and redox properties of adaptor Cys-X_n-Cys motifs could tailor the thiol oxidase of the ERV module activity to the particular substrates and physiological functions of each enzyme in the fold family.

Material and methods

Protein expression and purification

The *ERV2* coding region, lacking the first 29 amino acids, was inserted into the pET-21b(+) (Novagen) expression vector. The resulting Erv2-ΔN construct was transformed into BL21(DE3) pLysS (Novagen) cells. Single colonies were inoculated either into M9-ZB medium containing 4% (w/v) glucose or into LB. All cultures contained 100 mg l^{-1} ampicillin and 30 mg l^{-1} chloramphenicol. Cells were grown at 37 °C to an optical density of OD_{600} = 0.7-0.9, isopropyl-β-D-thiogalactoside (IPTG) and FAD were added to a final concentration of 0.5 mM and 10 μM, respectively, and the culture was shifted to 30 °C for a further 3-6 h. Cells were harvested by centrifugation and lysed by sonication in lysis buffer (20 mM KPO_4 [pH 7.4], 500 mM NaCl and 10 mM β-mercaptoethanol) supplemented with 50 μM FAD. Cell debris and membranes were sedimented by centrifugation, and the supernatant was applied at 4 °C to nickel affinity beads (Qiagen) preequilibrated with lysis buffer. After shaking gently overnight, the mixture was loaded onto a column and washed with 10 column volumes lysis buffer supplemented with 25 mM imidazole. Protein was eluted with 10 ml of 20 mM KPO_4 [pH

7.4], 500 mM NaCl, 10 mM β-mercaptoethanol and 300 mM imidazole. The protein was further purified by hydroxyapatite chromatography eluted with increasing phosphate. Fractions containing Erv2-ΔN were then pooled and dialyzed against 25 mM NaCl and 10 mM Tris-HCl [pH 8.0]. To obtain Erv2-c, the dialyzed protein was incubated with thermolysin (10 μg enzyme per 0.7 mg of protein) for 30 min at room temperature, and the protease-resistant domain was further purified by DEAE chromatography. The eluted protein was pooled and dialyzed against 25 mM NaCl and 10 mM Tris-HCl [pH 8.0], and concentrated by centricon (Amicon) to 19 mg ml^{-1}, as determined spectroscopically in 6 M guanidine-HCl and 10 mM $NaPO_4$ [pH 6.8], assuming an extinction coefficient of 21,980 at 280 nm.

Circular dichroism

CD was performed on an Aviv model 202 spectropolarimeter. Protein was dialyzed against a solution containing 2 mM citrate [pH 6.1], 2 mM KPO_4 [pH 6.8], 2 mM boric acid and 10 mM NaCl. Samples were diluted in the same buffer such that the absorbance at 454 nm was identical for Erv2-ΔN and Erv2-c and corresponded to 10 μM FAD. Spectra were recorded in a 1 mm pathlength cuvette at 25 °C.

Crystallization and structure determination

Small yellow crystals (~0.07 × ~0.07 × ~0.07 mm^3) were grown from the Erv2-ΔN preparation by hanging drop vapor diffusion over a well containing 0.1 M cacodylic acid [pH 6.2], 50 mM $MgCl_2$ and 32% (w/v) PEG 8000. For Erv2-c, initial crystals of poor morphology were grown over a well solution containing 0.1 M cacodylic acid [pH 6.2], 10 mM $CoCl_2$ and 22% (w/v) PEG 8000. Large crystals could be grown by seeding from these crystals into a variety of conditions. Crystals for data collection were grown in 0.1 M cacodylic acid [pH 6.2], 10% (v/v) dimethyl sulfoxide (DMSO), 15% (v/v) glycerol and 10% (w/v) PEG 1000. Crystals were transferred to a 1:1 mixture of mineral oil and Parabar oil (Exxon) before flash freezing. Diffraction data were collected to 2.0 Å (Erv2-ΔN preparation) and 1.5 Å (Erv2-c) resolution at 120 K on an RU-H3R generator (Rigaku, Tokyo) equipped with a RaxisIV detector (Rigaku) and osmic mirrors. Phasing was performed by MAD using a SeMet derivative of Erv2-c prepared according to published protocol (Van Duyne *et al.*, 1993), except that 10 μM FAD was added to the media at the time of induction, and the cells were allowed to grow for 3 h more before harvesting. SeMet-containing crystals were grown under similar conditions to the native crystals. Data for phasing were collected at 100 K on the ESRF ID14 4 beamline at three wavelengths around the selenium absorption edge (Table 1). All native and MAD data were processed and scaled using DENZO and SCALEPACK (Otwinowski and Minor, 1997). Heavy atoms sites were located, and phasing was performed with SOLVE (Terwilliger and Berendzen, 1999). The noncrystallographic symmetry operator for the Erv2-c crystals was determined using polarrfn (1994) and GETAX (Vonrhein and Schulz, 1999). The Erv2-c structure was built using O (2000), and an Erv2-c dimer was used as the molecular replacement search model in AMoRe (Navaza, 1994) to provide phases for the cleaved Erv2-ΔN crystals. Structure refinement was done using the Crystallography and NMR System (Brünger *et al*, 1998) without noncrystallographic symmetry restraints. A comparison of the Erv2p active site disulfide with Cys-X-X-Cys motifs in proteins of known structure was accomplished using SPASM (Kleywegt, 1999).

Construction and analysis of Cys mutants

Mutants of *ERV2* that converted Cys to Ala were made with the QuikChange site directed mutagenesis kit (Stratagene) using *ERV2-HA* in a *URA3*-marked plasmid as template. The mutated plasmids were verified by sequencing. P_{GAL1}-*ERV2* plasmids containing wild-type or mutant *ERV2-HA* were transformed into the yeast strain CKY598 (*MAT**a** GAL2 ura3-52 leu2-3,112 ero1-1*). Strains were grown in synthetic minimal media (SMM) minus uracil and methionine with 2% (w/v) galactose and 2% (w/v) raffinose to exponential phase. Cell proteins were radiolabeled with [^{35}S]methionine and cysteine (EXPRESS, NEN) for 60 min at 25 °C. Samples were collected by centrifugation and suspended in 10% (w/v) trichloroacetic acid (TCA). Cell membranes were disrupted by agitation with glass beads and proteins collected by centrifugation at 4 °C. Protein pellets were resuspended in sample buffer (80 mM Tris-HCl [pH 6.8], 2% (w/v) sodium dodecyl sulfate, 10% (v/v) glycerol, 1 mM phenylmethylsulfonyl fluoride (PMSF) and 0.01% (w/v) bromophenol blue) containing 40 mM N-ethylmaleimide (NEM, Sigma). The pH of the samples was adjusted by addition of 1 M Tris-HCl [pH 8.0], until samples turned blue. Samples were incubated for 15 min at 4 °C, followed by 10 min at 25 °C and 2 min at 100 °C. Samples were diluted 10-fold in IP buffer (50 mM Tris-HCl [pH 7.4], 150 mM NaCl, 1% (v/v) Triton X-100 and 1 mM PMSF) and incubated with HA antibody 12CA5 (Covance). Immune complexes were collected with protein A-sepharose (Pharmacia), washed twice in IP buffer and once in IP buffer minus detergent, and solubilized in sample buffer. Samples were resolved on a 10% SDS-PAGE gel and proteins were visualized with a 445si PhosphorImager (Molecular Dynamics).

Coordinates. Coordinates have been deposited in the Protein Data Bank (accession codes 1JR8 for Erv2-c and 1JRA for Erv2-ΔN).

References

Bader, M.W., Hiniker, A., Regeimbal, J., Goldstone, D., Haebel, P.W., Riemer, J., Metcalf, P. and Bardwell, J.C. (2001) Turning a disulfide isomerase into an oxidase: DsbC mutants that imitate DsbA. *Embo J*, **20**, 1555-1562.

Barbirz, S., Jakob, U. and Glocker, M.O. (2000) Mass spectrometry unravels disulfide bond formation as the mechanism that activates a molecular chaperone. *J Biol Chem*, **275**, 18759-18766.

Brünger, A.T., Adams, P.D., Clore, G.M., DeLano, W.L., Gros, P., Grosse-Kunstleve, R.W., Jiang, J.S., Kuszewski, J., Nilges, M., Pannu, N.S., Read, R.J., Rice, L.M., Simonson, T., Warren, G.L. (1998) Crystallography & NMR system: A new software suite for macromolecular structure determination. *Acta Crystallogr*, **D54**, 905-921.

Carson, M. (1997) Ribbons. *Methods Enzymol*, **277**, 493-505.

Chivers, P.T., Prehoda, K.E. and Raines, R.T. (1997) The CXXC motif: a rheostat in the active site. *Biochemistry*, **36**, 4061-4066.

Coppock, D., Kopman, C., Gudas, J. and Cina-Poppe, D.A. (2000) Regulation of the quiescence-induced genes: quiescin Q6, decorin, and ribosomal protein S29. *Biochem Biophys Res Commun*, **269**, 604-610.

Coppock, D.L., Cina-Poppe, D. and Gilleran, S. (1998) The quiescin Q6 gene (QSCN6) is a fusion of two ancient gene families: thioredoxin and ERV1. *Genomics*, **54**, 460-468.

Cowtan, K.A (1994) CCP4 density modification package. *Joint CCP4 and ESF-EACBM Newsletter on Protein Crystallography*, **31**, 34-38.

Fraaije, M.W. and Mattevi, A. (2000) Flavoenzymes: diverse catalysts with recurrent features. *Trends Biochem Sci*, **25**, 126-132.

Frand, A.R. and Kaiser, C.A. (1998) The ERO1 gene of yeast is required for oxidation of protein dithiols in the endoplasmic reticulum. *Mol Cell*, **1**, 161-170.

Frand, A.R. and Kaiser, C.A. (1999) Ero1p oxidizes protein disulfide isomerase in a pathway for disulfide bond formation in the endoplasmic reticulum. *Mol Cell*, **4**, 469-477.

Frand, A.R. and Kaiser, C.A. (2000) Two pairs of conserved cysteines are required for the oxidative activity of Ero1p in protein disulfide bond formation in the endoplasmic reticulum. *Mol Biol Cell*, **11**, 2833-2843.

Gerber, J., Muhlenhoff, U., Hofhaus, G., Lill, R. and Lisowsky, T. (2001) Yeast ERV2p is the first microsomal FAD-linked sulfhydryl oxidase of the Erv1p/Alrp protein family. *J Biol Chem*, **276**, 23486-23491.

Gleason, F.K., Lim, C.-J., Gerami-Nejad, M. and Fuchs, J.A. (1990) Characterization of Escherichia coli thioredoxins with altered active site residues. *Biochemistry*, **29**, 3701-3709.

Graumann, J., Lilie, H., Tang, X., Tucker, K.A., Hoffman, J.H., Vijayalakshmi, J., Saper, M., Bardwell, J.C.A. and Jakob, U. (2001) Activation of the redox-regulated molecular chaperone Hsp33-a two-step mechanism. *Structure*, **9**, 377-387.

Hagiya, M., Francavilla, A., Polimeno, L., Ihara, I., Sakai, H., Seki, T., Shimonishi, M., Porter, K.A. and Starzl, T.E. (1994) Cloning and sequence analysis of the rat augmenter of liver regeneration (ALR) gene: expression of biologically active recombinant ALR and demonstration of tissue distribution. *Proc Natl Acad Sci U S A*, **91**, 8142-8146.

Holm, L. and Sander, C. (1996) Mapping the protein universe. *Science*, **273**, 595-602.

Hoober, K.L., Glynn, N.M., Burnside, J., Coppock, D.L. and Thorpe, C. (1999a) Homology between egg white sulfhydryl oxidase and quiescin Q6 defines a new class of flavin-linked sulfhydryl oxidases. *J Biol Chem*, **274**, 31759-31762.

Hoober, K.L., Sheasley, S.L., Gilbert, H.F. and Thorpe, C. (1999b) Sulfhydryl oxidase from egg white. A facile catalyst for disulfide bond formation in proteins and peptides. *J Biol Chem*, **274**, 22147-22150.

Jakob, U., Muse, W., Eser, M. and Bardwell, J.C.A. (1999) Chaperone activity with a redox switch. *Cell*, **96**, 341-352.

Kamtekar, S. and Hecht, M.H. (1995) The four-helix bundle: what determines a fold? *FASEB J*, ***9***, 1013-1022.

Katzen, F. and Beckwith, J. (2000) Transmembrane electron transfer by the membrane protein DsbD occurs *via* a disulfide bond cascade. *Cell*, **103**, 769-779.

Kemmink, J., Darby, N.J., Dijkstra, K., Nilges, M. and Creighton, T.E. (1996) Structure determination of the N-terminal thioredoxin-like domain of protein disulfide isomerase using multidimensional heteronuclear 13C/15N NMR spectroscopy. *Biochemistry*, **35**, 7684-7691.

Kemmink, J., Dijkstra, K., Mariani, M., Scheek, R.M., Penka, E., Nilges, M. and Darby, N.J. (1999) The structure in solution of the b domain of protein disulfide isomerase. *J Biomol NMR*, **13**, 357-368.

Kleywegt, G.J. (1999) Recognition of spatial motifs in protein structures. *J Mol Biol*, **285**, 1887-1897.

Kraulis, P.J. (1991) MOLSCRIPT: a program to produce both detailed and schematic plots of protein structures. *J Appl Crystallogr*, **24**, 946-950.

Krishnaswamy, S. and Rossmann, M.G. (1990) Structural refinement and analysis of Mengo virus. *J Mol Biol*, **211**, 803-844.

Kuriyan, J., Krishna, T.S., Wong, L., Guenther, B., Pahler, A., Williams, C.H., Jr. and Model, P. (1991) Convergent evolution of similar function in two structurally divergent enzymes. *Nature*, **352**, 172-174.

Lee, J., Hofhaus, G. and Lisowsky, T. (2000) Erv1p from Saccharomyces cerevisiae is a FAD-linked sulfhydryl oxidase. *FEBS Lett*, **477**, 62-66.

Martin, J.L., Bardwell, J.C. and Kuriyan, J. (1993) Crystal structure of the DsbA protein required for disulphide bond formation *in vivo*. *Nature*, **365**, 464-468.

Massey, V. (1995) Introduction: flavoprotein structure and mechanism. *Faseb J*, **9**, 473-475.

McCarthy, A.A., Haebel, P.W., Torronen, A., Rybin, V., Baker, E.N. and Metcalf, P. (2000) Crystal structure of the protein disulfide bond isomerase, DsbC, from Escherichia coli. *Nat Struct Biol*, **7**, 196-199.

Navaza, J. (1994) AmoRe: an automated package for molecular replacement. *Acta Crystallogr*, **A50**, 157-163.

Noiva, R. (1999) Protein disulfide isomerase: the multifunctional redox chaperone of the endoplasmic reticulum. *Semin Cell Dev Biol*, **10**, 481-493.

Otwinowski, Z. and Minor, W. (1997) Processing of X-ray diffraction data collected in oscillation mode. *Methods Enzymol*, **276**, 307-326.

Pollard, M.G., Travers, K.J. and Weissman, J.S. (1998) Ero1p: a novel and ubiquitous protein with an essential role in oxidative protein folding in the endoplasmic reticulum. *Mol Cell*, **1**, 171-182.

Schulz, G.E., Schirmer, R.H., Sachsenheimer, W. and Pai, E.F. (1978) The structure of the flavoenzyme glutathione reductase. *Nature*, **273**, 120-124.

Senkevich, T.G., White, C.L., Koonin, E.V. and Moss, B. (2000) A viral member of the ERV1/ALR protein family participates in a cytoplasmic pathway of disulfide bond formation. *Proc Natl Acad Sci U S A*, **97**, 12068-12073.

Sevier, C.S., Cuozzo, J.W., Vala, A., Aslund, F. and Kaiser, C.A. (2001) A flavoprotein oxidase defines a new endoplasmic reticulum pathway for biosynthetic disulphide bond formation. *Nat Cell Biol*, **3**, 874-882.

Smith, C.A., Toogood, H.S., Baker, H.M., Daniel, R.M. and Baker, E.N. (1999) Calcium-mediated thermostability in the subtilisin superfamily: the crystal structure of Bacillus Ak.1 protease at 1.8 Å resolution. *J Mol Biol*, **294**, 1027-1040.

Stein, G. and Lisowsky, T. (1998) Functional comparison of the yeast scERV1 and scERV2 genes. *Yeast*, **14**, 171-180.

Terwilliger, T.C. and Berendzen, J. (1999) Automated MAD and MIR structure solution. *Acta Crystallogr*, **D55**, 849-861.

Tu, B.P., Ho-Schleyer, S.C., Travers, K.J. and Weissman, J.S. (2000) Biochemical basis of oxidative protein folding in the endoplasmic reticulum. *Science*, **290**, 1571-1574.

van Berkel, W.J.H., Benen, J.A.E., Eppink, M.H.M & Fraaije, M.W. (1999) Flavoprotein kinetics. In *Flavoprotein Protocols* (eds. Chapman, S.K. & Reid, G.A.), Humana Press, New Jersey, pp. 61-85.

Van Duyne, G.D., Standaert, R.F., Karplus, P.A., Schreiber, S.L. and Clardy, J. (1993) Atomic structures of the human immunophilin FKBP-12 complexes with FK506 and rapamycin. *J Mol Biol*, **229**, 105-124.

Vonrhein, C. and Schulz, G.E. (1999) Locating proper non-crystallographic symmetry in low-resolution electron-density maps with the program GETAX. *Acta Crystallogr*, **D55**, 225-229.

(1994) CCP4. Collaborative computational project number 4. The CCP4 suite programs for protein crystallography. *Acta Crystallogr*, **D50**, 760-763.

(2000) The O Files (29 November, 2000) http://origo.imsb.au.dk/~mok/o.

Table 1. Crystallographic and refinement statistics.

Data collection					
Crystal	Native 1	Native 2	MAD $\lambda 1$	MAD $\lambda 2$	MAD $\lambda 3$
Resolution (Å)	2.0	1.5	2.8	2.8	2.8
Wavelength (Å)	1.54	1.54	0.9797	0.9794	0.9393
completeness (%)[a]	99.8 (98.3)	99.4 (98.2)	99.9 (100)	98.9 (99.4)	99.7 (100)
R_{sym}[a]	0.082 (0.461)	0.047 (0.265)	0.042 (0.054)	0.032 (0.046)	0.041 (0.048)
$<I>/<\sigma>$[a]	21.7 (4.5)	32.0 (6.2)	34.1 (24.1)	33.9 (24.4)	34.3 (25.8)
Redundancy[a]	5.3 (4.8)	3.6 (3.7)	3.6 (3.7)	3.6 (3.7)	3.7 (3.8)
Overall figure merit[b]			0.52, 0.88		

Refinement		
Number of reflections	Reflection 1	Reflection 2
Working	26,812	33,466
Free	1,995	2,517
R_{work}[c]	0.196	0.208
R_{free}[c]	0.233	0.233
R.m.s. deviations		
bonds (Å)	0.008	0.006 Å
angles (°)	1.21	1.78
Number of atoms		
Protein	3,448	1,724
Water	292	283
FAD	212	106

[a] Numbers in parentheses correspond to the highest resolution shell (2.9-2.8 Å for MAD data, 2.07-2.00 Å for Native 1 and 1.55-1.50 Å for Native 2)

[b] Figure of merit from SOLVE (Terwilliger and Berendzen, 1999) and after solvent flattening and non-crystallographic symmetry averaging with DM (Kleywegt, 1999).

[c] $R_{work, free} = \Sigma||F_o| - |F_c||/|F_o|$, where the R_{work} and R_{free} are calculated using the working and free reflection sets, respectively. The free reflections (7% of the total) were held aside throughout refinement.

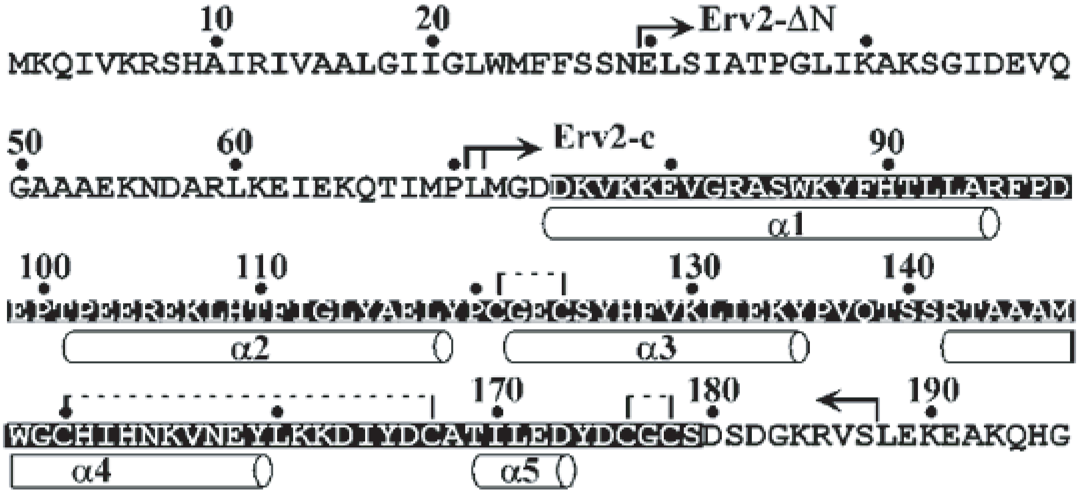
10
20
Erv2-ΔN
MKQIVKRSHAIRIVAALGIIGLWMFFSSNELSIATPGLIKAKSGIDEVQ
50
60
Erv2-c
90
GAAAEKNDARLKEIEKQTIMPLMGDDKVKKEVGRASWKYFHTLLARFPD
α1
100
110
130
140
EPTPEEREKLHTFIGLYAELYPCGECSYHFVKLIEKYPVQTSSRTAAAM
α2
α3
170
180
190
WGCHIHNKVNEYLKKDIYDCATILEDYDCGCSDSDGKRVSLEKEAKQHG
α4
α5

Figure 1. Sequence and secondary structure of Erv2p. The section of Erv2p corresponding to the structure determined crystallographically is shown in white lettering on a black background. Residues not present in the structure are in black on a white background. Black dots highlight every 10th residue. Helices are indicated by rods under the sequence, and disulfide bonds are shown by dotted lines between Cys residues. Bent arrows indicate the N terminus of the expression construct Erv2-ΔN, which extends to the natural C terminus of the protein, and the limits of the thermolysin-cleaved fragment Erv2-c. Different preparations of Erv2-c had either Leu71 or Met72 as the predominant N-terminal residue.

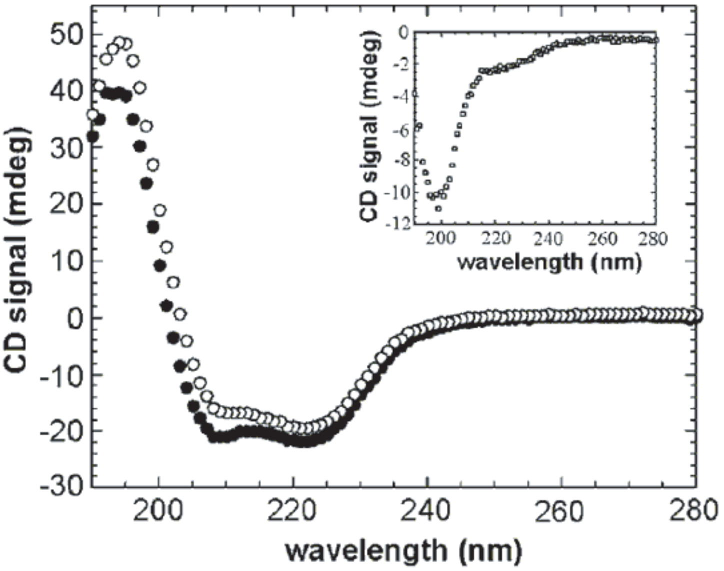

Figure 2. CD of Erv2-ΔN and Erv2-c. The CD signal as a function of wavelength is displayed for Erv2p lacking only the signal sequence (Erv2-ΔN; filled circles) and for thermolysin-cleaved enzyme (Erv2-c; open circles) at the same concentration. Both spectra are typical for highly helical proteins. The difference between these two spectra (inset) is indicative of random coil, demonstrating that the regions of Erv2p absent from the crystallographic study lack regular secondary structure.

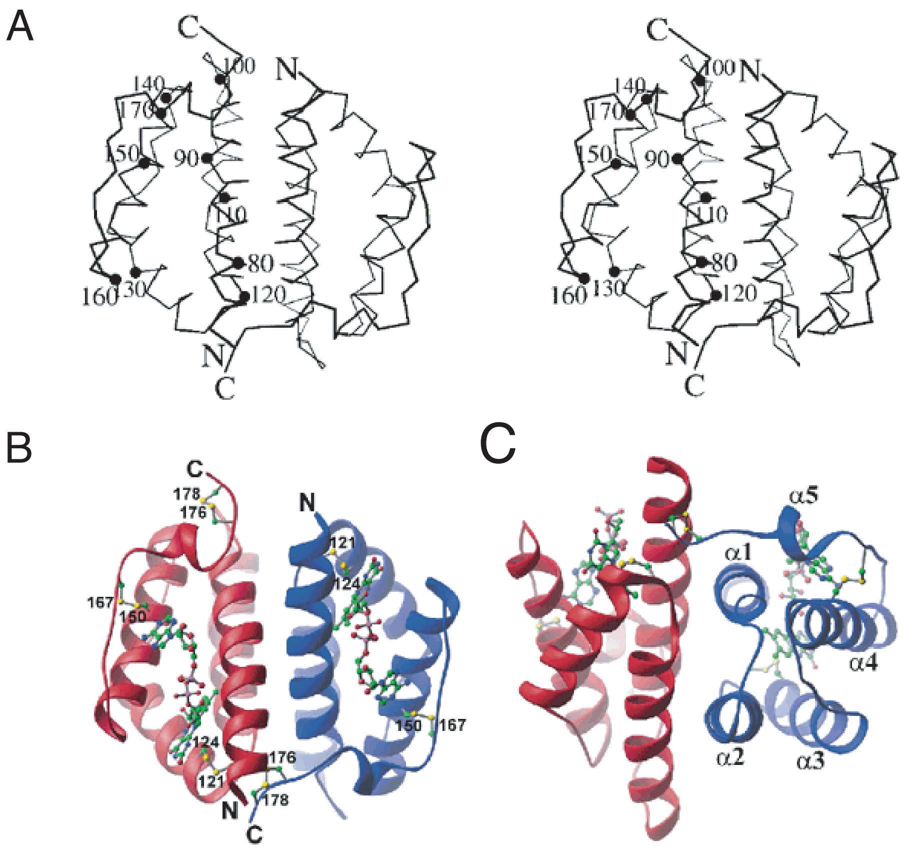
A
C
100
N
140
170
150
90
110
80
160
130
120
N
C
C
100
N
140
170
150
90
110
80
160
130
120
N
C
B
C
178
176
N
121
124
167
150
150
167
124
121
176
N
178
C
C
α5
α1
α4
α2
α3

Figure 3. Structure of Erv2p. **(A)** Stereo diagram of the Erv2-ΔN dimer viewed down the approximate two-fold symmetry axis. Every 10th residue in one protomer is indicated by a dot and labeled according to its position in the full Erv2p sequence. This figure was generated using MOLSCRIPT (Kraulis, 1991). **(B)** A ribbon diagram of the dimer in the same orientation as in the stereo diagram shows one protomer in red and the second in blue. Cys side chains are illustrated in ball-and-stick representation and numbered. The two FAD molecules bound by the dimer are shown as balls and sticks. The N and C termini of each chain is labeled "N" and "C," respectively. This and the following structure figures were generated with RIBBONS (Carson, 1997). **(C)** View down the four-helix bundle of one subunit with helices labeled α1-α5 according to their positions from N terminus to the C terminus along the polypeptide chain.

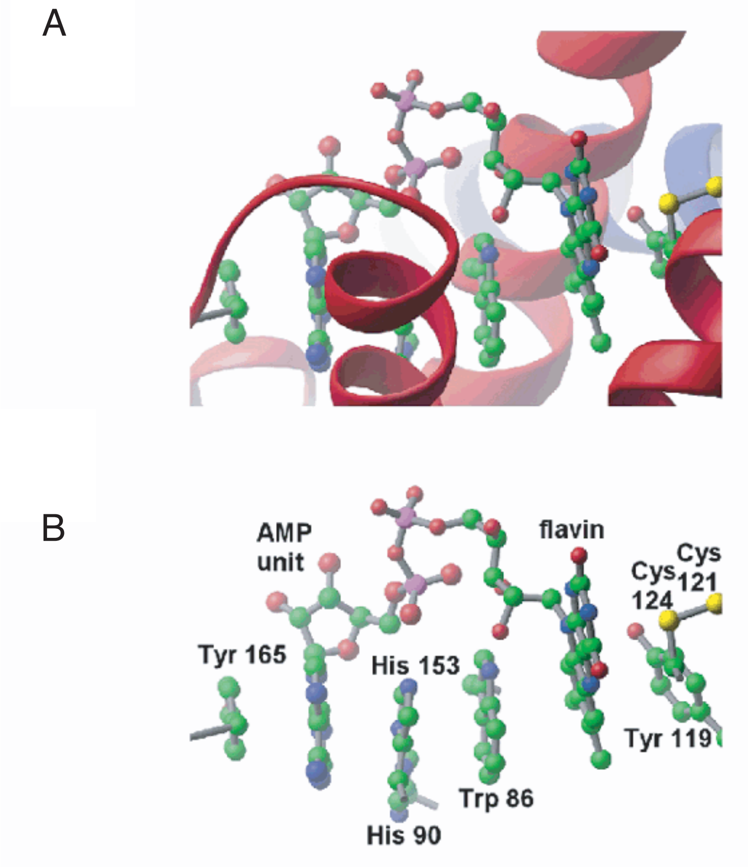
A
B
AMP unit
flavin
Cys 121
Cys 124
Tyr 165
His 153
Trp 86
Tyr 119
His 90

Figure 4. FAD binding site. **(A)** A ribbon diagram of the polypeptide backbone with some side chains and the bound FAD shown explicitly in ball-and-stick representation. The bent conformation of the FAD buries the isoalloxazine ring and adenine portions of the cofactor while keeping the intervening regions surface exposed. **(B)** The ribbon trace of the polypeptide backbone has been removed in this panel so that the residues involved in aromatic ring stacking with the FAD can be identified.

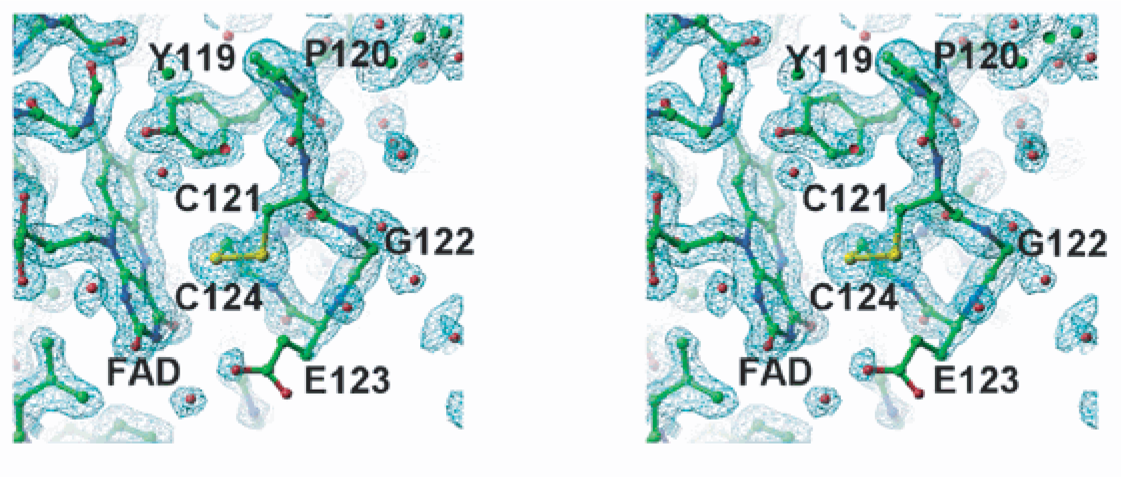
Y119
P120
C121
G122
C124
FAD
E123
Y119
P120
C121
G122
C124
FAD
E123

Figure 5. Electron density map in the vicinity of the Erv2p active site. A combined simulated annealing omit map calculated with CNS (Brünger et al., 1998) is displayed at 1.2 σ around the final model for the Erv2-c crystals. The Tyr-Pro-Cys-X-X-Cys motif is conserved among Erv1p, Erv2p, and ALR. In contrast, the residues corresponding to the Xs are highly variable, and these positions are surface-exposed. Electron density for the side chain of Glu123 is almost entirely lacking, indicating that this amino acid is flexible.

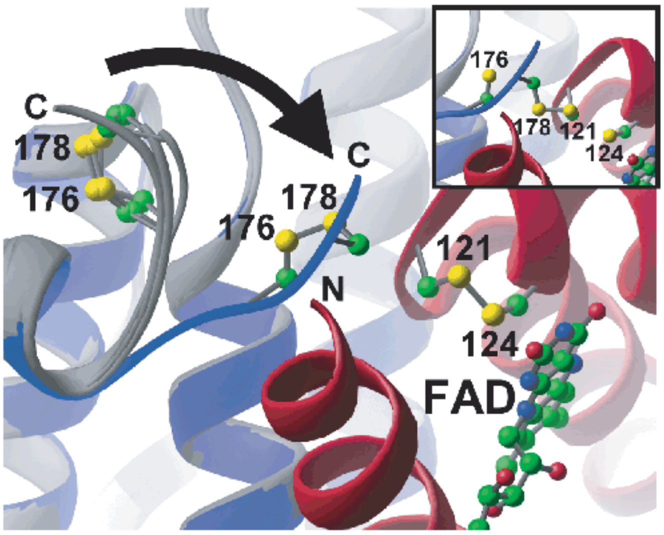

Figure 6. Erv2p flexible C-terminal tail. The four molecules in the asymmetric unit of the crystals grown from the original Erv2-ΔN preparation were superposed to compare the orientations of the C-terminal regions containing the Cys-Gly-Cys sequence. In this crystal, one of the four C-terminal tails packs against the neighboring active site. The arrow indicates the significant conformational differences between the superposed molecules. Shown in the inset is a model of an intersubunit disulfide bond constructed by changing the $\chi 1$ side chain torsion angles of Cys178 and Cys121 to decrease the sulfur-sulfur bond distance between these residues to 2.03 Å.

(Next page)

Figure 7. Cys residues required for disulfide bond formation between Erv2p protomers and for Erv2p function *in vivo*. Cells overproducing wild-type or Ala-substitution mutants of Erv2p-HA were labeled with [^{35}S]methionine and then lysed in 10% TCA to block disulfide exchange. Free thiols were alkylated with NEM prior to immunoprecipitation with HA antibody. **(A)** Wild-type Erv2p exists in monomeric and dimeric forms when resolved under non-reducing conditions, whereas the protein is entirely monomeric after reduction with 0.1 M DTT. **(B)** Comparison of the Cys mutants resolved under non-reducing conditions. **(C)** An *ero1-1* strain (CKY598) was transformed with the control plasmid, pRS316, with P_{GAL1}-*ERV2* or with P_{GAL1}-*ERV2* bearing Cys mutations. The failure of the Cys mutants to suppress the growth defect of *ero1-1* was shown by incubation at 37 ˚C for 2 d on minimal medium with 2% (w/v) galactose.

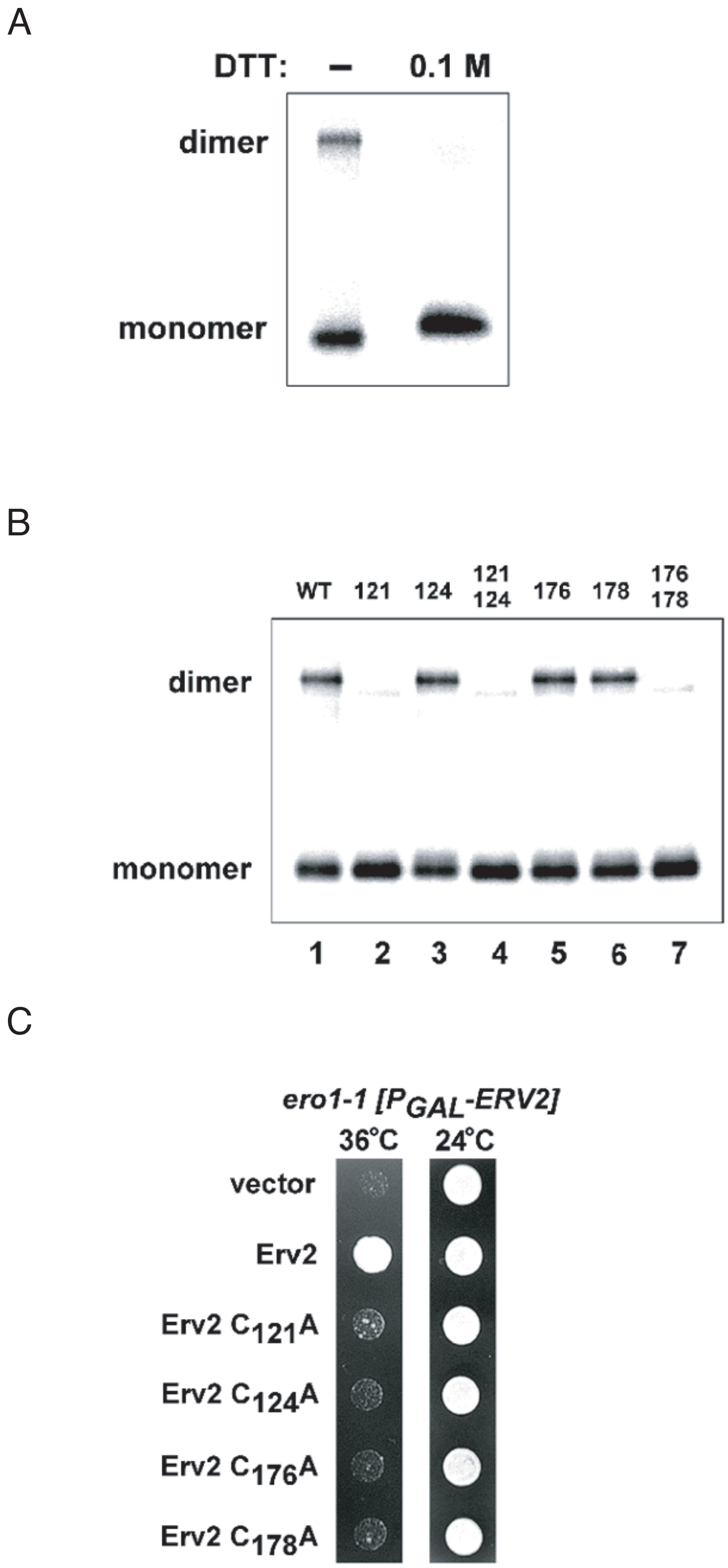
A
DTT:
–
0.1 M
dimer
monomer
B
WT
121
124
121
124
176
178
176
178
dimer
monomer
1
2
3
4
5
6
7
C
ero1-1 [PGAL-ERV2]
36°C
24°C
vector
Erv2
Erv2 C121A
Erv2 C124A
Erv2 C176A
Erv2 C178A

Chapter Three

Structural determinants of substrate access to the disulfide oxidase Erv2p

Preface

Chapter 3 represents primarily my own work and has been published as:

Vala, A., Sevier, C.S. and Kaiser, C.A. (2005) Structural determinants of substrate access to the disulfide oxidase Erv2p. *J Mol Biol*, **354**, 952-966.

Carolyn S. Sevier contributed with Figure 7C.

Summary

Erv2p is a small, dimeric FAD-dependent sulfhydryl oxidase that generates disulfide bonds in the lumen of the endoplasmic reticulum. Mutagenic and structural studies suggest that Erv2p uses an internal thiol-transfer relay between the FAD-proximal active site cysteine pair (Cys121-Cys124) and a second cysteine pair (Cys176-Cys178) located in a flexible, substrate accessible C-terminal tail of the adjacent dimer subunit. Here, we demonstrate that Cys176 and Cys178 are the only amino acids in the tail region required for disulfide transfer and that their relative positioning within the tail peptide is important for activity. However, intragenic suppressor mutations could be isolated that bypass the requirement for Cys176 and Cys178. These mutants were found to disrupt Erv2p dimerization and to increase the activity of Erv2p for thiol substrates such as glutathione. We propose that the two Erv2p subunits act together to direct the disulfide transfer to specific substrates. One subunit provides the catalytic domain composed of the active site cysteine residues and the FAD cofactor, while the second subunit appears to have two functions: it facilitates disulfide transfer to substrates *via* the tail cysteine residues while simultaneously shielding the active site cysteine residues from nonspecific reactions.

Introduction

Disulfide bond formation is often an essential step in the folding and assembly of extracellular proteins (Frand and Kaiser, 2000; Sevier and Kaiser, 2002). Recent studies have defined two pathways for disulfide bond formation in the endoplasmic reticulum (ER) of *Saccharomyces cerevisiae.* In both pathways, protein substrates are oxidized through thiol-disulfide exchange with protein disulfide isomerase (Pdi1p). Pdi1p, which has been reduced in the process of substrate oxidation, can be reoxidized by the membrane-associated flavoenzyme Ero1p, which itself can be oxidized by molecular oxygen or an anaerobic electron acceptor (Frand and Kaiser, 1998; Frand and Kaiser, 1999; Pollard *et al.*, 1998; Tu *et al.*, 2000). Alternatively, Pdi1p can be reoxidized independently of Ero1p by the sulfhydryl oxidase Erv2p (Sevier *et al.*, 2001).

Erv2p belongs to the QSOX/ERV family of FAD-dependent thiol oxidases that can couple the oxidation of substrate thiols to disulfides with the reduction of oxygen to hydrogen peroxide (Coppock *et al.*, 2000; Francavilla *et al.*, 1994; Lisowsky, 1992; Lisowsky *et al.*, 2001; Senkevich *et al.*, 2000b; Thorpe *et al.*, 2002). This family includes the small ERV-like proteins, which share a conserved core domain of about 100 amino acids including a conserved Cys-X-X-Cys motif (where X is any amino acid), and the larger QSOX proteins, which contain an ERV-like domain fused to a thioredoxin-like domain. Most eukaryotic genomes appear to encode at least one member of the ERV family; however, the presence of an ERV-like protein located within the ER appears to be unique to fungi. Conversely, QSOX proteins have been identified only in metazoans, and genes encoding these proteins are absent from the sequenced fungal genomes.

Members of the QSOX/ERV family have been localized to a variety of subcellular compartments and are involved in several cellular processes (Coppock *et al.*, 2000; Francavilla et al., 1994; Lisowsky, 1992; Lisowsky *et al.*, 2001; Senkevich *et al.*, 2000b). The ERV-like proteins Erv1p and ALR are mitochondrial proteins that participate in the assembly of cytoplasmic iron-sulphur proteins (Lange *et al.*, 2001), whereas the ERV-like protein E10R is a small vaccinia virus protein that uses the glutaredoxin-like protein G4L to transfer disulfides to viral coat proteins in the cytoplasm of infected cells (Senkevich *et al.*, 2004; Senkevich *et al.*, 2000a; Senkevich *et al.*, 2002; White *et al.*, 2002). The QSOX proteins chicken sulfhydryl oxidase and Quiescin Q6 are secreted proteins that are likely to be involved in the formation of disulfide bonds in the extracellular space (Thorpe *et al.*, 2002).

Erv2p is a homodimeric protein with two catalytic domains, each composed of a four-helix bundle holding an FAD cofactor in close proximity to the active site cysteine pair (Cys121-Cys124). In addition, a second cysteine pair (Cys176-Cys178) located in a flexible C-terminal region is also required for activity *in vivo* (Gross *et al.*, 2002). Structural and biochemical data indicate that Erv2p transfers disulfide bonds to substrate proteins by a shuttle mechanism. The following steps for disulfide formation and transfer have been deduced, but their reaction order has not yet been determined: (i) transfer of electrons from the active site cysteine pair to FAD leads to the formation of a disulfide bond at the active site, (ii) through an intermolecular disulfide exchange reaction the disulfide bond at the active site is transferred to the cysteine residues located in the C-terminal tail of the other subunit in an Erv2p dimer, and (iii) the disulfide bond in the tail can be transferred to thiol-containing substrates such as Pdi1p (Gross et al., 2002).

This disulfide shuttle mechanism is probably shared by all members of the QSOX/ERV family (Sevier and Kaiser, 2002). Mutagenic studies in Erv1p, human ALR and vaccinia virus E10R show that the active site cysteine pair, located within a conserved catalytic core, is required for activity *in vitro* and *in vivo* (Hofhaus *et al.*, 2003; Lisowsky *et al.*, 2001; Senkevich *et al.*, 2004; Senkevich *et al.*, 2000a; Senkevich *et al.*, 2000b; Sevier *et al.*, 2001). This pair reacts with a second pair of cysteine residues located near either the N or C terminus. In the case of Erv1p, a second cysteine pair located in an N-terminal domain was shown to be required for activity *in vivo* and *in vitro* (Gross *et al.*, 2002; Hofhaus *et al.*, 2003). Interestingly, the vaccinia virus protein E10R contains only one pair of cysteine residues but interacts with an adaptor protein, A2.5L, which contains a pair of cysteine residues that probably fulfills the function of the tail cysteine residues in Erv2p. Each cysteine in A2.5L is essential for the formation of disulfide bonds in substrate proteins (Senkevich *et al.*, 2000a; Senkevich *et al.*, 2000b; White *et al.*, 2002).

Despite the fact that the major ER oxidase Ero1p does not share obvious sequence similarity with Erv2p, the two proteins appear to have a common structure and mechanism (Gross *et al.*, 2004). Both Ero1p and Erv2p proteins share the same four helix bundle arrangement containing the FAD cofactor and the active site cysteine pair as catalytic domain (Gross *et al.*, 2004). In addition to an active site cysteine pair, both proteins require a second pair of cysteine residues for activity (Frand and Kaiser, 2000; Gross *et al.*, 2002). For both proteins the second cysteine pair is located in a relatively unstructured peptide exposed at the surface of the protein that appears to be able to engage in thiol-disulfide exchange with both the active site cysteine pair and thiols of substrate proteins. We have suggested previously that the internal disulfide relay mechanism may determine the selectivity of substrates by both proteins (Gross *et al*., 2004; Gross *et al*., 2002). Here we focus on the role of the subunit providing the C-terminal tail in conferring substrate specificity to Erv2p. By mutational studies we show that the latter subunit performs both a positive function to shuttle disulfide bonds to substrate proteins *via* the C-terminal peptide and a negative function to restrict relatively non-specific access of thiol compounds to the cysteine residues at the active site.

Results

Intragenic complementation of *erv2* mutations

Two key results provide evidence for a relay of oxidizing equivalents between the Cys121-Cys124 pair from one subunit and the Cys176-Cys178 pair of the adjacent subunit. First, these two pairs of cysteine residues are required for activity *in vivo*, and second, Cys121 and Cys176 or Cys178 are necessary for the formation of a disulfide-linked form, which is an intermediate of the reaction of the active site cysteine and the tail cysteine residues from the adjacent subunit (Gross *et al*., 2002).

As an explicit test of the ability of the active site cysteine residues from one subunit to functionally react with the tail cysteine residues of a different subunit we co-expressed a Cys121-Cys124 mutant (Erv2p-C121A-C124A) and a Cys176-Cys178 mutant (Erv2p-C176A-C178A) in an *ero1-1 erv2Δ* strain. When co-expressed, two different Erv2p mutants should form three different dimeric species: two homodimers of Erv2p-C121A-C124A or Erv2p-C176A-C178A, and a heterodimer of Erv2p-C121A-C124A and Erv2p-C176A-C178A. Co-expression of Erv2p-C121A-C124A and Erv2p-C176A-C178A was able to suppress the growth defect of the temperature-sensitive *ero1-1* mutant at the non-permissive temperature (Figure 1). This intragenic complementation of *erv2* cysteine mutants shows that Cys121-Cys124 from one subunit can work together with Cys176-Cys178 from the other subunit of a dimer to produce a functional enzyme. As shown previously, strains individually expressing Erv2p-C121A-C124A or Erv2p-C176A-C178A were unable to suppress the *ero1-1* growth defects (Figure 1) (Gross *et al*., 2002; Sevier *et al*., 2001). This result emphasizes that Erv2p catalytic domain requires components from both subunits. We will focus on the C-terminal tail and further study its role in disulfide transfer.

Cys176 and Cys178 are the only tail residues essential for Erv2p activity

The Erv2p tail region, defined structurally as the C-terminal segment beginning after the last α-helix of Erv2p (residues 171 to 196) is weakly conserved among the Erv2p fungal orthologs, yet only the Cys-Gly-Cys motif is conserved completely (Figure 2). Because previous studies suggested that the C-terminal tail of Erv2p confers specificity to its interaction with substrates (Gross *et al.*, 2002), we conducted site-directed mutagenesis of the tail and examined the effect on substrate oxidation. We individually mutated each of the amino acids from 171 to 183 to alanine, and determined that only the Erv2p-C176A and Erv2p-C178A mutants were not active *in vivo* (data not shown). In addition, the C-terminal tail contains many charged residues that we individually mutated to alanine (K184A, R185A, E189A, K190A, E191A, K193A and H195A). All of these mutants were active *in vivo*, and only the E191A mutation caused even a partial growth defect (data not shown).

We then generated a nested set of truncation mutants across the tail region (Figure 3A) and tested these mutants for their ability to suppress the growth defect of an *ero1-1* strain at the restrictive temperature. Only Erv2p truncation mutants that contained the tail cysteine residues (Erv2p-D182Stop, Erv2p-S187Stop and Erv2p-A192Stop) were active*,* while mutants lacking one or both tail cysteine residues (Erv2p-L171Stop, Erv2p-C176Stop and Erv2p-G177Stop) were inactive (Figure 3B). Erv2p-D182Stop, Erv2p-S187Stop and Erv2p-A192Stop mutants also displayed intersubunit disulfide-linked intermediates under denaturing conditions (Figure 3C). Interestingly, the majority of the Erv2p-G177Stop mutant protein was found in a disulfide-linked conformation, suggesting that a second cysteine normally plays a role in resolving the mixed disulfide between the tail and the active site cysteine residues. Alternatively, it is possible that the observed increase in the amount of disulfide-linked dimer in this truncation mutant is due to increased accessibility of Cys176 in the absence of the distal portion of the tail.

Erv2p activity depends on the spacing between Cys176 and Cys178

Studies with Cys-X_n-Cys peptides have shown that the number of residues between two cysteine residues affects the rate of the thiol-disulfide exchange reaction and that peptides containing only one residue between cysteine residues form a relatively unstable disulfide bond (Zhang and Snyder, 1989). These studies of model peptides suggest that the Cys-Gly-Cys arrangement of the Erv2p tail cysteine residues should create a relatively unstable disulfide bond, potentially facilitating the efficient transfer of oxidizing equivalents to substrate proteins (Gross *et al.*, 2002; Woycechowsky and Raines, 2003). The spacing between the cysteine residues of the second cysteine pair in other members of the QSOX/ERV family is variable. The second cysteine pair appears in a Cys-X_2-Cys motif in Erv1p, ALR and Quiescin Q6, in a Cys-X_3-Cys motif in the viral A2.5L protein, and in a Cys-X_4-Cys motif in Erv1p from *Arabidopsis thaliana*.

By adjusting the spacing between the Erv2p tail cysteine residues we expected to alter the redox characteristics of the Cys176-Cys178 pair and thus perhaps interfere with disulfide transfer either between the active site cysteine and the tail cysteine residues, or between the tail cysteine residues and the substrate protein. For this purpose, we either removed the glycine between the tail cysteine residues (Erv2p-G177Δ) or inserted alanine residues between the tail cysteine residues (Erv2p-CGA$_n$C, where *n* varies from one to four) (Figure 4A). Erv2p tolerated spacing of two, three or four residues between the tail cysteine residues but lost activity when we deleted the glycine residue between the tail cysteine residues (Erv2p-G177Δ) or increased the spacing between the tail cysteine residues to five amino acids (Erv2p-CGA$_4$C) (Figure 4B). The activity of these Erv2p mutants did not correlate with the predicted changes in the equilibrium constant for loop formation based on *in vitro* studies with model peptides (Zhang and Snyder, 1989).

A disulfide-linked form of Erv2p was detected by SDS-PAGE under non-reducing denaturing conditions for each of these mutants (Figure 4C), suggesting that the spacing between the tail cysteine residues does not affect the ability of the tail cysteines to interact with the active site cysteine residues. Because we can still capture Erv2p-CGA$_4$C and Erv2p-G177Δ in the disulfide-linked conformation, the inactivity of these mutants *in vivo* may result from either a particularly energetically unfavorable disulfide bond in these tail mutants or a constraint that causes resolution of the mixed disulfide bond between the active site cysteine and the tail cysteine to occur relatively slowly. Consistent with this latter possibility, kinetic studies of disulfide rearrangements with model peptides showed that Cys-Cys and Cys-Ala$_5$-Cys peptides are slow to undergo either oxidation or reduction reactions (Zhang and Snyder, 1989).

Erv2p activity depends on the position of Cys176 and Cys178 within the tail

Finally, we examined the effect of the distance between the active site cysteines and the tail cysteine residues on Erv2p activity by shortening the C-terminal tail by deleting residues before the tail cysteine pair (Figure 5A). Amino acids preceding

Cys176 in the tail (Asp173, Tyr174, and Asp175) were deleted to generate the Erv2p-(DYD)Δ mutant, which was inactive *in vivo* and failed to form disulfide-linked intermediates (Figure 5B and 5C). However, when we reintroduced two or three alanine residues at this position, creating Erv2p-(DYD)Δ+2A and Erv2p-(DYD)Δ+3A, the activity and the ability to form disulfide-linked intermediates was restored (Figure 5B and 5C).

Taken together, these mutagenesis studies show that Cys176 and Cys178 are the only residues in the C-terminal tail region required for Erv2p activity. Our data indicate two important factors for the cysteine residues in the tail to function *in vivo*: (i) the tail cysteine residues have to be separated by a peptide segment of an appropriate length for a disulfide bond to form between and (ii) the tail cysteine residues have to be separated from the body of Erv2p by a peptide tether sufficiently long to give access of the tail cysteine residues to the active site of the other subunit in the dimer.

Identification of intragenic suppressors of Erv2p tail cysteine mutants

To better understand how accessibility of substrates to the active site is controlled, we designed a screen for intragenic suppressors of a nonfunctional mutant with both tail cysteine residues mutated to alanine. Random PCR mutagenesis was performed on *ERV2-C176A-C178A*, and the resulting plasmids generated by *in vivo* gap repair were screened for their ability to bypass the need for the tail cysteine residues by allowing growth of an *ero1-1 erv2Δ* strain. Sequencing of 24 candidate suppressors revealed that each contained more than one mutation. However, all of the suppressor mutants had at least one mutation in the α2 helix: K107N (1 clone), K107E (1 clone), F111S (10 clones), F111V (1 clone) and F111L (2 clones), L114S (5 clones), F115S (1 clone), L118R (2 clones) and P120A (2 clones).

To identify individual point mutations with suppressor activity we tested three single mutants (F111S, L114S, and P120A) and found that each by itself was sufficient for the restoration of Erv2p activity in the absence of the tail cysteine pair (Figure 6A). These three mutants were also active *in vivo* when the Erv2p tail was truncated immediately after Cys176 yet required a functional Cys121-Cys124 pair for activity (Figure 6B and data not shown). Overexpression of the three intragenic suppressors decreases the sensitivity of *ero1-1* cells to the reducing agent dithiothreitol (DTT; data not shown) as does overexpression of wild-type Erv2p (Sevier et al., 2001). Constructs expressing the three intragenic suppressor mutants or wild-type Erv2p complemented an *ero1*Δ mutant, while those expressing an Erv2p mutant lacking the tail cysteine residues did not (data not shown).

The Phe111, Leu114 and Pro120 residues are located in the Erv2p dimer interface (Figure 6C), a region characterized by hydrophobic contacts between the α1 and α2 helices of both subunits (Gross *et al.*, 2002). To test whether elimination of these hydrophobic residues precludes dimer formation, we expressed and purified recombinant Erv2p wild-type and Erv2p variants (Erv2p-C176A-C178A, Erv2p-F111S-C176A-C178A and Erv2p-L114S-C176A-C178A) in *Escherichia coli*. We were unable to purify Erv2p-P120A-C176A-C178A due to its insolubility. After purification, all the recombinant proteins exhibited the characteristic absorbance peaks for bound FAD at 352 and 454 nm, and showed sulfhydryl oxidase activity as determined by the initiation of oxygen consumption and reduction of bound FAD by thiol substrates (data not shown).

In equilibrium analytical ultracentrifugation experiments, recombinant wild-type Erv2p and Erv2p-C176A-C178A each reached sedimentation equilibrium for a protein of a molecular weight of 41 kDa, a value close to that expected for a homodimeric protein (Table 1). In contrast, addition of the F111S or L114S mutation caused the mutant lacking the tail cysteine residues to sediment with a molecular weight of 22 or 23 kDa, respectively, suggesting that the intragenic suppressor mutants are monomeric proteins (Table 1).

In thermal denaturation experiments, recombinant wild-type Erv2p and Erv2p-C176A-C178A have a melting temperature of 59.2 ˚C and 56.5 ˚C, respectively, while the Erv2p-F111S-C176A-C178A has a lower melting temperature of 46.7 ˚C (Figure 7). The relative instability of monomeric Erv2p-F111S-C176A-C178A mutant indicates that molecular contacts at the dimer interface of the wild-type protein contribute to overall stability.

Monomeric Erv2p has decreased substrate selectivity

The Erv2p crystal structure suggests that the active site cysteine residues in the Erv2p dimer conformation are partially buried in the dimer interface, underneath the tail of the other subunit (Gross et al., 2002). To test whether thiol substrates have greater access to the active site cysteine residues in the monomeric form of Erv2p, we used the catalytic reduction of bound FAD in the presence of various thiol substrates as a measurement of *in vitro* sulfhydryl oxidase activity (Figure 8A). The observed time lag between the addition of Erv2p and the moment of reduction of bound FAD corresponds to the time that is necessary to consume the oxygen in the cuvette and is correlated with the amount of thiol used. We used a range of small thiol substrates, including the dithiol substrates DTT and (±)-trans-1,2-bis(2-mercaptoacetamido)cyclohexane (BMC), and the monothiol substrates cysteine, homocysteine, N-methylmercaptoacetamide (NMA), reduced glutathione (GSH) and β-mercaptoethanol (β-ME). Using an assay based on FAD bleaching we found that most thiol substrates (except for DTT and BMC) were not sufficiently soluble to derive K_m or V_{max} values. For example, Figure 8B shows that enzyme saturation when GSH was used as a substrate does not occur at the solubility limit of GSH (about 250 mM).

Comparison of the sulfhydryl oxidase activity of these proteins revealed higher reaction rates when using dithiols as substrates (Table 2). When we compared the activity of the recombinant proteins toward the dithiol substrates, we observed that they could oxidize the small dithiol DTT but have lower activity toward the bulkier dithiol substrate BMC (Table 2). The same relationship was observed for the monothiol substrates tested, with the exception of β-ME (Table 2). Of all the monothiols tested, β-ME has the highest pK_a value and thus probably has the least thiolate form at physiological pH.

Erv2p-C176A-C178A and Erv2p-C176Stop mutants could oxidize the small substrate DTT but have limited activity toward the bulkier substrates BMC, GSH and cysteine (Table 2 and data not shown). The addition of an intragenic suppressor mutation to the Erv2p-C176A-C178A mutant allowed this protein to oxidize a broader range of substrates (Table 2). The Erv2p-F111S-C176A-C178A had wild-type level activity toward all the monothiol substrates tested except GSH, which was twofold higher (Figure 8A, 8B and Table 2).

DTT is a strong reducing agent that is small enough to react directly with the Cys121-Cys124 pair. For each protein, the rate of O_2 consumption was highest with DTT as substrate (Table 2). Thus, we used the activity toward DTT as the standard for the intrinsic activity of each mutant protein. For all other substrates tested, the rates of O_2 consumption were highest for the Erv2p-F111S-C176A-C178A mutant. This result emphasizes that the intragenic suppressor mutants is less specific than wild-type Erv2p, tail mutant or the truncation mutant. From these *in vitro* experiments, we conclude that substrate accessibility to the active site is determined by steric occlusion by the adjacent subunit in a dimer.

Monomeric Erv2p mutants can oxidize Pdi1p in the absence of tail cysteine residues

We have previously shown that Erv2p is able to transfer oxidizing equivalents to Pdi1p *in vitro* (Sevier *et al.*, 2001). To test whether the intragenic suppressor mutations alter this property of Erv2p, we reduced 4 μM of recombinant Pdi1p and incubated it with 300 nM of Erv2p or its mutant variants at 30 °C. At various time points, an aliquot of the reaction mixture was TCA precipitated and the oxidation state of Pdi1p was determined by reaction with AMS, an alkylating agent that will react only with free cysteine residues. After AMS treatment, the samples were resolved by non-reducing SDS-PAGE. As a mobility standard for oxidized Pdi1p we incubated reduced Pdi1p with 1 mM diamide. Both Erv2p-C176A-C178A and Erv2p-C176Stop mutants did not oxidize Pdi1p, yet the Erv2p-F111S-C176A-C178A suppressor mutant reoxidized recombinant Pdi1p faster than wild-type Erv2p (Figure 8C). This result supports the idea that the active site cysteine pair in Erv2p-F111S-C176A-C178A is more accessible to bulkier substrates than in the wild-type.

The reaction of Erv2p with Pdi1p *in vitro* is much slower than the reaction of Erv2p with small-molecule thiols, raising the question of whether Pdi1p is a physiologically relevant substrate of Erv2p. It is possible that other as yet unidentified ER protein(s) are the preferred substrate of Erv2p *in vivo* or that our *in vitro* assay for oxidation of Pdi1p lacks an important component.

Discussion

The mechanism by which Erv2p generates a disulfide bond that can be transferred to thiol substrates has been deduced from structural data, mutagenesis studies, and biochemical assays (Gross *et al.*, 2002; Sevier *et al.*, 2001). A central feature of this mechanism, which Erv2p appears to share with other members of the family of QSOX/ERV proteins and the structurally related ER oxidase Ero1p, is a second pair of cysteine residues that can shuttle disulfide bonds from the active site to thiols of substrate proteins (Gross *et al.*, 2004; Hofhaus *et al.*, 2003; Thorpe *et al.*, 2002). In this manuscript we describe mutagenesis studies on Erv2p to define the features of the C-terminal tail in the vicinity of the second cysteine pair that allow efficient disulfide shuttling between the active site and *in vivo* substrates. In addition, we employed a genetic suppression strategy to explore the structural constraints that prevent substrate thiols from directly gaining access to the active site disulfide bond in the absence of cysteine residues in the C-terminal tail.

Mutagenesis of the Erv2p tail cysteine residues shows that they are required for activity and for the formation of the catalytically important intrasubunit disulfide-linked intermediate (Gross et al., 2002). By extensive mutagenesis of the C-terminal tail we show here that the most important features of the tail are the presence of two cysteine residues spaced appropriately such that a disulfide bond can form between them and positioned with a long enough flexible tether to engage in dithiol-disulfide exchange with the active site cysteine pair. Although the identity of other individual residues in the tail are not essential for the ability of Erv2p to suppress an *ero1-1* mutation *in vivo*, we cannot rule out the possibility that more subtle aspects of Erv2p function may be influenced by specific molecular recognition of the tail peptide.

Specificity conferred by the disulfide relay

Mutants that lack a cysteine pair in the C-terminal tail of Erv2p, such as Erv2p-C176A-C178A, exhibit greatly decreased capacity for protein disulfide bond formation *in vivo*. Nevertheless, such mutants should still be capable of forming a disulfide bond at the active site, and we wished to determine how access of thiol substrates to the active site is determined. Accordingly, we performed a screen for intragenic suppressor mutants that could oxidize substrates *in vivo* without relaying disulfides through the tail cysteine pair. The suppressor mutations that we isolated lie in the hydrophobic interface between subunits of the Erv2p dimer and convert Erv2p into a monomeric form bypassing the need for disulfide shuttling through the C-terminal tail by giving thiol substrates direct access to the active site cysteine residues.

Assays of purified Erv2p for the ability to oxidize different thiol-containing substrates *in vitro* show that wild-type Erv2p can readily oxidize the small, powerful reducing agent DTT. In addition, wild-type Erv2p can oxidize bulkier substrates more representative of the physiological substrates of Erv2p present in the ER, such as GSH or Pdi1p. Mutants lacking tail cysteine residues are slightly more active than the wild-type enzyme for oxidation of DTT, showing that this relatively small substrate can react with the active site without an active disulfide shuttle. In contrast to wild-type, the mutants lacking tail cysteine residues have greatly decreased activity for GSH and Pdi1p oxidation, showing that a disulfide shuttle is needed for oxidation of these substrates. Finally, the suppressor mutant exhibits restored activity for GSH and Pdi1p. The monomeric mutant of Erv2p has about one third the activity towards DTT (normalized to absorbance of the enzyme-bound FAD). Thermal denaturation experiments have shown that the suppressor mutant has a melting point about 10 ˚C lower than wild-type, indicating that the monomeric enzyme is intrinsically less stable than the native dimeric enzyme and this instability could account for the lower specific activity for reaction with DTT. Monomeric Erv2p has greater activity with GSH as a substrate than the wild-type enzyme, consistent with the greatly increased accessibility of the active site cysteine residues. Figure 9 uses the crystal structure of Erv2p to illustrate the relative accessibility of the active site cysteine residues for wild-type Erv2p, a truncation of the C-terminal tail (Erv2p-C176Stop), and monomeric Erv2p.

Specificity in the disulfide transfer reactions that occur in the ER must be tightly controlled to prevent crosstalk between the oxidation and the isomerization pathways, since unregulated activity might lead to activation or inactivation of proteins (Sevier and Kaiser, 2002). It is also important to regulate the activity of oxidoreductases in the ER, since their activity may generate reactive oxygen species as an unwanted byproduct (Harding *et al.*, 2003).

Mutational analysis suggests that the subunit contributing with the C-terminal tail governs Erv2p substrate selection in two different ways. In one sense the cysteine pair in the tail acts positively in the transfer of disulfide bonds to substrates. An attractive possibility is that this relatively unstructured region of Erv2p has evolved to interact efficiently with Pdi1p by displaying properties similar to nascent polypeptide chains that are in the process of folding (Gross *et al.*, 2004). In this way, Erv2p may optimize transfer of disulfides to the preferred catalyst of biosynthetic disulfide bonds.

In another sense, the tail along with the neighboring structure of the Erv2p monomer act negatively to restrict access of substrates to the active site, thus limiting the extent to which disulfides are transferred nonspecifically to bulk thiols within the ER, including glutathione. Truncations that removed the C-terminal tail (Erv2p-C176Stop and Erv2p-L171Stop) are inactive *in vivo* suggesting that residues from the opposing subunit bury the active site cysteine residues in this mutant. A truncation that removed the entire C-terminal tail (Erv2p-L171Stop) appeared to be unable to fold properly, since this mutant formed insoluble aggregates when expressed as recombinant protein (data not shown). However, Erv2p-C176Stop could fold into an enzymatically active dimer, and this mutant expressed as a recombinant protein could oxidize DTT but exhibited low activity for oxidation of bulkier substrates similar to the substrate specificity of Erv2p-C176A-C178A point mutants. Thus, even for dimeric proteins for which most of the C-terminal tail has been deleted the active site is not as accessible to substrates such as GSH as it is in the monomeric form of Erv2p.

Generality of the disulfide relay mechanism

Besides Erv2p and members of the QSOX/ERV family, several thiol oxidases, such as Ero1p, DsbB and high MW thioredoxin reductase (TrxR) (Gross *et al.*, 2004; Sandalova *et al.*, 2001) appear to have evolved a similar mechanism of transfer to substrate proteins: a cysteine pair located in a flexible region that mediates electron transfer between the substrate and the active site cysteine pair, which is located near a redox cofactor. However, this auxiliary cysteine pair can be located in the N or C terminus, either in the same subunit or in a different subunit, or as in the case of E10R, in a different protein.

A combination of structural, biochemical and mutagenesis studies show that there are striking similarities between the catalytic domains and disulfide transfer mechanisms of Erv2p and Ero1p (Gross *et al.*, 2004; Gross *et al.*, 2002). First, both require two pairs of cysteine residues for activity (Frand and Kaiser, 2000; Gross *et al.*, 2002; Sevier *et al.*, 2001). Second, both transfer disulfides from a buried FAD-proximal active site cysteine pair to Pdi1p *via* a second pair of cysteine residues located in an unstructured flexible region (Gross *et al.*, 2004; Gross *et al.*, 2002). This second pair of cysteine residues is located in a C-terminal tail in Erv2p and in a loop in Ero1p, and their structures suggest that these regions restrict substrate access to the active site cysteine pair (Gross *et al.*, 2004; Gross *et al.*, 2002). Like the Erv2p tail mutant, Ero1p lacking the second pair of cysteine residues (Ero1p-C100A-C105A) is incapable of forming disulfide bonds *in vivo* (Frand and Kaiser, 2000). Second-site suppressors of Ero1p-C100A-C105A seem to displace the loop, giving direct access to the active site cysteine residues (Sevier and Kaiser, 2005). As observed for Erv2p, these mutants are able to oxidize both small and large substrates, while Ero1p-C100A-C105A is only able to efficiently oxidize small substrates such as DTT (Sevier and Kaiser, 2005). Transfer between two pairs of cysteine residues seems to be an important mechanism used by Erv2p and Ero1p to control substrate specificity by directing the transfer of disulfides to specific substrates and thus preventing reduction of both proteins by reduced GSH, which is abundant in the ER.

A similar mechanism for substrate specificity is found in chicken QSOX, which is a fusion of a thioredoxin-like domain and an ERV-like domain (Raje and Thorpe, 2003).

While the thioredoxin-like fragment or the ERV-like fragment alone has little or no activity toward thiol substrates, the two fragments combined exhibit substantial activity. The ERV-like fragment is a dimer and probably shares the overall structure of Erv2p, including a flexible C-terminal tail containing the second cysteine pair (Raje and Thorpe, 2003). As in Erv2p, this second pair of cysteine residues in the ERV-like fragment confers specificity in the disulfide transfer to the redox active cysteine pair in the thioredoxin-like fragment.

High molecular mass TrxR and glutathione reductase are closely related reductases that exhibit distinct substrate specificities. A clear structural difference between the enzymes that may explain the marked preference of TrxR for thioredoxin rather than oxidized glutathione as a substrate is the presence of an extra C-terminal tail that has been shown to contain a second redox-active cysteine pair. Although the residues involved in GSH binding are conserved in both structures, high molecular mass TrxR is unable to reduce GSSG (Sandalova *et al.*, 2001). Structural data suggest that the presence of the C-terminal tail of the high molecular mass TrxR prevents interaction of GSSG with the active site cysteine residues by blocking access to them, thus conferring specificity (Sandalova *et al.*, 2001).

Mercuric ion reductase (MerA), a flavoenzyme involved in Hg(II) detoxification in bacteria, is a homodimer that catalyzes the transfer of electrons from NADPH to substrates *via* FAD and two pairs of cysteine residues, located in different subunits. Interestingly, a MerA mutant containing a mutated C-terminal cysteine pair is inactive *in vivo*, and yet it retains activity *in vitro*. MerA-C557A-C558A is able to reduce small HgX_2 substrates but is impaired in the reduction of larger substrates, which may be unable to access the active site cysteine residues (Engst and Miller, 1998; Engst and Miller, 1999). In the case of MerA, this internal transfer between two pairs of cysteine residues is important for the activity of this protein since all of the cellular Hg(II) seems to be associated with thiols, such as cysteine and GSH.

This flexibility in the transfer may allow these different proteins to perform in different locations or to perform diverse biological functions by acting upon different substrates. More importantly, the specificity in electron transfer obtained by this shuttle mechanism might allow for a better discrimination among different substrates, thus preventing inappropriate oxidation of substrates that are not on the pathway for formation of biosynthetic disulfide bonds.

Materials and methods

Media and yeast strains

All yeast strains used in this study have the genetic background of S288C. Cultures were either grown in rich medium (1% Bacto yeast extract and 2% Bacto-peptone containing either 2% dextrose (YPD) or 2% galactose (YPGal) as carbon sources) or minimal media (0.67% nitrogen base without amino acids supplemented with 16 amino acids not including cysteine) containing 2% galactose and 2% raffinose (SMM Gal/Raf). The isolation and characterization of the *ero1-1* mutant (CKY598) and the construction of an *erv2Δ* strain (CKY688) were described previously (Frand and Kaiser, 1998; Sevier *et al.*, 2001). CKY899 (*MAT**a** GAL2 ero1-1 erv2Δ::kanMX ura3-52 leu2-3,112*) was constructed by crossing an *erv2Δ* strain (CKY688) to an *ero1-1 GAL2* strain (CKY598).

Plasmid construction

The plasmids used in this study are listed in Table 3. The construction of *ERV2* Cys to Ala mutants was described previously (Gross *et al.*, 2002; Sevier *et al.*, 2001). A version of *ERV2-C121A-C124A* lacking an epitope tag (pAV36) was constructed by ligating a MluI fragment from *ERV2-C121A-C124A-HA* tagged (pJC15) to the same site in pFA11 (Gross *et al.*, 2002; Sevier *et al.*, 2001). To generate pAV106, a 738 bp BamHI-SacII fragment of pAV36 was placed under the *GAL1* promoter in a pRS315-based plasmid. The other mutants of *ERV2* were made using the QuikChange site directed mutagenesis kit (Stratagene) using pFA11 as template. The forward primers used for the site-directed mutagenesis are listed in Table 4. All mutated plasmids were verified by sequencing.

To construct *ERV2* truncation mutants, the *ERV2* gene was amplified from pFA11 by PCR with a primer from the *GAL1* promoter (Gal1) and one of the following primers: SacII-*-I170, SacII-*-D175, SacII-*-C176, SacII-*-S181, SacII-*-V186 or SacII-*-E191. The PCR products were cloned into BamHI-SacII restriction sites of pRS316 vector containing the *GAL1* promoter. The 3' untranslated region of *ERV2* was subcloned into these vectors using the SacII site.

ERV2 wild-type, *ERV2-C176A-C178A* and *ERV2-F111S-C176A-C178A* suppressor mutant lacking the first 29 amino acids encoding the hydrophobic N-terminal signal sequence and containing an N-terminal His_6 tag were constructed using NdeI-Erv2 and Erv2-BamHI primers. The resulting fragments were subcloned into the bacterial expression vector pET-14b (Novagen) using the NheI and BamHI sites. The *ERV2* mutant truncated at residue 176 (*ERV2-C176Stop*) was subcloned into pET-14b using NdeI-Erv2 and Erv2-C176Stop-BamHI primers.

Radiolabeling and immunoprecipitation

Radiolabeling and immunoprecipitation of Erv2p was done as described previously (Gross *et al.*, 2002). Briefly, strains overexpressing Erv2p or mutant alleles were grown in SMM Gal/Raf lacking uracil and methionine to about 1×10^7 cells/ml. Cells were suspended in the same medium at 1×10^8 cells/ml and labeled with [^{35}S]methionine and cysteine (EXPRESS, NEN) for 60 min at room temperature. Cells were then suspended in 10% (w/v) TCA and lysed with glass beads. Protein pellets were then incubated in sample buffer (80 mM Tris-HCl [pH 6.8], 2% SDS, 10% glycerol, 1 mM phenylmethylsulfonyl fluoride (PMSF), 0.01% bromophenol blue) containing 40 mM N-ethylmaleimide (Sigma) for 15 min at 4 °C followed by 10 min at room temperature. Cell extracts were suspended in 1 ml IP buffer (50 mM Tris-HCl [pH 7.4], 150 mM NaCl, 1% Triton X-100 and 1 mM PMSF) and pre-adsorbed with fixed *Staphylococcus* A cells (Sigma) before incubation with Erv2p antibody. Immune complexes were collected with protein A-Sepharose (Pharmacia), washed in IP buffer containing 0.1% SDS, washed in IP buffer without detergent, and solubilized in sample buffer. Samples were analyzed by 12% SDS-PAGE and visualized with a 445si PhosphorImager (Molecular Dynamics).

Erv2p antibody production

Erv2p lacking the first 29 amino acids and containing a C-terminal His_6 tag was purified as described previously (Sevier *et al.*, 2001). The protein was separated by SDS-PAGE and used to prepare polyclonal antibodies in rabbits by standard protocols at Covance.

Isolation of *ERV2-C176A-C178A* intragenic suppressors

PCR mutagenesis of *ERV2-C176A-C178A* (pAV41) was performed as described previously (Muhlrad *et al.*, 1992). pAV41 was amplified using AmpliTaq Gold (Perkin Elmer) in the presence of 0.65 mM or 0.25 mM $MnCl_2$ and 0.2 mM dATP (one fifth of the normal concentration) using the Gal1 and Erv2mut3 primers (Table 4).

CKY899 was co-transformed with the resulting randomly mutagenized PCR fragment and gapped pAV41 (cut with BamHI and StuI). Transformants were plated on SMM minus uracil plates and then replica plated in SMM Gal/Raf minus uracil plates at 24 ˚C and 37 ˚C. Plasmids from colonies that suppress the growth defect of CKY899 cells at 37 ˚C were obtained at a frequency of 3 or 4 colonies per 100 colonies tested. These plasmids were tested by retransformation and positive clones were sequenced.

Protein expression and purification

ERV2 wild-type and mutant allele expression plasmids were transformed into *E. coli* BL21(DE3) Gold pLysS cells (Novagen). Single colonies were inoculated into LB supplemented with 80 mg l^{-1} ampicillin and 30 mg l^{-1} chloramphenicol. Cultures were grown at 30 °C to an OD_{600} of 0.5-0.6, and isopropyl β-D-thiogalactoside (IPTG) and FAD were added to a final concentration of 0.4 mM and 10 μM, respectively. After 4 h of induction at 30 ˚C, cells were harvested by centrifugation and lysed by French press in lysis buffer (50 mM NaH_2PO_4 [pH 8], 350 mM NaCl and 10 mM imidazole with EDTA-free protease inhibitor cocktail). Insoluble material was sedimented by centrifugation and the supernatant was applied to a HiTrap Chelating HP column (Amersham Biotech) pre-equilibrated with lysis buffer.

The resin was washed with lysis buffer and with wash buffer (50 mM NaH_2PO_4 [pH 8], 300 mM NaCl and 20 mM imidazole). The bound protein was eluted with a gradient of 20 mM to 250 mM imidazole in 50 mM NaH_2PO_4 [pH 8], 300 mM NaCl. The fractions containing Erv2p were then dialyzed for at least 16 h against 50 mM NaH_2PO_4 [pH 8], 150 mM NaCl. The samples used for the determination of the molecular weight were further purified in an anion exchange HiTrap Q column (Amersham Biotech). The protein eluted from the HiTrap Chelating HP column (Amersham Biotech) was pooled and dialyzed against 20 mM Tris-HCl [pH 8]. The sample was applied to the HiTrap Q column and eluted with an increasing NaCl concentration. The fractions containing Erv2p were then dialyzed for at least 16 h against buffer A (50 mM KH_2PO_4 [pH 8], 150 mM KCl). All proteins were > 95% pure after the HiTrap Q column. Concentration of the protein samples was estimated using a molar extinction coefficient of 12.5 mM cm^{-1} at 454 nm (Sevier *et al.*, 2001).

Protein molecular mass determination

Protein samples were centrifuged in an optima XL-A centrifuge (Beckman-Coulter) using a 60 Ti rotor. For all protein samples absorbance readings at 280, 285 and 290 nm were taken. His$_6$-Erv2p at 10, 7 and 5 μM in buffer A was centrifuged at 25 ˚C at 9,000, 12,000 and 16,000 rpm. His$_6$-Erv2p-C176A-C178A at 13, 8 and 6 μM in buffer A was centrifuged at 25 ˚C at 12,000 and 16,000 rpm. His$_6$-Erv2p-F111S-C176A-C178A at 11, 7 and 5 μM and His$_6$-Erv2p-L114S-C176A-C178A at 11, 6 and 3 μM in buffer A were centrifuged at 25 ˚C at 12,000, 16,000 and 24,000 rpm. Absorbance measurements were made at 4 h intervals until equilibrium was reached (usually 24 h). Data were fit to a one-species model by the least squares method to determine the molecular weights (McRorie and Voelker, 1993).

Thermal denaturation assay

Thermal stability of Erv2p, Erv2p-C176A-C178A and Erv2p-F111S-C176A-C178A was studied by circular dichroism (CD) spectroscopy. CD spectra were recorded on an AVIV model 60CD spectropolarimeter (Aviv Associates, New Jersey) with a 1 mm pathlength cuvette. The proteins were at 12.5 μM in 50 mM NaH_2PO_4 [pH 8] and the ellipticity at 222 nm was measured from 4-90°C with an increased stepwise (1 °C/ min) and a 1 min equilibration at each temperature and a 20 s averaging time at each wavelength. Also, renaturation experiments (from 90 ˚C-4 ˚C) were carried out to ensure reversibility. The change in ellipticity at 222 nm was plotted against the temperature and the thermal denaturation midpoints (T_m) were interpolated.

Activity assay

Activity was also assayed by measuring the change in absorbance at 454 nm. The protein samples, at a final concentration of 3.75 μM, were added to a reaction mixture containing 50 mM NaH_2PO_4 [pH 8], 150 mM NaCl, 5 mM EDTA, and various concentrations of thiol substrates and absorbance changes were monitored at 454 nm. Thiol substrates were freshly prepared in buffer, pH was adjusted to pH 8 with NaOH and were standardized using 5,5'-dithio-bis(2-nitrobenzoic acid) (DNTB). The rates of bleaching were expressed as the amount of oxygen consumed per amount of time necessary to reduce half of the concentration of bound FAD (measured by a decrease in absorbance at 454 nm) per amount of Erv2p. In this assay, we observed a time lag between the addition of Erv2p and the moment of reduction of bound FAD. This delay in the reduction of bound FAD corresponds to the time that is necessary to consume 90% of the oxygen in the cuvette and is correlated with the amount of thiol used.

Pdi1p oxidation *in vitro*

His_6-tagged yeast Pdi1p lacking the signal sequence was purified as described previously (Sevier *et al.*, 2001). Purified Pdi1p was reduced by incubation with DTT-immobilized beads (BioVectra) for 1 h at room temperature. Samples containing 4 μM Pdi1p either alone or in combination with 1 mM diamide, 300 nM wild-type or mutant alleles of Erv2p or 300 nM FAD were incubated at 30 ˚C with intermittent mixing for up to 30 min. At different times, protein samples were precipitated with an equal volume of 20% (w/v) TCA and centrifuged for 15 min. The pellet was washed with cold acetone and suspended in urea sample buffer (50 mM Tris-HCl [pH 7.5], 2% SDS, 6 M urea, 1 mM PMSF, 0.01% bromophenol blue) with or without 15 mM 4-acetomido-4'-maleimidylstilbene-2,2'-disulphonic acid (AMS, Molecular Probes). Protein samples were incubated at 4 ˚C for 15 min and at 30 ˚C for 10 min. The samples were boiled for 2 min and were analyzed by 8% SDS-PAGE and immunoblotting. Yeast Pdi1p antibody (gift from Tom Stevens, University of Oregon, Eugene) was used at 1:10,000 and horseradish peroxidase-conjugated secondary antibody (Amersham Biosciences) was used at 1:10,000. Reduced Pdi1p protein concentrations were determined by the BCA protein assay (Sigma) using BSA as standard.

References

Coppock, D., Kopman, C., Gudas, J. and Cina-Poppe, D.A. (2000) Regulation of the quiescence-induced genes: quiescin Q6, decorin, and ribosomal protein S29. *Biochem Biophys Res Commun*, **269**, 604-610.

DeLano, W.L. (2002) *The Pymol Molecular Graphics System*. DeLano Scientific, San Carlos, CA, USA.

Engst, S. and Miller, S.M. (1998) Rapid reduction of Hg(II) by mercuric ion reductase does not require the conserved C-terminal cysteine pair using HgBr2 as the substrate. *Biochemistry*, **37**, 11496-11507.

Engst, S. and Miller, S.M. (1999) Alternative routes for entry of HgX2 into the active site of mercuric ion reductase depend on the nature of the X ligands. *Biochemistry*, **38**, 3519-3529.

Francavilla, A., Hagiya, M., Porter, K.A., Polimeno, L., Ihara, I. and Starzl, T.E. (1994) Augmenter of liver regeneration: its place in the universe of hepatic growth factors. *Hepatology*, **20**, 747-757.

Frand, A.R. and Kaiser, C.A. (1998) The ERO1 gene of yeast is required for oxidation of protein dithiols in the endoplasmic reticulum. *Mol Cell*, **1**, 161-170.

Frand, A.R. and Kaiser, C.A. (1999) Ero1p oxidizes protein disulfide isomerase in a pathway for disulfide bond formation in the endoplasmic reticulum. *Mol Cell*, **4**, 469-477.

Frand, A.R. and Kaiser, C.A. (2000) Two pairs of conserved cysteines are required for the oxidative activity of Ero1p in protein disulfide bond formation in the endoplasmic reticulum. *Mol Biol Cell*, **11**, 2833-2843.

Gross, E., Kastner, D.B., Kaiser, C.A. and Fass, D. (2004) Structure of Ero1p, source of disulfide bonds for oxidative protein folding in the cell. *Cell*, **117**, 601-610.

Gross, E., Sevier, C.S., Vala, A., Kaiser, C.A. and Fass, D. (2002) A new FAD-binding fold and intersubunit disulfide shuttle in the thiol oxidase Erv2p. *Nat Struct Biol*, **9**, 61-67.

Harding, H.P., Zhang, Y., Zeng, H., Novoa, I., Lu, P.D., Calfon, M., Sadri, N., Yun, C., Popko, B., Paules, R., Stojdl, D.F., Bell, J.C., Hettmann, T., Leiden, J.M. and Ron, D. (2003) An integrated stress response regulates amino acid metabolism and resistance to oxidative stress. *Mol Cell*, **11**, 619-633.

Hofhaus, G., Lee, J.E., Tews, I., Rosenberg, B. and Lisowsky, T. (2003) The N-terminal cysteine pair of yeast sulfhydryl oxidase Erv1p is essential for in vivo activity and interacts with the primary redox centre. *Eur J Biochem*, **270**, 1528-1535.

Lange, H., Lisowsky, T., Gerber, J., Muhlenhoff, U., Kispal, G. and Lill, R. (2001) An essential function of the mitochondrial sulfhydryl oxidase Erv1p/ALR in the maturation of cytosolic Fe/S proteins. *EMBO Rep*, **2**, 715-720.

Lisowsky, T. (1992) Dual function of a new nuclear gene for oxidative phosphorylation and vegetative growth in yeast. *Mol Gen Genet*, **232**, 58-64.

Lisowsky, T., Lee, J.E., Polimeno, L., Francavilla, A. and Hofhaus, G. (2001) Mammalian augmenter of liver regeneration protein is a sulfhydryl oxidase. *Dig Liver Dis*, **33**, 173-180.

McRorie, D.K. and Voelker, P.J. (1993) *Self-associating systems in the Analytical ultracentrifuge*.

Muhlrad, D., Hunter, R. and Parker, R. (1992) A rapid method for localized mutagenesis of yeast genes. *Yeast*, **8**, 79-82.

Pollard, M.G., Travers, K.J. and Weissman, J.S. (1998) Ero1p: a novel and ubiquitous protein with an essential role in oxidative protein folding in the endoplasmic reticulum. *Mol Cell*, **1**, 171-182.

Raje, S. and Thorpe, C. (2003) Inter-domain redox communication in flavoenzymes of the quiescin/sulfhydryl oxidase family: role of a thioredoxin domain in disulfide bond formation. *Biochemistry*, **42**, 4560-4568.

Sandalova, T., Zhong, L., Lindqvist, Y., Holmgren, A. and Schneider, G. (2001) Three-dimensional structure of a mammalian thioredoxin reductase: implications for mechanism and evolution of a selenocysteine-dependent enzyme. *Proc Natl Acad Sci U S A*, **98**, 9533-9538.

Sayle, R.A. and Milner-White, E.J. (1995) RASMOL: biomolecular graphics for all. *Trends Biochem Sci*, **20**, 374.

Senkevich, T.G., Ward, B.M. and Moss, B. (2004) Vaccinia virus A28L gene encodes an essential protein component of the virion membrane with intramolecular disulfide bonds formed by the viral cytoplasmic redox pathway. *J Virol*, **78**, 2348-2356.

Senkevich, T.G., Weisberg, A.S. and Moss, B. (2000a) Vaccinia virus E10R protein is associated with the membranes of intracellular mature virions and has a role in morphogenesis. *Virology*, **278**, 244-252.

Senkevich, T.G., White, C.L., Koonin, E.V. and Moss, B. (2000b) A viral member of the ERV1/ALR protein family participates in a cytoplasmic pathway of disulfide bond formation. *Proc Natl Acad Sci U S A*, **97**, 12068-12073.

Senkevich, T.G., White, C.L., Koonin, E.V. and Moss, B. (2002) Complete pathway for protein disulfide bond formation encoded by poxviruses. *Proc Natl Acad Sci U S A*, **99**, 6667-6672.

Sevier, C.S., Cuozzo, J.W., Vala, A., Aslund, F. and Kaiser, C.A. (2001) A flavoprotein oxidase defines a new endoplasmic reticulum pathway for biosynthetic disulphide bond formation. *Nat Cell Biol*, **3**, 874-882.

Sevier, C.S. and Kaiser, C.A. (2002) Formation and transfer of disulphide bonds in living cells. *Nat Rev Mol Cell Biol*, **3**, 836-847.

Sevier, C.S. and Kaiser, C.A. (2005) Disulfide transfer between two conserved cysteine pairs imparts selectivity protein oxidation by Ero1. *submited*.

Thompson, J.D., Gibson, T.J., Plewniak, F., Jeanmougin, F. and Higgins, D.G. (1997) The CLUSTAL_X windows interface: flexible strategies for multiple sequence alignment aided by quality analysis tools. *Nucleic Acids Res*, **25**, 4876-4882.

Thorpe, C., Hoober, K.L., Raje, S., Glynn, N.M., Burnside, J., Turi, G.K. and Coppock, D.L. (2002) Sulfhydryl oxidases: emerging catalysts of protein disulfide bond formation in eukaryotes. *Arch Biochem Biophys*, **405**, 1-12.

Tu, B.P., Ho-Schleyer, S.C., Travers, K.J. and Weissman, J.S. (2000) Biochemical basis of oxidative protein folding in the endoplasmic reticulum. *Science*, **290**, 1571-1574.

White, C.L., Senkevich, T.G. and Moss, B. (2002) Vaccinia virus G4L glutaredoxin is an essential intermediate of a cytoplasmic disulfide bond pathway required for virion assembly. *J Virol*, **76**, 467-472.

Woycechowsky, K.J. and Raines, R.T. (2003) The CXC motif: a functional mimic of protein disulfide isomerase. *Biochemistry*, **42**, 5387-5394.

Zhang, R.M. and Snyder, G.H. (1989) Dependence of formation of small disulfide loops in two-cysteine peptides on the number and types of intervening amino acids. *J Biol Chem*, **264**, 18472-18479.

Table 1. Molecular mass of His$_6$-Erv2p and His$_6$-Erv2p mutants.

Protein	**Calculated Molecular Mass (kDa)** [a]	**Predicted Molecular Mass (kDa)**
His$_6$-Erv2p	41.3 ± 0.1	21.2
His$_6$-Erv2p-C176A-C178A	41.0 ± 0.1	21.1
His$_6$-Erv2p-F111S-C176A-C178A	22.3 ± 0.1	21.0
His$_6$-Erv2p-L114S-C176A-C178A	23.0 ± 0.1	21.0

[a] Equilibrium analytical centrifugation of 7 μM His$_6$-Erv2p (16,000 rpm, 25 ˚C), 8 μM of His$_6$-Erv2p-C176A-C178A (16,000 rpm, 25 ˚C), 7 μM of His$_6$-Erv2p-F111S-C176A-C178A (24,000 rpm, 25 ˚C) and 6 μM of His$_6$-Erv2p-L114S-C176A-C178A (24000 rpm, 25 ˚C).

Table 2. Rate of O_2 consumption of His$_6$-Erv2p and His$_6$-Erv2p mutants.

		Rate of O_2 consumption (10^2 nmol O_2 per sec per nmol of Erv2p)[a]		
Thiol substrate	M_r[b]	His$_6$-Erv2p	His$_6$-Erv2p-C176A-C178A	His$_6$-Erv2p-F111S-C176A-C178A
DTT	152	99 ± 7.7 (100)	122 ± 7.8 (100)	34 ± 1.8 (100)
BMC	256	41 ± 3.3 (41)	22 ± 1.1 (18)	19 ± 2.1 (56)
NMA	208	17 ± 0.7 (17)	13 ± 0.6 (11)	19 ± 0.4 (56)
Cysteine	240	16 ± 2.4 (16)	2.9 ± 0.2 (3)	15 ± 1.0 (44)
Homocysteine	268	4.2 ± 0.2 (4)	1.9 ± 0.2 (2)	4.3 ± 0.2 (13)
β-ME	154	3.6 ± 0.1 (4)	1.8 ± 0.1 (2)	3.3 ± 0.3 (10)
GSH	613	2.2 ± 0.2 (2)	<0.9[c] (<1)	4.6 ± 0.2 (14)

[a] Rates of O_2 consumption were obtained using 5 mM dithiol substrates or 50 mM monothiol substrates. The average value ± standard deviation of at least three independent assays is presented. The activity relative to that of DTT (in percentage) is shown in parentheses.

[b] Molecular weight of the oxidized form (g/mol)

[c] Assays in which there was no decrease in absorbance at 454 nm after 2 h.

Table 3. Plasmids used in this work.

Name	**Description**	**Markers**	**Source or Reference**
pFA11	P_{GAL1}-*ERV2*	*CEN*, *URA3*	Sevier *et al.*, 2001
pJC15	P_{GAL1}-*ERV2-C121A-C124A-HA*$_3$	*CEN*, *URA3*	Gross *et al.*, 2002
pAV36	P_{GAL1}-*ERV2-C121A-C124A*	*CEN*, *URA3*	This study
pAV106	P_{GAL1}-*ERV2-C121A-C124A*	*CEN*, *LEU2*	This study
pAV41	P_{GAL1}-*ERV2-C176A-C178A*	*CEN*, *URA3*	Gross *et al.*, 2002
pAV364	P_{GAL1}-*ERV2-L171Stop*	*CEN*, *URA3*	This study
pAV363	P_{GAL1}-*ERV2-C176Stop*	*CEN*, *URA3*	This study
pAV437	P_{GAL1}-*ERV2-G177Stop*	*CEN*, *URA3*	This study
pAV365	P_{GAL1}-*ERV2-D182Stop*	*CEN*, *URA3*	This study
pAV366	P_{GAL1}-*ERV2-S187Stop*	*CEN*, *URA3*	This study
pAV367	P_{GAL1}-*ERV2-A192Stop*	*CEN*, *URA3*	This study
pAV70	P_{GAL1}-*ERV2-CC*	*CEN*, *URA3*	This study
pAV71	P_{GAL1}-*ERV2-CGAC*	*CEN*, *URA3*	This study
pAV92	P_{GAL1}-*ERV2-CGA*$_2$*C*	*CEN*, *URA3*	This study
pAV93	P_{GAL1}-*ERV2-CGA*$_3$*C*	*CEN*, *URA3*	This study
pAV94	P_{GAL1}-*ERV2-CGA*$_4$*C*	*CEN*, *URA3*	This study
pAV268	P_{GAL1}-*ERV2-(DYD)Δ*	*CEN*, *URA3*	This study
pAV404	P_{GAL1}-*ERV2-(DYD)Δ+2A*	*CEN*, *URA3*	This study
pAV403	P_{GAL1}-*ERV2-(DYD)Δ+3A*	*CEN*, *URA3*	This study
pAV161	P_{GAL1}-*ERV2-F111S-C176A-C178A*	*CEN*, *URA3*	This study
pAV283	P_{GAL1}-*ERV2-L114S-C176A-C178A*	*CEN*, *URA3*	This study
pAV176	P_{GAL1}-*ERV2-P120A-C176A-C178A*	*CEN*, *URA3*	This study
pAV284	P_{GAL1}-*ERV2-F111S-C121A-C124A*	*CEN*, *URA3*	This study
pAV377	P_{GAL1}-*ERV2-F111S-C176Stop*	*CEN*, *URA3*	This study
pJC11	*ERV2* (1-22Δ)-His$_6$	AMP	Sevier *et al.*, 2001
pET-14b	*E. coli* His$_6$-fusion vector	AMP	Novagen
pAV79	His$_6$-*ERV2*	AMP	This study
pAV87	His$_6$-*ERV2-C176A-C178A*	AMP	This study
pAV88	His$_6$-*ERV2-C176Stop*	AMP	This study
pAV276	His$_6$-*ERV2-F111S-C176A-C178A*	AMP	This study
pAV319	His$_6$-*ERV2-L114S-C176A-C178A*	AMP	This study
pAV287	His$_6$-*ERV2-P120A-C176A-C178A*	AMP	This study

Table 4. Primers used in this study.

Primer	**Sequence**
G177Del1	5’- GAGGACTACGATTGTTGTAGTGACAGCGAC-3’
G177insAla1	5’- GACTACGATTGTGGA**GCA**TGTAGTGACAGCGAC-3’
G177ins2Ala1	5'- GACTACGATTGTGGA**GCAGCA**TGTAGTGACAGCGAC-3'
G177ins3Ala1	5'- GACTACGATTGTGGA**GCAGCAGCA**TGTAGTGACAGCGAC-3'
G177ins4Ala1	5'-GACTACGATTGTGGA**GCAGCAGCAGCA**TGTAGTGACAGCGAC-3'
Δ(D173toD175)1	5'- GCTACCATCCTGGAGTGTGGATGTAGTGAC-3'
del(DYD)2Ala1	5'- GCTACCATCCTGGAG**GCTGCT**TGTGGATGTAGTGAC-3'
del(DYD)3Ala1	5'- GCTACCATCCTGGAG**GCTGCTGCT**TGTGGATGTAGTGAC-3'
F111S1	5'- GAGAAACTGCACACG**TCT**ATTGGGTTGTATGCA-3'
L114S1	5'- CACACGTTTATTGGG**TCT**TATGCAGAACTCTAT-3'
P120A1	5'- TATGCAGAACTCTAT**GCA**TGCGGGGAATGTTCA-3'
Gal1	5’- TGCATAACCACTTTAACT-3’
SacII-*-I170	5’- AAAA**CCGCGG**TTAGATGGTAGCACAGTCATATAT-3’
SacII-*-D175	5’- AAAA**CCGCGG**TTAATCGTAGTCCTCCAGGATGGT-3’
SacII-*-C176	5'- AAAA**CCGCGG**TTAACAATCGTAGTCCTCCAGGAT-3'
SacII-*-S181	5’- AAAA**CCGCGG**TTAGCTGTCACTACATCCACAAT-3’
SacII-*-V186	5’- AAAA**CCGCGG**TTACACGCGTTTACCGTCGCTGTC-3’
SacII-*-E191	5’- AAAA**CCGCGG**TTACTCCTTCTCGAGAGACACGCG-3’
NdeI-Erv2	5'- AAAAAA**CATATG**GAACTATCCATCGCTACGCCGGGC-3'
Erv2-BamHI	5'- AAAA**GGATCC**TCAACCGTGCTGTTTAGCCTCCTT-3'
Erv2-C176Stop-BamHI	5'- AAAA**GGATCC**TTAATCGTAGTCCTCCAGGATGGT-3'
Erv2mut3	5’- ATTAAGTTGGGTAACGCC-3’

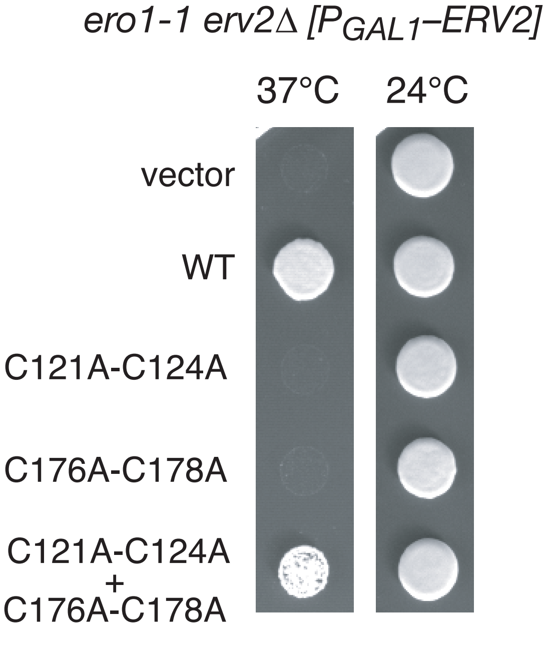
ero1-1 erv2Δ [PGAL1–ERV2]
37°C
24°C
vector
WT
C121A-C124A
C176A-C178A
C121A-C124A
+
C176A-C178A

Figure 1. Evidence of electron transfer between pairs of cysteine residues. An *ero1-1 erv2Δ* mutant strain (CKY899) was transformed with either pRS316 (empty vector), or plasmids expressing wild-type *ERV2* or *ERV2* cysteine mutants as indicated. The resulting strains were tested for growth on YPGal at the restrictive (37 ˚C) and permissive (24 ˚C) temperatures for *ero1-1*.

(Next page)

Figure 2. Conservation of the C terminus of Erv2p among fungal species. Multiple sequence alignment of the C-terminal half of Erv2p, among fungal species using ClustalX (Thompson *et al*., 1997). This segment shows both the conserved active site (Cys121-Cys124) and tail (Cys176-Cys178) cysteine pairs. The cysteine residues are colored in a dark grey. Light grey boxes show blocks of conserved residues with more than 70% identity. Abbreviations of the species names are as follows: Scer, *Saccharomyces cerevisiae*; Sbay, *Saccharomyces bayanus*; Smik, *Saccharomyces mikatae*; Skud*, Saccharomyces kudriavzevii;* Spar, *Saccharomyces paradoxus;* Ecun, *Encephalitozoon cuniculi*; Cgra, *Candida glabrata*; Sklu, *Saccharomyces kluyveri;* Klac, *Kluyveromyces lactis*; Scas, *Saccharomyces castellii*; Calb, *Candida albicans*; Dhan, *Debaryomyces hansenii*; Anid*, Aspergillus nidulans;* Fgra*, Fusarium graminearum*; Ylip*, Yarrowia lipolytica;* Mgri, *Magnaporthe grisea*; Ncra, *Neurospora crassa*; Umay, *Ustilago maydis*; Egos, *Eremothecium gossypii*; and Afum, *Aspergillus fumigatus*.

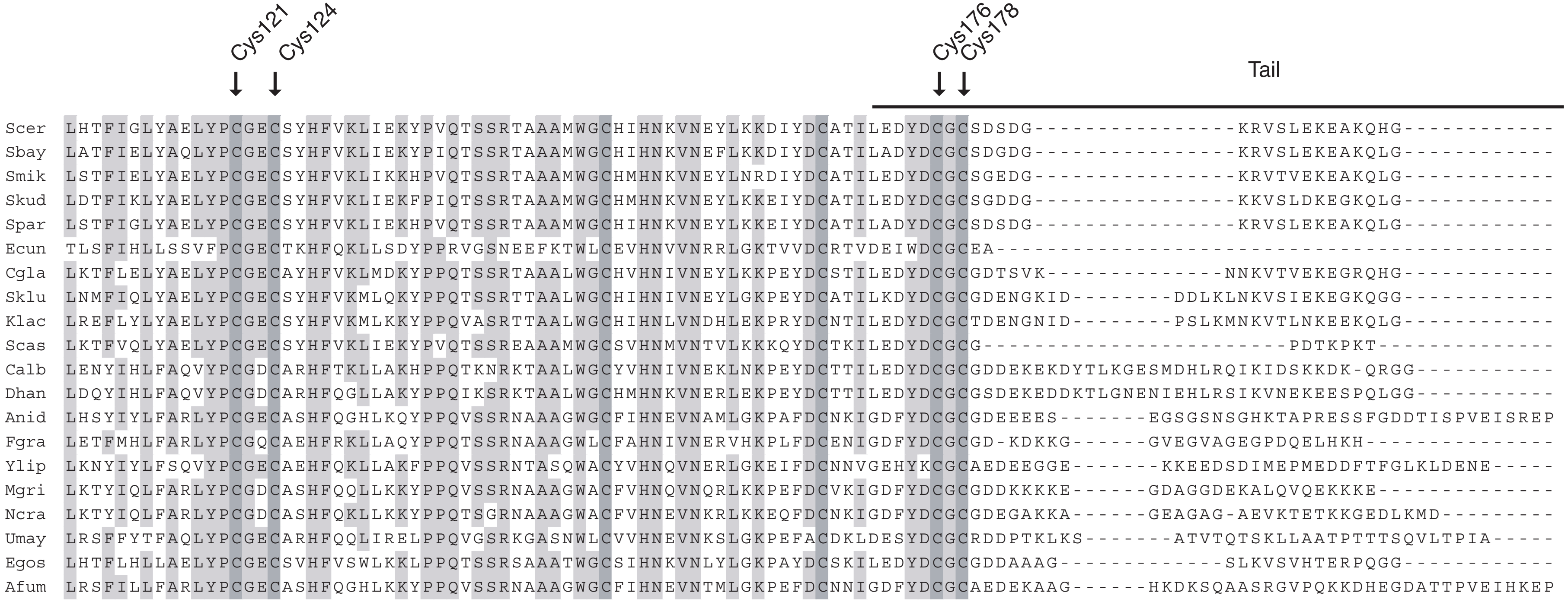

```
Scer LHTFIGLYAELYPCGECSYHFVKLIEKYPVQTSSRTAAAMWGCHIHNKVNEYLKKDIYDCATILEDYDCGCSDSDG----------------KRVSLEKEAKQHG------------
Sbay LATFIELYAQLYPCGECSYHFVKLIEKYPIQTSSRTAAAMWGCHIHNKVNEFLKKDIYDCATILADYDCGCSDGDG----------------KRVSLEKEAKQLG------------
Smik LSTFIELYAELYPCGECSYHFVKLIKKHPVQTSSRTAAAMWGCHMHNKVNEYLNRDIYDCATILEDYDCGCSGEDG----------------KRVTVEKEAKQLG------------
Skud LDTFIKLYAELYPCGECSYHFVKLIEKFPIQTSSRTAAAMWGCHMHNKVNEYLKKEIYDCATILEDYDCGCSGDDG----------------KKVSLDKEGKQLG------------
Spar LSTFIGLYAELYPCGECSYHFVKLIEKHPVQTSSRTAAAMWGCHIHNKVNEYLKKEIYDCATILADYDCGCSDSDG----------------KRVSLEKEAKQLG------------
Ecun TLSFIHLLSSVFPCGECTKHFQKLLSDYPPRVGSNEEFKTWLCEVHNVVNRRLGKTVVDCRTVDEIWDCGCEA--------------------------------------------
Cgla LKTFLELYAELYPCGECAYHFVKLMDKYPPQTSSRTAAALWGCHVHNIVNEYLKKPEYDCSTILEDYDCGCGDTSVK--------------NNKVTVEKEGRQHG------------
Sklu LNMFIQLYAELYPCGECSYHFVKMLQKYPPQTSSRTTAALWGCHIHNIVNEYLGKPEYDCATILKDYDCGCGDENGKID--------DDLKLNKVSIEKEGKQGG------------
Klac LREFLYLYAELYPCGECSYHFVKMLKKYPPQVASRTTAALWGCHIHNLVNDHLEKPRYDCNTILEDYDCGCTDENGNID--------PSLKMNKVTLNKEEKQLG------------
Scas LKTFVQLYAELYPCGECSYHFVKLIEKYPVQTSSREAAAMWGCSVHNMVNTVLKKKQYDCTKILEDYDCGCG------------------------PDTKPKT--------------
Calb LENYIHLFAQVYPCGDCARHFTKLLAKHPPQTKNRKTAALWGCYVHNIVNEKLNKPEYDCTTILEDYDCGCGDDEKEKDYTLKGESMDHLRQIKIDSKKDK-QRGG-----------
Dhan LDQYIHLFAQVYPCGDCARHFQGLLAKYPPQIKSRKTAALWGCHMHNKVNERLEKPEYDCTTILEDYDCGCGSDEKEDDKTLGNENIEHLRSIKVNEKEESPQLGG-----------
Anid LHSYIYLFARLYPCGECASHFQGHLKQYPPQVSSRNAAAGWGCFIHNEVNAMLGKPAFDCNKIGDFYDCGCGDEEEES-------EGSGSNSGHKTAPRESSFGDDTISPVEISREP
Fgra LETFMHLFARLYPCGQCAEHFRKLLAQYPPQTSSRNAAAGWLCFAHNIVNERVHKPLFDCENIGDFYDCGCGD-KDKKG------GVEGVAGEGPDQELHKH---------------
Ylip LKNYIYLFSQVYPCGECAEHFQKLLAKFPPQVSSRNTASQWACYVHNQVNERLGKEIFDCNNVGEHYKCGCAEDEEGGE-------KKEEDSDIMEPMEDDFTFGLKLDENE-----
Mgri LKTYIQLFARLYPCGDCASHFQQLLKKYPPQVSSRNAAAGWACFVHNQVNQRLKKPEFDCVKIGDFYDCGCGDDKKKKE------GDAGGDEKALQVQEKKKE--------------
Ncra LKTYIQLFARLYPCGDCASHFQKLLKKYPPQTSGRNAAAGWACFVHNEVNKRLKKEQFDCNKIGDFYDCGCGDEGAKKA------GEAGAG-AEVKTETKKGEDLKMD---------
Umay LRSFFYTFAQLYPCGECARHFQQLIRELPPQVGSRKGASNWLCVVHNEVNKSLGKPEFACDKLDESYDCGCRDDPTKLKS-------ATVTQTSKLLAATPTTTSQVLTPIA-----
Egos LHTFLHLLAELYPCGECSVHFVSWLKKLPPQTSSRSAAATWGCSIHNKVNLYLGKPAYDCSKILEDYDCGCGDDAAAG-------------SLKVSVHTERPQGG------------
Afum LRSFILLFARLYPCGECASHFQGHLKKYPPQVSSRNAAAGWGCFIHNEVNTMLGKPEFDCNNIGDFYDCGCAEDEKAAG------HKDKSQAASRGVPQKKDHEGDATTPVEIHKEP
```

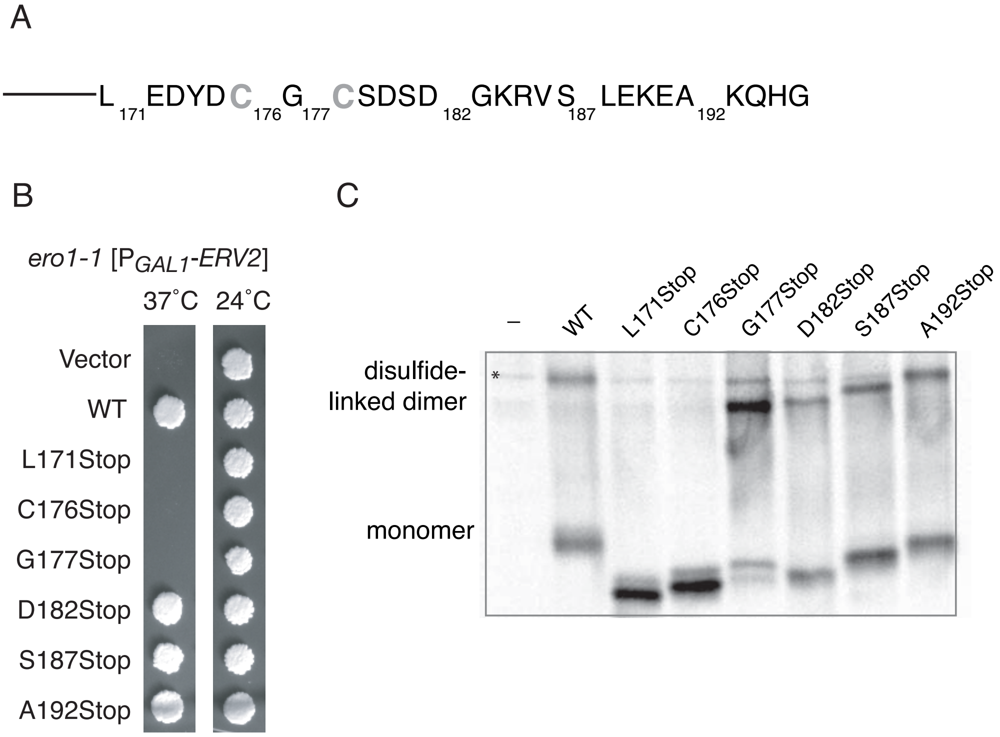

A
L171 EDYD C176 G177 C SDSD182 GKRV S187 LEKEA192 KQHG
B
ero1-1 [PGAL1-ERV2]
37˚C
24˚C
Vector
WT
L171Stop
C176Stop
G177Stop
D182Stop
S187Stop
A192Stop
C
–
WT
L171Stop
C176Stop
G177Stop
D182Stop
S187Stop
A192Stop
disulfide-linked dimer
monomer
*

Figure 3. In the tail, only Cys176 and Cys178 are required for activity. **(A)** Scheme representing residues in the Erv2p tail (residues 171 through 196). The numbers in subscript indicate the residues that were mutated to a stop codon, and the tail cysteine residues are colored grey. **(B)** The *ero1-1* mutant (CKY598) containing either pRS316 (empty vector) or various truncated mutant alleles of Erv2p were plated onto YPGal and grown at 24 ˚C or 37 ˚C for 4 d. **(C)** *ero1-1 erv2Δ* mutants (CKY899) containing either pRS316 (empty vector), wild-type Erv2p, or various truncated mutant alleles of Erv2p were labeled with [^{35}S]methionine and alkylated with NEM prior to immunoprecipitation with Erv2p antibody. A cross-reacting band not related to Erv2p is marked by an asterisk.

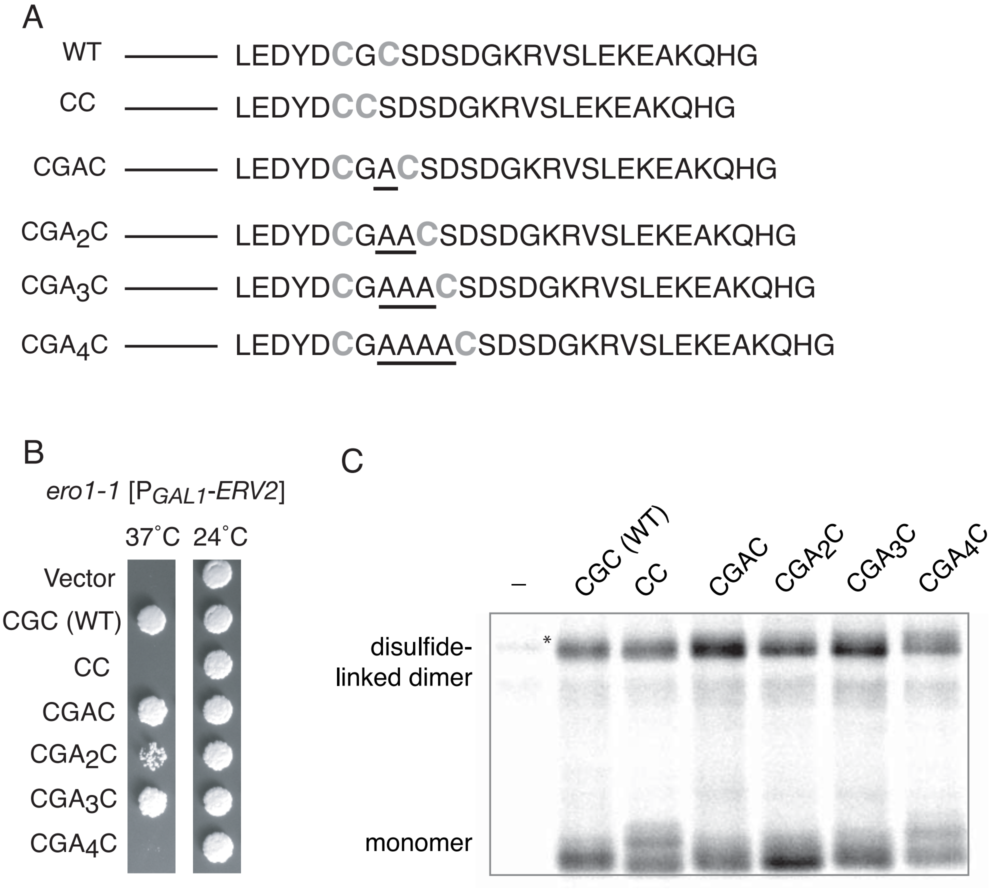
A
WT — LEDYDCGCSDSDGKRVSLEKEAKQHG
CC — LEDYDCCSDSDGKRVSLEKEAKQHG
CGAC — LEDYDCGACSDSDGKRVSLEKEAKQHG
CGA$_2$C — LEDYDCGAACSDSDGKRVSLEKEAKQHG
CGA$_3$C — LEDYDCGAAACSDSDGKRVSLEKEAKQHG
CGA$_4$C — LEDYDCGAAAACSDSDGKRVSLEKEAKQHG
B
ero1-1 [P$_{GAL1}$-ERV2]
37˚C
24˚C
Vector
CGC (WT)
CC
CGAC
CGA$_2$C
CGA$_3$C
CGA$_4$C
C
–
CGC (WT)
CC
CGAC
CGA$_2$C
CGA$_3$C
CGA$_4$C
disulfide-linked dimer
monomer
*

Figure 4. The position of Cys176 and Cys178 relative to the Cys121-Cys124 cysteine pair is important for disulfide transfer. **(A)** Scheme representing residues in the Erv2p tail (residues 171 through 196). The tail cysteine residues are colored grey, and inserted residues are underlined. **(B)** The *ero1-1* mutant (CKY598) containing either pRS316 (empty vector) or mutant alleles of *ERV2* were plated onto YPGal and grown at 24 ˚C and 37 ˚C for 4 d. **(C)** Radiolabeling and immunoprecipitation with Erv2p antibody of *ero1-1 erv2Δ* cells (CKY899) containing pRS316 (empty vector), wild-type *ERV2*, or *erv2* mutants as indicated. A cross-reacting band not related to Erv2p is marked by an asterisk.

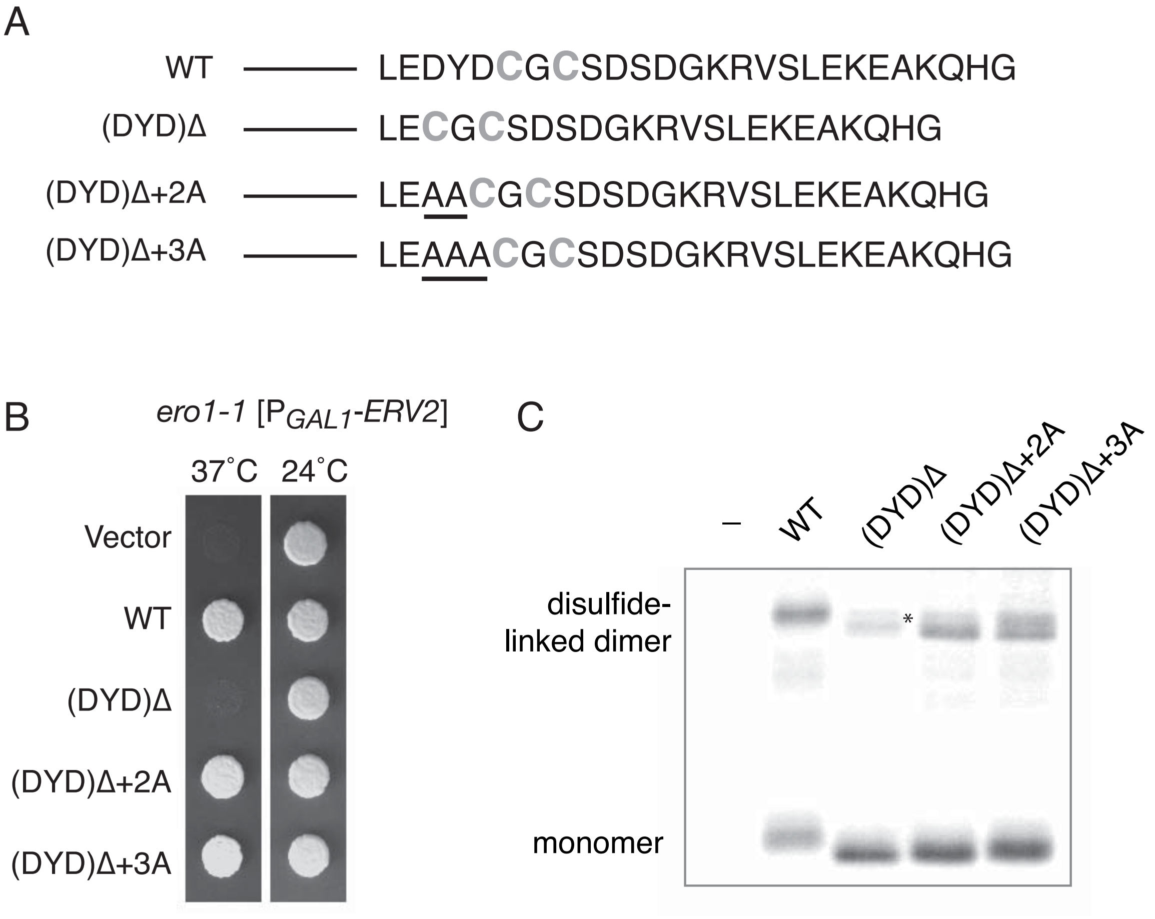
A
WT
LEDYDCGCSDSDGKRVSLEKEAKQHG
(DYD)Δ
LECGCSDSDGKRVSLEKEAKQHG
(DYD)Δ+2A
LEAACGCSDSDGKRVSLEKEAKQHG
(DYD)Δ+3A
LEAAACGCSDSDGKRVSLEKEAKQHG
B
ero1-1 [PGAL1-ERV2]
37˚C
24˚C
Vector
WT
(DYD)Δ
(DYD)Δ+2A
(DYD)Δ+3A
C
–
WT
(DYD)Δ
(DYD)Δ+2A
(DYD)Δ+3A
disulfide-linked dimer
*
monomer

Figure 5. Localization of Cys176 and Cys178 relative to Cys121-Cys124 is important for disulfide transfer. **(A)** Scheme representing residues in the Erv2p tail (residues 171 through 196). The residues underlined are the additional amino acid residues inserted back into the Erv2p-(DYD)Δ mutant. **(B)** The *ero1-1* mutant (CKY598) containing either pRS316 (empty vector) or various mutant alleles of *ERV2* were plated onto YPGal and grown at 24 ˚C and 37 ˚C for 4 days. **(C)** *ero1-1 erv2Δ* cells (CKY899) containing pRS316 (empty vector), wild-type *ERV2* or *erv2* mutants were labeled with [^{35}S]methionine and immunoprecipitated with Erv2p antibody. A cross-reacting band not related to Erv2p is marked by an asterisk.

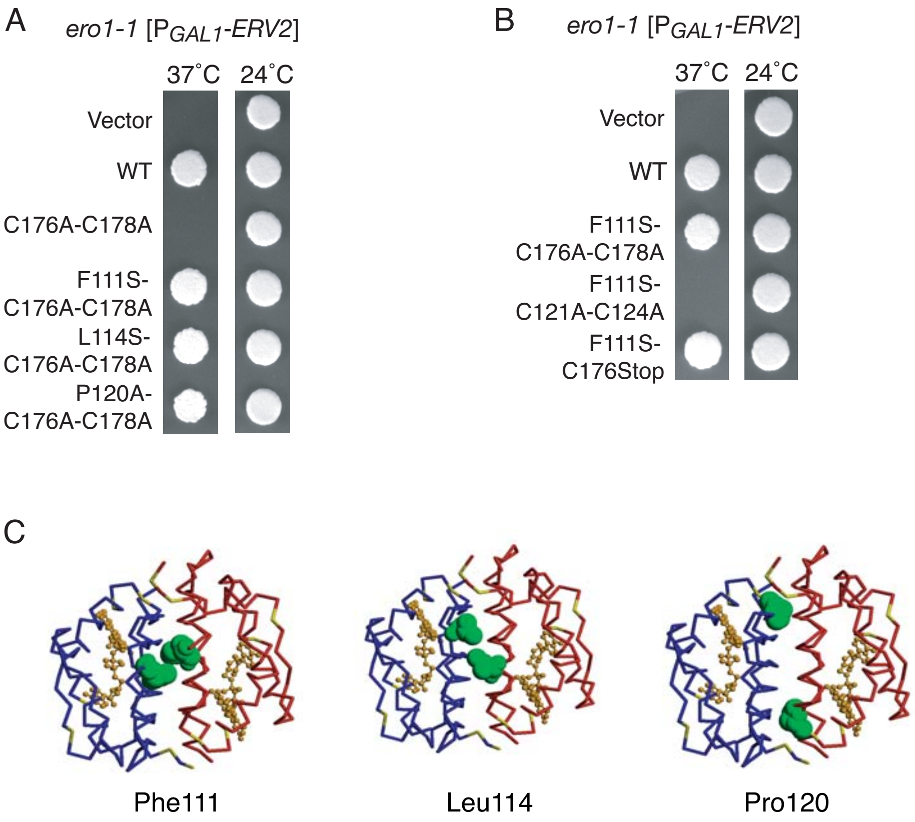
A
ero1-1 [P_{GAL1}-ERV2]
37˚C
24˚C
Vector
WT
C176A-C178A
F111S-C176A-C178A
L114S-C176A-C178A
P120A-C176A-C178A
B
ero1-1 [P_{GAL1}-ERV2]
37˚C
24˚C
Vector
WT
F111S-C176A-C178A
F111S-C121A-C124A
F111S-C176Stop
C
Phe111
Leu114
Pro120

Figure 6. Intragenic suppressors of the cysteine tail mutant. **(A)** and **(B)** The *ero1-1* mutant (CKY598) containing either pRS316 (empty vector) or various mutant alleles of *ERV2* were plated in rich medium containing 2% galactose at 24 ˚C and 37 ˚C for 4 d. **(C)** Structure of Erv2p showing the location of the residues identified as intragenic suppressors represented using Rasmol (Sayle and Milner-White, 1995). The FAD molecules are represented in a ball and stick representation. The cysteine residues are colored yellow and the residues obtained in the screen are shown in space-filling representation. Phe111, Leu114 and Pro120 are located in the dimer interface.

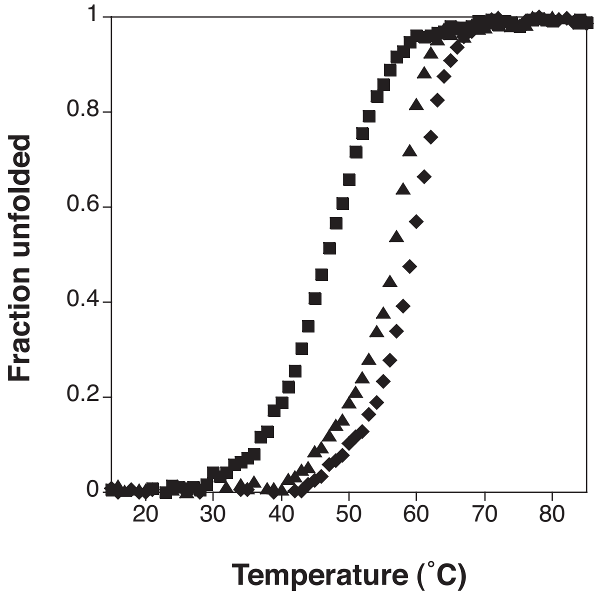

Figure 7. Thermal denaturation curves for Erv2p wild-type and mutant variants. Thermal stability of 12.5 μM recombinant His$_6$-Erv2p (◆), His$_6$-Erv2p-C176A-C178A (▲), and His$_6$-Erv2p-F111S-C176A-C178A (■) assayed by circular dichroism. The fraction of unfolded protein was plotted as a function of the temperature.

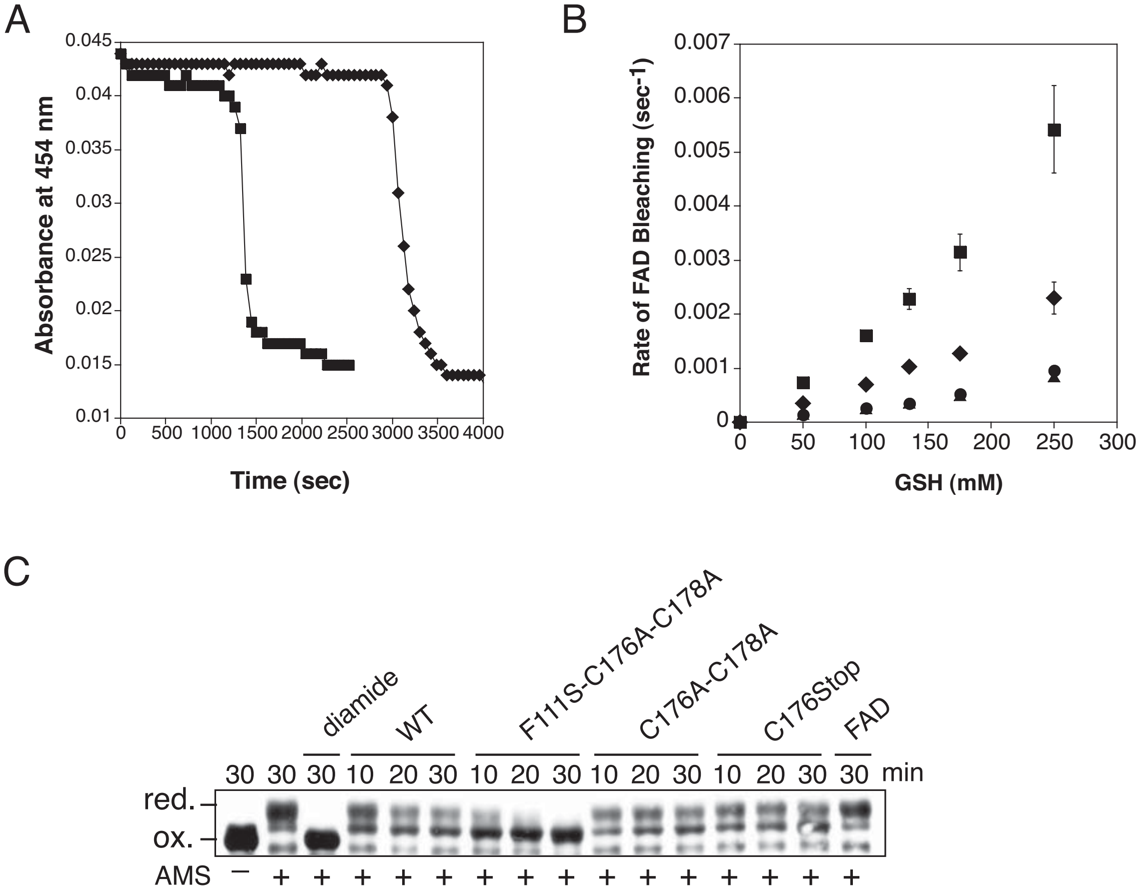

Figure 8. Erv2p intragenic suppressors have different substrate specificities. **(A)** Absorbance changes at 454 nm for 3.75 μM wild-type His$_6$-Erv2p (◆) or His$_6$-Erv2p-F111S-C176A-C178A (■) with 50 mM glutathione as a substrate. **(B)** Rate of reduction of bound FAD, measured by the decrease in absorbance at 454 nm, for 3.75 μM recombinant His$_6$-Erv2p (◆), His$_6$-Erv2p-F111S-C176A-C178A (■), His$_6$-Erv2p-C176A-C178A (▲) and His$_6$-Erv2p-C176Stop (●) measured as a function of glutathione concentration. **(C)** Pdi1p re-oxidation by His$_6$-Erv2p, His$_6$-Erv2p-F111S-C176A-C178A, His$_6$-Erv2p-C176A-C178A and His$_6$-Erv2p-C176Stop mutants *in vitro*. Reduced 4 μM Pdi1p was incubated in the presence of 300 nM FAD, 300 nM of wild-type or mutants of Erv2p, or 1 mM diamide. At the indicated time points, an aliquot was withdrawn, samples were TCA precipitated, and free thiols were trapped by alkylation with AMS. Reduced (red) and oxidized (ox) forms of Pdi1p are indicated.

(Next page)

Figure 9. Crystal-structure of Erv2p showing accessibility of the active site cysteine residues. The wild-type dimeric form of Erv2p **(A)**, and deduced structures of Erv2p-C176Stop **(B)**, and Erv2p-F111S-C176A-C178A **(C)** are displayed in space-filling representation using Pymol (DeLano, 2002). The active site cysteine residues for subunits labeled as dark blue are shown in red. The other subunit of the dimer is represented in light blue for wild-type and Erv2p-C176Stop, and the cysteine residues in the C-terminal tail of wild-type are shown in pink.

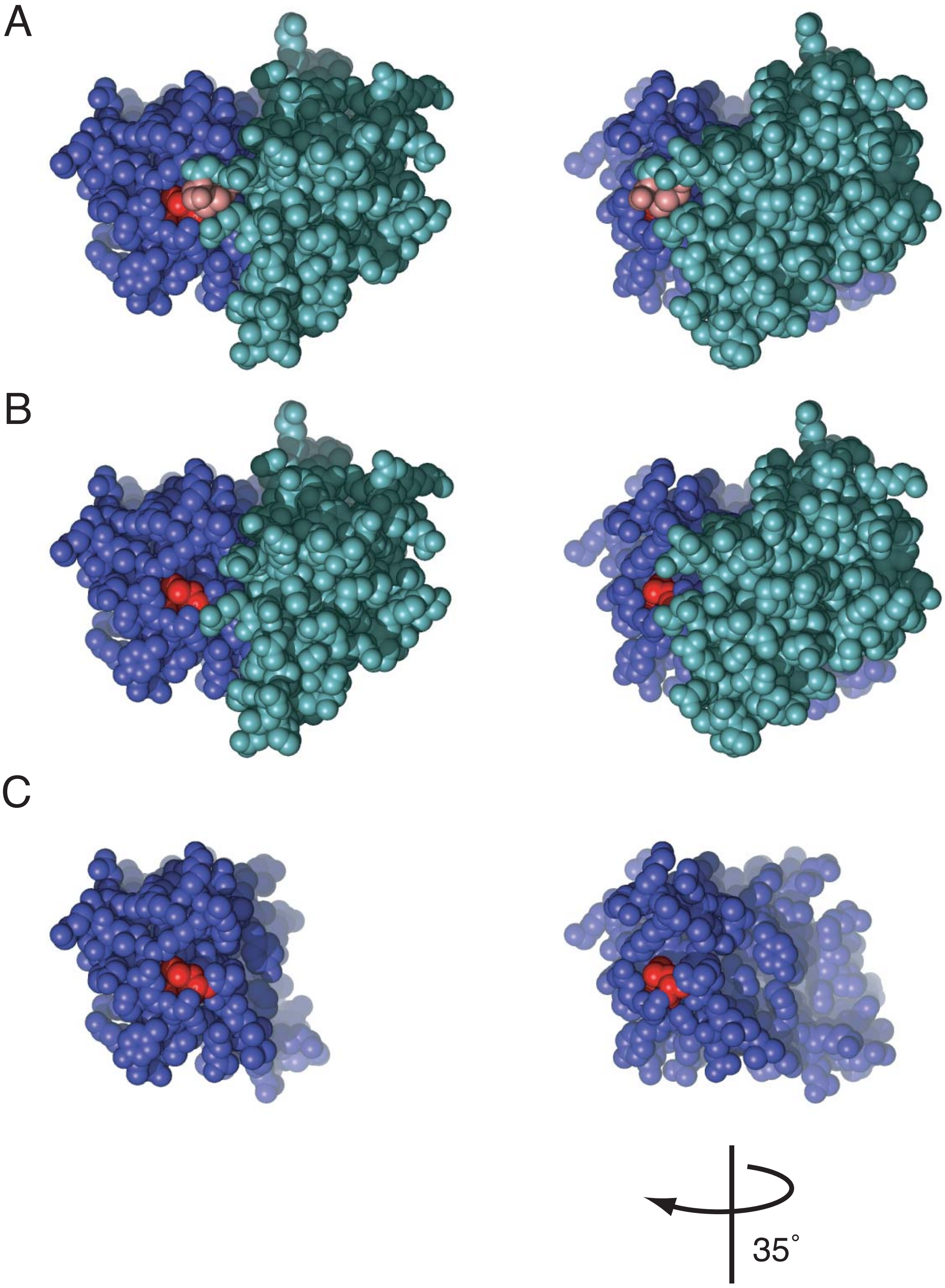
A
B
C
35°

Chapter Four

Further mutagenic studies performed in Erv2p

Preface

Additional pieces of data have been generated by me and have been included as an appendix to Chapter 3. In this chapter, I also extrapolate the data obtained for Erv2p to the QSOX/ERV family.

Results

An additional pair of cysteines seems to be required for Erv2p activity *in vivo*

In chapters 2 and 3, the roles of two conserved cysteine pairs in the catalytic mechanism of Erv2p are discussed. Additionally, Erv2p, Erv1p and ALR contain a third conserved pair of cysteines (Cys150 and Cys167 in Erv2p) that forms a disulfide bond between helix $\alpha4$ and the C-terminal helix $\alpha5$ (helix before the flexible tail). In the Erv2p and rat ALR (rALR) crystal structures this disulfide bond is near the adenine moiety of the FAD (Gross *et al.*, 2002; Wu *et al.*, 2003). In the rALR crystal structure, Cys91-Cys108 (corresponding to Cys150 and Cys167 in Erv2p) are in contact with the FAD ligand such that the oxygen of Cys91 forms a hydrogen bond with N6 of the adenine moiety (Wu et al., 2003). It has been suggested that this disulfide bond may be important for positioning the tail cysteine residues in close proximity to the conserved Cys-X-X-Cys motif in the other subunit and/or for stability of cofactor binding to the protein (Dym and Eisenberg, 2001; Gross *et al.*, 2002).

In order to determine the role of this disulfide bond in the disulfide transfer between subunits in Erv2p we created Cys to Ala mutants of these two residues (Erv2p-C150A and Erv2p-C167A). This pair of cysteines is required for activity *in vivo* as these mutants do not suppress the growth defect of *ero1-1* cells at the restrictive temperature (Figure 1A). Similarly, the corresponding pair of cysteines in Erv1p (Cys159 and Cys176) is also required for activity *in vivo*, since Cys to Ser mutants of these residues are unable to suppress the *erv1Δ* or the *erv1-1* temperature-sensitive mutant at the restrictive temperature (Hofhaus *et al.*, 2003).

The observation that Erv2p-C150A and Erv2p-C167A are still able to form a disulfide-linked dimer suggests that in these mutants the Cys121 and Cys176 or Cys178 are still able to interact (Figure 1B). Recombinant Erv2p-C150A and Erv2p-C167A were soluble but did not absorb light at the FAD characteristic peaks (data not shown) suggesting that these residues are probably involved in FAD binding. The same is observed for recombinant Erv1p-C159S mutant, which has lower affinity towards FAD (Hofhaus *et al.*, 2003), suggesting that Cys to Ala/Ser mutations of these cysteine residues cause instability of the FAD.

The tail of Erv2p is consisted mainly of charged residues

Sequence analysis of the C-terminal regions of Erv2p and fungi orthologs revealed that these regions are poorly conserved, that they can adopt various lengths and that the only common feature is the large number of charged residues (Figure 2). To analyze the role of the charged residues in the tail of Erv2p, we individually mutated these residues to alanine. The Erv2p charged residue mutants were able to suppress the growth defect of *ero1-1* at the restrictive temperature, suggesting that they were still active. Erv2p-E191A was the only mutant that had a slight growth defect (Table 1).

Altering Gly177 to a negatively charged residue affects Erv2p activity

It is well established that redox properties of protein thiol-disulfide oxidoreductases are strongly influenced by amino acid residues in close proximity to the redox-active cysteines (Chivers *et al.*, 1997). The properties of the amino acids between cysteine residues affect the propensity of those cysteine residues to be in a reduced or oxidized state (Bessette *et al.*, 2001). Analysis of the Cys-X-Cys motif in Erv2p and its fungal orthologs reveals that the residue between the tail cysteines (Gly177) is extremely conserved (Figure 2). To address the role of the Gly177, we mutagenized this residue to other amino acid residues. From the set of mutants studied, only Erv2p mutants where Gly177 was mutated to negatively charged residue had a slight defect in the ability to suppress the growth defect of *ero1-1* at the restrictive temperature (Table 2).

Cys121 of the active site cysteine pair is attacked by Cys176

To further address the role of the spatial localization of the cysteine residues of the Cys-X-Cys motif we added one to three alanine residues to the Erv2p-(DYD)Δ mutant before and after Gly177 (Figure 3A and Table 3). These mutants were still inactive and were still unable to transfer disulfide bonds through the tail, as suggested by the lack of a disulfide-linked intermediate (Figure 3B and C and Table 3). These results suggest that in the Erv2p-(DYD)Δ context, the Cys176 needs to be located near the active site cysteine pair for transfer to occur. It is also possible that in these mutants, the cysteine residue interacting with the active site cysteine is not facing the active site cysteine pair, thus not allowing the interaction to occur.

Intragenic suppressors of the tail cysteines mutants are monomers

In a screen for Erv2p mutants that were able to catalyze disulfide transfer without relaying through the tail cysteine we isolated three mutations (F111S, L114S and P120A). These residues lie in the dimer interface, a region characterized by hydrophobic contacts between the α1 and α2 helices of the two subunits (Gross *et al.*, 2002). The location of these residues suggested that these mutations convert the protein into a monomer, thus allowing direct access to the active site cysteines. To determine whether Erv2p-F111S-C176A-C178A was a monomeric protein, we expressed and purified Erv2p wild-type and Erv2p variants (Erv2p-C176A-C178A and Erv2p-F111S-C176A-C178A) in *Escherichia coli*. After purification, all the recombinant proteins exhibited the characteristic absorbance peaks for bound FAD at 352 and 454 nm and showed sulfhydryl oxidase activity (see below).

The purified proteins were analyzed by gel filtration in a Sephadex-200 column. Figure 4A shows the elution volume of Erv2p wild-type, Erv2p-C176A-C178A and Erv2p-F111S-C176A-C178A. A standard curve was generated with proteins of known molecular weight. The observed elution volumes correspond to apparent molecular weights of 47.7, 43.9 and 35.8 kDa for Erv2p wild-type, Erv2p-C176A-C178A and Erv2p-F111S-C176A-C178A, respectively (Figure 4 B). Erv2p wild-type and Erv2p-C176A-C178A showed a different behavior, suggesting that Erv2p wild-type has a more compact structure. Due to the difference in behavior of Erv2p wild-type and Erv2p-C176A-C178A proteins we decided to perform equilibrium analytical centrifugation studies (see Chapter 3)

Intragenic suppressor mutations do not rescue an Erv2p-C150A or Erv2p-C167A or Erv2p-C150A-C167A double mutant or an Erv2p-L171Stop mutant

It has been suggested that the Cys150-Cys167 disulfide bond tethers the C-terminal α5 helix to the core of the protein, thus positioning the tail cysteine residues near the active site cysteine pair (Gross *et al.*, 2002). Based on this, we expected that the addition of intragenic suppressor mutations to an Erv2p-C150A, Erv2p-C167A or Erv2p-C150A-C167A would suppress the *ero1-1* growth defect. Surprisingly, the Erv2p-F111S-C150A, Erv2p-L114S-C150A and Erv2p-P120A-C150A were still inactive (Table 4 and data not shown). This data is consistent with the idea that these residues are important for flavin binding.

While the addition of the intragenic suppressor mutations to Erv2p-C176Stop restored the activity, the addition of these mutations does not rescue an Erv2p-L171Stop mutant (Table 4). This inability to suppress could result from an overall instability of the protein due to the removal of helix α5. Consistent with this result, we were unable to purify Erv2p-L171Stop mutant.

Intragenic suppressor mutations are conserved in QSOX/ERV family

All the residues tested that cause Erv2p-C176A-C178A to become a monomeric protein are conserved among the QSOX/ERV family. The residue Phe111 is conserved between Erv2p, Erv1p and human and rat ALRp. In Erv2p or Erv1p-like fungal orthologs 70% of the aligned sequences have a Phe corresponding to the position 111 in Erv2p. The other sequences contain either a Tyr or a Leu. The residue Leu114 is conserved in Erv2p and rat ALR. In Erv2p-like homologs this residue is almost always a Leu except in 2 cases where is a Ser or Thr. In Erv1p-like fungi orthologs this residue is a Leu or Ile. Pro120 is conserved in Erv2p, Erv1p, human and rat ALR and E10R but not in Quiescin Q6. In both Erv2p-like and Erv1p-like fungi orthologs this residue is always a Pro.

Sulfhydryl oxidase activity of Erv2p

Erv2p catalyzes the oxidation of thiols to their corresponding disulfides, consuming oxygen and producing hydrogen peroxide. During oxidation of thiol substrates, the Cys121-Cys124 pair is reduced. The reoxidation of this pair is associated with the reduction of bound-FAD. In turn, reduced FAD is then reoxidized by oxygen, with a concomitant production of hydrogen peroxide. The sulfhydryl oxidase activity of Erv2p wild-type and mutant alleles can be determined by monitoring O_2 consumption, by measuring the reduction of bound FAD or by measuring the formation of oxidized substrate.

During the oxidation of a substrate, a mixed disulfide intermediate between Erv2p and the thiol of the substrate is formed. In the case of the oxidation of a dithiol substrate, a second thiol from the substrate is in close proximity and facilitates the release of the oxidized substrate. In the case of a monothiol substrate, another thiolate group has to be brought close to react (bi-molecular reaction). Because the mixed disulfide intermediate is unstable, the free thiolate group from Erv2p can attack, releasing reduced substrate. This difference in the mechanism typically leads to lower activities towards monothiols.

The kinetics of thiol/disulfide exchange reaction are influenced by many factors, including the redox potential, that determine the propensity of a thiol to be in the reduced or the oxidized state and by the thiol's acid dissociation constant (pK_a). Near physiological conditions, the lower the pK_a of a thiol, the more thiolate form will be present to initiate the thiol/disulfide exchange reaction (Chivers *et al.*, 1997).

Wild-type Erv2p was able to oxidize all small thiol substrates tested (Table 5). As expected, higher reaction rate was observed when using dithiols as substrates than when using monothiols. Recombinant Erv2p wild-type oxidizes dithiothreitol (DTT) faster than (±)-trans-1,2-bis(2-mercaptoacetamido)cyclohexane (BMC, Table 6). This result is consistent with the lower redox potential of DTT when compared to BMC (-0.33 V and -0.24 V, respectively). When we compared the oxidation of 50 mM of monothiol substrates by Erv2p wild-type, we observed that the rate of oxidation of cysteine and N-methylmercaptoacetamide (NMA) is the highest, followed by β-mercaptoethanol and homocysteine. The lowest rate of oxidation was observed for gluathione (GSH, Table 5). This result cannot be explained by redox potential alone and is probably due to a combination of the redox potential and pK_a of the thiols.

As discussed previously in Chapter 3, Erv2p-C176A-C178A and Erv2p-C176Stop mutants are able to oxidize the small substrate DTT but have limited activity toward the bulkier substrates BMC, GSH and cysteine (Table 5). The addition of an intragenic suppressor mutation to the Erv2p-C176A-C178A mutant allowed this protein to oxidize a broader range of substrates (Table 5). The Erv2p-F111S-C176A-C178A had wild-type level activity toward all the monothiol substrates tested except GSH, which was two-fold higher (Table 5).

Discussion

Structural data and mutational studies have suggested an intermolecular disulfide relay mechanism for Erv2p. The active site pair of cysteines (Cys121-Cys124), located near the FAD cofactor, transfers oxidizing equivalents from the FAD to the tail pair of cysteines (Cys176-Cys178) that, in turn, relays the disulfides obtained from the former cysteine pair to the substrate proteins, such as Pdi1p. Various evidence lead to the proposed mechanism: (i) two pairs of cysteines (Cys121-Cys124 and Cys176-Cys178) are required for Erv2p activity *in vivo*, as demonstrated by the inability of these mutants to suppress the growth defect of an *ero1-1* strain at the restrictive temperature (ii) Cys121, Cys176 or Cys178 are required for the intramolecular transfer of disulfides between the active site cysteines and the tail cysteines, as seen by the absence of a disulfide-linked dimer for Erv2 mutants that contain a Cys121, Cys176 or Cys178 mutated to alanine (iii) these two pairs of cysteines are close together in the crystal structure and we can model an interaction between Cys178 and Cys121 of the other subunit by rotating the $\chi 1$ side chain torsion angles of these residues.

The following steps for Erv2p catalytic mechanism have been deduced but their reaction order has not yet been determined: (i) transfer of electrons from the active site cysteine pair (Cys121-Cys124) to FAD leads to the formation of a disulfide bond at the active site, (ii) through an intermolecular disulfide exchange reaction, the disulfide bond at the active site is transferred to the cysteines located in the C-terminal tail of the other subunit of Erv2p dimer, and (iii) the disulfide bond in the tail is transferred to thiol-containing substrates, such as Pdi1p (see Figure 5A).

Erv2p and members of the in the QSOX/ERV family seem to share the same disulfide relay mechanism

All members of the QSOX/ERV family contain two pairs of cysteines that are required for activity, suggesting that members of this family share the same disulfide shuttle mechanism as Erv2p. Mutagenic studies performed in Erv1p and human ALR (hALR) show that two pairs of cysteines are required for activity *in vivo* and *in vitro*: an FAD-proximal active site cysteine pair and another cysteine pair located in a flexible region (that in the case of Erv1p and hALR is located at the N-terminus) (Hofhaus *et al.*, 2003; Lee *et al.*, 2000). As seen for Erv2p, the capture of disulfide-linked intermediates of Erv1p and hALR suggest that these two pairs of cysteines interact with each other during catalysis. This intermediate is absent when the N-terminal cysteine pair has been mutated to serine (Hofhaus *et al.*, 2003; Lisowsky *et al.*, 2001). The vaccinia virus homolog, E10R, contains only one pair of cysteines that is important for activity, as determined by the inability of these mutants to rescue virus replication and to oxidize L1R (Senkevich *et al.*, 2000). These cysteine residues form a mixed disulfide intermediate between E10R and A2.5L, that has been shown to be required for disulfide bond formation (Senkevich *et al.*, 2002). A2.5L contains a pair of cysteines that probably fulfills the function of the tail cysteines in Erv2p.

Truncation of the N-terminal regions of Erv1p and ALR, which contain the second pair of cysteines and are functionally homologous to the C-terminal tail of Erv2p, suggests that Erv1p and ALR require a second cysteine pair for disulfide transfer (Hofhaus *et al.*, 2003; Lee *et al.*, 2000). As observed in Erv2p, mutation of Cys30 and Cys33 in the N-terminal region of Erv1p or an N-terminal truncation of Erv1p (Erv1p-Δ1-

72) prevents the formation of the disulfide-linked Erv1p intermediate (Hofhaus *et al.*, 2003; Lee *et al.*, 2000). Similarly, a disulfide linked intermediate is not observed in an N-terminal truncation of ALR (ALR-Δ1-80) (Lisowsky *et al.*, 2001).

Varying the spacing between two cysteines affects the likelihood of disulfide bond formation by changing the rate of thiol-disulfide exchange (Zhang and Snyder, 1989). Accordingly, Erv2p-G177Δ, Erv2p-CGA$_2$C and Erv2p-CGA$_4$C mutants are inactive or slightly defective, although the tail cysteines in these mutants are still able to interact with the active site cysteines. The Erv2p tail cysteine pair is in a Cys-X-Cys motif, while other members of the QSOX/ERV family have a Cys-X$_n$-Cys, where n can be two (Erv1p, ALR and quiescin Q6) or four (*Arabidopsis thaliana* Erv1p). Interestingly, we were unable to find Erv2p homologs that have a Cys-X$_n$-Cys motif where n equals zero, three or five. It is possible that the difference in spacing between cysteines in the QSOX/ERV family reflects divergence in the redox properties of this cysteine pair, which has evolved either to confer specificity or to permit each protein to function in its specific environment. On the other hand, these variations in spacing may simply indicate robustness in the tail cysteine motif.

The C-terminal tail regions of Erv2p, the N-terminal regions of Erv1p and their fungal orthologs contain several hallmarks of unstructured regions: they are poorly conserved, can adopt various lengths and have an abundance of charged residues (Figure 2 and data not shown). The function of this unstructured region might be inferred from that of Ero1p, a protein that shares a similar disulfide shuttle mechanism (Gross *et al.*, 2004). Ero1p transfers disulfides from a buried active site cysteine pair to Pdi1p via a second pair of cysteine located in an unstructured region (Frand and Kaiser, 1999). It has been suggested that Pdi1p recognizes this region because it mimics its unfolded substrates (Gross *et al.*, 2004). Thus, it is possible that the Erv2p and Erv1p tails are also recognized by their substrate because they are unstructured. Another possibility is that the large number of charged residues might facilitate protein-protein interactions with the substrate (Zhu and Karlin, 1996). Also, it is possible that these regions have diverged to either allow these proteins to act in slightly different conditions or adapt to different substrates.

Transfer between two pairs of cysteines confers specificity in the disulfide transfer

Various evidences presented in Chapter 3 suggest that Erv2p tail sterically excludes larger substrates from reacting with the active site cysteine pair and that the Cys176-Cys178 pair is important for relaying disulfides from the buried active site cysteine pair to substrate proteins: (i) mutants lacking the tail cysteines (Erv2p-C176A-C178A and Erv2p-C176Stop) are unable to promote disulfide bond formation *in vivo*, (ii) addition of F111S to the previous mutants turns Erv2p into a monomeric form now able to promote disulfide bond formation *in vivo*, (iii) Erv2p-C176A-C178A and Erv2p-C176Stop are able to oxidize small substrate *in vitro*, but are unable to oxidize larger substrates such as GSH or Pdi1p, while Erv2p-F111S-C176A-C178A is able to oxidize small and large substrates.

The mutations that convert Erv2p into a monomeric form bypass the need for disulfide shuttling through the tail by giving thiol substrates direct access to the active site cysteines (see Figure 5 for the proposed differences between substrate oxidation by dimeric and monomeric forms of Erv2p)

Erv1p is able to oxidize lysozyme, DTT, and cysteine but not GSH (Hofhaus *et al.*, 2003; Hofhaus and Lisowsky, 2002; Lee *et al.*, 2000), but no studies have addressed the role of the tail cysteines in conferring specificity to the disulfide transfer. By analogy to Erv2p, it is plausible that the N-terminal cysteine pair of Erv1p may confer substrate specificity. Like the Erv2p truncation mutant, an N-terminal truncation of Erv1p (Erv1p-Δ1-72) is inactive *in vivo* (Lisowsky, 1996), but this could be due to mislocalization of the mutant protein, which lacks the mitochondrial signal sequence, and not a direct result of the absence of the cysteine pair in the N-terminus. *In vitro*, the Erv1p-Δ1-72 rate of oxidation of lysozyme is slightly lower than that of wild-type (Lee *et al.*, 2000; Lisowsky *et al.*, 2001). The observation that Erv1p-Δ1-72 is also able to oxidize DTT at a rate similar to wild-type, while Erv1p-C30S and Erv1p-C33S mutants have a reduced activity towards DTT (Hofhaus *et al.*, 2003), suggests that the active site pair in Erv1p-Δ1-72 is more accessible than in wild-type, which seems likely given that this truncation is larger than the truncations performed in the Erv2p tail. Thus, we expect that recombinant Erv1p-C30S and Erv1p-C33S would not efficiently oxidize lysozyme or GSH but that Erv1p-Δ1-72 would.

Specificity conferred by the disulfide transfer reaction

Besides Erv2p and members of the QSOX/ERV family, several other thiol oxidases, such as Ero1p, DsbB, TrxR appear to have evolved a similar mechanisms of transfer between two pairs of cysteines to control substrate specificity, directing the transfer of disulfides to specific substrates.

We observe that the Erv2p suppressor mutant is more active towards GSH than the tail cysteine mutant or wild-type, suggesting that the tail prevents random oxidation of thiols by blocking the active site cysteine pair. Also, studies on Erv1p, chicken QSOX and Ero1p have shown that these proteins are unable to oxidize GSH (Hofhaus and Lisowsky, 2002; Hoober *et al.*, 1996; Sevier and Kaiser, 2006). Furthermore, E10R infected cells seem to have the same GSH/GSSG ratio as non-infected cells, suggesting that E10R cannot use GSH in vivo. Unfortunately, we were unable to measure differences in oxidized glutathione in strains overexpressing Erv2p wild-type and Erv2p suppressor mutant, but this could be due to sensitivity of the method.

Interestingly, the mutation that renders Erv1p temperature-sensitive (Phe124Ser) is on a helix that forms the dimer interface of Erv1p (Lisowsky, 1994). We speculate that this mutation precludes Erv1p dimerization and also changes its substrate specificity, allowing it to oxidize a wider range of substrates.

Materials and methods

Media and yeast strains

All strains used in this study are isogenic to S288C. Cultures were grown either in rich medium (1% Bacto yeast extract and 2% Bacto-peptone (YP) containing either 2% dextrose (YPD) or 2% galactose (YPGal) as carbon sources) or in minimal media (0.67% nitrogen base without amino acids supplemented with 16 amino acids not including cysteine) containing 2% galactose and 2% raffinose (SMM Gal/Raf). The isolation and characterization of the *ero1-1* mutant (CKY598) were described previously (Frand and Kaiser, 1998). The construction of an *erv2Δ* strain (CKY688) was described previously (Sevier *et al.*, 2001). The *MAT**a** GAL2 ero1-1 erv2Δ::kanMX ura3-52 leu2-3,112* (CKY899) was constructed by crossing *erv2Δ* strain (CKY688) to an *ero1-1 GAL2* strain (CKY598). The resulting diploid was sporulated and tetrads dissected in YPD.

Plasmid construction

The plasmids used in this study are listed in Table 7. The *ERV2* cysteine, *ERV2-Gly177* and *ERV2* charged residues mutants were made using the QuikChange site directed mutagenesis kit (Stratagene) using pFA11 as template (Gross *et al.*, 2002;

Sevier *et al.*, 2001). The *ERV2-(DYD)Δ* spacing mutants were made using the QuikChange site directed mutagenesis kit (Stratagene) using pAV268 as template. The *ERV2* suppressor mutants in different backgrounds were made using the QuikChange site directed mutagenesis kit (Stratagene) using pAV41, pAV36, pAV37, pAV363 and pAV364 as templates. The forward primers used for the site-directed mutagenesis are listed in Table 8. The mutated plasmids were verified by sequencing, and the protein expression levels in each of the mutants were assessed by immunoprecipitation from the CKY598 strain overexpressing these plasmids using the Erv2p antibody as described below.

Erv2p wild-type, Erv2p-C150A and Erv2p-C167A mutants lacking the first 29 amino acids encoding the hydrophobic N-terminal signal sequence and containing an N-terminal His_6 tag were constructed using NdeI-Erv2 and Erv2-BamHI primers. The resulting fragments were subcloned into the bacterial expression vector pET-14b (Novagen) using the NheI and BamHI sites. The *ERV2* mutant truncated at residue 176 (ERV2-C176Stop) or 171 (*ERV2-L171Stop*) was subcloned into pET-14b using NdeI-Erv2 and Erv2-C176Stop-BamHI or Erv2-L171Stop-BamHI primers, respectively.

Radiolabeling and immunoprecipitation

Radiolabeling and immunoprecipitation of Erv2p was done as described previously (Gross *et al.*, 2002). Briefly, strains overexpressing Erv2p or mutant alleles were grown in SMM Gal/Raf lacking uracil and methionine to about 1×10^7 cells/ml. Cells were resuspended in the same medium at 1×10^8 cells/ml and labeled with $[^{35}S]$methionine and cysteine (EXPRESS, NEN) for 60 min at room temperature. Cells were then resuspended in 10% TCA and lysed with glass beads. Protein pellets were then incubated in sample buffer (80 mM Tris-HCl [pH 6.8], 2% SDS, 10% glycerol, 1 mM phenylmethylsulfonyl fluoride (PMSF), 0.01% bromophenol blue) containing 40 mM N-ethylmaleimide (Sigma) for 15 min at 4 °C followed by 10 min at room temperature. Cell extracts were resuspended in 1 ml IP buffer (50 mM Tris-HCl [pH 7.4], 150 mM NaCl, 1% Triton X-100 and 1 mM PMSF) and preadsorbed with fixed *Staphylococcus* A cells (Sigma) before incubation with Erv2p antibody. Immune complexes were collected with protein-A-sepharose (Pharmacia), washed in IP buffer containing 0.1% SDS and then washed in IP buffer without detergent and finally solubilized in sample buffer. Samples were analyzed by 12% SDS-PAGE and visualized with a 445si PhosphorImager (Molecular Dynamics).

Erv2p antibody production

An *E. coli* BL21(DE3) strain (Novagen) was transformed with pJC11 (Sevier *et al.*, 2001). Erv2p lacking the first 29 amino acids and containing a C-terminal His_6 tag was purified as described previously (Sevier *et al.*, 2001). The protein was separated by SDS-PAGE and used to prepare polyclonal antibodies in rabbits by standard protocols at Covance.

Protein expression and purification

ERV2 wild-type and mutant alleles expression plasmids were transformed into *E. coli* BL21(DE3) Gold pLysS cells (Novagen). Single colonies were inoculated into LB supplemented with 80 mg l^{-1} ampicillin and 30 mg l^{-1} chloramphenicol. Cells were grown at 30 °C to an OD_{600} of 0.5-0.6, and isopropyl β-D-thiogalactoside (IPTG) and FAD were added to a final concentration of 0.4 mM and 10 μM, respectively. After 4 hours of induction at 30 ˚C, cells were harvested by centrifugation and lysed by French press in lysis buffer (50 mM NaH_2PO_4 [pH 8], 350 mM NaCl and 10 mM imidazole with EDTA-free protease inhibitor cocktail). Insoluble material was sedimented by centrifugation and the supernatant was applied to a HiTrap Chelating HP column (Amersham Biotech) pre-equilibrated with lysis buffer.

The resin was washed with lysis buffer and with wash buffer (50 mM NaH_2PO_4 [pH 8], 300 mM NaCl and 20 mM imidazole). The bound protein was eluted with a gradient of 20 mM to 250 mM imizadole in 50 mM sodium phosphate [pH 8.0], 300 mM NaCl. The fractions containing Erv2p were then dialyzed for at least 16 h against 50 mM sodium phosphate [pH 8], 150 mM NaCl.

The samples used for the determination of the molecular weight were further purified in an anion exchange HiTrap Q column (Amersham Biotech). For this, the eluted protein from the affinity column was pooled and dialyzed against 20 mM Tris-HCl [pH 8]. The sample was applied to the HiTrap Q column and eluted with an increasing NaCl concentration. The fractions containing Erv2p were then dialyzed for at least 16 h against 50 mM KH_2PO_4 [pH 8], 150 mM KCl (Buffer A). All proteins were > 95% pure after the HiTrap Q column. Concentration of the protein samples was estimated using a molar extinction coefficient of 12.5 mM cm^{-1} at 454 nm (Sevier *et al.*, 2001).

Gel filtration

Analytical gel filtration of Erv2p variants was performed on a Superdex 200 PC 3.2/20 (Amersham Biosciences) in 50 mM sodium phosphate [pH 8], 150 mM NaCl and 2 mM DTT. A low molecular weight gel filtration calibration kit (Amersham Biosciences) was used to generate the standard curve in order to obtain the apparent molecular weights for the Erv2p variants.

FAD reduction assay

The protein samples, at a final concentration of 3.75 μM, were added to a reaction mixture containing 50 mM sodium phosphate [pH 8], 150 mM NaCl, 5 mM EDTA, and various concentrations of thiol substrates and absorbance changes were monitored at 454 nm. Thiol substrates were prepared fresh in buffer and were standardized using 5,5'-dithio-bis(2-nitrobenzoic acid) (DNTB). The rates of bleaching are expressed as the amount of oxygen consumed per amount of time necessary to reduce half of the concentration/signal of bound FAD (measured by a decrease in absorbance at 454 nm) per amount of Erv2p. In this assay, we observed a time lag between the addition of Erv2p and the moment of reduction of bound FAD. This delay in the reduction of bound FAD corresponds to the time that is necessary to consume the 90% of oxygen in the cuvette and is correlated with the amount of thiol used.

References

Bessette, P.H., Qiu, J., Bardwell, J.C., Swartz, J.R. and Georgiou, G. (2001) Effect of sequences of the active-site dipeptides of DsbA and DsbC on in vivo folding of multidisulfide proteins in Escherichia coli. *J Bacteriol*, **183**, 980-988.

Chivers, P.T., Prehoda, K.E. and Raines, R.T. (1997) The CXXC motif: a rheostat in the active site. *Biochemistry*, **36**, 4061-4066.

Dym, O. and Eisenberg, D. (2001) Sequence-structure analysis of FAD-containing proteins. *Protein Sci*, **10**, 1712-1728.

Frand, A.R. and Kaiser, C.A. (1998) The ERO1 gene of yeast is required for oxidation of protein dithiols in the endoplasmic reticulum. *Mol Cell*, **1**, 161-170.

Frand, A.R. and Kaiser, C.A. (1999) Ero1p oxidizes protein disulfide isomerase in a pathway for disulfide bond formation in the endoplasmic reticulum. *Mol Cell*, **4**, 469-477.

Gross, E., Kastner, D.B., Kaiser, C.A. and Fass, D. (2004) Structure of Ero1p, source of disulfide bonds for oxidative protein folding in the cell. *Cell*, **117**, 601-610.

Gross, E., Sevier, C.S., Vala, A., Kaiser, C.A. and Fass, D. (2002) A new FAD-binding fold and intersubunit disulfide shuttle in the thiol oxidase Erv2p. *Nat Struct Biol*, **9**, 61-67.

Hofhaus, G., Lee, J.E., Tews, I., Rosenberg, B. and Lisowsky, T. (2003) The N-terminal cysteine pair of yeast sulfhydryl oxidase Erv1p is essential for in vivo activity and interacts with the primary redox centre. *Eur J Biochem*, **270**, 1528-1535.

Hofhaus, G. and Lisowsky, T. (2002) Sulfhydryl oxidases as factors for mitochondrial biogenesis. *Methods Enzymol*, **348**, 314-324.

Hoober, K.L., Joneja, B., White, H.B., 3rd and Thorpe, C. (1996) A sulfhydryl oxidase from chicken egg white. *J Biol Chem*, **271**, 30510-30516.

Keire, D.A., Strauss, E., Guo, W., Noszal, B. and Rabenstein, D.L. (1992) Kinetics and Equilibria of thiol/disulfide interchange reactions of selected biological thiols and realted molecules with oxidized glutathione. *J Org Chem*, **57**, 123-127.

Lamoureux, G.V. and Whitesides, G.M. (1993) Synthesis of dithiols as reducing agents for disulfides in neutral aqueous solution and comparison of reduction potentials. *J Org Chem*, **58**, 633-641.

Lee, J., Hofhaus, G. and Lisowsky, T. (2000) Erv1p from Saccharomyces cerevisiae is a FAD-linked sulfhydryl oxidase. *FEBS Lett*, **477**, 62-66.

Lisowsky, T. (1994) ERV1 is involved in the cell-division cycle and the maintenance of mitochondrial genomes in Saccharomyces cerevisiae. *Curr Genet*, **26**, 15-20.

Lisowsky, T. (1996) Removal of an intron with unique 3' branch site creates an amino-terminal protein sequence directing the scERV1 gene product to mitochondria. *Yeast*, **12**, 1501-1510.

Lisowsky, T., Lee, J.E., Polimeno, L., Francavilla, A. and Hofhaus, G. (2001) Mammalian augmenter of liver regeneration protein is a sulfhydryl oxidase. *Dig Liver Dis*, **33**, 173-180.

Senkevich, T.G., White, C.L., Koonin, E.V. and Moss, B. (2000) A viral member of the ERV1/ALR protein family participates in a cytoplasmic pathway of disulfide bond formation. *Proc Natl Acad Sci U S A*, **97**, 12068-12073.

Senkevich, T.G., White, C.L., Weisberg, A., Granek, J.A., Wolffe, E.J., Koonin, E.V. and Moss, B. (2002) Expression of the vaccinia virus A2.5L redox protein is required for virion morphogenesis. *Virology*, **300**, 296-303.

Sevier, C.S., Cuozzo, J.W., Vala, A., Aslund, F. and Kaiser, C.A. (2001) A flavoprotein oxidase defines a new endoplasmic reticulum pathway for biosynthetic disulphide bond formation. *Nat Cell Biol*, **3**, 874-882.

Sevier, C.S. and Kaiser, C.A. (2006) Disulfide transfer between two conserved cysteine pairs imparts selectivity to protein oxidation by Ero1. *Mol Biol Cell*, **17**, 2256-2266.

Singh, R., Lamoureux, G.V., Lees, W.J. and Whitesides, G.M. (1995) Reagents for rapid reduction of disulfide bonds. *Methods Enzymol*, **251**, 167-173.

Thompson, J.D., Gibson, T.J., Plewniak, F., Jeanmougin, F. and Higgins, D.G. (1997) The CLUSTAL_X windows interface: flexible strategies for multiple sequence alignment aided by quality analysis tools. *Nucleic Acids Res*, **25**, 4876-4882.

Woycechowsky, K.J., Wittrup, K.D. and Raines, R.T. (1999) A small-molecule catalyst of protein folding in vitro and in vivo. *Chem Biol*, **6**, 871-879.

Wu, C.K., Dailey, T.A., Dailey, H.A., Wang, B.C. and Rose, J.P. (2003) The crystal structure of augmenter of liver regeneration: A mammalian FAD-dependent sulfhydryl oxidase. *Protein Sci*, **12**, 1109-1118.

Zhang, R.M. and Snyder, G.H. (1989) Dependence of formation of small disulfide loops in two-cysteine peptides on the number and types of intervening amino acids. *J Biol Chem*, **264**, 18472-18479.

Zhu, Z.Y. and Karlin, S. (1996) Clusters of charged residues in protein three-dimensional structures. *Proc Natl Acad Sci U S A*, **93**, 8350-8355.

Table 1. Erv2p C-terminal tail charge residues mutants.

Erv2p allele	**Suppression of *ero1-1* growth defect at 37 ˚C**[a]
Vector	–
Erv2p	+
Erv2p-E172A	+
Erv2p-D173A	+
Erv2p-D175A	+
Erv2p-D180A	+
Erv2p-K184A	+
Erv2p-R185A	+
Erv2p-E189A	+
Erv2p-K190A	+
Erv2p-E191A	+/–
Erv2p-K193A	+
Erv2p-H195A	+

[a] the *ero1-1* mutant (CKY598) containing either pRS316 (empty vector), wild-type Erv2p or the indicated mutant alleles of Erv2p were plated onto YPGal and grown at 24 ˚C or 37 ˚C for 4 d.

Table 2. Gly177 mutants of Erv2p.

Erv2p allele	**Suppression of *ero1-1* growth defect at 37 ˚C**[a]
Vector	–
Erv2p	+
Erv2p-G177A	+
Erv2p-G177S	+
Erv2p-G177V	+
Erv2p-G177L	+
Erv2p-G177M	+
Erv2p-G177P	+
Erv2p-G177F	+
Erv2p-G177D	+/–
Erv2p-G177E	+/–
Erv2p-G177Q	+
Erv2p-G177K	+
Erv2p-G177R	+

[a] the *ero1-1* mutant (CKY598) containing either pRS316 (empty vector), wild-type Erv2p or the indicated mutant alleles of Erv2p were plated onto YPGal and grown at 24 ˚C or 37 ˚C for 4 d.

Table 3. Erv2p-(DYD) mutants.

Erv2p allele	Suppression of *ero1-1* growth defect at 37 ˚C[a]	Disulfide-linked dimer[b]
Vector	−	NA
Erv2p	+	+
Erv2p-(YD)Δ	−	−
Erv2p-(DYD)Δ	−	−
Erv2p-(DYD)Δ+2A	+	+
Erv2p-(DYD)Δ+3A	+	+
Erv2p-(DYD)Δ CAGC	−	−
Erv2p-(DYD)Δ CAAGC	−	−
Erv2p-(DYD)Δ CAAAGC	−	−
Erv2p-(DYD)Δ CGAC	−	−
Erv2p-(DYD)Δ CGAAC	−	−
Erv2p-(DYD)Δ CGAAAC	−	−

[a] the *ero1-1* mutant (CKY598) containing either pRS316 (empty vector), wild-type Erv2p or the indicated mutant alleles of Erv2p were plated onto YPGal and grown at 24 ˚C or 37 ˚C for 4 d.

[b] the *ero1-1 erv2Δ* mutant (CKY899) containing either pRS316 (empty vector), wild-type Erv2p or the indicated mutant alleles of Erv2p were labeled with [^{35}S]methionine and alkylated with NEM prior to immunoprecipitation with Erv2p antibody.

NA, non applicable

Table 4. Erv2p suppressor mutants.

Erv2p allele	**Suppression of *ero1-1* growth defect at 37 ˚C**[a]
Vector	
Erv2p	+
Erv2p-C176A-C178A	−
Erv2p-F111S-C176A-C178A	+
Erv2p-L114S-C176A-C178A	+
Erv2p-P120A-C176A-C178A	+
Erv2p-F111S-C121A-C124A	−
Erv2p-F111S-C150A	−
Erv2p-F111S-C176Stop	+
Erv2p-F111S-L171Stop	−
Erv2p-L114S-C121A-C124A	−
Erv2p-L114S-C150A	−
Erv2p-L114S-C176Stop	+
Erv2p-L114S-L171Stop	−
Erv2p-P120A-C121A-C124A	−
Erv2p-P120A-C150A	−
Erv2p-P120A-C176Stop	+
Erv2p-P120A-L171Stop	−

[a] the *ero1-1* mutant (CKY598) containing either pRS316 (empty vector), wild-type Erv2p or the indicated mutant alleles of Erv2p were plated onto YPGal and grown at 24 ˚C or 37 ˚C for 4 d.

Table 5. Rate of O_2 consumption for of His$_6$-Erv2p and His$_6$-Erv2p mutants.

		Rate of O_2 consumption (10^2 nmol O_2 per sec per nmol of Erv2p)[a]			
Thiol substrate	M_r[b]	His$_6$-Erv2p	His$_6$-Erv2p-F111S-C176A-C178A	His$_6$-Erv2p-C176A-C178A	His$_6$-Erv2p-C176Stop
DTT	152	99 ± 7.7	34 ± 1.8	122 ± 7.8	116 ± 8.7
BMC	256	41 ± 3.3	19 ± 2.1	22 ± 1.1	9 ± 0.8
NMA	208	17 ± 0.7	19 ± 0.4	13 ± 0.6	11 ± 0.1
Cysteine	240	16 ± 2.4	15 ± 1.0	2.9 ± 0.2	2 ± 0.3
Homocysteine	268	4.2 ± 0.2	4.3 ± 0.2	1.9 ± 0.2	1.7 ± 0.1
β-ME	154	3.6 ± 0.1	3.3 ± 0.3	1.8 ± 0.1	1.7 ± 0.0
GSH	613	2.2 ± 0.2	4.6 ± 0.2	<0.9[c]	<0.9[c]

[a] Rates of O_2 consumption were obtained using 5 mM dithiol substrates or 50 mM monothiol substrates. The average value ± standard deviation of at least three independent assays is presented.

[b] Molecular weight of the oxidized form (g/mol).

[c] Assays in which there was no decrease in absorbance at 454 nm after 2 h.

Table 6. Structure and properties of thiol compounds used in this study.

Thiol substrate	Structure	Type of substrate	pK_a	$E^{0'}$ (V)	Reference
Dithiothreitol (DTT)	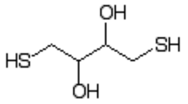	dithiol	9.2 10.1	-0.33	Lamoureux and Whitesides, 1993; Singh et al., 1995
(±)-trans-1,2-bis (2-mercaptoacetamido) cyclohexane (BMC)	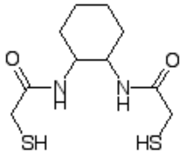	dithiol	8.3 9.9	-0.24	Woycechowsky et al., 1999
Glutathione (GSH)	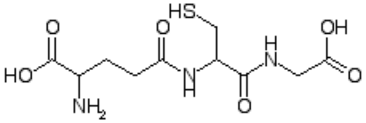	monothiol	9.3	-0.21	Keire et al., 1992
Cysteine	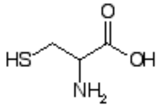	monothiol	8.9	-0.19	Keire et al., 1992
Homocysteine	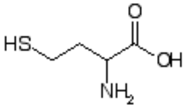	monothiol	9.7	-0.20	Keire et al., 1992
β-Mercaptoethanol (β-ME)	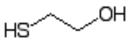	monothiol	10.1	-0.26	Keire et al., 1992
N-methylmercapto acetamide (NMA)	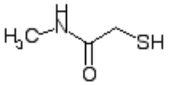	monothiol	8.3	ND	Singh et al., 1995; Woycechowsky et al., 1999

ND, non determined

Table 7. Plasmids used in this work.

Name	**Description**	**Markers**	**Source or Reference**
pFA11	P_{GAL1}-*ERV2*	*CEN*, *URA3*	Sevier et al., 2001
pJC15	P_{GAL1}-*ERV2-C121A-C124A-*HA_3	*CEN*, *URA3*	Gross et al., 2002
pAV37	P_{GAL1}-*ERV2-C150A*	*CEN*, *URA3*	This study
pAV38	P_{GAL1}-*ERV2-C167A*	*CEN*, *URA3*	This study
pAV532	P_{GAL1}-*ERV2-C150A-C167A*	*CEN*, *URA3*	This study
pAV538	P_{GAL1}-*ERV2-C150A-C167A-C176A-C178A*	*CEN*, *URA3*	This study
pAV60	P_{GAL1}-*ERV2-E172A*	*CEN*, *URA3*	This study
pAV61	P_{GAL1}-*ERV2-D173A*	*CEN*, *URA3*	This study
pAV63	P_{GAL1}-*ERV2-D175A*	*CEN*, *URA3*	This study
pAV66	P_{GAL1}-*ERV2-D180A*	*CEN*, *URA3*	This study
pAV68	P_{GAL1}-*ERV2-D182A*	*CEN*, *URA3*	This study
pAV294	P_{GAL1}-*ERV2-K184A*	*CEN*, *URA3*	This study
pAV189	P_{GAL1}-*ERV2-R185A*	*CEN*, *URA3*	This study
pAV190	P_{GAL1}-*ERV2-E189A*	*CEN*, *URA3*	This study
pAV191	P_{GAL1}-*ERV2-K190A*	*CEN*, *URA3*	This study
pAV192	P_{GAL1}-*ERV2-E191A*	*CEN*, *URA3*	This study
pAV193	P_{GAL1}-*ERV2-K193A*	*CEN*, *URA3*	This study
pAV194	P_{GAL1}-*ERV2-H195A*	*CEN*, *URA3*	This study
pAV71	P_{GAL1}-*ERV2-G177A*	*CEN*, *URA3*	This study
pAV96	P_{GAL1}-*ERV2-G177S*	*CEN*, *URA3*	This study
pAV183	P_{GAL1}-*ERV2-G177V*	*CEN*, *URA3*	This study
pAV95	P_{GAL1}-*ERV2-G177L*	*CEN*, *URA3*	This study
pAV75	P_{GAL1}-*ERV2-G177M*	*CEN*, *URA3*	This study
pAV77	P_{GAL1}-*ERV2-G177P*	*CEN*, *URA3*	This study
pAV270	P_{GAL1}-*ERV2-G177F*	*CEN*, *URA3*	This study
pAV73	P_{GAL1}-*ERV2-G177D*	*CEN*, *URA3*	This study
pAV184	P_{GAL1}-*ERV2-G177E*	CEN, URA3	This study
pAV269	P_{GAL1}-*ERV2-G177Q*	*CEN*, *URA3*	This study
pAV72	P_{GAL1}-*ERV2-G177K*	*CEN*, *URA3*	This study
pAV74	P_{GAL1}-*ERV2-G177R*	*CEN*, *URA3*	This study
pAV268	P_{GAL1}-*ERV2-(DYD)Δ*	*CEN*, *URA3*	This study
pAV404	P_{GAL1}-*ERV2-(DYD)Δ+2A*	*CEN*, *URA3*	This study
pAV403	P_{GAL1}-*ERV2-(DYD)Δ+3A*	*CEN*, *URA3*	This study
pAV422	P_{GAL1}-*ERV2-(DYD)Δ CAGC*	*CEN*, *URA3*	This study
pAV423	P_{GAL1}-*ERV2-(DYD)Δ CAAGC*	*CEN*, *URA3*	This study
pAV424	P_{GAL1}-*ERV2-(DYD)Δ CAAAGC*	*CEN*, *URA3*	This study
pAV425	P_{GAL1}-*ERV2-(DYD)Δ CGAC*	*CEN*, *URA3*	This study
pAV426	P_{GAL1}-*ERV2-(DYD)Δ CGAAC*	*CEN*, *URA3*	This study
pAV427	P_{GAL1}-*ERV2-(DYD)Δ CGAAAC*	*CEN*, *URA3*	This study

Table 7 Continued. Plasmids used in this work.

Name	Description	Markers	Source or Reference
pAV161	P_{GAL1}*-ERV2-F111S-C176A-C178A*	*CEN*, *URA3*	This study
pAV284	P_{GAL1}*-ERV2-F111S-C121A-C124A*	*CEN*, *URA3*	This study
pAV290	P_{GAL1}*-ERV2-F111S-C150A*	*CEN*, *URA3*	This study
pAV377	P_{GAL1}*-ERV2-F111S-C176Stop*	*CEN*, *URA3*	This study
pAV546	P_{GAL1}*-ERV2-F111S-L171Stop*	*CEN*, *URA3*	This study
pAV283	P_{GAL1}*-ERV2-L114S-C176A-C178A*	*CEN*, *URA3*	This study
pAV285	P_{GAL1}*-ERV2-L114S-C121A-C124A*	*CEN*, *URA3*	This study
pAV291	P_{GAL1}*-ERV2-L114S-C150A*	*CEN*, *URA3*	This study
pAV379	P_{GAL1}*-ERV2-L114S-C176Stop*	*CEN*, *URA3*	This study
pAV547	P_{GAL1}*-ERV2-L114S-L171Stop*	*CEN*, *URA3*	This study
pAV176	P_{GAL1}*-ERV2-P120A-C176A-C178A*	*CEN*, *URA3*	This study
pAV470	P_{GAL1}*-ERV2-P120A-C121A-C124A*	*CEN*, *URA3*	This study
pAV289	P_{GAL1}*-ERV2-P120A-C150A*	*CEN*, *URA3*	This study
pAV378	P_{GAL1}*-ERV2-P120A-C176Stop*	*CEN*, *URA3*	This study
pAV548	P_{GAL1}*-ERV2-P120A-L171Stop*	*CEN*, *URA3*	This study
pJC11	*ERV2 (1-22Δ)-His*$_6$	AMP	Sevier et al., 2001
pET-14b	*E. coli* His$_6$-fusion vector	AMP	Novagen
pAV79	His$_6$-*ERV2*	AMP	This study
pAV83	His$_6$-*ERV2-C150A*	AMP	This study
pAV84	His$_6$-*ERV2-C167A*	AMP	This study
pAV549	His$_6$-*ERV2-L171Stop*	AMP	This study
pAV276	His$_6$-*ERV2-F111S-C176A-C178A*	AMP	This study
pAV319	His$_6$-*ERV2-L114S-C176A-C178A*	AMP	This study
pAV287	His$_6$-*ERV2-P120A-C176A-C178A*	AMP	This study

Table 8. Primers used in this study.

Primer	Sequence
C150A1	5'- GCAATGTGGGGA**GCG**CACATTCACAAC-3'
C167A1	5'- GACATATATGAC**GCA**GCTACCATCCTG-3'
E172A1	5'- GCTACCATCCTG**GCG**GACTACGATTGT-3'
D173A1	5'- ACCATCCTGGAG**GCC**TACGATTGTGGA-3'
D175A1	5'- CTGGAGGACTAC**GCT**TGTGGATGTAGT-3'
D180A1	5'- TGTGGATGTAGT**GCC**AGCGACGGTAAA-3'
D182A1	5'- TGTAGTGACAGC**GCC**GGTAAACGCGTG-3'
K184A1	5'- AGTGACAGCGACGGT**GCT**CGCGTGTCTCTCGAG-3'
R185A1	5'- GACAGCGACGGTAAA**GCC**GTGTCTCTCGAGAAG-3'
E189A1	5'- AAACGCGTGTCTCTC**GCG**AAGGAGGCTAAACAG-3'
K190A1	5'- CGCGTGTCTCTCGAG**GCG**GAGGCTAAACAGCAC-3'
E191A1	5'- GTGTCTCTCGAGAAG**GCG**GCTAAACAGCACGGT-3'
K193A1	5'- CTCGAGAAGGAGGCT**GCA**CAGCACGGTTGAACA-3'
H195A1	5'- AAGGAGGCTAAACAG**GCC**GGTTGAACAAAGAAA-3'
G177N1	5'- GAGGACTACGATTGT**NNS**TGTAGTGACAGCGAC-3'
Δ(D173toD175)1	5'- GCTACCATCCTGGAGTGTGGATGTAGTGAC-3'
del(DYD)2Ala1	5'- GCTACCATCCTGGAG**GCTGC**TTGTGGATGTAGTGAC-3'
del(DYD)3Ala1	5'- GCTACCATCCTGGAG**GCTGCTGCT**TGTGGATGTAGTGAC-3'
(DYD) CAGC1	5'- ACCATCCTGGAGTGT**GCT**GGATGTAGTGACAGC-3'
(DYD) CAAGC1	5'- ACCATCCTGGAGTGT**GCTGCT**GGATGTAGTGACAGC-3'
(DYD) CAAAGC1	5'- ACCATCCTGGAGTGT**GCTGCTGCT**GGATGTAGTGACAGC-3'
(DYD) CGAC1	5'- ATCCTGGAGTGTGGA**GCT**TGTAGTGACAGCGAC-3'
(DYD) CGAAC1	5'- ATCCTGGAGTGTGGA**GCTGCT**TGTAGTGACAGCGAC-3'
(DYD) CGAAAC1	5'- ATCCTGGAGTGTGGA**GCTGCTGCT**TGTAGTGACAGCGAC-3'
F111S1	5'- GAGAAACTGCACACG**TCT**ATTGGGTTGTATGCA-3'
L114S1	5'- CACACGTTTATTGGG**TCT**TATGCAGAACTCTAT-3'
P120A1	5'- TATGCAGAACTCTAT**GCA**TGCGGGGAATGTTCA-3'
NdeI-Erv2	5'- AAAAAA**CATATG**GAACTATCCATCGCTACGCCGGGC-3'
Erv2-BamHI	5'- AAAA**GGATCC**TCAACCGTGCTGTTTAGCCTCCTT-3'
Erv2-C176Stop-BamHI	5'- AAAA**GGATCC**TTAATCGTAGTCCTCCAGGATGGT-3'
Erv2-L171Stop-BamHI	5'- AAAA**GGATCC**TTAGATGGTAGCACAGTCATATAT-3'
Gal1	5'- TGCATAACCACTTTAACT-3'
Erv2mut3	5'- ATTAAGTTGGGTAACGCC-3'

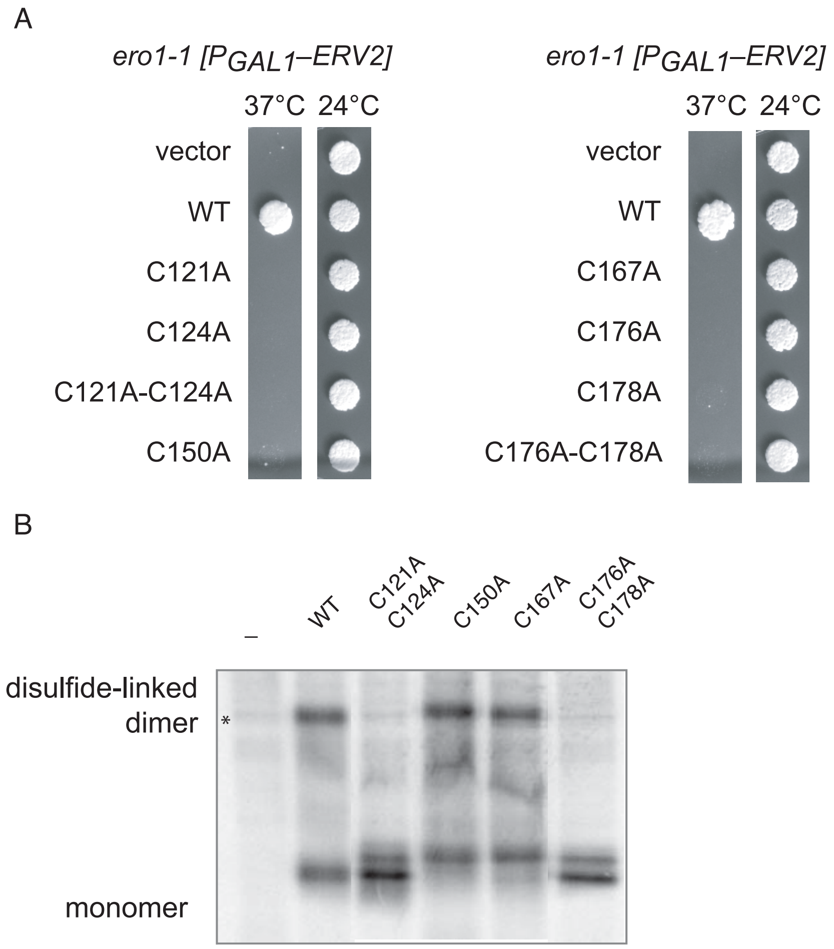
A
ero1-1 [PGAL1–ERV2]
37°C
24°C
vector
WT
C121A
C124A
C121A-C124A
C150A
ero1-1 [PGAL1–ERV2]
37°C
24°C
vector
WT
C167A
C176A
C178A
C176A-C178A
B
–
WT
C121A C124A
C150A
C167A
C176A C178A
disulfide-linked dimer
*
monomer

Figure 1. Erv2p Cys150 and Cys167 are required for activity. **(A)** The *ero1-1* mutant (CKY598) containing either pRS316 (empty vector) or various cysteine mutant alleles of Erv2p were plated onto YPGal and grown at 24 ˚C or 37 ˚C for 4 d. **(B)** *ero1-1 erv2Δ* mutants (CKY899) containing either pRS316 (empty vector), wild-type Erv2p, or various cysteine mutant alleles of Erv2p were labeled with [^{35}S]methionine and alkylated with NEM prior to immunoprecipitation with Erv2p antibody.

(next page)

Figure 2. Conservation of the C-terminus of Erv2p among fungal species. Multiple sequence alignment of the C-terminal half of Erv2p, among fungal species using ClustalX (Thompson *et al.*, 1997). This segment shows both the conserved active site (Cys121-Cys124) and tail (Cys176-Cys178) cysteine pairs. The cysteines are colored in a dark grey. Light grey boxes show blocks of conserved residues with more than 70% identity. Acidic and basic amino acid residues in the C-terminal tail are colored in red and blue, respectively. Abbreviations of the species names are as follows: Scer, *Saccharomyces cerevisiae*; Sbay, *Saccharomyces bayanus*; Smik, *Saccharomyces mikatae*; Skud*, Saccharomyces kudriavzevii;* Spar, *Saccharomyces paradoxus;* Ecun, *Encephalitozoon cuniculi*; Cgra, *Candida glabrata*; Sklu, *Saccharomyces kluyveri;* Klac, *Kluyveromyces lactis*; Scas, *Saccharomyces castellii*; Calb, *Candida albicans*; Dhan, *Debaryomyces hansenii*; Anid*, Aspergillus nidulans;* Fgra*, Fusarium graminearum*; Ylip*, Yarrowia lipolytica;* Mgri, *Magnaporthe grisea*; Ncra, *Neurospora crassa*; Umay, *Ustilago maydis*; Egos, *Eremothecium gossypii*, Afum, *Aspergillus fumigatus*, Kwal *Kluyveromyces waltii*, Ctro, *Candida tropicalis*, Clus, *Candida lusitaniae*, Cgui, *Candida guilliermondii*, Cglo, *Chaetomium globosum*, Cimm, *Coccidioides immitis*, Rory, *Rhizopus oryzae*, Ccin, *Coprinus cinereus*, Pnod, *Phaeosphaeria nodorum*, and Spom, *Schizosaccharomyces pombe*.

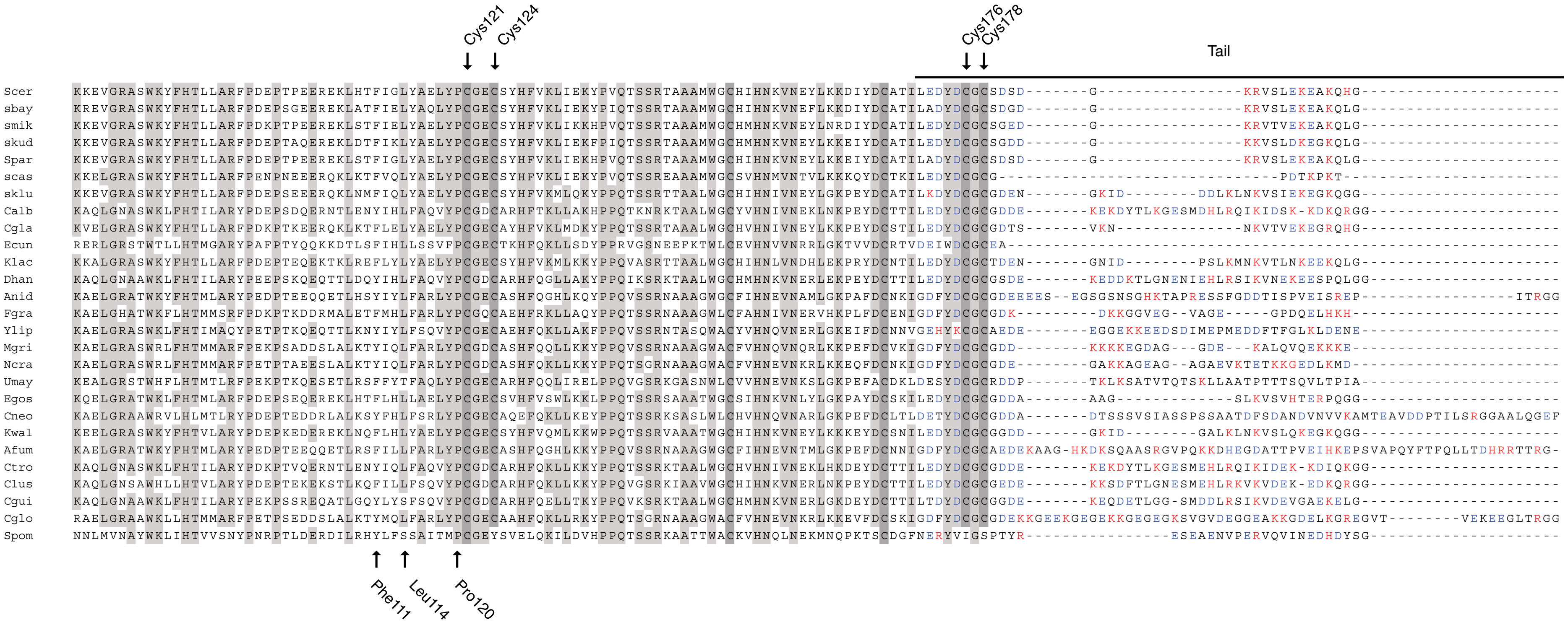
Cys121
Cys124
Cys176
Cys178
Tail
Scer
sbay
smik
skud
Spar
scas
sklu
Calb
Cgla
Ecun
Klac
Dhan
Anid
Fgra
Ylip
Mgri
Ncra
Umay
Egos
Cneo
Kwal
Afum
Ctro
Clus
Cgui
Cglo
Spom
Phe111
Leu114
Pro120

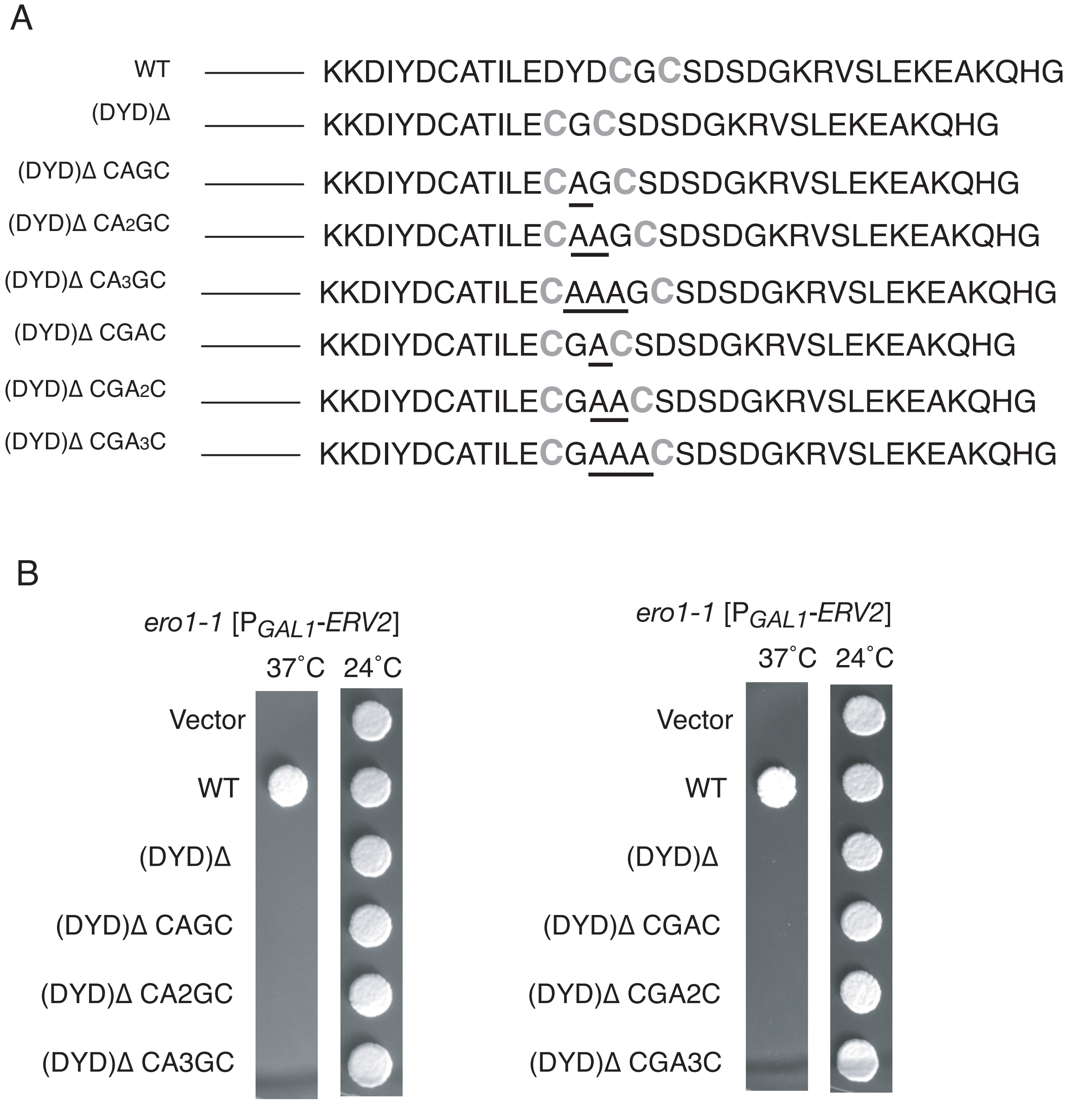
A
WT
KKDIYDCATILEDYDCGCSDSDGKRVSLEKEAKQHG
(DYD)Δ
KKDIYDCATILECGCSDSDGKRVSLEKEAKQHG
(DYD)Δ CAGC
KKDIYDCATILECAGCSDSDGKRVSLEKEAKQHG
(DYD)Δ CA2GC
KKDIYDCATILECAAGCSDSDGKRVSLEKEAKQHG
(DYD)Δ CA3GC
KKDIYDCATILECAAAGCSDSDGKRVSLEKEAKQHG
(DYD)Δ CGAC
KKDIYDCATILECGACSDSDGKRVSLEKEAKQHG
(DYD)Δ CGA2C
KKDIYDCATILECGAACSDSDGKRVSLEKEAKQHG
(DYD)Δ CGA3C
KKDIYDCATILECGAAACSDSDGKRVSLEKEAKQHG
B
ero1-1 [PGAL1-ERV2]
37˚C
24˚C
Vector
WT
(DYD)Δ
(DYD)Δ CAGC
(DYD)Δ CA2GC
(DYD)Δ CA3GC
ero1-1 [PGAL1-ERV2]
37˚C
24˚C
Vector
WT
(DYD)Δ
(DYD)Δ CGAC
(DYD)Δ CGA2C
(DYD)Δ CGA3C

Figure 3. Cys176 interacts with Cys121 in Erv2p-(DYD)Δ. **(A)** The *ero1-1* mutant (CKY598) containing either pRS316 (empty vector) or various cysteine mutant alleles of Erv2p were plated onto YPGal and grown at 24 ˚C or 37 ˚C for 4 d. **(B)** *ero1-1 erv2Δ* mutants (CKY899) containing either pRS316 (empty vector), wild-type Erv2p, or various mutant alleles of Erv2p were labeled with [^{35}S]methionine and alkylated with NEM prior to immunoprecipitation with Erv2p antibody.

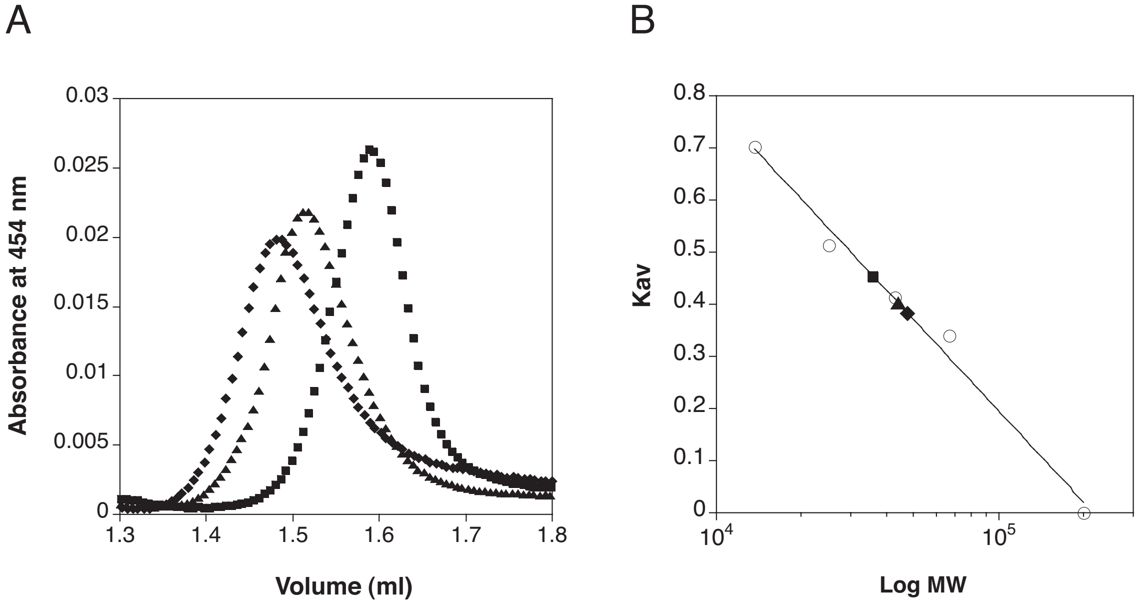

Figure 4. Erv2p-F111S-C176A-C178A is a monomer. **(A)** Analytical gel filtration of Erv2p His$_6$-Erv2p wild-type (◆), His$_6$-Erv2p-C176A-C178A (▲) and His$_6$-Erv2p-F111S-C176A-C178A (■). **(B)** Standard curve generated with proteins of known molecular weight (○): albumin (67 kDa), ovalbumin (43 kDa), chymotrysinogen A (25 kDa) and ribonuclease A (13.7 kDa). The apparent molecular weights of His$_6$-Erv2p (◆), His$_6$-Erv2p-C176A-C178A (▲) and His$_6$-Erv2p-F111S-C176A-C178A (■) were determined according this curve.

(Next page)

Figure 5. Catalytic mechanism of dimeric Erv2p **(A)** and monomeric Erv2p **(B)**. **(A)** Reduced substrate, illustrated here as Pdi1p, attacks the Cys176-Cys178 cysteine pair, resulting in the formation of a mixed-disulfide intermediate between the tail and the substrate (step 1-2). This intermediate is resolved by the attack of a second cysteine of Pdi1p, resulting on the formation of oxidized Pdi1p and reduced Cys176-Cys178 (step 2-3). The tail flips into close proximity of the Cys121-Cys124 pair (step 4) and the tail cysteines are reoxidized by interacting with the active site cysteine pair (step 5). The reduced Cys121-Cys124 pair is re-oxidized by FAD (step 2) and reduced FAD is subsequently reoxidized by O_2, with the concomitant production of H_2O_2 (step 3). **(B)** In contrast, in the monomeric form of Erv2p, the reduced substrate interacts directly with the Cys121-Cys124 pair, resulting in the formation of oxidized Pdi1p and reduced Cys121-Cys124 (step 1-3). Similarly, the reduced Cys121-Cys124 pair is re-oxidized by FAD (step 4) and the reduced FAD is reoxidized by O_2, with the concomitant production of H_2O_2 (step 5).

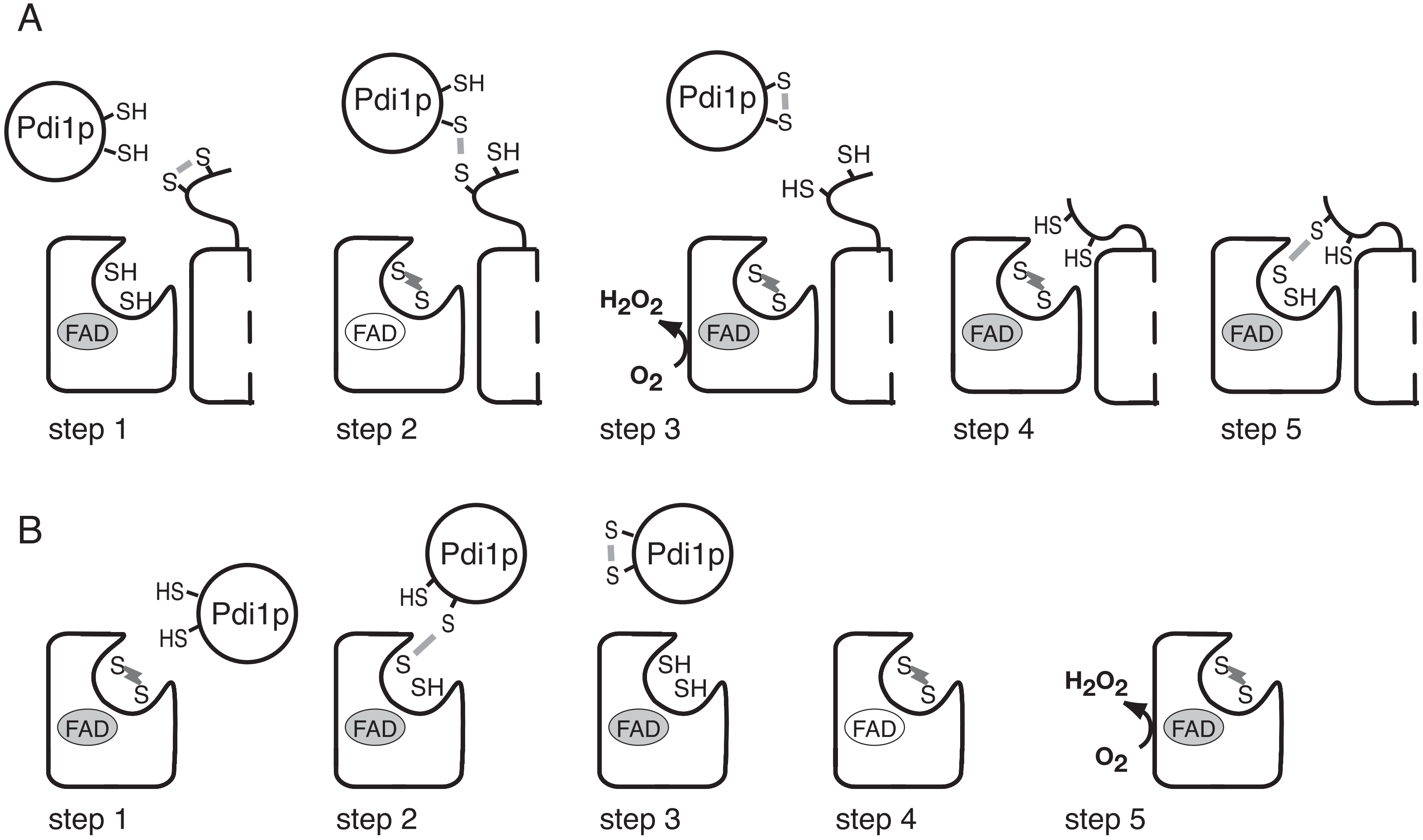
A
Pdi1p
SH
SH
S
S
SH
SH
FAD
step 1
Pdi1p
SH
S
S
SH
S
S
FAD
step 2
Pdi1p
S
S
SH
HS
H_2O_2
O_2
S
S
FAD
step 3
HS
HS
S
S
FAD
step 4
S
HS
S
SH
FAD
step 5
B
HS
HS
Pdi1p
S
S
FAD
step 1
Pdi1p
HS
S
S
SH
FAD
step 2
S
S
Pdi1p
SH
SH
FAD
step 3
S
S
FAD
step 4
H_2O_2
O_2
S
S
FAD
step 5

Chapter Five

Isolation and biochemical characterization of *pdi1* temperature-sensitive mutants

Preface

This chapter consists of preliminary data that is my own work. Some of the data shown in this chapter will be incorporated into a paper that is currently in preparation.

Sevier, C.S, **Vala, A.** and Kaiser, C.A. (2007) Role of glutathione in the isomerization of protein disulfide bonds in *S. cerevisiae*. *In preparation*.

Abstract

Pdi1p is an essential protein in *Sacharomyces cerevisiae*. Although the yeast Pdi1p was first described in the early 1990's, its main function *in vivo* is still debated. Pdi1p has been shown to catalyze disulfide bond formation by playing various roles in the endoplasmic reticulum (ER). First, together with Ero1p, it is involved in the formation of disulfide bonds in secretory proteins, thus working as an oxidoreductase. Second, it might also function as an isomerase, reshuffling disulfide bonds. Third, it might be involved in folding of proteins working as a chaperone. Recently, it has also been suggested that it might play an important role in ER-associated degradation (ERAD).

Although various functions have been attributed to Pdi1p, it is still unclear which of the catalytic activities of Pdi1p is essential for its function *in vivo*. To determine whether these functions exist *in vivo*, we have isolated temperature-sensitive alleles of Pdi1p. Characterization of these mutants revealed that Pdi1p might have two different functions in the ER. First, it seems that Pdi1p mainly acts as an oxidase. Secondly, Pdi1p might also be involved in translocation of secretory proteins. Initial charaterization of the *pdi1* ts mutants suggests that they might be a useful tool to trap PDI substrates.

Results

Isolation of temperature-sensitive *pdi1* alleles

Pdi1p plays an important role in the normal function of the ER. Because it is an essential gene, to further understand its role in the ER we isolated temperature-sensitive (ts) alleles of Pdi1p having a growth defect when placed at high temperature. The *pdi1* ts alleles were generated by random-PCR mutagenesis of *PDI1*, followed by homologous recombination into a *GAL1*-promoted gap plasmid. The *pdi1* ts alleles under the *GAL1* promoter that failed to grow at 37 ˚C were further tested. The *pdi1* alleles that were still temperature-sensitive under their own promoter were further studied.

We tested 45 *pdi1* ts alleles under their own promoter and selected five alleles that had the most severe growth phenotype at the restrictive temperature of 37 ˚C (Figure 1 A and Table 1).

Characterization of *pdi1* ts mutants

Addition of dithiothreitol (DTT) to yeast cells selectively perturbs the formation of disulfide bonds in the ER without interfering with protein synthesis or secretion of non-disulfide bonded proteins (Jamsa *et al.*, 1994). An *ero1-1* mutant at the restrictive temperature is highly sensitive to DTT (Frand *et al.*, 1998). Similarly, the *pdi1* ts alleles are more DTT sensitive than wild-type (Table 3). As observed for the *ero1-1* mutant, the unfolded protein response (UPR) is up-regulated in the *pdi1* ts mutants at the restrictive temperature ((Frand et al., 1998), and data not shown). With the exception of the *pdi1-16* allele, the *pdi1* ts mutants are also sensitive to other drugs that cause ER stress, such as tunicamycin and caffeine (Table 3). In contrast to the *ero1-1* strain, the *pdi1 ts* strains are able to grown under anaerobic conditions (data not shown).

Addition of exogenous oxidant, such as diamide, has been shown to allow *ero1-1* mutants to grow at the restrictive temperature, probably by providing exogenous oxidative equivalents that are missing in the *ero1-1* mutant (Frand et al., 1998). Likewise, addition of exogenous diamide to the medium was able to rescue all *pdi1* ts alleles tested except for *pdi1-16* mutant (Figure 2 and Table 2).

Addition of glycerol is known to rescue growth phenotypes associated with folding defects (Brown *et al.*, 1997; Hampsey, 1997). As observed for the *ero1-1* mutant, some of the temperature-sensitive defects of the *pdi1* ts alleles were rescued by exogenous glycerol (Table 2).

The *ero1-1* growth defect is rescued by lowering the GSH content, either by mutating the enzyme responsible for the first step of biosynthesis of GSH (*gsh1Δ background*) or by inhibiting the production by GSH by buthionine sulfoximine (BSO) (Cuozzo *et al.*, 1999). Similarly, with exception of *pdi1-16* allele, all *pdi1* ts mutants were rescued by either deletion of *GSH1* or by addition of BSO (Figure 3 and Table 4).

Analysis of the steady state protein levels of the *pdi1* ts mutants showed that in these mutants there are higher levels of Pdi1p than in the wild-type strain (data not shown). Under conditions of ER stress, cells up-regulate the protein levels of various ER resident proteins, including Pdi1p (Sidrauski *et al.*, 1998). Furthermore, Pdi1p levels are up-regulated by a cis-acting element CERP that is activated upon deficiency of protein disulphide isomerase activity (Norgaard *et al.*, 2003).

The temperature-sensitive alleles of *PDI*1 are impaired in oxidative folding

A common assay of ER oxidative folding is the maturation of carboxypeptidase Y (CPY), due to the fact that as CPY traverses the secretory pathway its molecular weight changes due to post-translational modifications. CPY is a non-essential yeast vacuolar protein that contains 5 disulfide bonds and a free thiol. It is initially synthesized as a pro-protein that is oxidized and glycosylated in the ER to a precursor form p1 (67 kDa). Upon formation of disulfide bonds it travels to the Golgi, where it acquires additional carbohydrates, forming precursor form p2 (69 kDa). When it reaches the vacuole, the pro sequence is cleaved, forming mature protein (m; 61 kDa) (Stevens *et al.*, 1982).

To determine if the *pdi1* ts alleles have a CPY maturation defect, we performed pulse chase experiments to follow the maturation of CPY *in vivo*. After shifting to the restrictive temperature of 37 °C for 1 h, the *pdi1-5*, *pdi1-6*, *pdi1-10* and *pdi1-11* alleles accumulated the p1 form of CPY, suggesting a defect in maturation of CPY due to retention in the ER (Figure 4A). Interestingly, the *pdi1-16* allele also had a defect in CPY maturation, but this mutant seems to accumulate a different form of CPY (prepro-CPY, non-translocated or non-glycosylated; which migrate in SDS-PAGE gels with similar mobilities). As expected, the CPY maturation defect on the *pdi1 ts* strains was rescued by addition of exogenous diamide (data not shown).

To further characterize the defect of *pdi1-16* ts allele upon temperature shift, we decided to compare the maturation of CPY in yeast mutants that are either defective in ER translocation (*kar2-159* and *sec61-2 mutants*) or in ER-to-golgi transport (*sec12-6* mutant) (Holkeri *et al.*, 1998; Nakano *et al.*, 1988; Pilon *et al.*, 1998; Vogel *et al.*, 1990).

For this purpose, we performed pulse chase experiments to follow the maturation of CPY with or without tunicamycin, a glycosylation inhibitor. After being shifted to the restrictive temperature of 38 ˚C for 1 h, the *pdi1-16* ts accumulates prepro-CPY as observed in *kar2-159* and *sec61-2* mutants (Figure 4B).

In *pdi1* ts mutants secretion of invertase is not impaired

Intracellular transport of secretory proteins that lack disulfides, such as the yeast periplasmic enzyme invertase, is not disrupted in the presence of DTT (Carlson *et al.*, 1983; Jamsa et al., 1994; Lodish *et al.*, 1993). To rule out that the *pdi1* ts mutants have a general secretion defect, we assayed these mutants for intracellular accumulation of invertase (Carlson et al., 1983). As observed for *ero1-1* mutants grown at the restrictive temperatures, the *pdi1* ts alleles do not accumulate intracellular forms of invertase, and thus do not show any defect in invertase secretion (data not shown).

To further characterize the translocation defect of *pdi1-16* mutant, we used the same assay. As controls, we used yeast mutants that are either defective in ER translocation (*kar2-159* and *sec61-2 mutants*) or ER-to-Golgi transport (*sec12-6* mutant). The intracellular ER form of invertase is observed in the *sec12-4* mutant, as this mutant is impaired in ER-to-Golgi transport. As in the *kar2-159* mutant, the *pdi1-16* ts mutant accumulates an intracellular, non-translocated form of invertase (Figure 5).

The pdi1 ts mutants are unable to oxidize CPY

To demonstrate that the CPY p1 form that accumulates after the temperature shift in the *pdi1* ts alleles (*pdi1-5*, *pdi1-6*, *pdi1-10* and *pdi1-11*) does not contain disulfide bonds, we used a thiol-modifying agent that reacts only with free thiols. As controls for mobility shifts, we treated the cells with DTT to reduce all the CPY prior to the 4-acetomido-4'-maleimidylstilbene-2,2'-disulphonic acid (AMS) modification. We observed that in the presence of AMS, the protein runs with the same mobility as CPY treated with DTT prior to AMS modification, suggesting that this CPY p1 form in these mutants is in the reduced form (Figure 6). As observed previously, the CPY form observed in *pdi1-16* ts mutant is of higher mobility suggesting that this mutant accumulates a different form of CPY (non-translocated).

Under hyperoxidizing conditions (e.g. treatment of yeast cells with the thiol oxidant diamide) proteins that contain reactive thiols, such as CPY, are withheld in the ER in oxidized forms (p1 form) and are likely to contain inappropriate intra- or intermolecular disulfide bonds, while the intracellular transport of proteins without cysteines, such as prepro-α-factor, proceeds with normal kinetics (Cuozzo et al., 1999). Mature CPY can be obtained from cells grown under hyperoxidizing conditions by washing out the oxidant and allowing cells to isomerize misoxidized CPY to mature CPY. The isomerization process occurs by an initial reduction step followed by an oxidation step (Sevier *et al.*, 2007). These results suggest that misoxidation of CPY is a reversible process and points to the existence of a reduction system in *S. cerevisiae* (Sevier et al., 2007). In the *pdi1* ts *mutants* (*pdi1-5*, *pdi1-6*, *pdi1-10* and *pdi1-11*) misoxidized CPY formed by hyperoxidizing conditions is reduced after washing out the oxidant, suggesting that the *pdi1* ts alleles are not defective in the oxidase activity thus not able to reoxidize reduced CPY (data not shown and (Sevier et al., 2007)).

From this screen we have isolated two different types of *pdi1* ts mutants: 1) mutants defective in oxidation of disulfide bond in the ER and, 2) mutants defective in the translocation or glycosylation of proteins into the ER.

Function of Ero1p and Pdi1p in oxidative folding

Although *ERO1* is an essential gene, it is possible to grow cells lacking the *ERO1* gene by addition of exogenous oxidant (diamide) or by lowering the GSH content (*gsh1Δ* background), suggesting that it is possible to overcome the need for Ero1p (Cuozzo et al., 1999; Frand et al., 1998). In contrast, we were unable to rescue cells lacking *PDI1* by either addition of exogenous oxidant (diamide) or by lowering the GSH content (*gsh1Δ* background), suggesting a fundamental differences in the role played by these two proteins (data not shown). These results suggest that the essential function of Pdi1p is its oxidoreductase activity.

Genetic interactions of *pdi1* mutations with mutations in the disulfide bond pathway genes

The *ero1-1* mutant is synthetic lethal with *ire1Δ, hut1-1 (Hut1p-A265T) and pdi1-1 (Pdi1p-P106S) mutants (Frand et al., 1998; Tu, 2003)*. In contrast to what is observed for *ero1-1* mutants, only *pdi1-16* and *pdi1-5* mutants were synthethic lethal or sick with *ire1Δ*, respectively (Table 5).

It has been shown previously that *ero1-1 hut1Δ* mutants are more sensitive to DTT than *ero1-1* (Nakanishi *et al.*, 2001). We tested the ability of the *pdi1* ts mutants to suppress the growth defect of *pdi1Δ hut1Δ*. We found that the *pdi1-5* and *pdi1-16* ts mutants are synthetic lethal with *hut1Δ*, while cells containing all other *pdi1* ts alleles are only synthetic sick (Table 5).

To address the effect of deletion of the other genes encoding protein disulfide isomerases in the yeast ER, we tested the *pdi1* ts mutants for their ability to suppress the growth defect of double mutants lacking *PDI1* and one of the yeast PDI homologs or the quintuple mutant lacking *PDI1* and all of its homologs (*pdi1Δ mpd1Δ, pdi1Δ mpd2Δ*, *pdi1Δ eug1Δ*, *pdi1Δ eps1Δ* and *pdi1Δ mpd1Δ mpd2Δ eug1Δ eps1Δ* strains). The *pdi1-16* ts allele is unable to suppress the growth defect of double mutant *pdi1Δ mpd1Δ* or the quintuple mutant (Table 6). The *pdi1-5* ts allele was synthetic sick with all strains tested except *pdi1Δ eps1Δ* (Table 6).

Location of the mutations in the predicted secondary structure of Pdi1p

Sequence analysis of the *pdi1 ts* alleles shows that these carry mutations in both the active and inactive thioredoxins domains of Pdi1p (Table 7). Attempts to separate individual mutations or mutations by domains were unsuccessful, suggesting that it is necessary to have mutations in at least two domains of Pdi1p to obtain the temperature-sensitivity defect (Figure 7).

Trapping *pdi1* ts-substrate mixed disulfides *in vivo*

To further investigate why the *pdi1* ts mutants are defective in oxidative folding, we analyzed the *in vivo* redox state of the *pdi1* ts proteins. The oxidation state was analyzed by covalent modification with AMS, a thiol-modifying agent that reacts to free thiols only, and the reduced and oxidized forms of the proteins were resolved by SDS-PAGE. As controls for mobility shifts, we treated the cells with DTT to reduce all the *pdi1* ts protein prior to the AMS modification. We were unable to determine the redox state of the *pdi1* ts proteins, because even in the absence of AMS these *pdi1* ts proteins were trapped in higher molecular weight complexes (Figure 8). Under reducing conditions we no longer detect these higher molecular complexes, suggesting that they are disulfide-linked complexes of *pdi1* ts and substrate proteins (data not shown).

As reported for mutants of DsbA, the bacterial homolog of Pdi1p, it is possible that the mutations contained in the *pdi1* ts mutants slow the thiol-exchange reaction between the *pdi1* ts proteins and its substrates, thus allowing us to detect mixed-disulfide complexes (Kadokura *et al.*, 2004). Since lowering the GSH content of cells rescued the growth defect of the *pdi1* ts mutants, we analysed the formation of the *pdi1* ts-substrate complexes in cells lacking the *GSH1* gene. Interestingly, the amount of *pdi1* ts-substrate complexes in these cells was slightly increased (Figure 8). As a control we overexpressed wild-type Pdi1p and were unable to obtain the formation of *pdi1* ts-substrate complexes.

Future directions

The initial characterization of the *pdi1* ts mutants was performed. The *pdi* ts mutants are a tool for analyzing further the function of Pdi1p *in vivo* but also an important tool for the potential trapping of substrates. It will also be interesting to further analyze the role of Pdi1p in ER translocation.

Materials and methods

Strains, plasmids and media

S. cerevisiae strains are listed in Table 8. Isolation and characterization of the *ero1-1* strain (CKY598) has been described previously (Frand et al., 1998). Cultures were either grown in rich medium (1% Bacto yeast extract and 2% Bacto-peptone containing either 2% dextrose (YPD) or 2% galactose (YPGal) as carbon sources) or minimal media (0.67% nitrogen base without amino acids supplemented with 16 amino acids not including cysteine) containing 2% galactose and 2% raffinose (SMM Gal/Raf). For anaerobic conditions, strains were grown in sealed BBL GasPak chamber envelope (Becton Dickinson). Standard genetic manipulations and yeast transformations were performed as described (Adams *et al.*, 1997).

To generate AVY115, the coding sequence of *PDI1* was replaced by *kanMX6* by homologous recombination in AVY111 (a homozygous *GAL2 ura3-52 leu2-3, 112* diploid background). The resulting heterozygous diploid was transformed with pCS213. After sporulation, a viable *MAT**a** Ura+ kanMX* segregant was selected (CSY314). The viability of CSY314 depends on the episomal *PDI1* allele, since this strain is not able to grown on medium containing 5-fluorootic acid (5-FOA; Toronto Research Laboratories, Canada).

Complete gene deletion of *GSH1* in a *pdi1Δ* background was constructed by gene replacement with the *kanMX6* cassette by homologous recombination in AVY800 (Wach *et al.*, 1994). To make AVY800 the *kanMX6* cassette was substituted by *natMX6* cassette by homologous recombination in AVY115 (Goldstein *et al.*, 1999). Tagging of

ERO1 at its C terminus with 13xmyc was performed by homologous recombination, resulting in AVY758 (Longtine *et al.*, 1998).

The *ero1-1 pdi1Δ [pCS213]* strain (AVY704) was constructed by crossing an *ero1-1* strain (CKY598) to a wild type strain (CKY264). The coding sequence of *PDI1* was replaced by *kanMX6* by homologous recombination in AVY704. After transformation with pCS213, this strain was sporulated and a viable *MAT**a** Ura+ kanMX6* temperature-sensitive spore was selected (AVY769). The *ire1Δ pdi1Δ [pCS213]* strain (AVY802) was constructed by replacing the *IRE1* coding sequence in AVY115. The *gsh1Δ pdi1Δ [pCS213]* strain (AVY831) was constructed by replacing the *GSH1* coding sequence in AVY800. The resulting diploid strains were transformed with pCS213 and sporulated. A viable *MAT**a** Ura+ kanMX6 natMX6* was selected (AVY844 and AVY876, respectively). The viability of AVY769, AVY844 and AVY876 depends on the episomal *PDI1* allele, since these strains are not able to grown on medium containing 5-FOA.

The *mpd1Δ pdi1Δ [pCS213], mpd2Δ pdi1Δ [pCS213], eug1Δ pdi1Δ [pCS213] and eps1Δ pdi1Δ [pCS213]* strains were constructed replacing the *MPD1*, *MPD2*, *EUG1* or *EPS1* coding sequences by *kanMX6* by homologous recombination in AVY800. After transformation with pCS213, these strains were sporulated and a viable *MAT**a** Ura+ kanMX6 natMX6* temperature-sensitive spore was selected (AVY882, AVY888, AVY894 and AVY900, respectively). The *mpd1Δ mpd2Δ eug1Δ eps1Δ pdi1Δ [pCS213]* strain (AVY967) was constructed by crossing an *mpd1Δ mpd2Δ eug1ΔI strain* (AVY918) to an *eps1Δ pdi1Δ [pCS213]* strain (AVY897). The viability of AVY882, AVY888, AVY894, AVY900 and AVY967 depends on the episomal *PDI1* allele, since these strains are not able to grown on medium containing 5-FOA.

To generate strains AVY580-596, CSY314 was transformed with *LEU2*-based plasmids carrying the *pdi1* ts alleles under their own promoter (pAV336-pAV458). The transformants were streaked in 5-FOA containing medium to select for colonies that only contain the *pdi1* ts allele and that have lost the wild-type *PDI1*-containing plasmids.

The *pdi1Δ suc2-Δ9 [pCS213]* strain was constructed by crossing a *suc2-Δ9* strain (CKY406) to a *pdi1Δ* strain carrying an exogenous copy of wild-type *PDI1* [pCS213] (CYY314). This strain was sporulated and a viable *MATa Ura+ natMX6* temperature-sensitive spore was selected (AVY957). The *pdi1Δ suc2-Δ9 [pAV458]* strain was constructed by transforming AVY957 with *LEU2*-based plasmid carrying the *pdi1* ts allele under their own promoter (pAV458). The transformants were streaked in 5-FOA containing medium to select for colonies that only contain the *pdi1* ts allele and that have lost the wild-type *PDI1*-containing plasmids (AVY1030).

Plasmid construction

Plasmids used in this work are listed in Table 8. To make pAV9 an ApaI-SacI fragment of 2572 bp from pCT37, containing the *GAL1* promoter and *PDI1*, was subcloned into the same sites of pRS315 (Sikorski *et al.*, 1989).

To generate pCS213, pBH1966 was cut with BamHI and SalI and gap repair by homologous recombination with genomic PDI1 from CKY263. To create a plasmid containing the 5' untranslated region (UTR) of *PDI1*, we amplified genomic DNA with SalI-5'UTR-Pdi1, 5'-AAA AAA **GTC GAC** GGA AAT TGG TAC CAC CCA GGT CGG CGG CTA-3' and 5'UTR-Pdi1-BamHI primers 5'-AAA AAA **GGA TCC** TGC TTG CAA CAA GAA AAT GCA CGC GTA ACA-3'. This PCR product was inserted into SalI and BamHI sites of pRS315 (Sikorski et al., 1989). To create plasmids containing the *pdi1* alleles under their own promoter, DNA fragments containing the *pdi1* alleles that conferred temperature sensitivity under the *GAL1* promoter were subcloned into BamHI and SacII sites of pAV320. The same DNA fragments were subcloned into the same sites in pRS306 (Sikorski et al., 1989) for integration at the *PDI1* locus by two-step gene replacement.

Isolation and integration of pdi1 temperature-sensitive alleles

PCR mutagenesis of the *PDI1* gene was preformed as described (Muhlrad *et al.*, 1992). A 1762 bp DNA fragment containing 196 base pair of the 5' UTR was amplified from pAV9 with the following primers Gal1, 5'-TGCATAACCACTTTAACT-3' and Pdi3, 5'-CAATTCATCGTGAA TGGCATC-3' using AmpliTaq Gold (Perkin Elmer) in the presence of 0.25 mM $MgCl_2$ and one-fifth the normal concentration of dATP (0.2 mM dATP).

The resulting PCR fragment and pAV9 (described above) cut with BamHI and SacII were transformed into CKY564. Transformants in SC Gal/Raff-leucine plates were replica-plated onto plates with 5-FOA at 24 °C versus 37 °C. Plasmids that conferred temperature-sensitivity were obtained at a frequency of 1-2 colonies per 100 colonies tested and were tested by retransformation. The *pdi1* alleles that conferred temperature sensitivity under the *GAL1* promoter were subcloned into pAV320 (pRS315 vector containing *PDI1* promoter). These plasmids were further tested and the ones that still conferred temperature sensitivity under the *PDI1* promoter were studied further.

Assays for growth in the presence of DTT, diamide or BSO

Strains were grown selectively to exponential phase at 24 ˚C. Triplicate lawns of 2×10^6 cells were plated into YPD and 10 μl of 2 M DTT applied to lawns in 6 mm filter disks (Fisher Scientific). Diameters of the zone of inhibition were measured after incubation for 1-2 d at 30 ˚C.

To test for diamide (Sigma) and DL-buthionine-[S,R]-sulfoximine (BSO; Sigma) rescue of temperature-sensitive strains, lawns of 1×10^6 cells were plated into YPD or SC, respectively. Then, 10 μl of 0.6 M diamide or 10 μl of 50 mg ml^{-1} BSO were applied to the lawns in 6 mm filter disks before incubation at 37 ˚C (for *pdi1 ts* mutants) or 30 ˚C (for CSY314).

CPY immunoprecipitation

For CPY immunoprecipitation, strains were grown at 24 ˚C in synthetic minimal medium (SMM) lacking methionine with 2% glucose to exponential phase. Cells were resuspended in overnight medium at a concentration of 1.8 OD_{600} ml^{-1} at 24 ˚C and shifted to 38 ˚C for 1 h before labeling with [35^S]methionine and cysteine (EXPRESS, NEN). Cells were then suspended in 10% (w/v) TCA and lysed with glass beads. Protein pellets were then incubated in sample buffer (80 mM Tris-HCl [pH 6.8], 2% SDS, 10% glycerol, 1 mM phenylmethylsulfonyl fluoride (PMSF), 0.01% bromophenol blue). Cell extracts were suspended in 1 ml IP buffer (50 mM Tris-HCl [pH 7.4], 150 mM NaCl, 1% Triton X-100 and 1 mM PMSF) and preadsorbed with fixed *Staphylococcus* A cells (Sigma) before incubation with CPY antibody (1 OD_{600} units of cells were incubated with 1 μl of anti-CPY). Immune complexes were collected with protein A-Sepharose (Pharmacia), washed in IP buffer containing 0.1% SDS, washed in IP buffer without detergent, and solubilized in sample buffer. Samples were analyzed on a non-reducing 8% SDS-PAGE and visualized with a 445si PhosphoImager (Molecular Dynamics). When necessary tunicamycin (10 μg ml^{-1}, Sigma) was added to cells 10 min before labeling. Cells were labeled with [35^S]methionine and cysteine (EXPRESS, NEN) for 10 min at 38 ˚C and chased for 15 min.

To examine the redox state of CPY, strains were grown as described before. Strains were resuspended in overnight medium at a concentration of 1.8 OD ml^{-1} at 24 ˚C and shifted to 38 ˚C for 1 h before labeling with [35^S]methionine and cysteine (EXPRESS, NEN). When necessary strains were treated with 5 mM DTT 10 min before labeling. After labeling, samples were TCA precipitated and incubated in sample buffer containing 15 mM 4-acetoamido-4'-maleimidylstilbene-2,2'-disulfonic acid (AMS, Molecular Probes). Samples were resolved on a non-reducing 8% SDS-PAGE gel and analyzed with a 445si PhosphorImager (Molecular Dynamics).

Induction of the unfolded protein response

Strains expressing pJC104 (Sidrauski *et al.*, 1996) were grown in selective medium at 24 ˚C and resuspended 1 x 10^7 cells ml^{-1} in YPD. Cultures were given 0 or 2.5 μg ml^{-1} of tunicamycin (Sigma) and incubated at 30 °C or 37 °C for 2.5 h. Cells were permeabilized and β-galactosidase activity assayed as described (Guarente, 1983). Two transformants were assayed per strain and the experiment repeated twice.

Protein extracts, and immunoblotting

Whole-cell extracts were prepared by resuspending 5 OD_{600} units of cells in 30 μl sample buffer (60 mM Tris-HCl [pH 6.8], 2% SDS, 100 mM DTT, 10% glycerol, 0.001% bromophenol Blue) and boiled for 2 min. Cells were lysed by agitation with glass beads, and an additional 70 μl of sample buffer was added. The equivalent to 0.75 OD_{600} units of cells were analyzed by 8% SDS-PAGE and analyzed by immunoblotting with antiserum to Pdi1p.

For invertase assay, cells were grown to the exponential phase in YEP with 2% glucose. Two OD_{600} units of cells were centrifuged and resuspended in YEP medium 0.1% glucose (derepressing conditions) and aerated at 37°C for 2-3 h. Cells were washed with 10 mM sodium azide. Cell pellets were suspended in 20 μl of sample buffer (80 mM Tris-HCl [pH 6.8], 10% glycerol, 2% SDS, 100 mM DTT, 2 mM PMSF, 0.01% bromphenol blue) and boiled for 2 min followed by disruption by glass bead lysis. An additional 130 μl of sample buffer was added, and samples were heated to 95°C for 3 min. Proteins were separated on 7.5% SDS-PAGE and analyzed by immunoblotting with antiserum to invertase.

To examine the redox state of *Pdi1* ts protein, strains were grown as described above. When necessary strains were treated with 5 mM DTT for 10 min. Samples were TCA precipitated and cells were lysed by agitation with glass beads. Cell pellets were resuspended in sample buffer containing 15 mM AMS. Samples were resolved on a non-reducing 8% SDS-PAGE gel and analyzed by immunoblotting with antiserum to Pdi1p.

Immunoblotting was performed as described (Elrod-Erickson *et al.*, 1996). The following antibodies were used for western blot detection: rabbit anti-invertase at 1:1,000 dilution, and rabbit polyclonal anti-PDI 1:10,000 (a gift from T. Stevens, University of Oregon, Eugene, Oregon), and donkey anti-rabbit IgG-HRP (1:10,000 dilution; Amersham). Blots were developed by chemiluminescence (ECL system; Amersham) and detected on a Kodak Image Station 440.

References

Adams, A., Gottschling, D.E., Kaiser, C.A. and Stearns, T. (1997) *Methods in Yeast Genetics*. Cold Spring Harbor Laboratory Press.

Brown, C.R., Hong-Brown, L.Q. and Welch, W.J. (1997) Correcting temperature-sensitive protein folding defects. *J Clin Invest*, **99**, 1432-1444.

Carlson, M., Taussig, R., Kustu, S. and Botstein, D. (1983) The secreted form of invertase in Saccharomyces cerevisiae is synthesized from mRNA encoding a signal sequence. *Mol Cell Biol*, **3**, 439-447.

Cuozzo, J.W. and Kaiser, C.A. (1999) Competition between glutathione and protein thiols for disulphide-bond formation. *Nat Cell Biol*, **1**, 130-135.

Elrod-Erickson, M.J. and Kaiser, C.A. (1996) Genes that control the fidelity of endoplasmic reticulum to Golgi transport identified as suppressors of vesicle budding mutations. *Mol Biol Cell*, **7**, 1043-1058.

Frand, A.R. and Kaiser, C.A. (1998) The ERO1 gene of yeast is required for oxidation of protein dithiols in the endoplasmic reticulum. *Mol Cell*, **1**, 161-170.

Goldstein, A.L. and McCusker, J.H. (1999) Three new dominant drug resistance cassettes for gene disruption in Saccharomyces cerevisiae. *Yeast*, **15**, 1541-1553.

Guarente, L. (1983) Yeast promoters and lacZ fusions designed to study expression of cloned genes in yeast. *Methods Enzymol*, **101**, 181-191.

Hampsey, M. (1997) A review of phenotypes in Saccharomyces cerevisiae. *Yeast*, **13**, 1099-1133.

Holkeri, H., Paunola, E., Jamsa, E. and Makarow, M. (1998) Dissection of the translocation and chaperoning functions of yeast BiP/Kar2p in vivo. *J Cell Sci*, **111 (Pt 6)**, 749-757.

Jamsa, E., Simonen, M. and Makarow, M. (1994) Selective retention of secretory proteins in the yeast endoplasmic reticulum by treatment of cells with a reducing agent. *Yeast*, **10**, 355-370.

Kadokura, H., Tian, H., Zander, T., Bardwell, J.C. and Beckwith, J. (2004) Snapshots of DsbA in action: detection of proteins in the process of oxidative folding. *Science*, **303**, 534-537.

Lodish, H.F. and Kong, N. (1993) The secretory pathway is normal in dithiothreitol-treated cells, but disulfide-bonded proteins are reduced and reversibly retained in the endoplasmic reticulum. *J Biol Chem*, **268**, 20598-20605.

Longtine, M.S., McKenzie, A., 3rd, Demarini, D.J., Shah, N.G., Wach, A., Brachat, A., Philippsen, P. and Pringle, J.R. (1998) Additional modules for versatile and economical PCR-based gene deletion and modification in Saccharomyces cerevisiae. *Yeast*, **14**, 953-961.

Muhlrad, D., Hunter, R. and Parker, R. (1992) A rapid method for localized mutagenesis of yeast genes. *Yeast*, Vol. 8, pp. 79-82.

Nakanishi, H., Nakayama, K., Yokota, A., Tachikawa, H., Takahashi, N. and Jigami, Y. (2001) Hut1 proteins identified in Saccharomyces cerevisiae and Schizosaccharomyces pombe are functional homologues involved in the protein-folding process at the endoplasmic reticulum. *Yeast*, **18**, 543-554.

Nakano, A., Brada, D. and Schekman, R. (1988) A membrane glycoprotein, Sec12p, required for protein transport from the endoplasmic reticulum to the Golgi apparatus in yeast. *J Cell Biol*, **107**, 851-863.

Norgaard, P., Tachibana, C., Bruun, A.W. and Winther, J.R. (2003) Gene regulation in response to protein disulphide isomerase deficiency. *Yeast*, **20**, 645-652.

Norgaard, P., Westphal, V., Tachibana, C., Alsoe, L., Holst, B. and Winther, J.R. (2001) Functional differences in yeast protein disulfide isomerases. *J Cell Biol*, **152**, 553-562.

Pilon, M., Romisch, K., Quach, D. and Schekman, R. (1998) Sec61p serves multiple roles in secretory precursor binding and translocation into the endoplasmic reticulum membrane. *Mol Biol Cell*, **9**, 3455-3473.

Sevier, C.S., Vala, A. and Kaiser, C.A. (2007) Role of glutathione in the isomerization of protein disulfide bonds in S. cerevisiae. **in preparation**,

Sidrauski, C., Chapman, R. and Walter, P. (1998) The unfolded protein response: an intracellular signalling pathway with many surprising features. *Trends Cell Biol*, **8**, 245-249.

Sidrauski, C., Cox, J.S. and Walter, P. (1996) tRNA ligase is required for regulated mRNA splicing in the unfolded protein response. *Cell*, **87**, 405-413.

Sikorski, R.S. and Hieter, P. (1989) A system of shuttle vectors and yeast host strains designed for efficient manipulation of DNA in Saccharomyces cerevisiae. *Genetics*, **122**, 19-27.

Stevens, T., Esmon, B. and Schekman, R. (1982) Early stages in the yeast secretory pathway are required for transport of carboxypeptidase Y to the vacuole. *Cell*, **30**, 439-448.

Tachibana, C. and Stevens, T.H. (1992) The yeast EUG1 gene encodes an endoplasmic reticulum protein that is functionally related to protein disulfide isomerase. *Mol Cell Biol*, **12**, 4601-4611.

Tu, B.P.-C. (2003) Biochemical basis of oxidative protein folding in the endoplasmic reticulum. University of California, San Francisco, California.

Vogel, J.P., Misra, L.M. and Rose, M.D. (1990) Loss of BiP/GRP78 function blocks translocation of secretory proteins in yeast. *J Cell Biol*, **110**, 1885-1895.

Wach, A., Brachat, A., Pohlmann, R. and Philippsen, P. (1994) New heterologous modules for classical or PCR-based gene disruptions in Saccharomyces cerevisiae. *Yeast*, **10**, 1793-1808.

Table 1. Temperature-sensitive alleles of Pdi1p.

Pdi1p allele[a]	**Suppression of *pdi1Δ* growth defect at 24 ˚C**	**Suppression of *pdi1Δ* growth defect at 37 ˚C**
Vector	−	NA
PDI1	+	+
pdi1-5	+	−
pdi1-6	+	−
pdi1-10	+	−
pdi1-11	+	−
pdi1-16	+	−

[a] The CSY314 strain (*pdi1Δ pCS213*) was transformed with either pRS316 (empty vector), *PDI1* or *pdi1* temperature-sensitive alleles. The transformants were streaked on SC + 5-FOA plates and grown at RT for 3 d.

NA - non applicable

Table 2. Characterization of *pdi1* temperature-sensitive alleles.

Pdi1p allele[a]	**CPY defect**	**Growth YPD + DIA 37 ˚C**	**Growth YPGly 37 ˚C**
PDI1	No	+	+
pdi1-5	Yes	+	−
pdi1-6	Yes	+	+
pdi1-10	yes	+	+
pdi1-11	yes	+	+
pdi1-16	yes	−	−

[a] the various yeast strains (AVY580, AVY585-6, AVY590-1 and AVY596) were platted onto YPD containing diamide or YPGly plates and grown at RT for 3 d.

Table 3. Further characterization of *pdi1* temperature-sensitive alleles.

Pdi1p allele[a]	**Growth YPD + 7.5mM DTT**	**Growth YPD + 10 mM Caff**	**Growth YPD+ 1 μg/ml Tun**
PDI1	+	R	R
pdi1-5	–	VS	VS
pdi1-6	–	VS	VS
pdi1-10	+	R	S
pdi1-11	–	S	S
pdi1-16	+/–	R	R

[a] the various yeast strains (AVY580, AVY585-6, AVY590-1 and AVY596) were platted onto YPD containing either DTT, Caffeine or Tunicamycin plates and grown at RT for 3 d. R, resistant; S, sensitive; VS, very sensitive.

Table 4. Suppression of growth defect of the temperature-sensitive alleles of Pdi1p by blocking GSH synthesis.

Pdi1p allele[a]	**Growth YPD 37 ˚C**	**gsh1Δ background Growth YPD 37 ˚C**	**Growth SC 37 ˚C**	**Growth SC + BSO 37 ˚C**
PDI1	+	+	+	+
pdi1-5	–	+/-	–	+
pdi1-6	–	+/-	–	+
pdi1-10	–	+	–	+
pdi1-11	–	+	–	+
pdi1-16	–	–	–	–

[a] the various yeast strains (AVY580, AVY585-6, AVY590-1, AVY596 and AVY1018-AVY1023) were plated on YPD or SC medium containing BSO grown at 24 ˚C and 37 ˚C for 3 d.

Table 5. Synthetic lethality of temperature-sensitive alleles of Pdi1p with *ero1-1*, *ire1Δ*, and *hut1Δ*.

Pdi1p allele[a]	**Suppression of *ero1-1 pdi1Δ* growth defect at 24 ˚C**	**Suppression of ire1Δ *pdi1Δ* growth defect at 37 ˚C**	**Suppression of *hut1Δ pdi1Δ* growth defect at 24 ˚C**
PDI1	+	+	+
pdi1-5	+/–	–	–
pdi1-6	+	–	+/–
pdi1-10	+	+	+
pdi1-11	+	–	+/–
pdi1-16	–	–	–

[a] AVY769, AVY844 and AVY870 strains were transformed with either pRS316 (empty vector), *PDI1* or *pdi1* temperature-sensitive alleles. The transformants were streaked on SC + 5-FOA plates and grown at RT for 3 d.

Table 6. Synthetic lethality of temperature-sensitive alleles of Pdi1p with genomic deletion of Pdi1p homologs.

Pdi1p mutant allele[a]	***mpd1Δ pdi1Δ*** **growth defect at 24 ˚C**	***mpd2Δ pdi1Δ*** **growth defect at 24 ˚C**	***eug1Δ pdi1Δ*** **growth defect at 24 ˚C**	***eps1Δ pdi1Δ*** **growth defect at 24 ˚C**	***mpd1Δ mpd2Δ eug1Δ eps1Δ pdi1Δ*** **growth defect at 24 ˚C**
PDI1	+	+	+	+	+
pdi1-5	+/–	+/–	+/–	+	+/–
pdi1-6	+	+	+	+	+
pdi1-10	+	+	+	+	+
pdi1-11	+/–	+	+	+	+/–
pdi1-16	–	+/–	+/–	+/– –	–

[a] the AVY882, AVY888, AVY894, AVY900 and AVY967 strains were transformed with either pRS316 (empty vector), *PDI1* or *pdi1* temperature-sensitive alleles. The transformants were streaked on SC + 5-FOA plates and grown at RT for 3 d.

Table 7. Mutations in *pdi1* temperature-sensitive alleles.

Allele	Base change	Amino acid change	PDI domain
pdi1-5	T62C	F21S	SS
	G132C	E44D	a
	T155C	V52A	a
	T491C	V164A	b
	A557G	N186S	b
	A628T	M210L	b
	A689T	E230V	b
	A902T	H301L	b'
	A970G	K324E	b'
	A1024G	I342V	b'
	A1049G	E350G	b'
	T1111C; T1112G	F371R	
	A1231G	R411G	a'
	A1262G	D421G	a'
	A1317T	E439D	a'
	A1378G	K460E	a'
pdi1-6	T59C	V20A	SS
	A368G	E123G	a
	A443G	D148G	b
	C448G	P150A	b
	T529C	F177L	b
	A689G	E230G	b
	A728T	E243V	b'
	A1019C	D340A	b'
	A1024G	I342V	b'
	A1034G	E345G	b'
	A1165G	I389V	a'
	T1418C	L473S	a'

Table 7 Continued. Mutations in *pdi1* temperature-sensitive alleles.

Allele	Base change	Amino acid change	PDI domain
pdi1-10	T44C	L15P	SS
	T94G	S32A	a
	T395C	V132A	a
	A548G	K183R	b
	T554A	F185Y	b
	A628G	M210V	b
	T685A	F229I	b
	T770C	L257S	b'
	A797T	D266V	b'
	A816T	E272D	b'
	A1121T	Q374L	
	T1190C	V397A	a'
pdi1-11	T137C	I46T	
	T506C	I169T	b
	A752G	Q251R	b'
	A791G	Y264C	b'
	T980C	L327S	b'
	A1061T	K354M	b'
	T1070G	L357W	b'
	A1103G	Q368R	
	A1329T	R443S	a'
	T1429C	F477L	a'
	T1463C	V488A	

Table 7 Continued. Mutations in *pdi1* temperature-sensitive alleles.

Allele	Base change	Amino acid change	PDI domain
pdi1-16	A5G	K2R	SS
	G79A	V27M	
	T151A	L51M	a
	A304G	I102V	a
	A521G	N174S	b (abolish N-linked Glyc.)
	A549C	K183N	b
	A590G	D197G	b
	A649G	N217D	b
	A658C	K220Q	b
	A865T	N289Y	b'
	A996T	E332D	b'
	A1121C	Q374P	
	T1133C	V378A	a'
	A1172T	N391I	a'
	A1273G	N425D	a' (abolish N-linked Glyc.)
	T1439C	I480T	a'
	A1499G	K500R	

Table 8. Yeast strains used in this study.

Strain	**Genotype**	**Source**
CKY263	*MAT**a** ura3-52 leu2-3,112 GAL2*	Kaiser lab collection
CKY598	*MAT***a** *ero1-1 ura3-52 leu2-3,112 GAL2*	Kaiser lab collection
CSY314	*MATα ura3-52 leu2-3, 112 GAL2 pdi1Δ::kanMX6 [pCS213]*	Sevier collection
AVY111	*MAT**a**/α ura3-52/ura3-52 leu2-3, 112/leu2-3, 112 GAL2/GAL2*	This study
AVY115	*MAT**a**/α ura3-52/ura3-52 leu2-3, 112/leu2-3, 112 GAL2/GAL2 PDI1/pdi1Δ:kanMX6*	This study
AVY800	*MAT**a**/α ura3-52/ura3-52 leu2-3, 112/leu2-3, 112 GAL2/GAL2 PDI1/pdi1Δ::natMX6*	This study
AVY840	*MAT**a** ura3-52 leu2-3, 112 GAL2 pdi1Δ::natMX6 [pCS213]*	This study
CKY598	*MAT**a** ura3-52 leu2-3, 112 ero1-1 GAL2*	Kaiser lab collection
AVY769	*MAT**a** ura3-52 leu2-3, 112 GAL2 ero1-1 pdi1Δ::kanMX6 [pCS213]*	This study
AVY844	*MAT**a** ura3-52 leu2-3, 112 GAL2 ire1Δ::natMX6 pdi1Δ::kanMX6 [pCS213]*	This study
AVY876	*MAT**a** ura3-52 leu2-3, 112 GAL2 pdi1Δ::natMX6 gsh1Δ::kanMX6 [pCS213]*	This study
AVY870	*MATa ura3-52 leu2-3, 112 GAL2 pdi1Δ::natMX6 hut1Δ::kanMX6 [pCS213]*	This study
AVY880	*MAT**a** ura3-52 leu2-3, 112 GAL2 mpd1Δ::kanMX6*	This study
AVY886	*MAT**a** ura3-52 leu2-3, 112 GAL2 mpd2Δ::kanMX6*	This study
AVY892	*MAT**a** ura3-52 leu2-3, 112 GAL2 eug1Δ::kanMX6*	This study
AVY898	*MAT**a** ura3-52 leu2-3, 112 GAL2 eps1Δ::kanMX6*	This study
AVY882	*MAT**a** ura3-52 leu2-3, 112 GAL2 pdi1Δ::natMX6 mpd1Δ::kanMX6 [pCS213]*	This study
AVY888	*MAT**a** ura3-52 leu2-3, 112 GAL2 pdi1Δ::natMX6 mpd2Δ::kanMX6 [pCS213]*	This study
AVY894	*MAT**a** ura3-52 leu2-3, 112 GAL2 pdi1Δ::natMX6 eug1Δ::kanMX6 [pCS213]*	This study
AVY900	*MAT**a** ura3-52 leu2-3, 112 GAL2 pdi1Δ::natMX6 eps1Δ::KanMX6 [pCS213]*	This study
CSY304	*MATα mpd1Δ::kanMX6 eug1Δ::kanMX6 ura3-52 leu2-3, 112 GAL2*	Sevier collection
CSY306	*MATα mpd1Δ::kanMX6 mpd2Δ::kanMX6 ura3-52 leu2-3, 112 GAL2*	Sevier collection
CSY308	*MATα mpd1Δ::kanMX6 mpd2Δ::kanMX6 eug1Δ::kanMX6 ura3-52 leu2-3, 112 GAL2*	Sevier collection
AVY967	*MAT**a** ura3-52 leu2-3, 112 GAL2 pdi1Δ::natMX6 mpd1Δ::kanMX6 mpd2Δ::kanMX6 eug1Δ::kanMX6 eps1Δ::kanMX6 [pCS213]*	This study
AVY580	*MATa a pdi1Δ::kanMX6 ura3-52 leu2-3, 112 GAL2 [pAV336]*	This study
AVY585	*MATa pdi1Δ::kanMX6 ura3-52 leu2-3, 112 GAL2 [pAV341]*	This study
AVY586	*MATa pdi1Δ::kanMX6 ura3-52 leu2-3, 112 GAL2 [pAV342]*	This study
AVY590	*MATa pdi1Δ::kanMX6 ura3-52 leu2-3, 112 GAL2 [pAV452]*	This study
AVY591	*MATa pdi1Δ::kanMX6 ura3-52 leu2-3, 112 GAL2 [pAV453]*	This study
AVY596	*MATa pdi1Δ::kanMX6 ura3-52 leu2-3, 112 GAL2 [pAV458]*	This study

Table 8 Continued. Yeast strains used in this study.

Strain	Genotype	Source
AVY1018	*MATa ura3-52 leu2-3, 112 GAL2 pdi1Δ::natMX6 gsh1Δ::kanMX6 [pAV336]*	This study
AVY1019	*MATa ura3-52 leu2-3, 112 GAL2 pdi1Δ::natMX6 gsh1Δ::kanMX6 [pAV341]*	This study
AVY1020	*MATa ura3-52 leu2-3, 112 GAL2 pdi1Δ::natMX6 gsh1Δ::kanMX6 [pAV342]*	This study
AVY1021	*MATa ura3-52 leu2-3, 112 GAL2 pdi1Δ::natMX6 gsh1Δ::kanMX6 [pAV452]*	This study
AVY1022	*MATa ura3-52 leu2-3, 112 GAL2 pdi1Δ::natMX6 gsh1Δ::kanMX6 [pAV453]*	This study
AVY1023	*MATa ura3-52 leu2-3, 112 GAL2 pdi1Δ::natMX6 gsh1Δ::kanMX6 [pAV458]*	This study
CKY406	*MATa ura3-52 leu2-3, 112 suc2-Δ9*	Kaiser Lab collection
EHY33	*MATa ura3-52 leu2-3, 112 kar2-159 suc2-Δ9*	Elisabeth Hong collection
CKY156	*MATα ura3-52 leu2-3, 112 ade2 pep4-3 sec61-2*	Kaiser Lab collection
CKY407	*MATα ura3-52 leu2-3, 112 sec12-4 suc2-Δ9*	Kaiser Lab collection
AVY957	*MATa ura3-52 leu2-3, 112 GAL2 pdi1Δ::natMX6 suc2-Δ9 [pCS213]*	This study
AVY1030	*MATa ura3-52 leu2-3, 112 GAL2 pdi1Δ::natMX6 suc2-Δ9 [pAV458]*	This study

Table 9. Plasmids used in this work

Name	**Description**	**Markers**	**Source or Reference**
pCT37	*pGal1-PDI1*	*CEN*, *URA3*	Tachibana *et al.*, 1992
pAV9	*pGal1-PDI1*	*CEN*, *LEU2*	This study
pBH1966	pP_{PDI1}-*PDI1*-CGHS-CGHS	*CEN, TRP1*	Norgaard *et al.*, 2001
pCS213	pP_{PDI1}-*PDI1*	*CEN*, *URA3*	This study
pAV336	pP_{PDI1}-*PDI1*	*CEN*, *LEU2*	This study
pAV337	pP_{PDI1}-*pdi1-1*	*CEN*, *LEU2*	This study
pAV338	pP_{PDI1}-*pdi1-2*	*CEN*, *LEU2*	This study
pAV339	pP_{PDI1}-*pdi1-3*	*CEN*, *LEU2*	This study
pAV340	pP_{PDI1}-*pdi1-4*	*CEN*, *LEU2*	This study
pAV341	pP_{PDI1}-*pdi1-5*	*CEN*, *LEU2*	This study
pAV342	pP_{PDI1}-*pdi1-6*	*CEN*, *LEU2*	This study
pAV449	pP_{PDI1}-*pdi1-7*	*CEN*, *LEU2*	This study
pAV450	pP_{PDI1}-*pdi1-8*	*CEN*, *LEU2*	This study
pAV451	pP_{PDI1}-*pdi1-9*	*CEN*, *LEU2*	This study
pAV452	pP_{PDI1}-*pdi1-10*	*CEN*, *LEU2*	This study
pAV453	pP_{PDI1}-*pdi1-11*	*CEN*, *LEU2*	This study
pAV454	pP_{PDI1}-*pdi1-12*	*CEN*, *LEU2*	This study
pAV455	pP_{PDI1}-*pdi1-13*	*CEN*, *LEU2*	This study
pAV456	pP_{PDI1}-*pdi1-14*	*CEN*, *LEU2*	This study
pAV457	pP_{PDI1}-*pdi1-15*	*CEN*, *LEU2*	This study
pAV458	pP_{PDI1}-*pdi1-16*	*CEN*, *LEU2*	This study
pAV637	pP_{PDI1}-*pdi1-5 N-term*	*CEN*, *LEU2*	This study
pAV644	pP_{PDI1}-*pdi1-5 C-term*	*CEN*, *LEU2*	This study
pAV638	pP_{PDI1}-*pdi1-6 N-term*	*CEN*, *LEU2*	This study
pAV645	pP_{PDI1}-*pdi1-6 C-term*	*CEN*, *LEU2*	This study
pAV639	pP_{PDI1}-*pdi1-10 N-term*	*CEN*, *LEU2*	This study
pAV642	pP_{PDI1}-*pdi1-10 C-term*	*CEN*, *LEU2*	This study
pAV640	pP_{PDI1}-*pdi1-11 N-term*	*CEN*, *LEU2*	This study
pAV646	pP_{PDI1}-*pdi1-11 C-term*	*CEN*, *LEU2*	This study

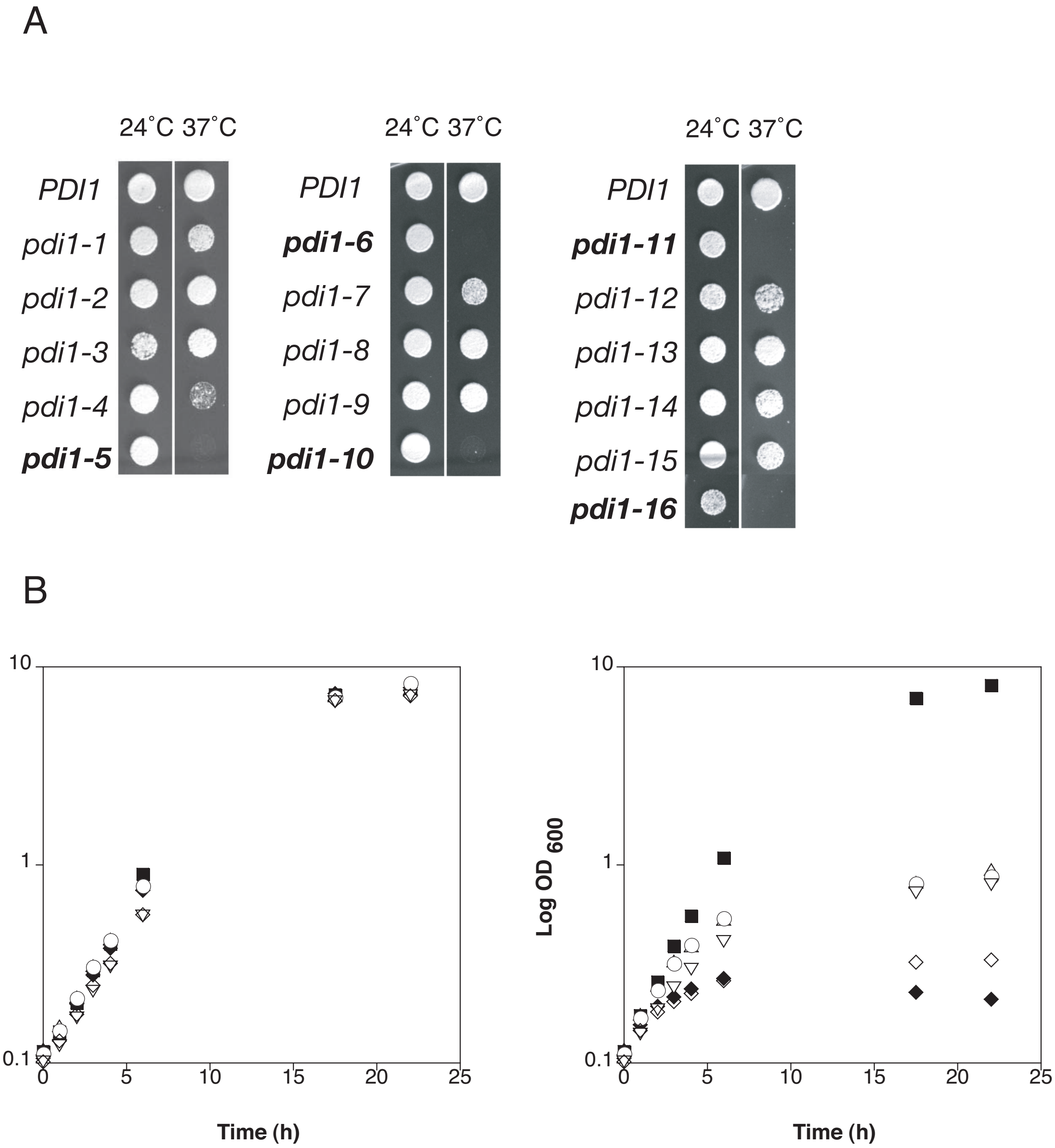

Figure 1. Isolation of a *pdi1* ts alleles. **(A)** The *pdiΔ* strain covered by *PDI1* (pAV336) or the indicated *pdi1* ts alleles (pAV337-pAV342, pAV449-pAV458) were plated on rich medium and incubated at 24 ˚C and 37 ˚C for 2 d. **(B)** Growth curve of the *pdi1Δ* strain covered by *pdi1* ts alleles at 24 ˚C (left panel) and 37 ˚C (right panel). (◆) *ero1-1*, (■) *pdi1Δ PDI1*, (△) *pdi1Δ pdi1-6*, (○) *pdi1Δ pdi1-10*, (▽) *pdi1Δ pdi1-11*, and (◇) *pdi1Δ pdi1-16*.

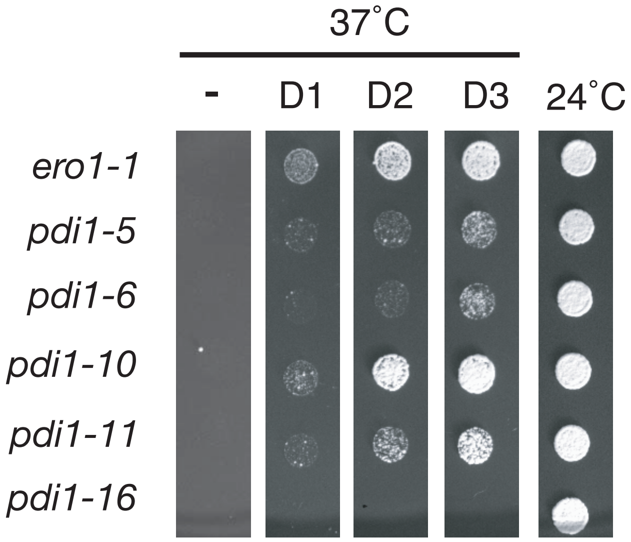
37˚C
-
D1
D2
D3
24˚C
ero1-1
pdi1-5
pdi1-6
pdi1-10
pdi1-11
pdi1-16

Figure 2. Addition of oxidant rescues *pdi1 ts* alleles. The *ero1-1* (CKY598), *pdi1Δ [pCS213]* (AVY580) and *pdi1Δ [pdi1 ts* alleles] (AVY585-6, AVY590-1 and AVY596) strains were plated on rich medium containing increasing concentrations of diamide (D1 - 0.1 mM diamide, D2 - 0.25 mM diamide, D3 - 0.5mM diamide) and incubated at 37 ˚C for 3 d.

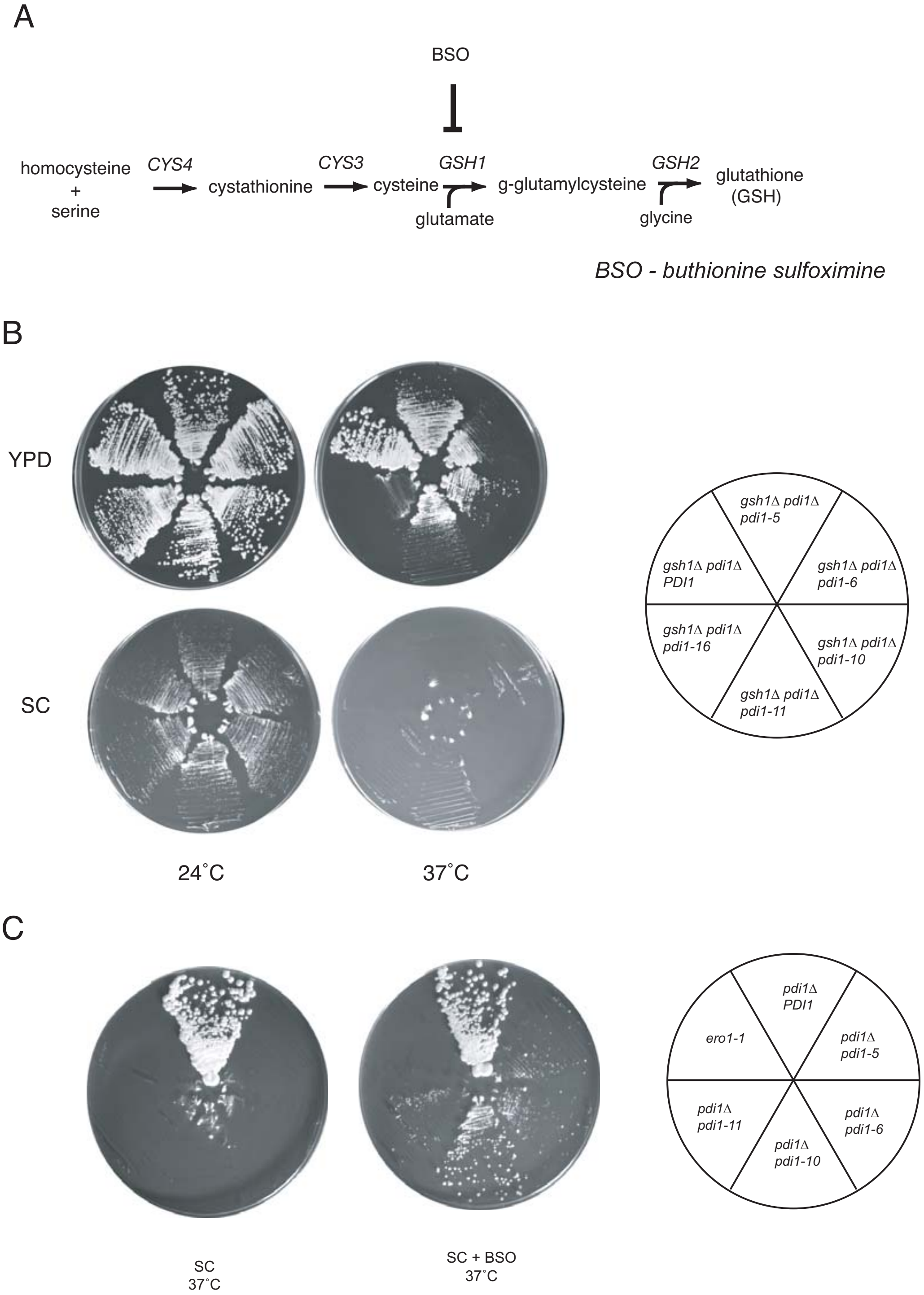
A
BSO
homocysteine
+
serine
CYS4
cystathionine
CYS3
cysteine
GSH1
glutamate
g-glutamylcysteine
GSH2
glycine
glutathione
(GSH)
BSO - buthionine sulfoximine
B
YPD
SC
24˚C
37˚C
gsh1Δ pdi1Δ pdi1-5
gsh1Δ pdi1Δ pdi1-6
gsh1Δ pdi1Δ pdi1-10
gsh1Δ pdi1Δ pdi1-11
gsh1Δ pdi1Δ pdi1-16
gsh1Δ pdi1Δ PDI1
C
pdi1Δ PDI1
pdi1Δ pdi1-5
pdi1Δ pdi1-6
pdi1Δ pdi1-10
pdi1Δ pdi1-11
ero1-1
SC
37˚C
SC + BSO
37˚C

Figure 3. Blocking the excess of GSH rescues the *pdi1* ts alleles. **(A)** Scheme of GSH biosynthesis. **(B)** The *pdi1Δ gsh1Δ PDI*1 (AVY1018) and *pdi1Δ gsh1Δ pdi1* ts alleles (AVY1019-AVY1023) were plated on rich medium YPD and incubated at 37 ˚C for 3 d. **(C)** The *ero1-1* (AFY397), *pdi1Δ PDI1* (AVY580) and *pdi1Δ pdi1* ts alleles (AVY585-6, AVY590-1 and AVY596) were plated on complete minimal medium containing BSO and incubated at 37 ˚C for 3 d.

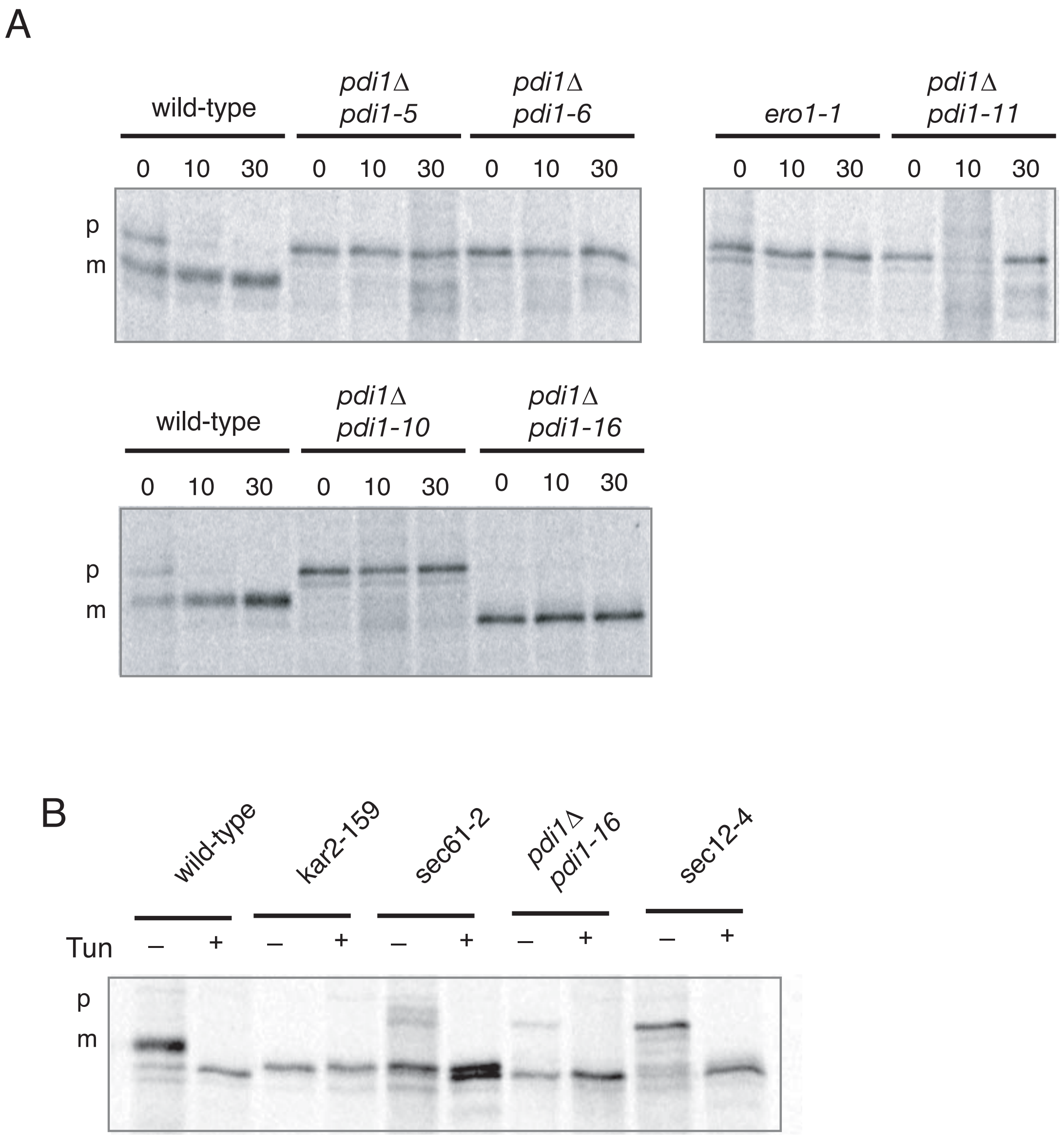
A
wild-type
pdi1Δ pdi1-5
pdi1Δ pdi1-6
ero1-1
pdi1Δ pdi1-11
0 10 30 0 10 30 0 10 30
0 10 30 0 10 30
p
m
wild-type
pdi1Δ pdi1-10
pdi1Δ pdi1-16
0 10 30 0 10 30 0 10 30
p
m
B
wild-type
kar2-159
sec61-2
pdi1Δ pdi1-16
sec12-4
Tun – + – + – + – + – +
p
m

Figure 4. CPY transport is impaired in *pdi1* ts alleles. Wild type (CKY263), *ero1-1* (CKY598), *pdi1Δ [pCS213]* (AVY580) and *pdi1Δ [pdi1 ts* alleles] (AVY585-6, AVY590-1 and AVY596) were shifted to the restrictive temperature of 38 ˚C for 1 h and pulse labeled with [^{35}S]methionine for 10 min, followed by a chase for the indicated times, and immunoprecipitated with CPY antibody.

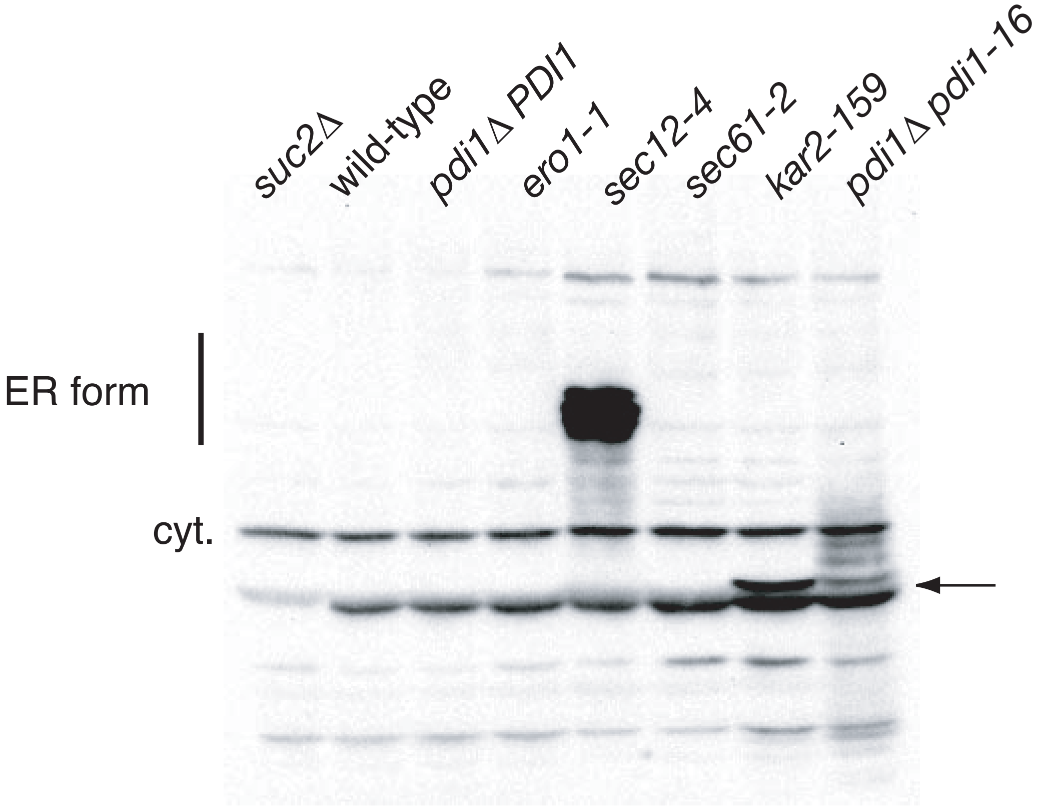
suc2Δ
wild-type
pdi1Δ PDI1
ero1-1
sec12-4
sec61-2
kar2-159
pdi1Δ pdi1-16
ER form
cyt.

Figure 5. The *pdi1-16* ts mutant accumulates the intracellular form of invertase. Wild-type (CKY263), *ero1-1 (AFY397) , kar2-159 (AVY etc)* were shifted to the restrictive temperature of 38 ˚C for 1 h. Intracellular invertase was detected by immunoblotting.

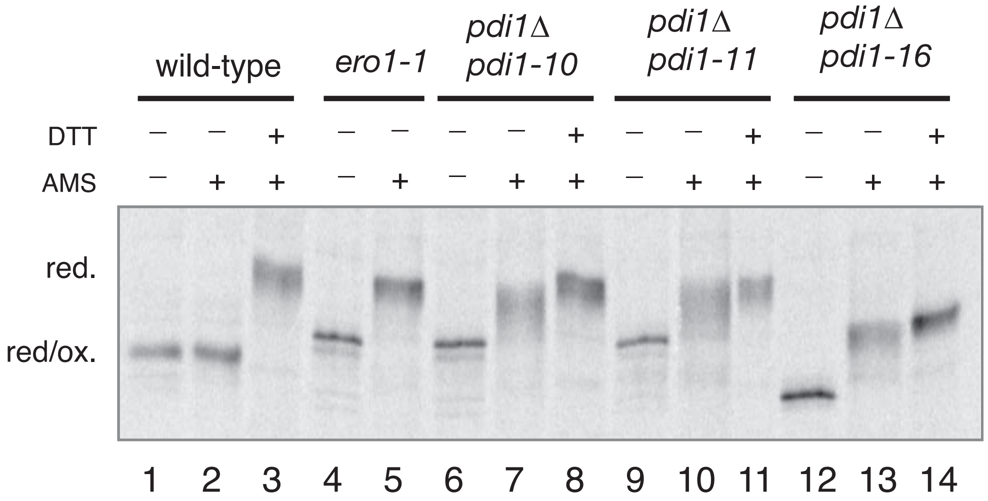
wild-type
ero1-1
pdi1Δ pdi1-10
pdi1Δ pdi1-11
pdi1Δ pdi1-16
DTT – – + – – – – + – – + – – +
AMS – + + – + – + + – + + – + +
red.
red/ox.
1 2 3 4 5 6 7 8 9 10 11 12 13 14

Figure 6. The *pdi1* ts alleles are required for oxidation of CPY. Wild type (CKY263), *ero1-1* (CKY598), *pdi1Δ [pCS213]* (AVY580) and *pdi1Δ [pdi1 ts* alleles] (AVY585-6, AVY590-1 and AVY596) were shifted to the restrictive temperature of 38 ˚C for 1 h and pulse labeled with [^{35}S]methionine for 10 min. DTT was added to a final concentration of 5 mM to samples 3, 8 and 11, 10 min before labeling. Cells pellets were lysed under non-reducing conditions in the presence of 20 mM AMS (lanes 2-3, 5, 7-8, 10-11 and 13-14) or in the absence of AMS (lanes 1, 4, 6, 9 and 12). CPY was immunoprecipitated and samples resolved by non-reducing SDS-PAGE.

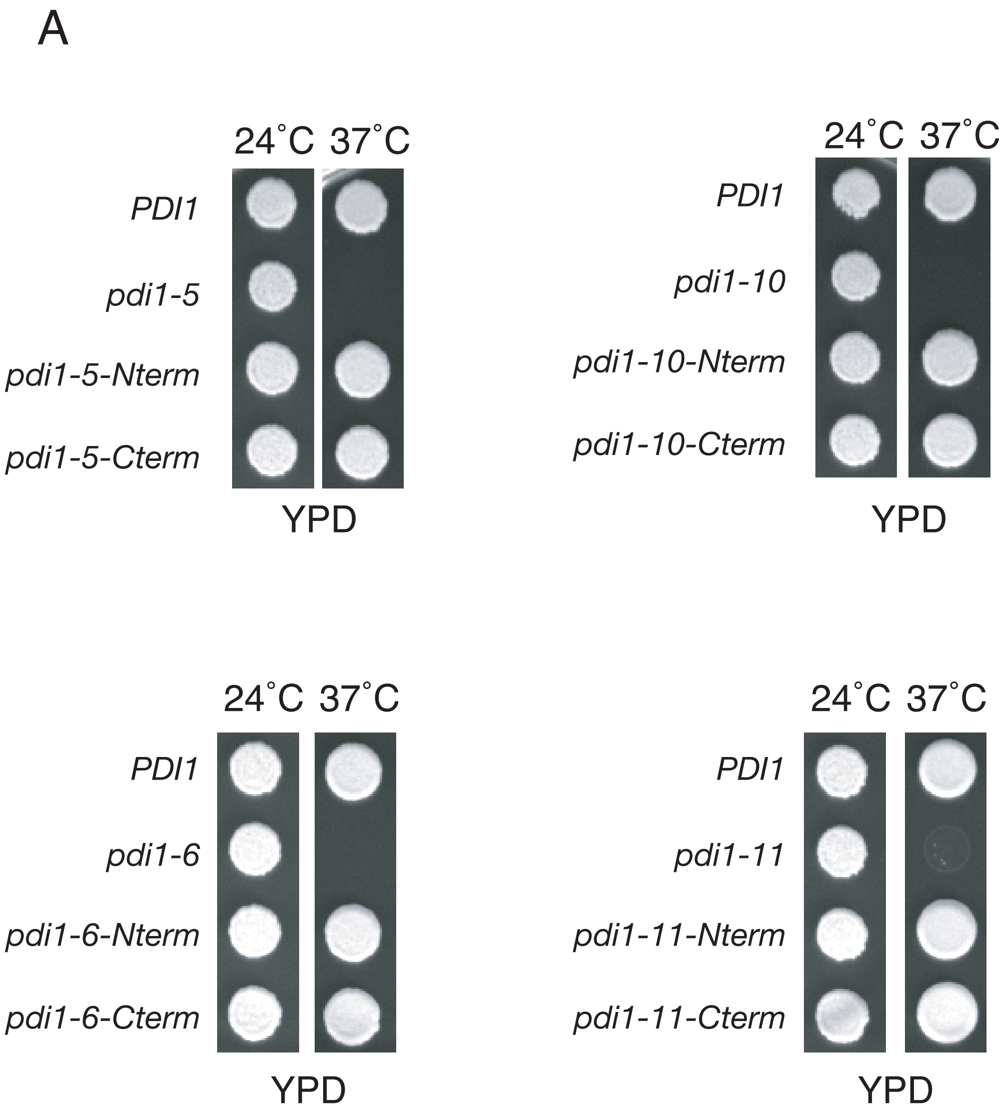
A
24˚C 37˚C
PDI1
pdi1-5
pdi1-5-Nterm
pdi1-5-Cterm
YPD
24˚C 37˚C
PDI1
pdi1-10
pdi1-10-Nterm
pdi1-10-Cterm
YPD
24˚C 37˚C
PDI1
pdi1-6
pdi1-6-Nterm
pdi1-6-Cterm
YPD
24˚C 37˚C
PDI1
pdi1-11
pdi1-11-Nterm
pdi1-11-Cterm
YPD

Figure 7. Isolation of mutaions of *pdi1* ts alleles. The *pdiΔ* strain covered by *PDI1* (pAV336) or the indicated *pdi1* ts alleles (pAV637-646) were plated on rich medium and incubated at 24 ˚C and 37 ˚C for 2 d.

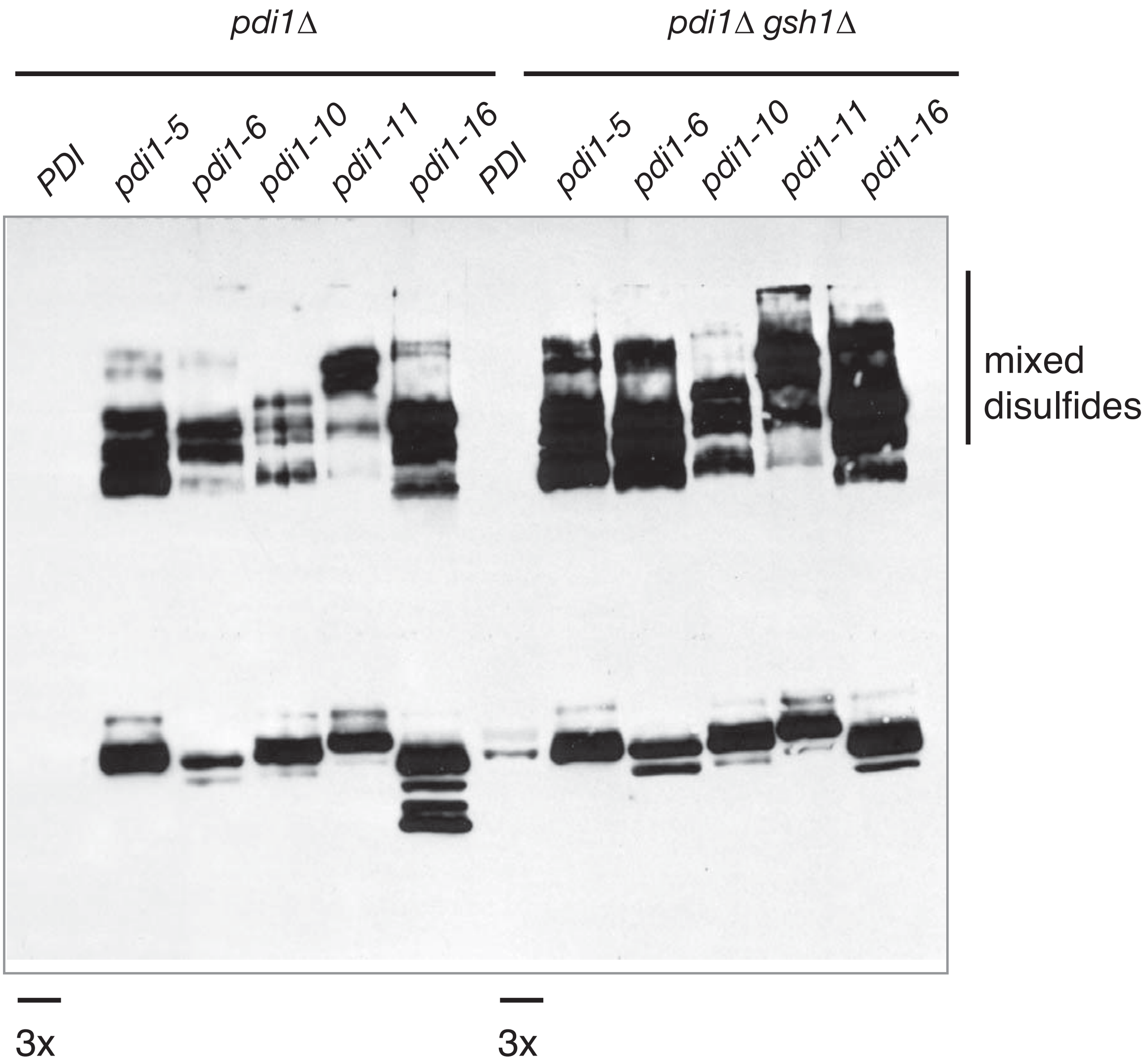
pdi1Δ
pdi1Δ gsh1Δ
PDI
pdi1-5
pdi1-6
pdi1-10
pdi1-11
pdi1-16
PDI
pdi1-5
pdi1-6
pdi1-10
pdi1-11
pdi1-16
mixed disulfides
3x
3x

Figure 8. The *pdi1* ts alleles accumulate *pdi1* ts-substrate complexes. The *pdi1Δ [pCS213]* (AVY580) and *pdi1Δ [pdi1* ts alleles] strains (AVY585-6, AVY590-1 and AVY596) or the *pdi1Δ gsh1Δ [pCS213]* (AVY1018) and *pdi1Δ gsh1Δ [pdi1* ts alleles*]* (AVY1019-23) were shifted to the restrictive temperature of 38 ˚C for 1 h. Pdi1p was detected by immunoblotting.

Chapter Six

Players in disulfide bond formation pathways: Open questions

Ero1-dependent and -independent disulfide bond formation pathways

The main pathway of disulfide bond formation in the ER of *S. cerevisiae* uses two essential proteins, Ero1p and Pdi1p, that by means of a shuttle mechanism, transfer disulfide bonds to secretory proteins (Frand et al., 1998). Recently, a second pathway has been defined, in which in the absence of Ero1p, overexpressed Erv2p can transfer oxidizing equivalents to Pdi1p (Sevier *et al.*, 2001). In this thesis, the isolation and biochemical and structural characterization of Erv2p are described (Chapter 2). The catalytic mechanism of disulfide transfer in Erv2p is described in detail in Chapter 3 and Chapter 4.

Search for substrates of Erv2p

When overexpressed, Erv2p can be found in mixed disulfides with Pdi1p (Sevier et al., 2001). Furthermore, recombinant Erv2p is able to oxidize Pdi1p *in vitro*, although this reaction is extremely slow. For this reason, it is unclear whether Pdi1p is a physiological substrate of Erv2p (Sevier et al., 2001, and Chapter 3). Besides Pdi1p, it is unknown whether there are other physiological substrates of Erv2p. Intermediates of a disulfide exchange reaction are short-lived and difficult to observe; therefore, despite various efforts, other Erv2p substrate(s) are still unknown.

Although *in vitro* studies (described in Chapter 3) suggested that Erv2p suppressor mutants are more promiscuous, it is also unknown if wild-type Erv2p and suppressor mutants share the same substrates *in vivo* or if wild-type Erv2p is a more specific oxidoreductase. Mutants that are impaired in the resolution of mixed disulfides with substrate proteins have been used by other groups to find physiological substrates (Frand *et al.*, 1999; Kadokura *et al.*, 2004). Some of the mutants designed in this study (see Chapters 3 and 4), such as Erv2p-E191A and Erv2p-CGA$_2$C, have a slight defect in activity and might be useful for this end. Identification of physiological substrates of wild-type and suppressor mutant Erv2p will be valuable for our understanding of the mechanism of disulfide bond transfer and its specificity.

The function of Erv2p: still a mystery

The question concerning the physiological function of Erv2p still remains open. One interesting hypothesis is that in yeast, Erv2p acts in stationary phase when the ATP and FAD levels drop and when the activity of Ero1p might be compromised. It has been reported that the mRNA levels of Erv2p are increased during stationary phase (Stein *et al.*, 1998).

Erv2p homologs are involved in disulfide bond formation in non-ER locations

For a long time, the formation of disulfide bonds was viewed as a process that occurs exclusively in the ER. The isolation of members of the QSOX/ERV family that are localized to non-ER compartments, such as the mitochondrial intermembrane space or the cytoplasm of virus-infected cells, changed this view.

Recent studies showed that Erv1p, a member of the ERV/QSOX family that has FAD-dependent sulfhydryl oxidase activity, together with Mia40p, oxidizes proteins in the intramembrane space of the mitochondria (Mesecke *et al.*, 2005; Rissler *et al.*, 2005; Tokatlidis, 2005). The importance of Erv1p function is indicated by the fact that it is an essential gene necessary for the proper function of the mitochondria (Lange *et al.*, 2001; Lisowsky, 1994). Both flavin and GSH play a role in the ER disulfide bond formation pathway, but it is still unknown whether these factors play a role in the disulfide bond formation pathway in the mitochondria as well. Interestingly, there is a flavin transporter, FLX1, and a GSH transporter system in mitochondria (Bafunno *et al.*, 2004; Rebbeor *et al.*, 1998; Tzagoloff *et al.*, 1996).

A pathway for disulfide bond formation in viral proteins in the cytosol of the host cell is also performed by a homolog of Erv2p named E10R (Senkevich *et al.*, 2000). It is currently unknown how disulfide bond formation can occur in such a reducing environment. Surely, future studies will reveal new mechanisms of disulfide bond formation in other cellular compartments.

How is FAD transported into the ER lumen?

Both Ero1p and Erv2p are FAD-dependent oxidoreductases (Sevier et al., 2001; Tu *et al.*, 2002). One interesting question is how the FAD is transported into the ER to fulfill the requirements of Ero1p and the sulfhydryl oxidase Erv2p. Since the ER membrane seems to be impermeable to free FAD, the existence of a FAD transporter has been suggested but its identity is still unknown (Tu et al., 2002).

ER redox homeostasis and oxidative folding

The activities of Ero1p and Erv2p are directly linked with the formation of H_2O_2 (Gross *et al.*, 2006; Sevier et al., 2001). Thus, inappropriate oxidation of substrates or heavy load of protein thiols in the secretory pathway would lead to increased H_2O_2 formation, which could be very damaging to the cell. Lowering the levels of Ero1p in *C. elegans* by RNAi eliminates the significant accumulation of peroxides in the cell due to ER stress (Harding *et al.*, 2003).

A remaining challenge is to discover how the ER copes with this oxidative stress and how this information is integrated into other related signaling pathways. In Chapter 3, I discuss a mechanism of shuttle of disulfides between two cysteine pairs in Erv2p that seems to confer specificity to disulfide transfer to substrate proteins, which is also used by Ero1p (Sevier *et al.*, 2006). Regulating the activity of these enzymes. can be used to control the amount of ROS produced. Another potential mechanism to control ROS production is by the enzymatic removal of H_2O_2; thus there may be a catalase in the ER, which would disprotonate H_2O_2.

Specificity in disulfide transfer - variations on a theme

Transfer between two cysteine pairs is a conserved mechanism of some thiol disulfide oxidoreductase such as Ero1p, Erv2p and DsbB. In general, specificity of disulfide transfer reactions can also be achieved in various other ways.

DsbB, a transmembrane protein involved in disulfide bond formation pathways in *E. coli*, preferentially oxidizes DsbA, a monomeric protein, and not DsbC or DsbG, which are dimeric proteins. Converting DsbC into a monomeric protein, by mutation of residue Gly49 to Arg or Glu or by truncating the N-terminal domain (which is necessary for dimerization), allows DsbC to become a substrate of DsbB (Bader *et al.*, 2001).

High MW thioredoxin reductase and glutathione reductase have the same fold, except that the former has a C-terminal tail containing a second redox cysteine pair (Sandalova *et al.*, 2001). GSSG is the natural substrate of glutathione reductase, yet GSSG is not a substrate for high MW thioredoxin reductase. A comparison between the crystal structure of these two enzymes revealed that the residues involved in GSH binding are conserved in both structures. However, the presence of the C-terminal tail in thioredoxin reductase prevents interaction of GSSG with the active site cysteines by blocking access to them (Sandalova et al., 2001).

Thus, specificity of disulfide bond formation has evolved in various ways, and future studies will likely reveal other mechanisms.

Is there an isomerization pathway in yeast? PDI, GSH or an uncharacterized reductase - who's to blame?

The *E. coli* disulfide bond isomerization pathway has been fairly well characterized: the periplasmic membrane protein DsbD gives reducing equivalents to the soluble periplasmic protein DsbC, which shuffles disulfide bonds in protein substrates until the native conformation is achieved (Rietsch *et al.*, 1996). In contrast, the precise mechanism and players of the disulfide bond isomerization pathway in the ER have not been identified.

It is still in debate whether the reduced form of Pdi1p (or Pdi1p containing only one of the Cys-X-X-Cys motif reduced) can function as an isomerase (Tian *et al.*, 2006). If so, and if indeed there is an analogous pathway of isomerization in the ER, it is possible that either glutathione or an uncharacterized ER reductase may be responsible for maintaining a portion of Pdi1p in the reduced form, allowing it to function as an isomerase *in vivo*. The other possibility is that Pdi1p is not involved in the isomerization pathway in the yeast ER and that glutathione or an uncharacterized ER reductase is responsible for this activity.

To study disulfide bond isomerization in the yeast ER we need to find a secretory marker protein that contains at least two disulfide bonds. Carboxypeptidase Y is a good model, since it contains 11 cysteines and therefore has numerous potential disulfide bond connectivities. As it traverses the secretory pathway it acquires various post-translational modifications that allow the various forms to be differentiated by SDS-PAGE. Furthermore, it has been shown that under hyperoxidizing conditions (e.g. treatment of yeast cells with the thiol oxidant diamide) proteins that contain reactive thiols, such as CPY, are withheld in the ER in oxidized form (p1 form) likely to contain inappropriate intra- or intermolecular disulfide bonds, while the intracellular transport of proteins without cysteines, such as prepro-α-factor, proceeds with normal kinetics (Cuozzo *et al.*, 1999). Therefore, the ability of the cell to isomerize disulfide bonds can be easily assayed. The oxidative folding of misoxidized CPY can be assessed in cells deficient in glutathione, Pdi1p or any of the Pdi1p-homologs to test whether each is involved in the isomerization pathway.

Role of PDI homologs? Different specificity?

Despite the increasing number of PDI family members and the large number of reports being made in the last five years, there are still a lot of questions regarding the physiological role of these proteins, their mechanism of action and their substrates. For example, the yeast ER contains five PDI-like proteins, namely Pdi1p, Eug1p, Mpd1p, Mpd2p and Eps1p (Norgaard *et al.*, 2001). Their role in disulfide bond formation and their substrate specificity is still unknown.

Recent studies suggest that PDI homologs may participate in discrete protein maturation pathways. ERp57 promote disulfide bond formation in glycoproteins, including MHC class I, thought the interaction with lectin chaperones calnexin and calreticulin (Ellgaard *et al.*, 2003). Furthermore, preferential expression of members of the human PDI family in different tissues, suggests these proteins contribute the folding of tissue specific proteins. For example, PDIp, EndoPDI, and PDILT are highly expressed in pancreas, endothelia, and testis cells, respectively (Sullivan *et al.*, 2003; van Lith *et al.*, 2005; Volkmer *et al.*, 1997).

References

Bader, M.W., Hiniker, A., Regeimbal, J., Goldstone, D., Haebel, P.W., Riemer, J., Metcalf, P. and Bardwell, J.C. (2001) Turning a disulfide isomerase into an oxidase: DsbC mutants that imitate DsbA. *Embo J*, **20**, 1555-1562.

Bafunno, V., Giancaspero, T.A., Brizio, C., Bufano, D., Passarella, S., Boles, E. and Barile, M. (2004) Riboflavin uptake and FAD synthesis in Saccharomyces cerevisiae mitochondria: involvement of the Flx1p carrier in FAD export. *J Biol Chem*, **279**, 95-102.

Cuozzo, J.W. and Kaiser, C.A. (1999) Competition between glutathione and protein thiols for disulphide-bond formation. *Nat Cell Biol*, **1**, 130-135.

Ellgaard, L. and Frickel, E.M. (2003) Calnexin, calreticulin, and ERp57: teammates in glycoprotein folding. *Cell Biochem Biophys*, **39**, 223-247.

Frand, A.R. and Kaiser, C.A. (1998) The ERO1 gene of yeast is required for oxidation of protein dithiols in the endoplasmic reticulum. *Mol Cell*, **1**, 161-170.

Frand, A.R. and Kaiser, C.A. (1999) Ero1p oxidizes protein disulfide isomerase in a pathway for disulfide bond formation in the endoplasmic reticulum. *Mol Cell*, **4**, 469-477.

Gross, E., Sevier, C.S., Heldman, N., Vitu, E., Bentzur, M., Kaiser, C.A., Thorpe, C. and Fass, D. (2006) Generating disulfides enzymatically: reaction products and electron acceptors of the endoplasmic reticulum thiol oxidase Ero1p. *Proc Natl Acad Sci U S A*, **103**, 299-304.

Harding, H.P., Zhang, Y., Zeng, H., Novoa, I., Lu, P.D., Calfon, M., Sadri, N., Yun, C., Popko, B., Paules, R., Stojdl, D.F., Bell, J.C., Hettmann, T., Leiden, J.M. and Ron, D. (2003) An integrated stress response regulates amino acid metabolism and resistance to oxidative stress. *Mol Cell*, **11**, 619-633.

Kadokura, H., Tian, H., Zander, T., Bardwell, J.C. and Beckwith, J. (2004) Snapshots of DsbA in action: detection of proteins in the process of oxidative folding. *Science*, **303**, 534-537.

Lange, H., Lisowsky, T., Gerber, J., Muhlenhoff, U., Kispal, G. and Lill, R. (2001) An essential function of the mitochondrial sulfhydryl oxidase Erv1p/ALR in the maturation of cytosolic Fe/S proteins. *EMBO Rep*, **2**, 715-720.

Lisowsky, T. (1994) ERV1 is involved in the cell-division cycle and the maintenance of mitochondrial genomes in Saccharomyces cerevisiae. *Curr Genet*, **26**, 15-20.

Mesecke, N., Terziyska, N., Kozany, C., Baumann, F., Neupert, W., Hell, K. and Herrmann, J.M. (2005) A disulfide relay system in the intermembrane space of mitochondria that mediates protein import. *Cell*, **121**, 1059-1069.

Norgaard, P., Westphal, V., Tachibana, C., Alsoe, L., Holst, B. and Winther, J.R. (2001) Functional differences in yeast protein disulfide isomerases. *J Cell Biol*, **152**, 553-562.

Rebbeor, J.F., Connolly, G.C., Dumont, M.E. and Ballatori, N. (1998) ATP-dependent transport of reduced glutathione on YCF1, the yeast orthologue of mammalian multidrug resistance associated proteins. *J Biol Chem*, **273**, 33449-33454.

Rietsch, A., Belin, D., Martin, N. and Beckwith, J. (1996) An in vivo pathway for disulfide bond isomerization in Escherichia coli. *Proc Natl Acad Sci U S A*, **93**, 13048-13053.

Rissler, M., Wiedemann, N., Pfannschmidt, S., Gabriel, K., Guiard, B., Pfanner, N. and Chacinska, A. (2005) The essential mitochondrial protein Erv1 cooperates with Mia40 in biogenesis of intermembrane space proteins. *J Mol Biol*, **353**, 485-492.

Sandalova, T., Zhong, L., Lindqvist, Y., Holmgren, A. and Schneider, G. (2001) Three-dimensional structure of a mammalian thioredoxin reductase: implications for mechanism and evolution of a selenocysteine-dependent enzyme. *Proc Natl Acad Sci U S A*, **98**, 9533-9538.

Senkevich, T.G., White, C.L., Koonin, E.V. and Moss, B. (2000) A viral member of the ERV1/ALR protein family participates in a cytoplasmic pathway of disulfide bond formation. *Proc Natl Acad Sci U S A*, **97**, 12068-12073.

Sevier, C.S., Cuozzo, J.W., Vala, A., Aslund, F. and Kaiser, C.A. (2001) A flavoprotein oxidase defines a new endoplasmic reticulum pathway for biosynthetic disulphide bond formation. *Nat Cell Biol*, **3**, 874-882.

Sevier, C.S. and Kaiser, C.A. (2006) Disulfide transfer between two conserved cysteine pairs imparts selectivity to protein oxidation by Ero1. *Mol Biol Cell*, **17**, 2256-2266.

Stein, G. and Lisowsky, T. (1998) Functional comparison of the yeast scERV1 and scERV2 genes. *Yeast*, **14**, 171-180.

Sullivan, D.C., Huminiecki, L., Moore, J.W., Boyle, J.J., Poulsom, R., Creamer, D., Barker, J. and Bicknell, R. (2003) EndoPDI, a novel protein-disulfide isomerase-like protein that is preferentially expressed in endothelial cells acts as a stress survival factor. *J Biol Chem*, **278**, 47079-47088.

Tian, G., Xiang, S., Noiva, R., Lennarz, W.J. and Schindelin, H. (2006) The crystal structure of yeast protein disulfide isomerase suggests cooperativity between its active sites. *Cell*, **124**, 61-73.

Tokatlidis, K. (2005) A disulfide relay system in mitochondria. *Cell*, **121**, 965-967.

Tu, B.P. and Weissman, J.S. (2002) The FAD- and O(2)-dependent reaction cycle of Ero1-mediated oxidative protein folding in the endoplasmic reticulum. *Mol Cell*, **10**, 983-994.

Tzagoloff, A., Jang, J., Glerum, D.M. and Wu, M. (1996) FLX1 codes for a carrier protein involved in maintaining a proper balance of flavin nucleotides in yeast mitochondria. *J Biol Chem*, **271**, 7392-7397.

van Lith, M., Hartigan, N., Hatch, J. and Benham, A.M. (2005) PDILT, a divergent testis-specific protein disulfide isomerase with a non-classical SXXC motif that engages in disulfide-dependent interactions in the endoplasmic reticulum. *J Biol Chem*, **280**, 1376-1383.

Volkmer, J., Guth, S., Nastainczyk, W., Knippel, P., Klappa, P., Gnau, V. and Zimmermann, R. (1997) Pancreas specific protein disulfide isomerase, PDIp, is in transient contact with secretory proteins during late stages of translocation. *FEBS Lett*, **406**, 291-295.